Intrinsic and Extrinsic Regulation of MeCP2 in Brain Cell Types and Their Implications in MeCP2-Related Neurodevelopmental Disorders

By

Vichithra Rasangi Batuwita Liyanage

A thesis submitted to the Faculty of Graduate Studies of

The University of Manitoba

In partial fulfillment of the requirements of the degree of

DOCTOR OF PHILOSOPHY

Department of Biochemistry and Medical Genetics

Rady Faculty of Health Sciences

University of Manitoba

Winnipeg, Manitoba, Canada

THESIS ABSTRACT

MeCP2 is a key epigenetic regulator in the brain, which regulates gene expression. There are two *Mecp2/*MeCP2 isoforms - MeCP2E1 and MeCP2E2 - with both overlapping and non-overlapping expression and functions in the brain. MeCP2 is widely expressed in different brain cell types but predominantly expressed in neurons. *MECP2*/MeCP2-deficiency and overexpression are associated with Rett Syndrome (RTT), *MECP2* duplication syndrome (MDS) and alcohol (ethanol)-mediated neurological damage, such as Fetal Alcohol Spectrum Disorders (FASD). These disorders have no cure. Rescuing the expression levels of MeCP2 could be a potential therapeutic approach for these diseases. A thorough understanding of MeCP2 expression regulation is essential to achieve this goal. The objective of my Ph.D. project presented in this thesis is to address the knowledge gap on *Mecp2* regulation in the brain, which has been carried out using cellular models of *in vitro* neural stem cell (NSC) differentiation and *in vivo* differentiated neurons and astrocytes. As such, the intrinsic regulation of *Mecp2* isoforms by epigenetic and transcriptional mechanisms, and extrinsic regulation of *Mecp2* isoforms by the insult of ethanol exposure were explored in this thesis.

We identified six regulatory elements (REs) within the *Mecp2* promoter and intron 1, DNA methylation of which correlated with the expression of *Mecp2* isoforms during NSC differentiation [Liyanage *et al.* (2013), Molecular Autism]. The role of DNA methylation in *Mecp2* regulation was studied by treatment with a DNA demethylating agent decitabine, which was identified as a potential drug that induces *Mecp2*/MeCP2 expression in an isoform-specific manner. In terms of the extrinsic regulation by ethanol, dynamic DNA methylation patterns at these REs was associated with the alterations of *Mecp2* levels by ethanol exposure and withdrawal during NSC differentiation [Liyanage *et al.* (2015), Experimental Neurology]. We also found that expression

of *Mecp2* isoforms in primary neurons and astrocytes is cell type- and sex-specific. The higher expression of *Mecp2* isoforms in neurons as compared to astrocytes is possibly mediated through lower DNA methylation levels in these identified REs.

Taken together, my studies provide evidence for the role of DNA methylation in epigenetic regulation of *Mecp2* in these brain cells, under normal conditions and in response to extrinsic deregulation by ethanol exposure. The ability of the DNA methylation inhibitor decitabine to upregulate *Mecp2* levels provides insights on potential future drug treatment strategies for MeCP2-deficiency-associated neurological conditions. The knowledge gained from this study will hold promise for utilizing these intrinsic and extrinsic regulatory mechanisms of *Mecp2* isoforms for a better understanding of diseases pathology and provides insights into translational knowledge on further MeCP2 research and therapy strategies for MeCP2-associated neurological disorders.

ACKNOWLEDGEMENTS

It has been a long six years during which I experienced and embraced victory, success, many achievements as well as challenges, failures, and pain. I am indebted to all who were there for me, who helped me and encouraged me.

First and foremost, my deepest gratitude is offered to my supervisor Dr. Mojgan Rastegar. The guidance and opportunities you provided were invaluable for my progress as a graduate student. I am proud to be one of your students, and any student would be lucky to have you as their mentor. Secondly, I extend my thanks to my advisory committee members, Dr. Jim Davie, Dr. John Wilkins and Dr. Chris Anderson. Over the last six years, there were numerous individual and group meetings to revise my project. Your input and guidance, as well as the faith you had in me, are deeply appreciated. I especially thank Dr. Jim Davie, whom I consider as a second mentor to me. From the days that I participated in your Gene Expression classes, I idealized you as a scientist I want to be one day.

Special thanks go to my external thesis examiner Dr. Vince Tropepe. Thank you very much for your insightful comments. They had a significant impact on my perspectives on my thesis studies.

Dr. Louise Simard, the Head of the Department of Biochemistry and Medical Genetics, I am indebted to you for your kindness, empathy, guidance and mentorship during the most difficult period of my life. I learned a lot from you. You are and will always be an inspiration to me. I owe my heartfelt appreciation to the Chairs of Graduate Student Affairs, Dr. Leigh Murphy, Dr. Mark Nachtigal and Dr. Jeff Wigle.

Rastegar lab was a friendly environment, where I considered as a second home and worked hard day and night for six years. I am highly appreciative of the impacts it had on my life. Carl

During the last two years of my Ph.D. studies, I fell severely ill. There were a handful of people who supported me, encouraged me and helped me to ease my pain. Molly, Santhosh, Pratima and Sumanta, I am so thankful for all your kindness and empathy. The accessibility/disability services of the University of Manitoba and Mr. Jamie Penner who was my

accessibility advisor during this time helped me immensely. Words fail to express my gratitude to you.

Big thanks go to my 'gang' Ariff, Kannan, Vasu, Anjali, Manoj, Bhavya, Nivedita, Jit, Glen, and Hardeep. Thank you so much for the laughter, high-fives, support, encouragement and many meals together. You made life much more bearable and joyful. Thank you so much, Soma Didi. You showed me the spiritual path to take during the most difficult period of my life. You are truly a life savior for me. Anupama Konara and Sanzida Jahan, you are the two sisters I never had. Both of you and your families have been with me in every happiness and sorrow. Without you, I would not have come this far. I am so lucky to be your best friend.

Words are not enough to thank my parents (Ammi and Thaththi). Without your never-ending love, support and faith in me, I would not have come so far. My brother Chamara has always been a wonderful brother and great support. Thank you, Shamika akki for taking care of my family while I am far away from them.

Last but not least, I am eternally grateful to my soul mate, Robby Zachariah. This thesis is a tribute to you because, without you, this thesis would not have been possible. You supported me as a lab member, my best friend, and my fiancé. Thank you so much for loving me endlessly, even when I am stubborn, crabby and cranky. You raised me up every time I fell and held me when I was depressed and so sick. I am so lucky to have you in my life. I cannot ever thank you enough for the everlasting love, inspiration, encouragement and faith.

"It is not the critic who counts; not the man who points out how the strong man stumbles, or where the doer of deeds could have done them better. The credit belongs to the man who is actually in the arena, whose face is marred by dust and sweat and blood; who strives valiantly; who errs, who comes short again and again, because, there is no effort without error and shortcoming; but who does actually strive to do the deeds; who knows great enthusiasms, the great devotions, who spends himself in a worthy cause; who at the best knows in the end triumph of high achievement, and who at the worst, if he fails, at least fails daring greatly, so that his place shall never be with those cold and timid souls who neither know victory nor defeat…."

-Theodore Roosevelt-

'Man in the Arena' Speech

April 23, 1910

Dedicated to my loving parents

Mr. Wijesena Batuwita Liyanage & Mrs. Mithila Sarathchandra

who believed in me and taught me never to give up

TABLE OF CONTENTS

xiii

xiv

LIST OF FIGURES

Chapter 1_Main figures

Chapter 2_Main figures

Chapter 3_Main figures

Chapter 3_Supplementary figures

Chapter 4_Main figures

Chapter 4_Supplementary figures

Chapter 5_Main figures

Appendix

LIST OF TABLES

LIST OF ABBREVIATIONS

The abbreviations are defined at the first mention as they appear on the text. Note that the abbreviations found within the figure legends directly adapted from published articles and abbreviations within published chapters have kept unchanged. Also, the first letter of gene/protein names was capitalized to be consistent with the published articles reprinted in this thesis.

Term	Abbreviation
$\Delta\Delta C_T$	comparative C_T
5CaC	5-carboxycytosine
5fC	5-formylcytosine
5hmc	5-hydroxymethylcytosine
5mC	5-methylcytosine
ac	acetyl
ADH	Alcohol dehydrogenase
ADP	adenosine diphosphate
AGO	Protein argonaute-2
AGRE	Autism genetic resource exchange
AID	Activation-induced cytidine deaminase
ALC	acetyl-L-carnitine
ALDH2	Aldehyde dehydrogenase 2
ANOVA	analysis of variance
APOBEC1	Apolipoprotein B mRNA editing enzyme catalytic polypeptide 1
APOBEC1	Apolipoprotein B mRNA editing enzyme catalytic polypeptide 1

ARBD	alcohol related birth defects
ARND	alcohol-related neurodevelopmental disorders
ASD	Autism Spectrum Disorders
ASTFs	astrocyte-specific TFs
AT-hook	adenine-thymine (AT)-rich
ATP	adenosine triphosphate
ATRX	ATP-dependent helicase ATRX
ATRX	ATP-dependent helicase ATRX
BDNF	Brain-derived neurotrophic factor
BER	base excision repair
bFGF	basic fibroblast growth factor
BIRC4	Baculoviral IAP repeat-containing protein 4
bp	base pairs
BRE^d	TFIIB recognition element downstream
BRE^u	TFIIB recognition element upstream
BS	brain stem
BSA	bovine serum albumin
C	cytosine
C/EBP	CCAAT-enhancer-binding proteins
cDNA	complementary DNA
CER	cytoplasmic extraction reagent
CERE	cerebellum

CETS	cell epigenotype-specific
ChIPseq	Chromatin immunoprecipitation sequencing
circRNAs	circular RNAs
CNPase	2',3'-Cyclic-nucleotide 3'-phosphodiesterase
CNTF	Ciliary neurotrophic factor
CNVs	copy number variations
CpH methylation	non-CpG methylation
CREB	cAMP response element-binding protein
Creb1	cAMP Responsive Element Binding Protein 1
Ct	threshold cycle values
CTCF	CCCTC-binding factor
CTD	C-terminal Domain
CTX	cortex
CYP2E1	Cytochrome P450 2E1
D	day
DAPI	4′,6-diamidino-2-phenylindole
DCE	downstream core element
DMEM	Dulbecco's modified eagle medium
DMS-V	diagnostic and statistical manual of mental disorders
Dnmt	DNA methyltransferases
dNTPs	deoxynucleotides
DPE	downstream promoter element

DTT	dithiothreitol
E	embryonic day
EDTA	ethylenediaminetetraacetic acid
EMSA	electrophoretic mobility shift assay
ENCODE	encyclopedia of DNA elements
eRNAs	enhancer RNAs
ESC	embryonic stem cells
Ex	exon
EZH2	Enhancer of zeste homolog 2
F	female
FAE	fetal alcohol effects
FAS	fetal alcohol syndrome
FASD	Fetal Alcohol Spectrum Disorders
FBS	fetal bovine serum
FOX1	Forkhead box 1
FP	forward PCR primer
GAB3	GRB2-associated- binding protein 3
GAD1	Glutamate decarboxylase 1
GAPDH	Glyceraldehyde-3- phosphate dehydrogenase
GFAP	Glial fibrillary acidic protein
Gli	GLI Family Zinc finger
GR	glycine and arginine residues

Grhl1	Grainyhead Like Transcription Factor 1
GTFs	general transcription factors
h	hours
H1/H2/H3/H4	histones
HCl	hydrochloric Acid
Hdac6	Histone deacetylase 6
HEPES	4-(2-hydroxyethyl)-1-piperazineethanesulfonic acid
HIPPO	hippocampus
hMeDIP	hydroxymethylated DNA immunoprecipitation
HMGB	High-mobility group box
hnRNP	heterogeneous nuclear ribonucleoproteins
HOTAIR	HOX transcript antisense RNA
HP1	Heterochromatin protein 1
hPTMs	histone post-translational modifications
HRP	horseradish peroxidase
ICC	immunocytochemistry
ID	inter-domain
IF	immunofluorescence
Igf2r	Insulin-like growth factor 2 receptor
IHC	immunohistochemistry
Il3	Interleukin 3
Inr	initiator element

IRAK1	Interleukin 1 receptor associated kinase 1
JARID1C	Jumonji/ARID domain-containing protein 1C
K	lysine
KAT	histone/lysine acetyltransferases
KDM	lysine demethylases
Kdm6a	Lysine demethylase 6A
KMT	histone/lysine methyltransferases
lncRNA	long non-coding RNA
M	male
m^6A	RNA N6-methyladenosine
MB	methylene blue
MBP	Myelin basic protein
MD	mean difference
MDS	*MECP2* Duplication Syndrome
me	methyl
MeCP2/*MECP2/ Mecp2*	Methyl CpG Binding Protein 2, protein/human gene/ mouse gene
MeDIP	methylated DNA immunoprecipitation
MEF2A/C	Myocyte enhancer factor 2A/C
MEIS1	Myeloid ecotropic viral integration site 1 homolog
MEM	minimum essential medium
MIA	maternal immune activation
min	minutes

miRNA	microRNA
MRE	miRNA response elements
MTE	motif ten element
N/A	not available
NA	numerical aperture
NAD^+	nicotinamide adenine dinucleotide
NaOH	sodium hydroxide
NCBI	national center for biotechnology information
ncRNAs	non-coding RNAs
NEC	neuroepithelial cells
NER	nuclear extraction reagent
NEUN	NEUronal nuclei
NeuroD1	Neuronal differentiation 1
NGS	normal goat serum
Nhlh2	Nescient helix-loop-helix 2
NLS	nuclear localization signal
NOVA1	NOVA alternative splicing regulator 1
Nrf1	Nuclear respiratory factor 1
NSC	neural stem cells
NSTFs	neuron-specific TFs
NTD	N-terminal domain
O_2	oxygen

OB	olfactory bulb
OCT	optimal cutting temperature compound
OLIG2	Oligodendrocyte lineage transcription factor 2
OPN1LW	Opsin 1, long wave sensitive
Otx1	Orthodenticle homeobox 1
oxBS-seq	oxidative bisulfite sequencing
P	postnatal day
P	P value
PBS	phosphate-buffered saline
PBST	PBS with 0.2% tween20
PCR	polymerase chain reaction
PCV	packed cell volume
PDD-NOS	pervasive developmental disorder not otherwise specified
PDGF	platelet-derived growth factor
PFA	paraformaldehyde
PIC	pre-initiation complex
PolII-S5p	RNA polymerase phosphorylated at Ser 5
PRC2	polycomb repressive complex 2
QK1	Quaking homolog 1
qRT-PCR	quantitative reverse transcription polymerase chain reaction
r	Pearson's correlation coefficient
R	region

RA	retinoic acid
RBPs	RNA binding proteins
RELN	Reelin
REs	regulatory elements
RGC	radial glial cells
rhEGF	recombinant human epidermal growth factor
RNR	ribonucleotide reductase
ROS	reactive oxygen species
RP	reverse PCR primer
rpm	revolutions per minute
RPS4X	Ribosomal protein S4-X-linked
rRNA	ribosomal RNAs
RT	room temperature
RTT	Rett Syndrome
s	seconds
S	Silencer
S100B	S100 calcium-binding protein B
SAM	S-adenosyl methionine
SDS-PAGE	Sodium dodecyl sulfate-polyacrylamide gel electrophoresis
SEM	standard error of mean
SF1	Splicing factor 1
SHANK3	SH3 and multiple ankyrin repeat domains 3

SIG	Significance
SLC16A2	Solute carrier family 16 member 2
snRNAs	small nuclear RNAs
SP	sequencing primer
SP1/4	Specificity protein 1/4
SR	serine-arginine
SRP20/40	Serine and arginine rich splicing factor 3
Sry	Sex-determining region protein gene on the Y chromosome
SSC	saline-sodium citrate
STR	striatum
SVZ	subventricular zone
TAB-seq	Tet-assisted bisulfite sequencing
TAE	tris-acetate-EDTA
TAF1	TATA-Box binding protein associated factor 1
TBP	TATA-box binding protein
TBS	tris-buffered saline
TBST	tris-buffered saline with 0.2% Tween20
TDG	Thymine DNA glycosylase
TEMED	tetraacetylethylenediamine
TET	Ten-eleven translocation
TFs	transcription factors
THAL	thalamus

tr	triton X-100
TRD	transcription repression domain
tRNA	transfer RNAs
TSS	transcription start site
TUB III	TUBULIN III
U	uracil
U2AF	U2 auxiliary factor
UBE1	Ubiquitin-like modifier activating enzyme 1
UTR	untranslated region
vs	versus
VZ	ventricular zone
WB	western blot
XCI	X chromosome inactivation
XCPE1	X core promoter element 1
XCR	X chromosome reactivation
Xi	Inactive X chromosome
Xist	X-inactive specific transcript
YB-1	Y-Box Binding Protein 1
αKG	alpha-ketoglutarate
ω-3 PUFAs	ω-3 polyunsaturated fatty acids

COPYRIGHT PERMISSION

1. Liyanage *et al.* (2013) Molecular Autism

Chapter 3 contains the reprint of my first-authored article from Molecular Autism, published by Biomed Central and Springer. The full citation for the article is below.

> *Liyanage, V. R., Zachariah, R. M., & Rastegar, M. (2013). Decitabine alters the expression of Mecp2 isoforms via dynamic DNA methylation at the Mecp2 regulatory elements in neural stem cells. Mol Autism, 4(1), 46. doi:10.1186/2040-2392-4-46*

The copyright information is as follows as directly quoted from Biomed Central website.

2. Liyanage *et al.* (2015) Experimental Neurology

Chapter 4 contains the reprint of my first-authored article from Experimental Neurology, published by Elsevier. The full citation for the article is below.

Liyanage, V. R., Zachariah, R. M., Davie, J. R., & Rastegar, M. (2015). Ethanol deregulates Mecp2/MeCP2 in differentiating neural stem cells via interplay between 5-methylcytosine and 5-hydroxymethylcytosine at the Mecp2 regulatory elements. Exp Neurol, 265, 102-117. doi:10.1016/j.expneurol.2015.01.006

The copyright license/permission to reuse the article in my thesis is indicated below.

Licensee: Vichithra Batuwita Liyanage

License Date: Aug 21, 2016; License Number: 3933710063004

Publication: Experimental Neurology

3. Figures/tables in the introduction and discussion

3.1 Neuromolecular Medicine

Liyanage VR, Rastegar M (2014) Rett syndrome and MeCP2. Neuromolecular Med 16: 231-264.

Order detail ID:70326369; Order License Id:4064380292924; ISSN:1535-1084

Publication Type: Journal; Publisher: HUMANA PRESS, INC.

3.2 Biology MDPI

Liyanage VR, Jarmasz JS, Murugeshan N, Del Bigio MR, Rastegar M, Davie JR (2014) DNA modifications: function and applications in normal and disease States. Biology (Basel) 3: 670-723.

MDPI copyright policy indicates as follows: "This is an open access article distributed under the Creative Commons Attribution License, which permits unrestricted use, distribution, and reproduction in any medium, provided the original work is properly cited. (CC BY 4.0)."

3.3 Current topics in medicinal chemistry

Liyanage VR, Curtis K, Zachariah RM, Chudley AE, Rastegar M (2017) Overview of the Genetic Basis and Epigenetic Mechanisms that Contribute to FASD Pathobiology. Curr Top Med Chem 17: 808-828.

License number: 4096840308433

3.4 PLoS One

Olson CO, Zachariah RM, Ezeonwuka CD, Liyanage VR, Rastegar M (2014) Brain region-specific expression of MeCP2 isoforms correlates with DNA methylation within Mecp2 regulatory elements. PLoS One 9: e90645.

PLoS One copyright policy indicates as follows: "This is an open-access article distributed under the terms of the Creative Commons Attribution License, which permits unrestricted use, distribution, and reproduction in any medium, provided the original author and source are credited."

THESIS OVERVIEW

This thesis is written in sandwich-type thesis format. An introduction to the subjects included in this thesis, which includes a literature review, rationale, hypothesis and aims of my Ph.D. project can be found in Chapter 1. Detailed methodologies used in the studies are described in Chapter 2. My Ph.D. project has three objectives, each of which is included as a separate results chapter. Chapters 3 and 4 contain results from aims 1 and 2, which have been published in Molecular Autism [Liyanage *et al.* (2013)] and Experimental Neurology [Liyanage *et al.* (2015)], respectively. Chapter 5 is work-in-progress of aim 3, written as a manuscript in progress to comply with the consistency of sandwich thesis type. A general discussion of the findings of Chapters 3-5, representation of the bigger picture, conclusions, future directions and limitations of the study are discussed in Chapter 6.

CHAPTER 1. INTRODUCTION

1.1 Chromatin structure and gene expression

The complex morphology, physiology, and behavior of eukaryotes are regulated by a limited number of genes. Yet, these genes are governed by even further complex transcriptional, co-transcriptional splicing, post-transcriptional, translational and post-translational regulatory mechanisms. Highly structured chromatin dynamics and epigenetic mechanisms are postulated to be involved in these processes [1,2].

1.1.1 Chromatin structure

An organism's genetic information is stored in genomic DNA that is organized into a higher order 'chromatin' structure. Eukaryotic chromatin is composed of nucleosome arrays arranged into 10-nm chromatin fibers that are also called the 'beads on a string' [3,4]. Nucleosomes are the fundamental building blocks and the basic repeating units of chromatin, which are composed of core histone octamer-DNA complexes and are linked to each other by linker DNA. Genomic DNA that is 146 base pairs (bp) long is wrapped around an octamer of histone proteins consisting of dimers of H2A-H2B, and H3-H4 to form a tetramer (reviewed in [5,6]). The linker DNA is more accessible for transcription factors (TFs) binding for gene regulation in contrast to nucleosomal DNA. Therefore, nucleosomes are considered to be negative regulators of transcription [7]. For the same reason, nucleosome-depleted regions are found around transcriptionally active and regulatory regions upstream of the transcription start site (TSS), the genomic location where transcription of a particular gene is initiated [8]. Through the dynamics of the chromatin structure, chromatin governs the regulation of fundamental cellular functions including gene expression regulation and DNA replication [9].

Chapter 1

Chromatin structure is not uniform throughout the genome, and it is highly context-dependent. Depending on the state of chromatin condensation, chromatin can form either euchromatin or heterochromatin. Euchromatin is a state with an 'open chromatin structure' with less chromatin compaction, dispersed nucleosomes, a particular set of histone post-translational modifications (hPTMs) and DNA modifications that render the chromatin more accessible to the transcription machinery. On the other hand, heterochromatin is a more condensed form of chromatin where the presence of nucleosomes, repressive hPTMs, and DNA modifications render the chromatin inaccessible to the transcription machinery. Therefore, heterochromatin is generally associated with transcriptional silencing or repression (reviewed in [5,6]).

1.1.2 Regulatory elements

Specific genomic regions serve as footprints for binding of specific regulatory proteins that are involved in transcription activation, repression, and splicing. These regions are referred to as *cis*-regulatory elements, which are recognized and bound by *trans*-acting factors. Examples of major regulatory elements are a promoter, proximal and distal promoter regions, silencers, enhancers and insulators **(Figure 1.1)** [1].

The core promoter is the region flanking the TSS (denoted as +1) of a gene, which facilitates the recruitment of transcription machinery and other regulatory proteins [10]. It is the minimally essential region for basal transcription initiation. Studies from genome-wide studies suggest that generally, a core promoter may range from 70-150 bp in size [11]. The core promoter contains specific DNA elements onto which specific regulatory proteins are bound. A typical core promoter may contain a TATA-box, initiator element (Inr), TFIIB recognition element (BRE[u], upstream and BRE[d] downstream) and downstream promoter element (DPE) **(Figure 1.1)**. Additionally, a core

2

promoter may contain motif ten elements (MTE), a downstream core element (DCE) and an X core promoter element 1 (XCPE1). The TATA-box is an AT-rich regulatory sequence onto which the TATA-box binding protein (TBP) is recruited to initiate transcription. While some of the eukaryotic gene promoters contain a TATA-box, only a smaller percentage of these gene promoters contain a 'canonical TATA-box' sequence, TATAWAWR (W = A /T, Y = C /T, R = A/G) [12].
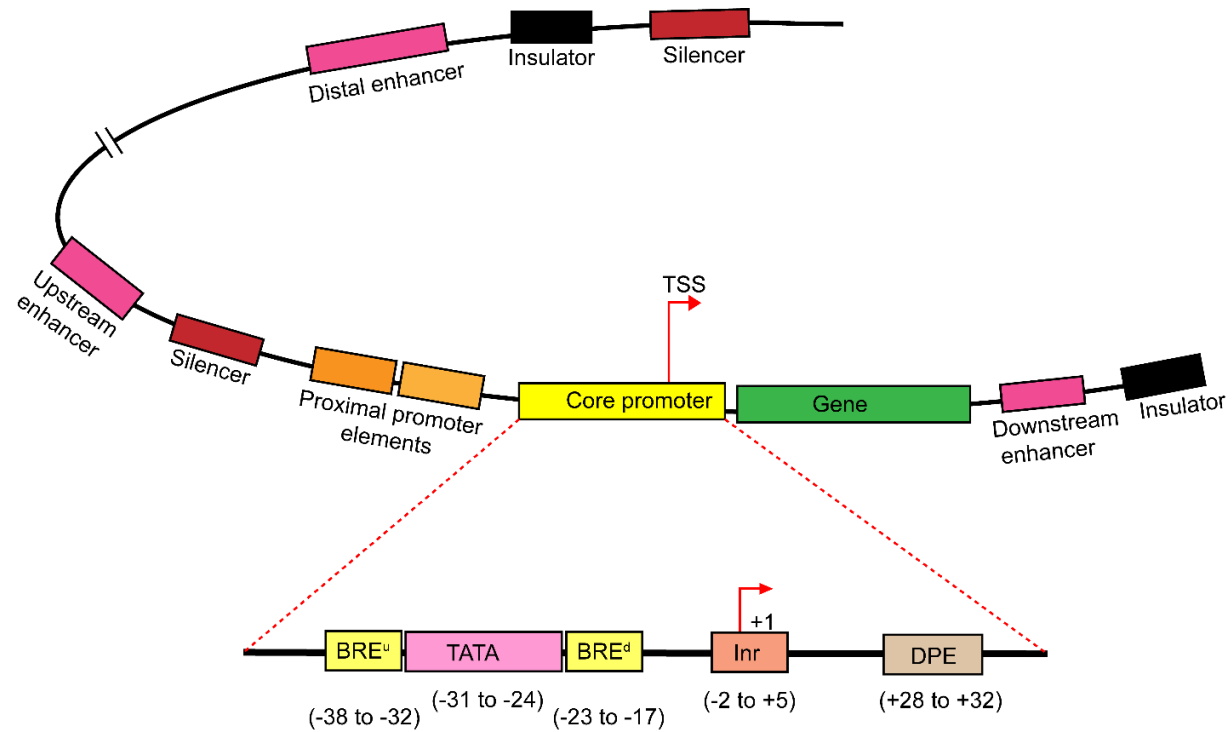
Figure 1.1 Mammalian gene regulatory elements.

The figure illustrates typical regulatory elements of a mammalian gene. There are *cis*-regulatory elements such as promoter regions, silencers, enhancers and insulators that bind *trans*-acting factors to regulate gene expression. The figure also illustrates the core promoter elements, Inr, TATA-box, DPE, BRE[u], and BRE[d]. TSS is marked as +1.

Figure designed based on [2,13,14].

Chapter 1

The Inr is located exactly around the TSS and is considered to be the smallest functional promoter that can initiate the transcription through binding of transcription factor II D (TAF) [15]. Inr is characterized by the consensus sequence YYANWYY where W = A /T, Y = C /T, N = G/A/T/C [16]. In addition to the TATA-box and Inr, the DPE is also capable of recruiting TFIID onto the transcription machinery. The proximal promoter elements are considered as tethering elements that support distal enhancers to interact with the core promoter [17]. Distal promoter elements are located far away (up to several kb) from the core promoter and yet facilitate transcription through interactions with enhancers [18].

The prevalence of these core promoter element varies with the species as well as the genes. **Table 1.1** summarizes the prevalence of these elements in human, mouse and Drosophila. Unfortunately, many of these studies produce highly conflicting results. Nevertheless, these studies suggest that certain core promoter elements are preferably chosen by different species.

Table 1.1 Prevalence or frequency of core promoter elements			
Core promoter element	**Human**	**Mouse**	*Drosophila*
Inr	~50-63%	~45-53%	~67%
TATA	~11-76%	~6-16%	~43%
BRE	~22-25%	~22%	-
DPE	~12-25%	~7-12%	-
References	[12,19-23]	[12,21]	[12,24]

Inr: Initiator; TATA: TATA box; BRE: TFIIB recognition element; DPE: downstream promoter element

Enhancers are distantly located DNA motifs that have the capability to sequester regulatory proteins such as TFs to induce/enhance/upregulate transcription through supporting the formation of the transcription machinery [25]. They can be located both upstream and downstream of the TSS within the same gene, inter or intragenic locations. Therefore, chromatin loop formation and

long-range chromatin interactions are necessary for the function of enhancers [26]. Silencers or silencer elements are negative regulators of transcription [27]. Position-independent silencers are located in proximity and upstream of the TSS and interfere with the assembly of the transcription pre-initiation complex (PIC) *via* the repressor proteins bound to them. In contrast, position-dependent silencer elements interfere with the recruitment of TFs to *cis*-regulatory elements. They can be located both downstream and upstream of TSS [1,27]. Insulators are another type of *cis*-acting regulatory DNA motifs that prevent interactions between promoters and enhancers/silencers to regulate gene expression [1]. If an insulator is located in between an enhancer and a promoter, it is able to interfere with their interaction, and therefore, such insulators are called enhancer-blocking insulators. On the other hand, insulators can also act as barriers, which prevent crawling or advancement of adjacent heterochromatin into gene promoters. Therefore, they are considered as safeguards of promoters. CCCTC binding factor (CTCF) is a regulator that binds to barrier- and enhancer blocking-insulators [28,29].

1.1.3 Alternative splicing

A limited number of eukaryotic genes can be utilized to attain the diversity of physiology and function by generation of multiple protein isoforms from the same gene. This process is achieved by alternative splicing. During the alternative splicing process, some of the exons and introns are spliced out, and different exons are combined to generate different isoforms. There are various mechanisms of alternative splicing [30,31] **(Figure 1.2)**. They include: 1) exon skipping during which an exon from the gene is spliced out; 2) alternative donor site in which another 5'donor site is used; 3) alternative acceptor site in which another 3' acceptor site is used; 4) mutually exclusive exons during which only one of two exons is kept in the spliced mRNA, and

both exons never coexist in one transcript and 5) intron retention, which is a rare splicing mechanism that retains an intron sequence as a coding sequence. The consensus sequences of 5'donor sites and 3'acceptor sites are G-**G**-U-R-A-G-U and (Y-rich)-N-C-A-**G**-G, respectively (splice site is designated by red nucleotide and R = A/G, Y = C /U, N = G/A/U/C). Alternative splicing is carried out by a protein complex called the spliceosome, which is composed of five small nuclear RNAs (snRNAs: U1, U2, U4, U5, and U6) and other splicing proteins such as Splicing factor 1 (SF1), U2 auxiliary factor (U2AF) and serine-arginine (SR) proteins [31]. Recent studies suggest that splicing may co-occur with transcription and is therefore known as 'co-transcriptional splicing.' In this case of transcription and pre-mRNA splicing being coupled, the splicing machinery is recruited onto the nascent RNA that is being transcribed. SR proteins that are involved in splicing interact with the C-terminal domain (CTD) of RNA Pol II to carry out splicing [32]. Moreover, DNA methylation-dependent binding of CTCF regulates the rate of RNA Pol II movement along the nascent mRNA and thereby regulates splicing [33]. Additionally, different isoforms can be generated by utilizing alternative promoters or different TSSs [34]. Transcripts with different polyadenylations are also considered to be different isoforms [35].
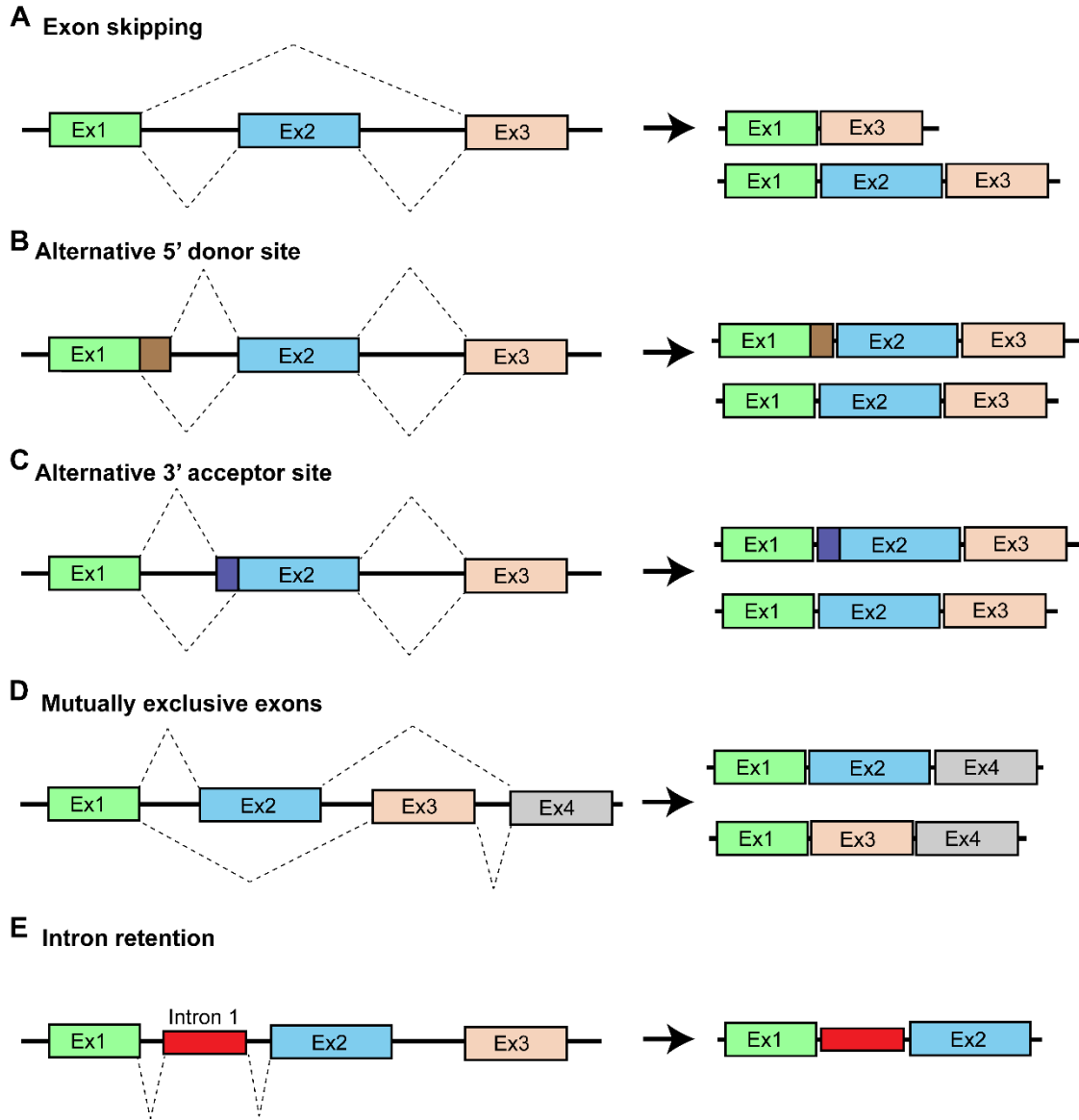
Figure 1.2 Different mechanisms of alternative splicing.

A) Exon skipping, **B)** Alternative 5' donor site, **C)** Alternative 3' acceptor site, **D)** Mutually exclusive exons, and **E)** Intron retention.

1.2 Epigenetic mechanisms in gene expression regulation

Genetics determine heritable changes to gene expression through DNA sequence and can be affected by genomic changes, including mutations, translocations, deletions or insertions. On the other hand, epigenetic mechanisms are defined as heritable changes in gene expression that are not caused by alterations in the underlying genomic DNA sequences, but mechanisms that change how the information is interpreted [5,6]. Such changes that occur on the genomic DNA and histone proteins are DNA methylation and hPTMs, respectively. Non-coding RNAs (ncRNAs), which regulate genes post-transcriptionally, are also part of epigenetic mechanisms. These epigenetic mechanisms determine whether a gene is '*on*' or '*off*' in particular cell types and under different conditions such as exposure to environmental insults.

1.2.1 Histone post-translational modifications

Covalent modifications to the N-terminal tails of histone proteins allow chromatin to adopt two interchangeable states: active/open/euchromatin or inactive/repressive/closed/ heterochromatin. Since the discovery of the first hPTMs by Vincent Allfrey in the 1960s [36,37], a wide range of hPTMs has been identified. The major hPTMs include acetylation, methylation, phosphorylation, ubiquitination, sumoylation, and ADP-ribosylation. These hPTMs generate an epigenetic landscape along gene loci, including promoters, enhancers, silencers and insulator elements [38] **(Table 1.2)**. For example, different lysine (K) moieties on H3 can get epigenetically modified, and their distribution and hence functional significance differ based on the genomic context **(Table 1.2)**. The 'histone code' hypothesis postulates that "PTMs function as a signal platform to recruit effector modules to local chromatin, and it is the effectors/readers that ultimately determine the functional outcome of certain PTMs" [39]. Regardless of the fact that the

Chapter 1

histone code hypothesis has been subjected to many controversies regarding the structural alternatives of chromatin [40], the role of specific hPTMs and their cross-talks with other epigenetic mechanisms such as DNA methylation in transcription can not be undermined [41]. As stated, there are specific proteins or enzymes that bind to specific hPTMs. Examples are bromodomain-, chromodomain, tudor domain- containing proteins, which function upon binding to acetylated and methylated histone tails. They are capable of interacting or cross-talking with other hPTMs and DNA methylation to carry out their major functions as transcriptional regulators [39].

Table 1.2 Examples of the distribution of hPTMs along gene loci																					
Gene loci		hPTMs																			
		H3K4				H3K9				H3K27				H3K20				H3K36			
		ac	me	me2	me3	ac	me	me2	me3	ac	me	me2	me3	ac	me	me2	me3	ac	me	me2	me3
Promoter	Active		✓	✓	✓	✓				✓											
	Inactive						✓				✓		✓								
Enhancer	Active		✓	✓		✓				✓			✓								
	Inactive		✓						✓				✓								

9

Transcription	Start Site			✓												
	Elongation											✓				✓

1.2.2 DNA methylation

DNA methylation at the 5th position of cytosine residues in DNA was first discovered by Rollin Hotchkiss in 1948 [42]. Since then, 5-methylcytosine (5mC) was studied as a major component of DNA and RNA [43-45]. In the early 1980s, the role of DNA methylation in gene regulation and cellular differentiation was determined by inhibition of DNA methylation by 5-azacytidine and 5-aza-2'-deoxycytidine treatments [46].

Writing DNA methylation: The 5mC, or the 'fifth base of DNA', is established by a family of enzymes known as DNA methyltransferases (DNMTs). They transfer methyl groups (-CH₃/me) from methyl donor *S*-adenosyl methionine (SAM) to a cytosine in the context of CpG dinucleotides (**Figure 1.3**). DNMT1 is accountable for the maintenance of DNA methylation during DNA replication [47]. Therefore, the inherited DNA modifications are transferred to the daughter DNA strands from the parental DNA strands during DNA replication. DNMT3A and DNMT3B are *de novo* DNMTs. They carry out DNA methylation and proof-read DNA methylation patterns that are established by DNMT1 during replication, propagating the inherited DNA modifications [48].

Cytosine → 5-methylcytosine (5mC) → 5-hydroxymethylcytosine (5hmC) → 5-formylcytosine (5fC) → 5-carboxycytosine (5CaC)
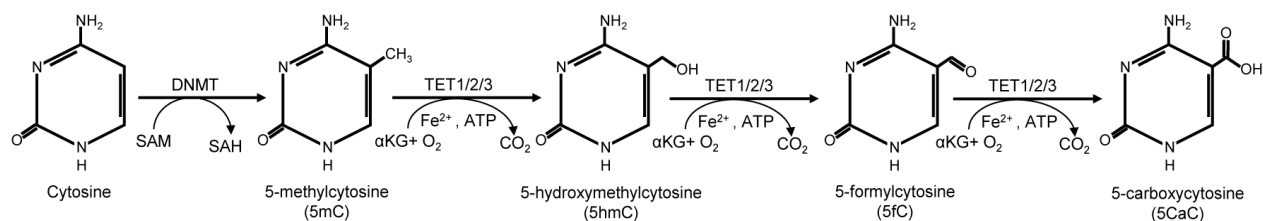
Figure 1.3 Generation of DNA methyl modifications.

Cytosines are converted to 5-methylcytosine (5mC) by DNA methyltransferase (DNMT) enzymes through the transfer of a methyl group from S-adenosyl methionine (SAM). Ten-eleven translocation (TET) enzymes catalyze the oxidation of 5mC to 5-hydroxymethylcytosine (5hmC) through a chemical reaction, which involves alpha-ketoglutarate (αKG), oxygen (O_2), adenosine triphosphate (ATP) and Fe^{2+}. Similar reactions further oxidize 5hmC into 5-formylcytosine (5fC) and 5-carboxycytosine (5CaC).

Figure and figure legend reprinted with permission from [6].

Oxidation of 5mC by TET proteins (TET1-3) generates the 'sixth base' 5hmC, which is considered as active DNA demethylation [49]. Additionally, 5hmC is further oxidized by TET proteins to generate 5CaC and 5fC.

Erasing DNA methylation: Mechanisms of direct conversion of 5mC to an unmodified cytosine or direct demethylation remain elusive [50]. However, the models of active demethylation provide evidence that conversion of 5mC to 5hmC, 5fC, and 5CaC can be considered as active demethylation. These methyl modifications can then be demethylated through the base excision repair (BER) pathway. In this mechanism, 5mC is deaminated to thymine by activation-induced cytidine deaminase (AID) and Apolipoprotein B mRNA editing enzyme catalytic polypeptide 1 (APOBEC1) deaminases. Thymine DNA glycosylase (TDG) is then able to carry out the rest of the BER process to generate unmodified cytosine [47].

Reading DNA methylation: The role of DNA methylation is genomic context-dependent. In other words, the localization of DNA methylation at TSSs, CpG islands, enhancers, promoters and exonic and intronic regions determines whether they play a role in transcriptional repression, activation, alternative splicing or co-transcriptional splicing [6]. Prior to the discovery of alternate forms of DNA modifications, the role of DNA methylation (5mC) was thought to be repressive

when localized at promoter regions [51]. DNA methylation represses transcription through chromatin remodeling and generates a more closed chromatin conformation, which hinders transcription machinery recruitment. DNA methylation can also be read and interpreted by DNA methyl binding proteins such as Methyl CpG Binding Protein 2 (MeCP2) and MBD1-4, which then recruit repressor complexes containing Sin3 and histone deacetylases (HDAC) [52]. However, recent studies show the ability of MeCP2 in binding to 5hmCs as well, which are localized in active chromatin domains [53]. The association of MeCP2 with 5hmC-establishing TET1 adds further evidence to the role of DNA methylation and its readers in transcription activation [54]. However, the association of 5hmC and MeCP2 with repression of Reelin *(RELN)* and Glutamate decarboxylase 1 *(GAD1)* genes in autism [55], raises the question whether additional factors determine the precise role of DNA methylation and its readers.

Non-CpG methylation: For many years, DNA methylation was studied exclusively in the context of CpG dinucleotides. However, emerging evidence from several recent studies suggests that methyl groups can also be added to cytosines upstream to nucleotides other than guanine, and this type of modification is referred to as non-CpG methylation or CpH methylation (H=A, T or C) [56,57]. CpH methylation is highly abundant in neurons, neuronal lineage cells, differentiating cells and during neuronal maturation, mostly associated with transcriptionally active domains [58,59]. Based on *in vitro* studies, both the maintenance DNMT (DNMT1) and *de novo* DNMTs (DNMT3A and DNMT3B) are capable of methylating CpH nucleotides [60,61]. The MBD family member MeCP2 is thought to be the primary reader of CpH methylation in the brain [62].

Methods of DNA methylation detection: Several approaches can be used to detect and quantify DNA methylation. The most basic technique and the gold standard is bisulfite sequencing **(Figure 1.4A)**. Bisulfite treatment can convert unmodified cytosines into uracil (U), while it

cannot convert both 5mC and 5hmC to U. For this reason, this technique is unable to differentially identify and quantify 5mC and 5hmC [63,64]. Oxidative bisulfite sequencing (oxBS-seq) and Tet-assisted bisulfite sequencing (TAB-seq) were identified later as methods that can be used to differentiate not only 5mC and 5hmC but also 5fC and 5CaC [65,66] **(Figure 1.4B)**. Use of 5mC or 5hmC-specific antibodies provides a means of immunoprecipitating 5mC or 5hmC DNA, which are referred to as MeDIP and hMeDIP, respectively [67,68]. Methylated DNA can then be quantified using high throughput sequencing techniques (MeDIP-seq) or by using gene specific-primers in quantitative real-time PCR.
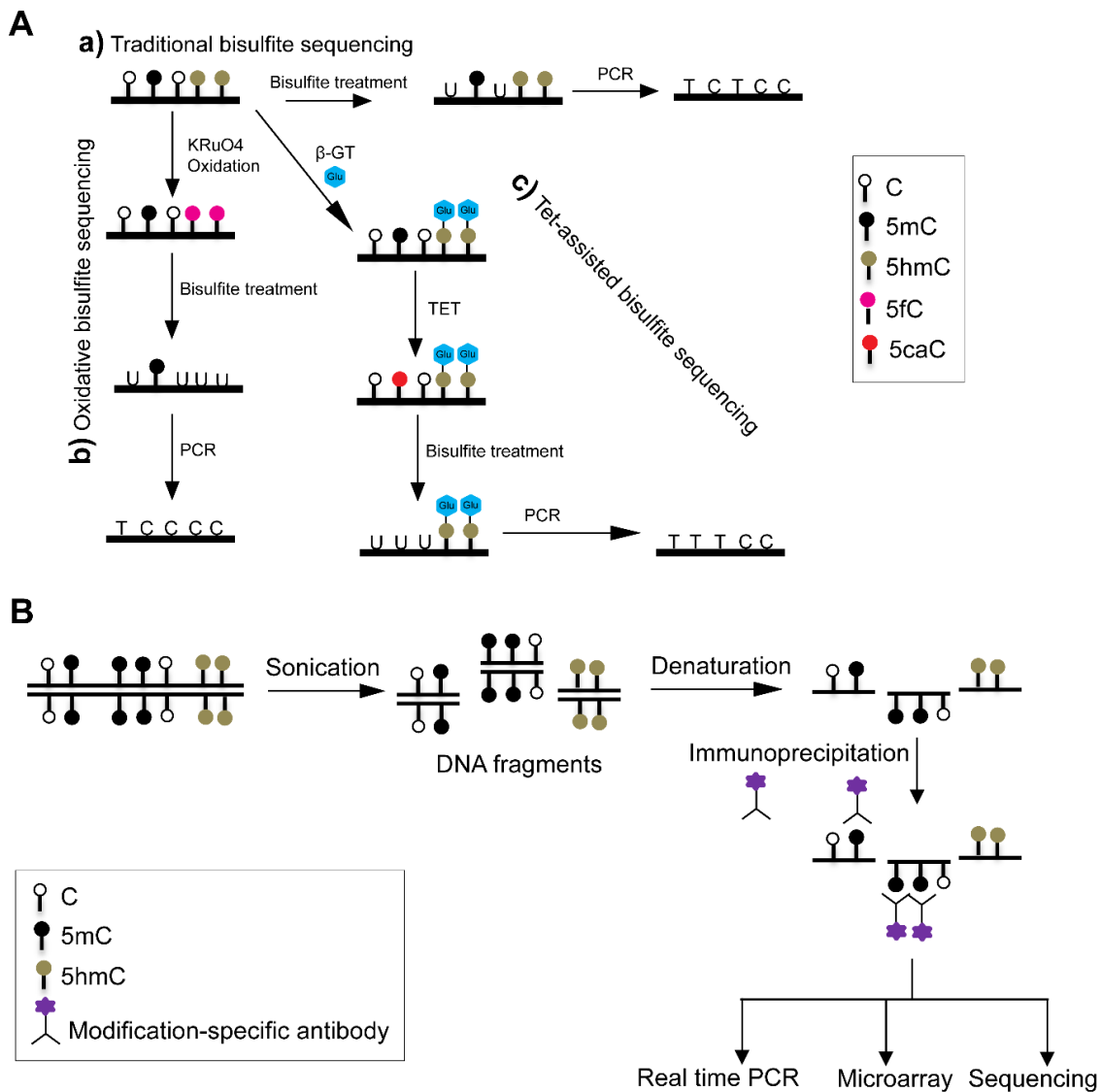
Figure 1.4 Methods of DNA methylation detection and quantification.

A) Bisulfite sequencing: **a**) Traditional bisulfite sequencing, which cannot differentiate 5mC and 5hmC. **b**) oxBS-Seq and **c**) TAB-seq. **B)** Immunoprecipitation of methylated DNA with antibodies specific for 5mC (methylated DNA immunoprecipitation: MeDIP) or 5hmC (hydroxymethylated DNA immunoprecipitation: hMeDIP).

1.2.3 Post-transcriptional regulation by ncRNAs

Post-transcriptional regulation: The physical compartmentalization of transcription and translation in eukaryotes enables an additional layer of gene regulation in the form of post-transcriptional gene regulation [69]. Various forms of post-transcriptional gene regulation include mRNA processing (polyadenylation, capping, and splicing), mRNA export, localization and mRNA decay. Although these events occur through distinct molecular and biochemical mechanisms, they are capable of influencing each other in terms of specificity and efficiency [70]. More recent studies have also unveiled specific mRNA modifications such as RNA *N6*-methyladenosine (m^{6}A), that are capable of modulating post-transcriptional regulatory processes such as mRNA export [71,72].

Role of non-coding RNAs: RNAs that are not translated into a protein product, yet acts as an independent functional entity are known as ncRNAs [73]. The major examples of ncRNAs are microRNA (miRNA), long non-coding RNA (lncRNA), ribosomal RNAs (rRNA), transfer RNAs (tRNA*)*, enhancer RNAs (eRNAs) and circular RNAs (circRNAs). Among these ncRNAs, miRNA and lncRNA are extensively studied as epigenetic regulators in the brain [74]. MiRNAs are short (22 nucleotides) that are involved in post-transcriptional regulation. A review by Cech and Steitz defines miRNA as "RNA that, in complex with AGO protein, uses seed sequences near its 5′ end

to base pair with a target mRNA to induce deadenylation and decay or translational regulation"
[75]. Thereby, miRNAs determine how their target mRNAs are post-transcriptionally regulated
through translation repression followed by mRNA decay [76]. LncRNAs, on the other hand, are
>200 nucleotides long, and were previously thought to be transcriptional noise. Moreover, they
have many diverse functions compared to miRNAs. Some of the lncRNAs that are considered to
be 'macro' in size, such as *Airn,* a lncRNA involved in imprinting by induction of the imprinted
gene Insulin-like growth factor 2 receptor (*Igf2r*) [77] and is postulated to be doing so through
dueling polymerases [75]. LncRNAs use their capacity to base pair with another transcript to
reduce the target mRNAs' functional significance. *Xist* is another well-known lncRNA that plays
a significant role in X-chromosome inactivation [78]. Additionally, lncRNAs can interact with
proteins to promote the functions of the interacting proteins. For example, the recruitment of
H3K27 methyltransferase PRC2 onto genomic regions by *HOTAIR* lncRNA [79], and to act as a
decoy to repress functions such as when B2 RNA inhibits transcription upon heat shock by binding
to RNA Pol II [80]. Enhancer RNAs are ncRNAs that are transcribed from enhancer regions and
known to play a role in contributing to the functions of its enhancer through recruitment of other
regulatory proteins [81]. The precise role of eRNAs is still highly debated. CircRNAs are
generated during RNA processing reactions such as splicing by ligation of 5′ and 3′ ends of linear
RNAs. They function as intermediates during RNA processing, templates for viroids and miRNA
regulation [82].

1.2.4 Epigenetic modifiers

Dynamics of epigenetic modifications and subsequent chromatin structure changes govern the regulation of transcription activation, repression, splicing, DNA damage repair and DNA replication. These functions are carried out with the aid of epigenetic regulatory proteins, which are generally referred to as 'epigenetic modifiers' and are of three kinds based on their functions. These are epigenetic writers, readers, and erasers (**Figure 1.5**).
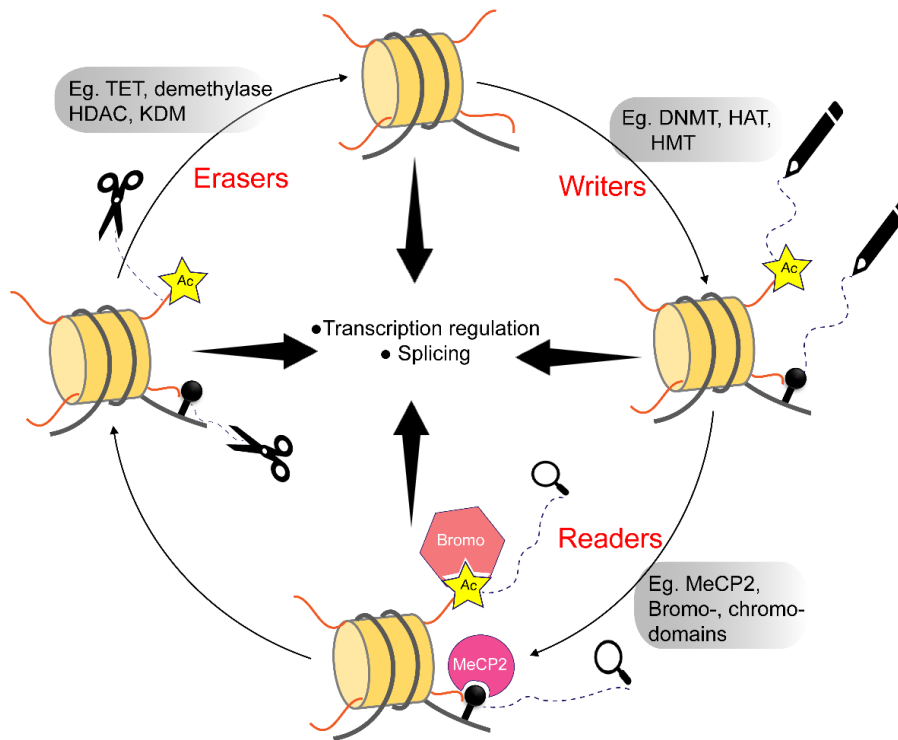
Figure 1.5 Epigenetic modifiers involved in gene expression regulation

Gene regulation by epigenetic modifiers is a dynamic process. The 'writers' such as DNMTs, histone/lysine acetyltransferases (KAT) and histone/lysine methyltransferases (KMT) establish DNA methylation, histone acetylation, and histone methylation, respectively. Epigenetic modifications are read by 'readers' such as MeCP2, which reads DNA methyl marks, and bromo- and chromo-domain containing proteins, which read acetylated and methylated histones. Once their function in gene regulation, splicing or DNA replication are completed, 'erasers' such as DNA demethylases, HDAC, and lysine demethylases (KDM) remove these modifications.

Writers: These are the proteins that establish or lay down epigenetic modifications onto DNA and histone proteins. For instance, 5mC methylation is carried out by DNMTs, which is subsequently converted to 5hmC by TET proteins. The addition of modifications on to histone tails is done by writers such as KAT [add acetyl (ac) groups] and KMT [add methyl (CH_3)-groups] [83].

Readers: DNA and histone modifications written by writers are then recognized and read by 'readers'. One of the major epigenetic readers is MeCP2, which has the capability to recognize both 5mC and 5hmC and carry out transcriptional repression or activation [53,84]. Readers of hPTMs have bromodomains to recognize and bind to acetylated histone and/or chromodomains to bind to methylated histones. Many of the KAT enzymes have bromodomains, which enable them to write and read the histone code [85]. Similarly, histone methylases such as SET proteins use their SET domain to add CH_3 groups which are then recognized and read by chromodomains [85].

Erasers: The modifiers that remove the DNA and histone modifications are 'erasers.' Erasers of DNA methylation can be of two kinds depending on how DNA demethylation is defined. First, DNA demethylases can convert 5mC back to an unmodified C. Secondly, the conversion of 5mC to subsequently reduced forms are considered as active DNA demethylation, which is carried out by TET proteins [6]. HDAC and KDM remove ac and CH_3 groups, respectively [83].

These modifiers can also be targeted using inhibitors that interfere with their functions/activity or expression and thereby regulate gene expression. For instance, DNA demethylating agents such as 5-azacytidine and 5-aza-2´deoxycytidine (decitabine) can inhibit DNMT activity and/or reduce their expression [86].

1.3 MeCP2

1.3.1 MeCP2 as a multifunctional epigenetic modulator in the brain

Functional domains of MeCP2: MeCP2 is known as a key epigenetic regulator of the brain due to its multifunctional role in brain cell types [87]. This multifunctionality is governed by different domains of the protein that allow interactions with DNA or specific regulatory protein complexes [88]. MeCP2 belongs to a family of proteins that employ a methyl binding domain (MBD) to recognize and bind to methylated CpGs and thus function as a 'methyl reader' **(Figure 1.6A)** [89,90]. Members of this protein family include MeCP2, MBD1, MBD2, MBD3, and MBD4, among which, MBD3 is incapable of binding to methylated DNA due to two extra amino acids within its MBD [91]. MeCP2 protein has five major functional domains, the N-terminal domain (NTD), MBD, inter-domain (ID), transcription repression domain (TRD) and CTD (**Figure 1.6B**). There are two MeCP2 isoforms MeCP2E1 and MeCP2E2, which differ only at the N-terminal sequence, and they will be discussed in more detail in the next section.
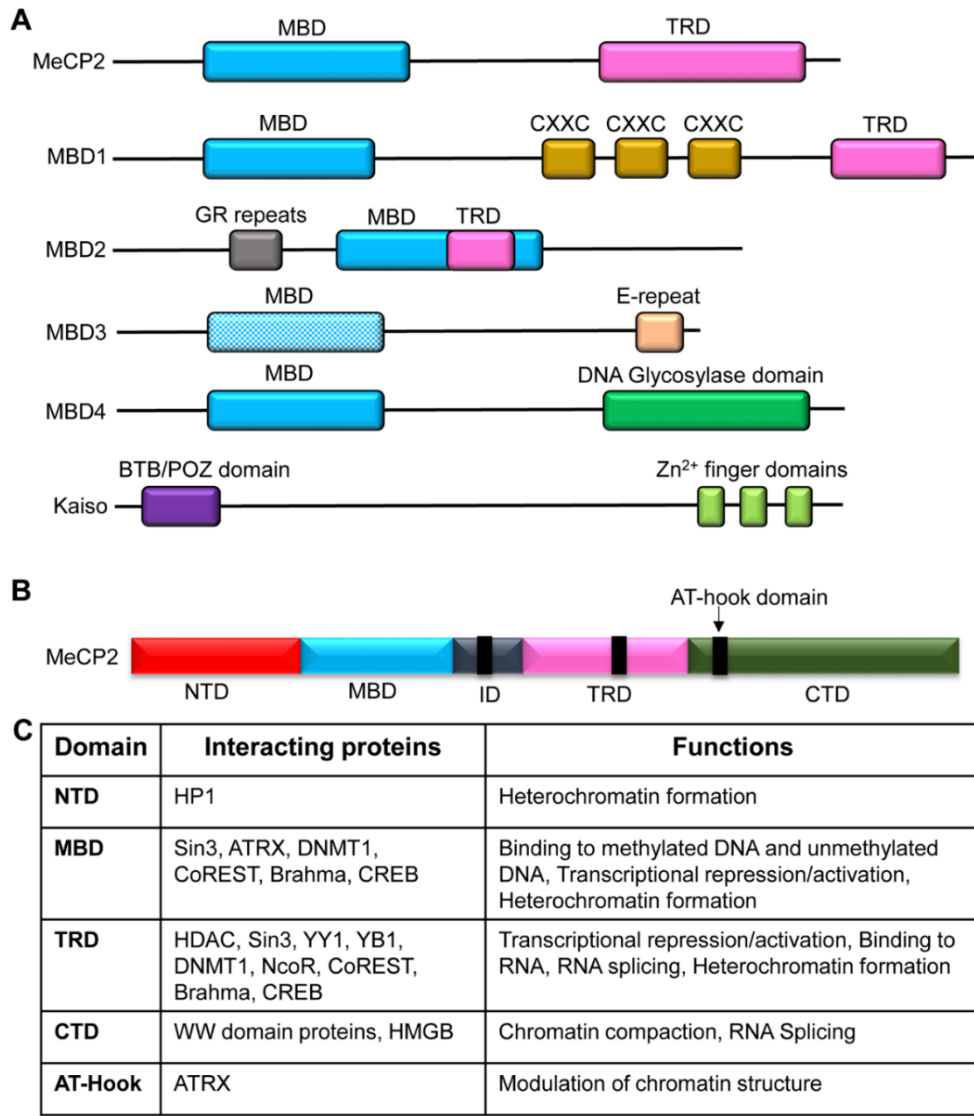
Figure 1.6 The structure of the methyl-CpG-binding protein (MBP) family.

A) Comparison of the structure of MBPs. The MBP family shares the characteristic methyl-CpG-binding domain (MBD), which enables the recognition of and binding to methylated DNA. However, MBD3 is unable to bind to methylated DNA. The transcription repression domain (TRD) is found in MeCP2 and MBD1-2. Apart from the MBD, the binding of specific MBDs to DNA can be mediated through CXXC zinc-finger (Zn^{2+}) motifs, glycine and arginine residues (GR), and thymine glycosylase. The Kaiso family of proteins is characterized by a BTB/POZ domain and a triple zinc-finger domain. **B**) Domains of MeCP2. Apart from the characteristic MBD, there are other domains which are important in protein interactions and functions.

Abbreviations: NTD: N-terminal domain; MBD: Methyl-CpG-binding domain; TRD: Transcription repression domain; ID: interdomain; CTD: C-terminal domain; AT-hook: Adenine-thymine (AT)-rich DNA binding domain. **C**) Interacting protein partners and functions of MeCP2. HP1: Heterochromatin Protein 1; ATRX: ATP-dependent helicase ATRX; DNMT1: DNA methyltransferase 1; HDAC: Histone deacetylase; CREB: cAMP response element-binding protein; HMGB: High-mobility group box.

Figure and figure legend reprinted with permission from [6].

While the overall protein structure of MeCP2 is essential for its multifunctional behavior, two major domains are essential for its most critical functions. They are MBD and TRD, which recruit MeCP2 onto methylated DNA and interact with protein partners to mediate transcriptional regulation, respectively. Upon binding to methylated DNA, MeCP2 may act as transcriptional repressor, activator, chromatin architectural protein or splicing regulator (reviewed in [88,92]). The other domains seem to aid MeCP2 to maintain interactions with chromatin and proteins to regulate the formation of heterochromatin as a chromatin architectural protein and RNA splicing. Therefore, interacting protein partners play a critical role in defining MeCP2 functions. Some examples of the interacting proteins or DNA interactions with MeCP2 domains and their associated functions are listed in **Figure 1.6C**. When the overall protein structure of MeCP2 is considered, MeCP2 is rather a highly unstructured protein (60%) making it an intrinsically disordered protein [93]. The structured component (40%) of the MeCP2 protein is composed of 21% β-sheets, 4% α-helices and 13% β-turns, which are the basic secondary structures of protein.

Functions of MeCP2: In the brain, MeCP2 regulates a plethora of functions and processes, which include brain development [94-98], neuronal differentiation [99,100], neuronal maturation [101-103], neuronal morphology [104-109] and protein synthesis [110,111]. Initially, MeCP2 was considered to function solely as a transcriptional regulator. However, its functions and associations

with a wide range of genomic locations suggested a rather global epigenetic regulator [112]. Evidence suggests that MeCP2 has a role beyond a conventional transcriptional regulator. It functions not only by binding to proximal promoter elements (which are mostly located approximately 250 bp upstream of theTSS) but also by mediating long-range chromatin interactions [113]. This concept was further supported by MeCP2 binding to CpH methylation in the central nervous system [57]. As a chromatin architectural protein, the influence of MeCP2 binding to either methylated or unmethylated DNA on chromatin structure is significant [5,114,115]. MeCP2 is capable of mediating long-range chromatin interactions through bridge or loop formation [116-118]. In neurons, astrocytes and other brain cell types, both MeCP2 isoforms are localized to the DAPI-counterstained heterochromatin regions, which are usually referred to as chromocenters in mouse cells [119-121]. For this reason, disrupted high-order chromatin structures have been observed in cells with Rett Syndrome (RTT)-causing *MECP2* mutations [122-124]. Increased chromocenter clustering has been observed upon MeCP2 overexpression [125]. Recruitment of MeCP2 to the exons of specific genes has been shown to regulate their splicing [126]. Altered splicing of multiple genes has also been observed in an RTT mouse model [127]. MeCP2 also plays a role in miRNA expression and processing either by binding to the promoters of miRNA genes [128] or through binding to the DGCR8/Drosha Complex, which is an important component of the miRNA processing pathway [129]. In agreement, with these findings, altered levels of miRNAs have been observed in RTT mouse models [130,131]. Collectively, the level of MeCP2 protein is important as it functions as a global regulator and thus any change in overall MeCP2 levels may make significant changes to gene regulation, chromatin architecture, nuclear structure and cellular morphology.

Chapter 1

1.3.2 Gene and protein structure of MECP2/Mecp2/MeCP2

MECP2 and *Mecp2* genes are found in the long arm of the X-chromosome (Xq28) and XqA7.3, respectively. *MECP2* is ~76 kb in size and is flanked by *IRAK1* and *OPN1LW* (also known as *RCP*) while *Mecp2* is ~60 kb in size and flanked by the same genes **(Figure 1.7A)**. The *Mecp2*/*MECP2* gene has four exons, three introns, and a 3' untranslated region (UTR) that are different based on how it is polyadenylated or depending on the isoform **(Figure 1.7B-C)**. As stated earlier, there are two *MECP2/Mecp2* isoforms that are generated by alternative splicing, MeCP2E1 (MeCP2B/α) and MeCP2E2 (MeCP2A/β), which are illustrated in **Figure 1.7C-D** [132,133]. *MECP2E1/Mecp2e1* is composed of exon 1, 3, and 4, and skips the exon 2. Using the translation start site (ATG) in exon 1, MeCP2E1 is generated. In contrast, *MECP2E2/Mecp2e2* may have exons 1-4 or exons 2-4. It uses an ATG within exon 2 to generate MeCP2E2 protein with exons 2-4. Studies conducted in mouse embryonic day (E) 14 brain cortex have shown that the two isoforms may be utilizing the same TSS within the 5'UTR of the exon 1, while *Mecp2e2* may also use a TSS within exon 2 5'UTR [134]. MeCP2 isoforms differ in their N-terminal sequence where MeCP2E1 and MeCP2E2 have 21 (MAAAAAAAPSGGGGGGEEERL) and 9 (MVAGMLGLR) unique amino acids, respectively (**Figure 1.7D)**.
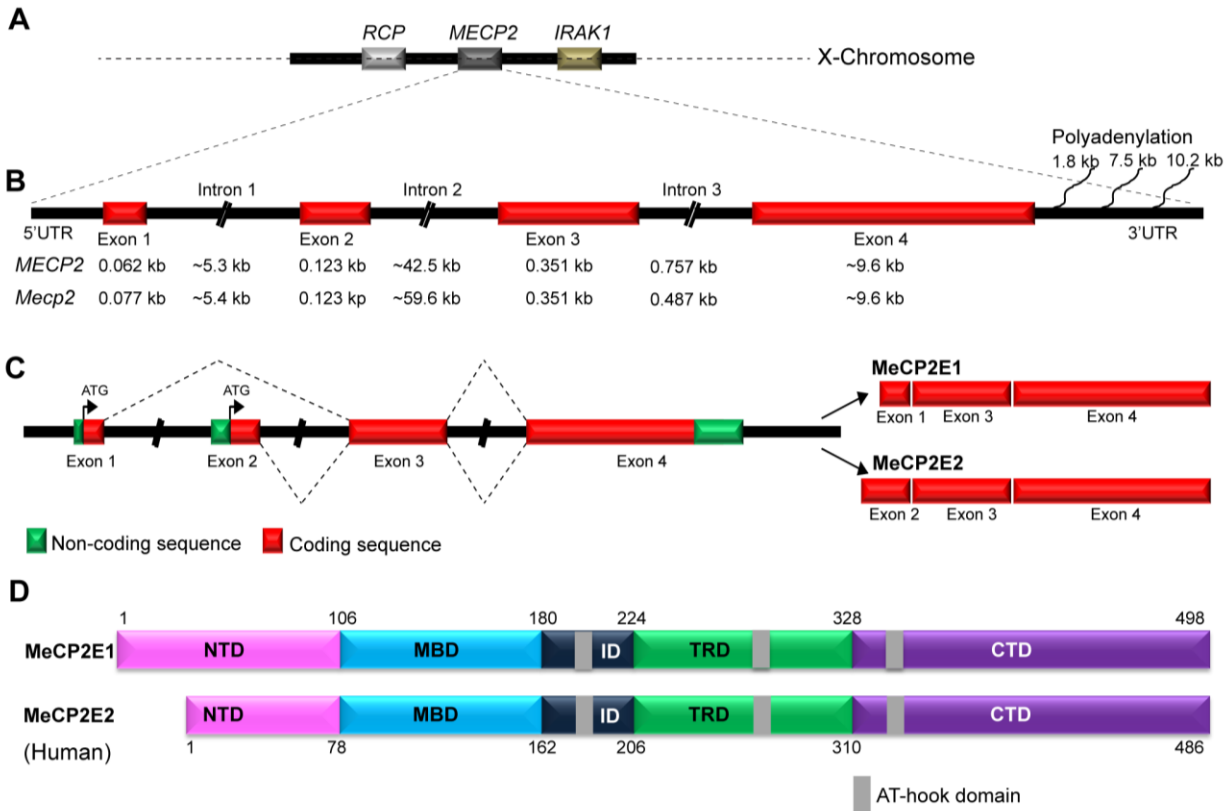
Figure 1.7 The structure of the *MECP2/Mecp2* gene and MeCP2 protein.

A) The *MECP2/Mecp2* gene is located on the X chromosome (Xq28), flanked by the *RCP* and *IRAK* genes. **B)** The schematic of the *MECP2/Mecp2* gene showing that it is composed of four exons (exon 1-4) and three introns (intron 1-3). The gene has three polyadenylation sites in the 3'UTR. The sizes of each exonic and intronic region in human *MECP2* and mouse *Mecp2* genes are indicated. **C)** The generation of two MeCP2 isoforms; MeCP2E1 and MeCP2E2. The translation start site (ATG) for each isoform is indicated by arrows. The MeCP2E1 isoform is encoded by exons 1, 3 and 4. The MeCP2E2 isoform is encoded by exons 2, 3 and 4. Red: coding sequence. Green: non-coding sequence. **D)** Protein domains of human MeCP2E1 and MeCP2E2. The human MeCP2E1 and MeCP2E2 are 498 and 486 amino acids in size, respectively. In contrast, the mouse MeCP2E1 and MeCP2E2 are 501 and 484 amino acids in size, respectively. MBD: methyl-CpG-binding domain, ID: Inter domain, TRD: transcriptional repression domain, CTD: C-terminal domain, NTD: N-terminal domain, AT-hook: A domain found within the TRD, which allows binding to adenine-thymine (AT) rich DNA.

Figure and figure legend adapted/reprinted with permission from [88].

1.3.3 Expression of MeCP2 in mammalian brain and brain cell types

MeCP2 is a ubiquitously expressed protein with higher abundance in the brain [135]. MeCP2 expression and functions in the brain are extensively investigated due to neurological phenotypes seen in MeCP2-associated neurological disorders, mainly RTT and *MECP2* Duplication Syndrome (MDS) [136]. However, these patients also display phenotypes outside the central nervous system such as cardiac issues and respiratory abnormalities, implicating a role for MeCP2 outside the central nervous system [137-141]. In the brain, we have reported MeCP2 localization in the nucleus, mainly at chromocenters with a punctate detection pattern [119,120]. However, several other studies have observed cytoplasmic [142] as well as diffuse MeCP2 detection [143].

Brain region-specific Mecp2/MeCP2 expression: The significance of properly regulated brain region-specific expression of MeCP2 was suggested by many studies conducted in relation to RTT, which is caused by loss of MeCP2. In an RTT mouse model, the levels of MeCP2 in mouse brain regions correlated with the severity of behavioral impairments [144]. Mouse models, which lack MeCP2 or have *MECP2* mutations in specific brain regions, have displayed distinct phenotypes. For instance, the loss of MeCP2 in forebrain neurons lead to autistic features and anxiety [145-147], in contrast to the impaired fear-learning observed by mice lacking MeCP2 in basolateral amygdala [148,149]. Our lab has reported that MeCP2E1 is the major protein isoform in the mouse brain [119,120]. By transcript analysis, a previous study also showed that *Mecp2e2* is the minor isoform in newborn (P1), juvenile (P21) and adult (P60) mouse brain [150]. Among olfactory bulb, cortex, striatum, hippocampus, thalamus, cerebellum and brain stem, *Mecp2e1*/MeCP2E1 expression was relatively even [119]. However, in the same brain regions, *Mecp2e2*/MeCP2E2 levels were different. Another study showed 12-fold higher *MECP2E1* levels than *MECP2E2* in

the whole brain and 9-fold higher *MECP2E1* in the cerebellum in contrast to *MECP2E2* levels [132].

MeCP2 expression during neurodifferentiation: Mouse neurogenesis starts around E10. At E10.5, trace MeCP2 levels have been found in the marginal zone. By E14.5, MeCP2 detection spreads to the marginal zone, deep cortical layers, thalamus, caudate putamen, pons, medulla, and cerebellum. At E18.5 when neurogenesis is almost concluded, MeCP2 expression is detected in almost all brain regions [143]. This expression increment of MeCP2 also correlates with brain maturation in both human and mouse brain [143]. Studies conducted before 2009 have reported that MeCP2 expression increases during neuronal differentiation, but is absent in differentiated astroglia or oligodendrocytes [101]. The same study showed that MeCP2 is detected in neural precursor cells, yet does not play a role in cell fate commitment during neuronal differentiation [101]. A recent study using neural differentiation of mesenchymal stem cells from healthy individuals and RTT patients demonstrated that MeCP2 is detected throughout differentiation and that the lack of MeCP2 leads to perturbation of cell fate commitment [151]. Moreover, MeCP2 expression in the brain is preferentially higher in neurons and increases during neuronal maturation [101,143]. Collectively, it is possible that the expression of *Mecp2/MECP2*/MeCP2 is tightly regulated during neurodifferentiation and neuronal maturation.

Cell type-specific expression of MECP2/Mecp2/MeCP2: Until 2009, the accepted belief in the MeCP2 field was that MeCP2 is absent in glial cells in the brain. Later on, several groups demonstrated the detection of MeCP2 in glia, albeit at lower levels in contrast to neurons [104,107,119-121]. Studies from our lab also show that MeCP2E1 level in astrocytes is five times less than in neurons [120]. In neurons, astrocytes, and oligodendrocytes of the adult mouse hippocampus, both MeCP2E1 and MeCP2E2 are primarily localized to the heterochromatin

regions (chromocenters) of the nucleus [119,120]. The expression of MeCP2 is also known to act in a non-cell autonomous fashion. For instance, *MECP2*-deficiency in RTT glial cells cause aberrations in neuronal morphology and neuronal functions [152,153]. The significance of MeCP2 expression in neurons and glia (both astrocytes and oligodendrocytes) have been further validated by the rescue the RTT-like phenotypes by re-expression MeCP2 in these cell types [107,154-156]. However, mechanisms by which this differential cell type-specific *Mecp2*/MeCP2 expression is driven are currently unknown.

1.3.4 Known regulatory mechanisms of MeCP2

A handful of regulatory mechanisms of *MECP2/Mecp2*/MeCP2 expression at the transcript and protein levels have been reported in the literature. A summary of these mechanisms is illustrated in **Figure 1.8**. Unfortunately, the regulatory mechanisms of *MECP2/Mecp2*/MeCP2 isoform-specific expression are largely unknown as most of the studies are limited to total MeCP2 without differentiating between the two isoforms.
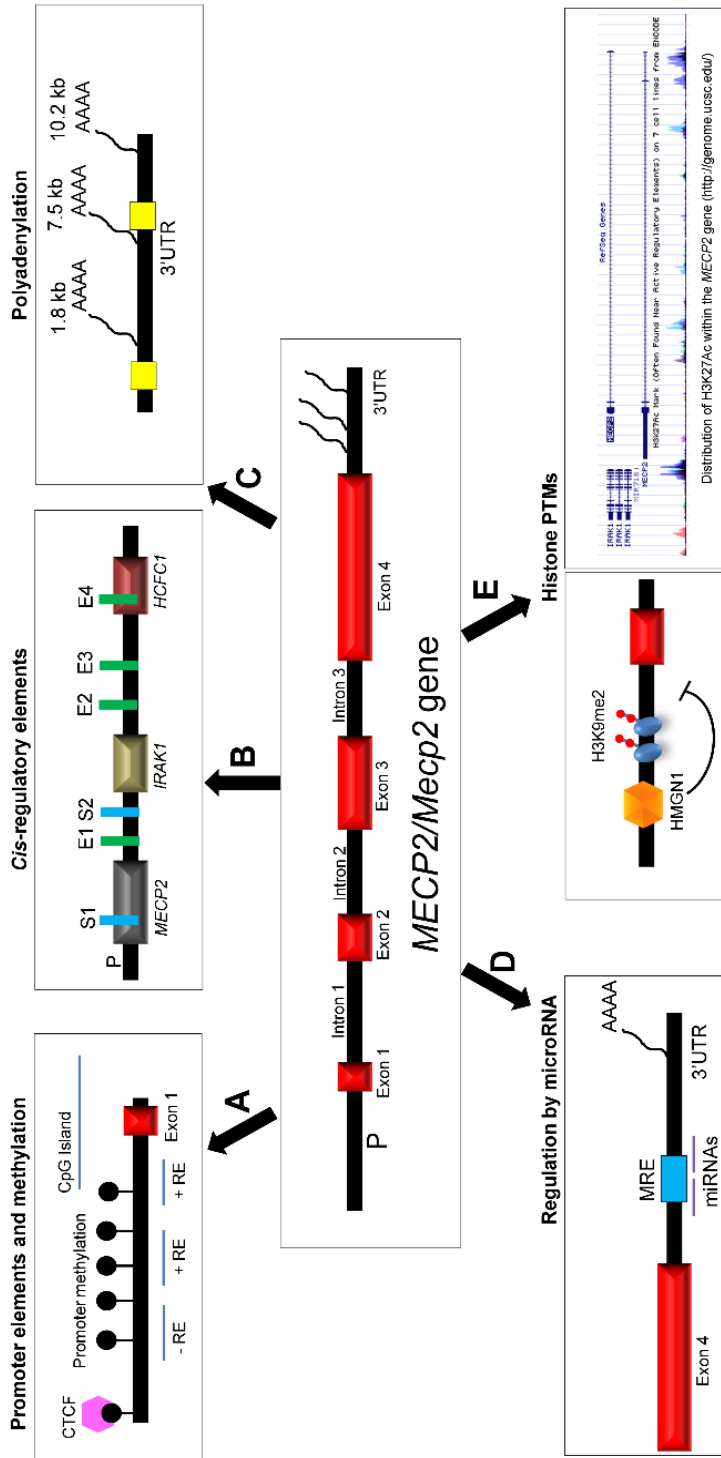
Figure 1.8 Known regulatory mechanisms of *MECP2/Mecp2* gene.

The *MECP2/Mecp2* gene is regulated transcriptionally and post-transcriptionally by multiple mechanisms. **A)** The *MECP2* promoter contains positive and negative regulatory elements (+RE

and -RE), which are known to regulate *MECP2* expression. Both *MECP2/Mecp2* genes harbor CpG islands and several CpG dinucleotides regulated by DNA methylation. **B)** *Cis*-regulatory elements are found in intragenic regions of the *MECP2* gene as well as intragenic regions. There are two silencer elements (S1-S2) and four enhancer elements (E1-E4). P: Promoter. **C)** the *MECP2/Mecp2* 3'UTR contains polyadenylation sites and *cis*-acting elements (yellow boxes), which harbor binding sites for *trans*-acting factors involved in polyadenylation. Three transcript variants are generated by polyadenylation (1.8, 7.5 and 10.2 kb). **D)** Binding of miRNAs to miRNA response elements (MRE) at the 3'UTR involves post-transcriptional regulation of *MECP2/Mecp2*. **E)** Changes in histone modification in response to binding of regulatory proteins regulate *Mecp2/MECP2* expression. For example, binding of HMGN1 induces modifications in histones and thereby changes the chromatin structure. There is a differential enrichment of hPTMs across the *MECP2/Mecp2* gene. As an example, the distribution of active histone marks H3K9ac and H3K27ac across the *MECP2* gene in three cell types (HeLa, HepG2, and HUVEC) is shown (data extracted from http://genome.ucsc.edu/; February 2009 assembly).

Figure and figure legend adapted/reprinted with minor modification with permission from [88].

Promoter methylation: Promoters of the mouse and human *MECP2/Mecp2* genes are epigenetically regulated by promoter DNA methylation **(Figure 1.8A)** [157,158]. The first evidence that the *MECP2* promoter is regulated by DNA methylation was shown by Nagarajan *et al.* (2006) in a male autistic patient [157]. A section of the *MECP2* promoter (-531 to -243) was hypermethylated in the cerebral cortex of male autistic patients in contrast to age-matched controls. The *MECP2* promoter hypermethylation negatively correlated with the repressed *MECP2* expression in autistic brain. In 2008, they further analyzed the -700 to -509 region of the *MECP2* promoter, which was hypermethylated in the autistic brain, in association with the loss of CTCF binding [159]. CTCF is an insulator protein and an epigenetic regulator of gene expression and splicing upon recruitment to its binding sites in a DNA methylation-dependent manner [6,160]. Their hypothesis was that loss of CTCF binding to the upstream *MECP2* promoter allows the

nearby heterochromatin to be crawled (advanced) into the promoter and thereby increases *MECP2* promoter methylation. In 2010, another research group demonstrated that alterations in *Mecp2* promoter methylation caused by early stress due to maternal separation are inherited and thus transmitted as transgenerational epigenetic inheritance [158]. Increased *Mecp2* promoter methylation (1 to -164 region) was observed in sperm of F1-pups exposed to maternal separation, and F2-pups' brains reflected similar *Mecp2* hypermethylation in association with reduced *Mecp2* expression.

Regulatory elements (REs): Previous studies on the *MECP2/Mecp2* promoter have been done by Liu and Franke (2006), Singh *et al.* (2008) and Adachi *et al.* (2005) [90,134,161]. They report that the *MECP2* core promoter, which is located at -179 to -309, is able to drive *MECP2* expression in SK-N-SH, HT1080, CRL1718 and HeLa cells. They also identified three upstream REs, which showed cell type-specific activity **(Figure 1.8A)**. A negative RE or a silencer element was detected at -309 and -370, which functions predominantly in an astrocytoma CRL1718 cell line. Another weak negative RE (-553 and -681) was found to be active mainly in neuronal SK-N-SH cells and fibrosarcoma HT1080 cells. A positive RE or an enhancer (-847 to -1071) was found to be universally active. The core *MECP2* promoter contains binding sites for RNA Pol II, TAP1, SP1/SP3, C/EBP, E2F1 and CTCF [90,161]. In studies conducted in mouse cell types, an essential core promoter region (-677/-56) was found to be sufficient to drive *Mecp2* expression in neurons but not glia [134], suggesting at least three possibilities; 1) this promoter region may not contain all or part of the REs that are required for *Mecp2* expression in glia, 2) TFs that drive *Mecp2* expression in glia and neurons may be different, and 3) while the *Mecp2* promoter sequence is the same in both cell types, the role of epigenetic mechanisms such as DNA methylation may extend beyond the sequence of the *Mecp2* promoter. In other words, epigenetic mechanisms may play a

role in differential *Mecp2* expression in different cell types. Moreover, binding of TFs including SP1 to this essential *Mecp2* promoter segment was detected in mouse brain cortex, striatum, cerebellum and brain stem [134].

Liu and Franke also discovered six *cis*-REs; four enhancers (E1-E4) and two silencers (S1-S2) that regulate *MECP2* expression **(Figure 1.8B)** [161]. The enhancers were localized as follows, E1: *MECP2* 3'UTR, E2-E3: intergenic region between *IRAK1* and *CXorf12* and E3: within *HCFC1*. The role of these enhancers on *MECP2* regulation has not been studied since then. The two silencer elements are located within the *Mecp2* intron 1 (S1) and the 3'UTR (S2). Reporter assays suggested that the S1 silencer element may act as an alternative promoter in non-neuronal cells [161]. DNA methylation at this silencer element will be one of the focuses of my thesis.

MECP2/Mecp2 TSSs: Both the human and mouse *MECP2/Mecp2* promoters are broad promoters with multiple TSSs, which were not allocated to specific isoforms [162]. The analysis of mouse *Mecp2* TSSs in E14 mouse cortex illustrated that *Mecp2* has a promoter with dispersed TSSs, yet the majority of the TSSs were localized to a site 47 nucleotides upstream of exon 1 [134]. This major TSS was common for both *Mecp2* isoforms. Some TSSs for *Mecp2e2* were found within the 5'UTR of exon 2 suggesting the possibility of alternative promoters.

Polyadenylation of MECP2/Mecp2: Multiple polyadenylation sites have been discovered in the 3'UTR of *MECP2*/*Mecp2*, which generate transcripts of varying length (~1.8, ~5.4, ~7.5, and ~10.2 kb) **(Figure 1.8C)**. Based on observations from previous studies, the expression of these transcripts appears to be tissue-specific. For instance, the 10.2 kb transcript has been observed predominantly in the brain whereas a shorter transcript of ~8.5 kb was found in the lymphoid system and muscle [163,164]. Moreover, short- and long-length polyadenylated *Mecp2* transcripts have been shown to have similar stability, despite their tissue-specific expression [165]. The longer polyadenylated

transcript harbors many putative miRNA-binding sites, including the miRNAs that downregulate MeCP2 protein levels such as *miR132/212* [166-168]. In contrast, short *Mecp2* polyadenylated transcripts are associated with increased protein expression [169,170]. Several putative *cis*-acting factors (CstF binding site, G-rich element, and upstream sequence elements) and a *trans*-acting factor (hnRNPF) have been shown to regulate *MECP2*/*Mecp2* polyadenylation [171]. Indirect observations by two independent studies suggest that *MECP2E1*/*Mecp2e1* might be associated with the longer polyadenylated 3'UTR [172]. Moreover, *Mecp2e2* was associated with the 1.8-kb transcript and the less abundant 5.4-kb transcript [150]. Therefore, cell type, species, and isoforms are potential factors that determine the length of the polyadenylated 3'UTR associated with individual *MECP2/Mecp2* isoforms [172].

Mecp2/MeCP2 post-transcriptional regulation by miRNAs: Many studies have indicated that MeCP2 is regulated by multiple miRNAs. This is in accordance with previous studies that discovered multiple MREs in the long 3'UTR of *MECP2/Mecp2* (**Figure 1.8D**) [168]. Regulation of MeCP2 by *miR-483-5p* has been shown to be critical for optimal MeCP2 expression during human fetal development [166]. Using an *in vitro* human embryonic stem cell (ESC) differentiation model, Rodriguez *et al.* (2016) demonstrated that miRNAs, along with RNA binding proteins (RBPs), regulate *MECP2* transcript stability and translational efficiency during neuronal differentiation [172]. These studies indicate that miRNAs play a critical role in regulating MeCP2 expression during neurodevelopment. Regulation of MeCP2 expression levels also influences its function. For instance, Zhang *et al.* (2016) demonstrated that expression of *miR-130a* in rat cortical neurons inhibited neurite outgrowth, reduced dendritic spine density as well as dendritic complexity. Subsequent experiments showed that *miR-130a* decreases MeCP2 levels, and overexpression of MeCP2 rescues the *miR-130a*-induced neuronal phenotype [173].

Moreover, homeostatic regulation of MeCP2 by *miR-132* is critical for maintaining the expression levels of MeCP2 and BDNF both *in vitro* and *in vivo* [168]. A similar homeostatic interaction between MeCP2, BDNF, and *miR-132* has also been observed in major depressive disorder patients and animal models as well [174]. Regulation of MeCP2 by miRNAs has been observed under multiple disease conditions. In Down syndrome, for instance, *miR-155* and *miR-802* have been shown to downregulate MeCP2 expression, thereby causing altered expression of MeCP2 targets *Creb1* and *Mef2c* [167]. MeCP2 has also been identified as a target of *miR-152*, *mir199a-3p,* and *mir-685* in cortical neurons exposed to ethanol [175]. Whether this observation indicates a potential mechanism for MeCP2 regulation specifically in Fetal Alcohol Spectrum Disorders (FASD) remains to be determined. More recently, Yan *et al.* (2017) have demonstrated that *miR-218* inhibits heroin-induced behavioral plasticity by targeting MeCP2 [176]. Collectively, these studies indicate that miRNA-mediated regulation of MeCP2 plays a vital role in the pathobiology of many brain disorders.

Influence of XCI on MECP2/Mecp2 expression: XCI is an evolutionary mechanism found in mammals to balance gene expression dosage (dosage compensation) in males and females [177]. XCI is initiated by the transcription of the X-inactive specific transcript (*XIST/Xist*), a long non-coding RNA from one X-chromosome. The transcribed *XIST* RNA covers the X-chromosome in *cis* and recruits a protein complex, which deposits repressive histone marks, inactivating the chromosome in terms of transcription. As a result of these events, the inactivated X-chromosome (Xi) becomes condensed and heterochromatic [178-183]. A subset of genes, however, escapes silencing by X inactivation, which is referred to as 'XCI escape'. These genes are thus expressed by both X chromosomes in females and exhibit higher expression in females [178,184,185]. Patterns of X-linked gene transcription are of particular relevance to brain function because the

mammalian X-chromosome is enriched in genes showing brain-specific expression [186,187].
Mutations in more than 100 human X-linked genes have been linked to intellectual disability
[188,189]. Previous studies have indicated that MeCP2 is one such X-linked gene that escapes
XCI and exhibits biallelic expression [190]. Many X-linked genes that escape inactivation show
cell type-, tissue-specific expression and sex biases [191]. The effect of these regulatory
mechanisms on *MECP2/Mecp2* expression remains to be fully determined.

1.4 Consequences of MeCP2 regulation deficits: MeCP2-associated neurological disorders

MeCP2 functional and/or expression deficits have been linked to many neurological
disorders (**Table 1.3**). For instance, reduced levels of *MECP2*/MeCP2 are found in RTT, ASD,
Angelman syndrome, Prader-Willi syndrome and Down syndrome (reviewed in [6,192]). *MECP2*
overexpression has been observed in MDS, rare cases of RTT and some cases of ASD. Among
these disorders, *MECP2* mutations have been found in RTT, ASD, as well as in FASD [193].
These disorders also show a sex-bias in phenotypes (**Table 1.3**), possibly due to X-linkage of many
of the genes involved, specifically, *MECP2*. As these disorders are caused by or associated with
altered expression and altered regulatory mechanisms of *MECP2*, it is possible to utilize the
knowledge on *Mecp2/MECP2* regulation in restoring its expression as a treatment for these
disorders. This section will summarize, RTT, ASD, MDS, and FASD as major disorders caused
by MeCP2 misregulation and how knowledge on *Mecp2/MECP2* regulation may aid in future
therapeutic strategies.

Table 1.3 Association of total MeCP2 and/or MeCP2 isoforms with neurological disorders				
Disorder	**RTT**	**ASD**	**MDS**	**FASD/Alcohol-related disorders**
Prevalence	1:10000-15000 [194]	1:68 [195]	Unknown (~150 cases reported so far)	~1% in Canada 13% in Manitoba [196]
Sex-biasness	Predominantly female [197]	Predominantly male (1:42); female (1:189) [195]	Predominantly male [198]	Biasness in male, but also found in females [196]
MeCP2 alterations	Mutations [197], decreased expression [157], changes in splicing [199]	Mainly decreased expression [157,200], but also increased expression.	Increased expression [198]	*MECP2* mutation in one patient with FASD and RTT [193]; Both increased and decreased expression in FASD rodent models and *in vitro* cellular models [175,201-208]
MeCP2 isoform levels	Major mutations affect both isoforms [197]; exon 1 mutations, which affect MeCP2E1 [209,210]; exon 1 mutations may affect transcription or translation of *MECP2E2* [211]; mutations causing	No reports on levels of individual isoforms.	No reports on levels of individual isoforms	No reports on levels of individual isoforms

	MECP2 splicing changes [212]; mice with exon 1 mutations have increased MeCP2E2 [121]			
Causes of MeCP2 alterations	Mutations [213]	Increased promoter methylation and CTCF binding [157,159]; altered transcriptional and post-transcriptional regulation [200]	Duplication of gene coding for MeCP2 [214]	DNA methylation changes at *Mecp2* regulatory elements [215]
Implications on therapy strategies by studying MeCP2 regulation	• Activation of non-mutated allele • Induce changes in splicing to increase the expression of unaffected isoform (e.g., If MeCP2E1 is not functional, induce MeCP2E2)	Promoter demethylation to induce expression	• Use of miRNA to decrease *MECP2/Mecp2* expression • Use of drugs to target transcriptional repression	Understanding the complex molecular mechanisms and determine suitable rescue methods based on the observed expression changes.

1.4.1 Rett Syndrome

Phenotypes of RTT: RTT is a neurological disorder with an incidence of approximately 1:10000, and is the leading cause of mental retardation in young females [216,217]. Patients with RTT appear to develop normally for the first 6-18 months of their life, followed by a variable period of developmental delay and regression. Regression of developmental milestones includes loss of purposeful hand use and speech. These regression patterns also constitute the main criteria for the

diagnosis of classic RTT [218]. The regression of skills stabilizes by 30-36 months, after which many patients exhibit stereotypic hand movements and gait abnormalities. Partial reacquisition of skills lost during the regression phase has been observed in a few RTT patients, but the loss of purposeful hand movements and language skills remain as predominant characteristics [219].

MECP2 mutations in RTT: Mutations in the *MECP2* gene were identified as the genetic cause of Rett Syndrome in 1999 [220]. The discovery that a DNA methyl reader was the underlying cause of a neuronal disorder led to a plethora of subsequent studies that attempted to unravel the precise connection between *MECP2* mutations and RTT. The majority of the *MECP2* mutations are located in the two main functional domains, the MBD domain, and the TRD domain, thus indicating that defective function of MeCP2 is a major underlying cause of RTT [221].

To date, only a few studies have analyzed RTT mutations specifically in individual *MECP2* isoforms. This is primarily due to the concept that the functions of MeCP2 isoforms are largely similar. However, previous studies have reported differential temporal and region-specific expression patterns for MeCP2E1 and MeCP2, as well as isoform-specific functions. Mutations specifically located in exon 1 have been identified in RTT patients, which may affect both isoforms, yet more profound effects on *MECP2E1* have been observed [121,209,210,212,222-226]. However, to date, no exon 2-specific mutations and thus *MECP2E2*-specific mutations have been identified. This could be due to two reasons: 1) *MECP2E2* mutations do not lead to RTT, a concept strengthened by previous reports on mouse models [227], or 2) *MECPE2* mutations lead to milder phenotypes in humans, who are not diagnosed as RTT patients.

MECP2 expression changes in RTT: RTT-causing *MECP2* mutations can result in expression and/or functional deficiency of MeCP2. The major focus of RTT research field has been the functional defects caused by *MECP2* mutations while few studies have described their effects on *MECP2* expression. **Figure 1.9** illustrates the *MECP2* gene/protein mutations that are known to cause expression changes. The reports on decreased *MECP2* expression or protein stability are in agreement with the notion that *MECP2*-deficiency is associated with RTT. However, many of these studies have not considered *MECP2E1* and *MeCP2E2* and potential dynamics between their expression. Petel-Galil *et al.* (2006) reported transcript levels of *MECP2E1* and *MeCP2E2* in lymphoblast cells from RTT patients with many deletions and mutations in the *MECP2* gene [228]. Known RTT-causing *MECP2* mutations, which lead to changes in *MECP2*/MeCP2 expression, are listed in **Table 1.4** and illustrated in **Figure 1.9**.
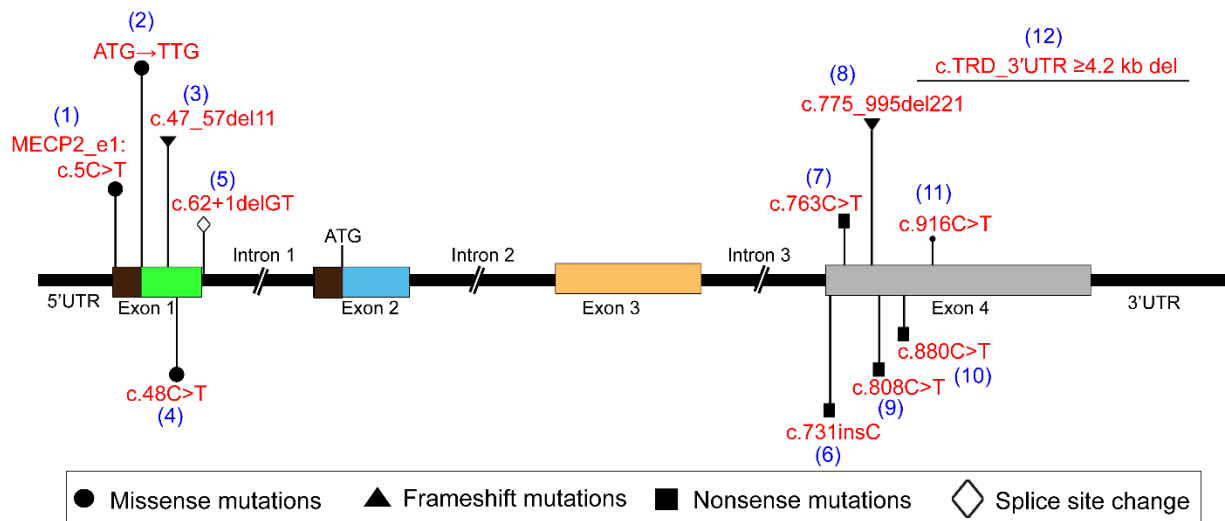
 Figure 1.9 RTT-causing *MECP2* mutations that change *MECP2* expression.
The figure illustrates known *MECP2* mutations that cause expression changes on *MECP2E1* and *MeCP2E2* transcripts and their translation efficiency. The *MECP2* expression changes associated with these mutations are summarized in **Table 1.4**.

#	Mutation	Type	Location	Tissue/cell type	Changes to *MECP2*/MeCP2 expression	Ref
(1)	MECP2_e1: c.5C>T (MeCP2_e1: p.A2V)	missense mutation	exon 1	fibroblasts	*MECP2E1*/ MeCP2E1 ↓ MeCP2E2 translation inhibited; *MECP2E2* unaffected	[229]
(2)	ATG→TTG	missense mutation	exon 1	mouse brain	Ablated MeCP2E1, Increased MeCP2E2	[121]
(3)	c.47_57del11 (G16EfsX22)	frameshift deletion	5'UTR-exon 1	lymphocytes	Translation efficiency of MeCP2E1 ↓ & MeCP2E2 ↓ *MECP2E2* transcription unaffected.	[211].
(4)	c.48C>T	missense mutation	exon 1	lymphocytes	*MECP2E1* ↓ *MECP2E2* ↑	[230]
(5)	c.62+1delGT	splice donor site deletion	intron 1	lymphoblast cells	*MECP2E1* ↓ *MECP2E2* ↓	[228]
(6)	c.731insC (Q244fs258X)	insertion/ nonsense mutation	exon 4 TRD	lymphoblast cells	*MECP2E1* ↓ *MECP2E2* ↓	[228]
(7)	c.763C>T (R255X)	nonsense mutation	exon 4 TRD NLS	lymphoblast cells	Unchanged *MECP2E1* & *MECP2E2*	[228]

Table 1.4 RTT-causing *MECP2* mutations and effects on *MECP2* expression

(8)	c.775_995del221 (A259fs266X)	frameshift deletion	exon 4 TRD NLS	lymphoblast cells	*MECP2E1* ↓ *MECP2E2* ↓	[228]
(9)	c.808C>T (R270X)	nonsense mutation	exon 4 TRD NLS	lymphoblast cells	*MECP2E1* ↓ *MECP2E2* ↓	[228]
(10)	c.880C>T (R294X)	nonsense mutation	exon 4 TRD-NLS	lymphoblast cells	*MECP2E1* ↓ *MECP2E2* ↓	[228]
(11)	c.916C>T (R306C)	missense mutation	TRD	lymphoblast cells	*MECP2E1* ↓ *MECP2E2* ↓	[228]
(12)	c.TRD_3′UTR ≥4.2 kb del	large rearrangement/ deletion	TRD to 3'UTR	lymphoblast cells	*MECP2E1* ↓ *MECP2E2* ↓	[228]

MECP2 mutations in gene regulatory elements such as the *MECP2* promoter, exon/intron boundaries critical for splicing and 3'UTR have been linked to *MECP2* expression deficits in RTT patients. Petel-Galil *et al.* (2006) demonstrated that in lymphoblasts, many of the RTT-causing *MECP2* gene deletions, nonsense mutations that are listed in **Table 1.4**, lead to reduced levels of both *MECP2* isoforms relative to control samples [228]. They also demonstrated that expression of both *MECP2* isoforms is decreased in some atypical RTT patients, who lack known RTT-causing *MECP2* mutations [228]. Another atypical RTT patient showed increased *MECP2E2* levels and decreased *MECP2E1* levels suggesting the splicing was affected. This observation was in agreement with the increased MeCP2E2 levels observed in a mouse model carrying a *MECP2* exon 1 point mutation at the MeCP2E1 translation start site (ATG→TTG) which ablated MeCP2E1 expression [121]. Similarly, another RTT patient with an exon 1 missense mutation showed reduced translation of both MeCP2E1 and MeCP2E2 without affecting *MECP2E2*

transcription [229]. Exon 1 mutation c.47_57del11-carrying RTT patient lymphocytes showed reduced translation of both MeCP2E1 and MeCP2E2 [211]. Mutations that target the splice acceptor/donor sites have also been shown to affect the transcript levels of *MECP2E1* and *MeCP2E2*, for instance, the c.62+1delGT mutation/deletion caused reduced levels of both *MECP2E1* and *MECP2E2* in RTT patients [228]. On the contrary, the exon 1 splice donor site mutation c.48C>T (p.Gly16Gly) causes reduced levels of *MECPE1* with a truncated MeCP2E1 and increased levels of *MECP2E2* that may suggest a splicing change [212]. Finally, nonsense mutations such as c.763C→T, also known as R255X, generates a truncated protein. In a mouse model of *Mecp2*[R255X/Y], reduced mRNA and absence of a truncated protein product were observed [231]. These observations are summarized in **Table 1.4**.

Some studies suggest that *MECP2* promoter methylation could also contribute to RTT. For example, in a rare variant of RTT in a girl, *MECP2* overexpression was observed in association with decreased *MECP2* promoter methylation [232]. However, monozygotic twins with RTT caused by *MECP2* exon 4 mutations did not have DNA methylation differences at the *MECP2* promoter (-225 to -637 region) or expression differences in their fibroblasts [233]. However, as RTT patients were not compared to age-matched controls, this analysis does not necessarily mean that *MECP2* promoter methylation does not play any role in RTT pathology.

XCI in RTT: As *MECP2* is an X-linked gene, another confounding factor that determines RTT phenotypes plus the sex-bias to females is XCI. Even though, some studies have suggested that *Mecp2* undergoes XCI-escape [234], it is unknown whether XCI-escape of *MECP2* occurs in all cell types, brain regions and all patients. Skewing of XCI, in which the X chromosome carrying the mutant *MECP2* allele has been identified in phenotypically normal or mildly affected mothers of RTT patients [235-237]. Increased frequencies of skewed XCI patterns have been reported in

RTT patients in contrast to the controls, but their direct association with clinical phenotypes have yet to be fully determined [238-240]. Transgenic expression of individual MeCP2 isoforms has been shown to prevent the development of RTT phenotypes in a mouse model, albeit in a limited capacity. These results suggest that both isoforms are required for the proper functioning of the brain and thus relevant to RTT pathogenesis [241].

Current treatments for RTT: At the moment, there is no cure for RTT. Current therapy strategies tested in *in vitro* cellular models, *in vivo* rodent models and/or human patients are of three kinds, 1) restoration of MeCP2 expression by gene therapy and/or genetic engineering [107,156,242-244]; 2) use of chemical compounds that can read-through nonsense mutations, examples of such compounds are aminoglycosides such as NB54, gentamicin, amikacin and paromomycin. [245-248]; 3) activation of silenced *MECP2* using drugs. They can be either inhibitors of HDACs such as trichostatin A and valproic acid, or DNMT inhibitors such as 5-azacytidine and decitabine [249]; 4) use of MeCP2 targets to rescue a subset of phenotypes. Such treatable MeCP2 targets are BDNF [109,250,251] and IGF1 [252-254]; 5) dietary supplementation with ω-3 polyunsaturated fatty acids (ω-3 PUFAs), acetyl-L-carnitine (ALC), folic acid and choline, some of which can restore methylation cycle components [255-258] and finally, 6) environmental and behavioural enrichment [259-261].

1.4.2 MECP2 Duplication Syndrome

Duplication of the Xq28, which contains *MECP2* gene, is frequently identified in males with overlapping phenotypes to RTT [262-264]. These male MDS patients experience a diverse range of phenotypes such as autistic features, recurrent respiratory infections, hypotonia, progressive encephalopathy, severe mental retardation, cerebellar degeneration, developmental

regression and epilepsy [265]. The duplicated region within the Xq28 region can vary from 0.3 to 4 Mb in size (reviewed in [266]). Genotype-phenotype correlation analyses have suggested the minimal critical region that leads to MDS phenotypes includes *MECP2* and *IRAK1* [267] (**Figure 1.10A**). Among them, *MECP2* appears to be the major dosage-sensitive gene and the primary cause of the majority of the Xq28 duplication or MDS [266]. However, in some MDS cases, partial *MECP2* duplication has been observed. In one such case, the duplicated *MECP2* lacked the 3'UTR region (**Figure 1.10B**) that is critical for its post-transcriptional regulation, which also implicated the absence of 3'UTR in mitigation of MDS disease severity [267]. As the full-length *MECP2* containing all four exons is duplicated in all reported cases of MDS, it is possible that both *MECP2* isoforms are upregulated. However, these studies have not reported the levels of *MECP2* isoforms, which would be important in using the regulatory mechanisms to recapitulate normal *MECP2* levels, if the two isoforms are regulated differently.
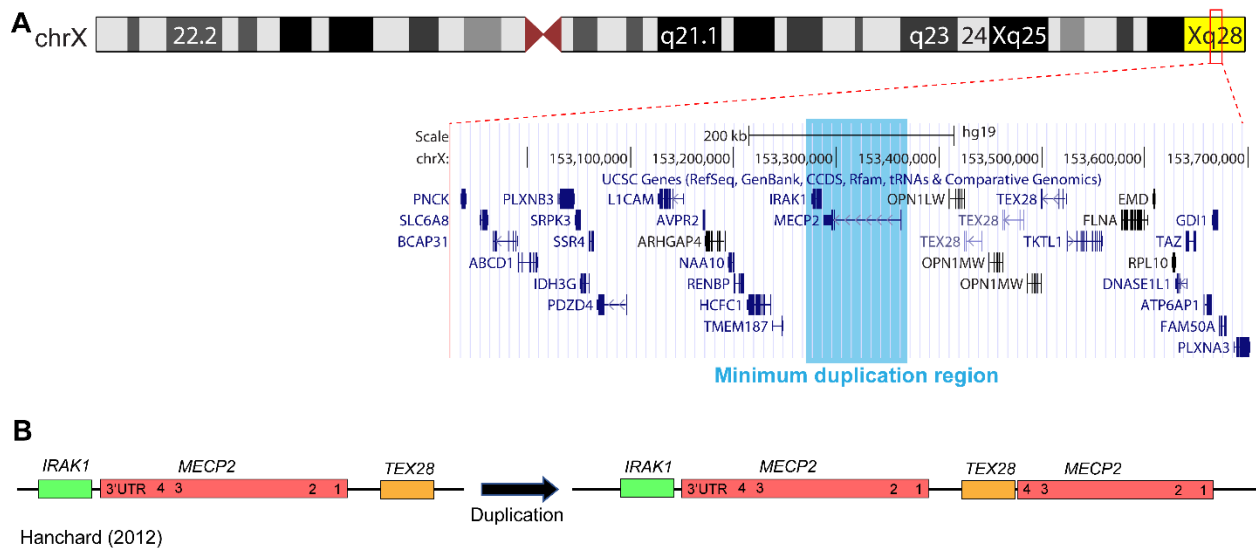
Figure 1.10 Genomic regions duplicated in Xq28 duplication or *MDS*.
A) Chromosome ideogram illustrating the location of Xq28. The zoomed-in region demonstrates a segment of the Xq28 region, which contains the minimum duplication region observed in many patients. It contains *MECP2* and *IRAK1*. **B)** Partial duplication of *MECP2,* which lacks the 3'UTR

of the gene [267]. Numbers on the *MECP2* gene indicate the exons. *Figure panel modified from [267].*

There are rare reports of MDS in females who are usually asymptomatic [268]. As of 2014, there were only 15 symptomatic MDS female patients reported and only six of them displayed interstitial duplications in contrast to X;autosome translocations displayed by the others. One reason for these symptoms is the increased *MECP2* expression due to the skewed XCI and activation of the X chromosome with the *MECP2* duplication [269].

Understanding *MECP2/Mecp2* regulatory mechanisms will be necessary for treating MDS at a few major checkpoints of the *MECP2/Mecp2* regulatory network. 1) transcription regulation: use of specific transcription inhibitors or TF-inhibitors to repress *MECP2/Mecp2* expression; 2) epigenetic regulation by DNA methylation: use of DNA remethylating agents/agents that increase DNA methylation (Eg. diminazene aceturate and SAM) to hypermethylate the *MECP2* promoter, and 3) post-transcriptional regulation: use of miRNAs that specifically bind to *MECP2/Mecp2*. Therefore, the current study, which aims to explore the effect of DNA methylation on *Mecp2* regulation (Chapters 3-5), will provide some new insight towards developing therapy options for MeCP2-associated brain disorders. As an advancement of such knowledge on *Mecp2* gene structure and regulation, antisense oligonucleotides targeting *Mecp2* intron 2 and exon 4 have been proven to be successful in reversing the phenotypes in an MDS mouse model [270].

Current treatment for MDS: Similar to RTT, MDS has no cure, and only a subset of phenotypes are rescued or managed due to the wide range of phenotypes [271]. Similar to many disorders with autistic behaviors, MDS also depends on developmental intervention therapies such as physical therapy, speech therapy, rehabilitation and behavioral therapy [214]. Moreover, phenotypes such

as seizures are managed by deep brain stimulation or anti-seizure drugs [272]. In a mouse model

of MDS, antisense oligonucleotides treatment caused reversal of phenotypes [270].

1.4.3 Autism Spectrum Disorders (ASD)

Genetics and epigenetics of ASD: According to the Metropolitan Atlanta developmental

disabilities surveillance program (MADDSP), "Autism Spectrum Disorders are defined as a

constellation of behaviors, indicating social, communicative and behavioral impairment or

abnormalities. The essential features of autism spectrum disorders are: 1) impaired reciprocal

social interactions, 2) delayed or unusual communication styles, and 3) restricted or repetitive

behavior patterns" [273]. The Diagnostic and statistical manual of mental disorders (DMS-V)

identifies autistic disorder, Asperger's disorder, and pervasive developmental disorder not

otherwise specified (PDD-NOS) included in the diagnostic criteria of ASD [274].

The complex nature of the phenotypes can be attributed to multiple genes that are being

involved in numerous cellular pathways in brain development and neuronal functions [275]. The

Autism genome project has utilized genome-wide sequencing studies, linkage analyses and

advanced sequencing technologies to identify numerous copy number variations (CNVs) and *de

novo* mutations in autism susceptibility genes [276]. Further complicating the multigenic and wide

range of phenotypes, the role of epigenetics, mainly DNA methylation and DNA methyl binding

proteins such as MeCP2 have also been highly implicated as major factors contributing to ASD

pathogenesis [6,277]. The contribution from epigenetics to ASD pathology was thought to be

significant as only 2% of ASD cases have an established genetic cause [278].

MECP2 misexpression in ASD: MeCP2 is among the major autism candidate genes and perhaps

one of the mostly-studied factors in relation to its regulatory role in controlling autism

susceptibility genes such as *RELN* [279]. The initial link between MeCP2 and autism was based on the diagnostic criteria that included RTT within the ASD category. However, RTT is no longer considered as an ASD [273]. Moreover, *MECP2* gene duplication may also lead to autistic phenotypes, however, whether MDS is currently considered as an ASD is unclear [280,281]. It has been established that both increased and decreased levels of MeCP2 lead to neurological complications [282-284]. Similarly, *MECP2* expression changes have been observed in patients diagnosed with ASD and examples of some of these studies are listed in **Table 1.5**.

Table 1.5 Changes in *MECP2* expression and regulation in ASD				
Ref	**Tissue/cell type**	**Sex**	***MECP2* change**	**Proposed mechanisms**
[157]	brain frontal cortex	F	↓	promoter variant
		M	↓	increased *MECP2* promoter methylation
[159]	brain frontal cortex and neurons	F, M	↓	increased *MECP2* promoter methylation, loss of CTCF binding to upstream promoter (loss of insulator function), skewed XCI
[285]		M F M	3′-UTR variants c.1558insA, c.1638 G > C, c.6809 T > C Expression was not reported.	structural changes to *MECP2* and 3'UTR
[286]	peripheral blood mononuclear cells	M, F	↓	3′UTR variations caused by following mutations at highly conserved regions c.1832G > C, c.2015G > A,

				c.4017T > A, and c.4417G >A. Decreased stability of *MECP2* mRNA.
[200]	frontal cerebral cortex		↑	differences in long to short transcript ratio suggesting post-transcriptional change
			↓	possible C-terminal changes associated with reduced post-translational stability. Increase in long 3'UTR, which is translated less efficiently.

Expression changes of the *MECP2* gene have been reported in autistic patients, which were the result of either mutations or deletions of regulatory regions of *MECP2* such as the 3'UTR. The 3'UTR of a gene is involved in transcript stability and translation [287]. Therefore, it is possible that mutations found in the 3'UTR of *MECP2* gene might contribute to the autistic features [288]. The possibility of these mutations in the 3'UTR of *MECP2* gene reducing the mRNA stability and inducing decay was suggested by Coutinho *et al.* (2007) [289]. Similarly, other studies have also reported mutations or rare polymorphisms (availability of more than one allele) in the 3'UTR of the *MECP2* gene in male ASD patients [290]. However, they did not report *MECP2/*MeCP2 levels to accurately postulate the exact role of 3'UTR mutations in misregulating *MECP2*/MeCP2 expression. Many of the studies also imply the possibility that mutations within the *MECP2* coding region are rare in ASD [290,291]. Possibly due to the same reason, the roles of *MECP2* mutations in ASD pathology have been uncertain [291,292] until subsequent studies linked epigenetic, transcriptional and post-transcriptional regulation of MeCP2 to ASD pathology [157,200].

Nagarajan *et al.* (2006) reported *MECP2* promoter hypermethylation (-541 to -243) in male autistic patients' brain frontal cortex [157]. Through correlation analysis, they suggested that increased *MECP2* promoter DNA methylation is an 'epigenotype' for the reduced *MECP2* expression in these patients. Two years later, the same groups investigated the DNA methylation profile further upstream of the promoter (-700 to -509). They reported that the loss of insulator protein CTCF binding to the upstream promoter leads to crawling of adjacent heterochromatin regions to the *MECP2* promoter and thereby causing *MECP2* repression [159]. Samaco *et al.* (2004) suggested both post-transcriptional and post-translational regulatory mechanisms of *MECP2*/MeCP2 might be impaired in ASD. They reached this conclusion based on the observations of altered ratio of long/short *MECP2* transcripts and protein level changes [200].

Current treatment for ASD: Currently, there are no cure or universal treatment strategies for all ASD cases. Due to the complex genetic and epigenetic contributions to these disorders, the major treatment available for patients is the management of the disability rather than the reversal of defects [293]. Educational programs are available to increase exposure of the patient families to the ways that can be used to improve the quality of life and reduce behavioral adaptations. Moreover, some research groups have succeeded in managing a subset of ASD phenotypes using targeted approaches such as repetitive transcranial magnetic stimulation in brain executive functional deficits [294-296]. Interestingly, the epigenetic changes, more specifically, DNA and histone methylation changes in ASD patients have been targeted by metabolic treatments such as methyl B12 treatment, which has been shown to restore the cellular methylation capacity and improved ASD symptoms [297]. It is our anticipation that increased understanding of *MECP2* alterations and regulatory mechanisms may provide novel concepts that can be used to restore genetic and/or epigenetic defects in ASD patients.

1.4.4 Fetal Alcohol Spectrum Disorders (FASD)

Complexity: Consumption of alcohol by the mother during pregnancy and/or pre-conception alcohol intake by the mother and/or the father may lead to a spectrum of disorders that are collectively referred to as FASD (reviewed in [196]). The disorders that come under the umbrella of FASD are fetal alcohol syndrome (FAS), fetal alcohol effects (FAE), partial fetal alcohol syndrome (pFAS), alcohol related neurodevelopmental disorders (ARND), static encephalopathy alcohol-exposed (SEAE) and alcohol-related birth defects (ARBD) [298,299]. Even though FASD is a 100% preventable condition, it is a global health issue with a prevalence rate of 1% in Canada [299]. Among its broader spectrum of subtypes, FAS, pFAS, and ARBD represent the tip of the FASD iceberg as these conditions show the majority of visible phenotypes. On the other hand, ARND is considered to be the invisible and most dangerous set of phenotypes as these defects directly affect brain function, cognition and behavioral defects, among others [196]. Therefore, the investigation of how alcohol causes these defects using *in vitro* cellular or *in vivo* models is critical to find treatments for this devastating set of conditions.

The confounding factors that determine the extent of damage by alcohol are quantity, frequency, and timing of alcohol consumption. In other words, the amount of alcohol consumed, the duration of the alcohol consumption (binge or chronic) and the time of consumption in terms of gestational period [196]. Studies on the transmission of epigenetic changes through generations (transgenerational epigenetic inheritance) have shown that the intake of alcohol by either or both parents prior to conception can also cause FASD [300]. Early diagnosis of FASD phenotypes is critical and essential as the majority of both visible and invisible phenotypes cannot be reversed or rescued after birth. Health and behavioral management, educational programs and environmental enrichment programs are available for the patients who continue living with FASD.

However, *in vitro* and *in vivo* studies have shown that the use of retinoic acid supplementation [301], and supplementations, which contain components of the methylation cycle, methyl donor, choline, and folate, were able to ameliorate at least partly the effects of alcohol (reviewed in [196]).

Alcohol metabolism: The damage to the central nervous system by alcohol can occur directly from alcohol or toxic metabolites of alcohol. Once entered into the blood stream, alcohol (ethanol) gets absorbed into other organ cells through diffusion **(Figure 1.11A)**. Then ethanol is metabolized *via* the oxidative ethanol metabolism pathway (~95%) **(Figure 1.11B)** or non-oxidative ethanol metabolism pathway (~1%) **(Figure 1.11C)** [302]. During oxidative alcohol metabolism, cytosolic alcohol dehydrogenase (ADH) converts ethanol into acetaldehyde in a reaction involving nicotinamide adenine dinucleotide (NAD^+) being reduced to NADH. Both peroxisomal catalases and cytochrome P450 2E1 (CYP2E1) in the endoplasmic reticulum are capable of oxidation of alcohol to acetaldehyde. The acetaldehyde is then transported into mitochondria, and aldehyde dehydrogenase 2 (ALDH2) mediates catalysis of acetaldehyde to acetate, NADH and reactive oxygen species (ROS).

Chapter 1
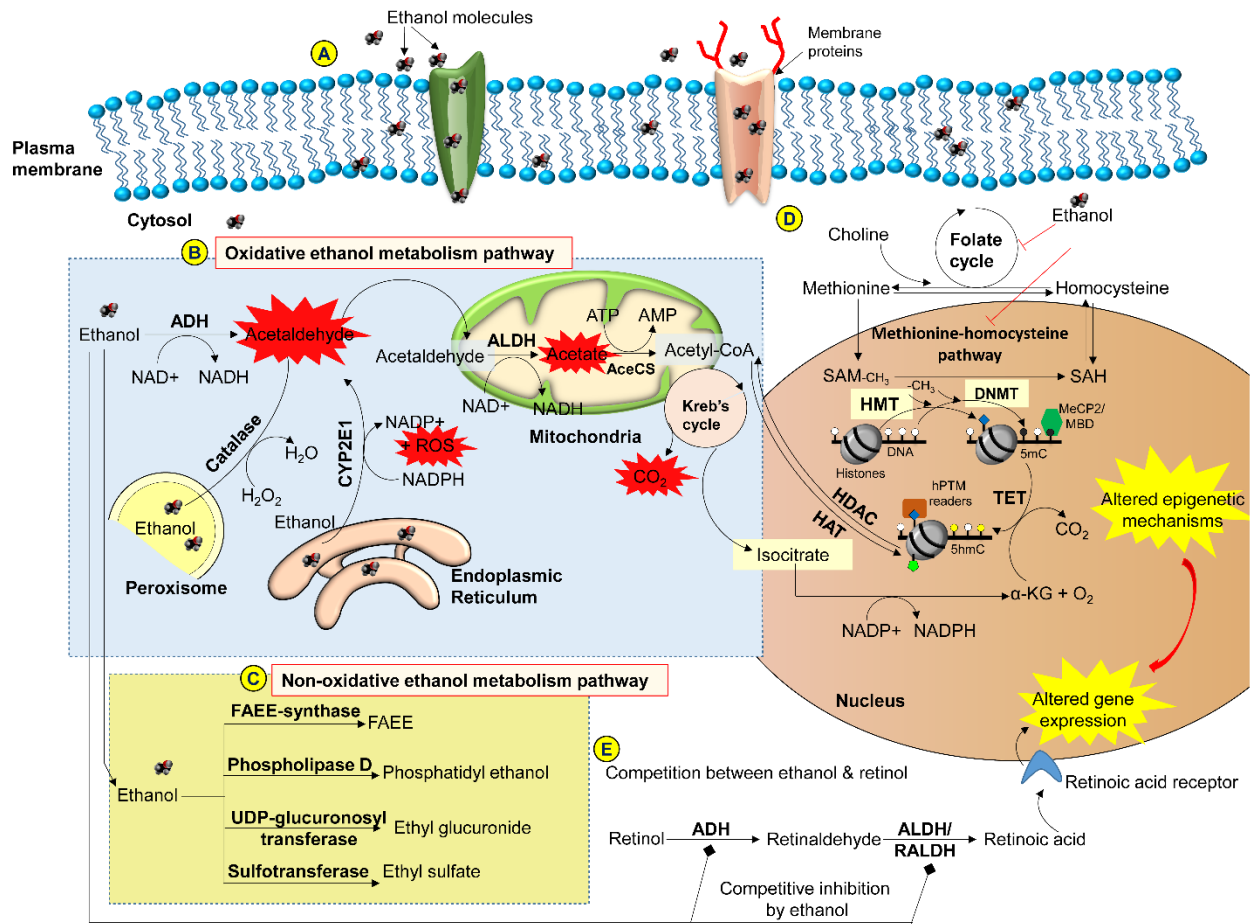
Figure 1.11 Alcohol metabolism and effects of ethanol on epigenetic mechanisms and gene expression.

A) Ethanol enters the cell through simple diffusion across the plasma membrane. **B)** Oxidative alcohol metabolism pathway. **C)** Non-oxidative alcohol metabolism pathway. **D)** Effects of ethanol and its metabolites on epigenetic mechanisms and gene expression. **E)** Competition between ethanol and retinol for metabolizing enzymes, which reduces the metabolism of retinol to retinoic acid. This leads to altered retinoic acid-dependent genes expression.

Figure and figure legend adapted/reprinted with permission from [196].

Epigenetics, MeCP2, and FASD: The broad spectrum of the phenotypes seen in the patients under the umbrella of FASD can only be explained by complex mechanisms involving both genetic and

epigenetic factors [196]. Ethanol can be considered as an 'epigenetic modifier' as ethanol, and its metabolites can alter DNA methylation, hPTMs and ncRNA expression and regulation [196,303]. Recent links between alcohol and MeCP2 have broadened the scope of FASD research towards the elucidation of the role of MeCP2 and DNA methylation, especially in brain and brain cell types. The first link between MeCP2 and FASD was established in 2004 when the *MECP2* c.808T>C (R270X) mutation was found in a girl with both FASD and RTT phenotypes [193]. This nonsense mutation has been shown to cause reduced *MECP2E1* and *MECP2E2* in RTT patients [228]. Since then, Lee *et al.* (2015) have suggested the *MECP2* promoter methylation be used as an 'epigenotype' for maternal alcohol consumption. Even though they did not report the expression changes of *MECP2* in the patients; it was speculated that induced DNA methylation in these patients might have a repressive role in regulating *MECP2* [304]. The remaining evidence on the role of MeCP2 in alcohol-mediated neurological phenotypes come from *in vitro* and *in vivo* animal model studies. The complexity of the damage caused by alcohol exposure on MeCP2 and its gene network was demonstrated by rather discordant expression changes of MeCP2 in these studies [175,201-208,305]. These observations led to the assumption that the effect of ethanol on *Mecp2*/MeCP2 expression is influenced by a multitude of factors including cell type, mode of alcohol exposure (binge or chronic), exposure time during pregnancy and the amount of alcohol used. While these studies provided valuable insights regarding the diverse effects of ethanol on MeCP2 expression and possibly its functions; how ethanol alters MeCP2 expression was unknown. Restoring altered levels of MeCP2 in alcohol-exposed systems may be a possible way to rescue the phenotypes.

Chapter 1

1.5 Cellular models to study *Mecp2* regulatory mechanisms

1.5.1 Differentiating neural stem cell model

Stem cells: Stem cell-based cellular models have been previously employed in studying the functions of MeCP2 [107,306-308]. Stem cells are types of unspecified cell types, which are capable of giving rise to similar (self-renewal) or different cell types through differentiation [309]. Based on their ability or potential to differentiate, stem cells can be of three main types, namely, totipotent, pluripotent or multipotent. Totipotent stem cells are found at the top of the stem cell hierarchy, with the potential of generating all the cell types of an organism and are found in the embryo proper and extraembryonic tissue in mammals [310]. Pluripotent stem cells have a more restricted potency for lineage differentiation and can differentiate into different cell types of the three germ layers, endoderm, mesoderm, and ectoderm [311]. The ectoderm gives rise to the nervous system [311]. Multipotent stem cells have further restricted differentiation potential and can differentiate into a set of specific cell types within one lineage. Neural stem cells are multipotent stem cells, which can differentiate into neurons, astrocytes, and oligodendrocytes [309].

Mouse neurogenesis and gliogenesis: The differentiation of NSC generates neurons and glial cells in the embryonic and early postnatal mouse brain [312]. The process by which multipotent NSC are transitioned into terminally differentiated neurons is called 'neurogenesis' while the transition of NSC into glial cell types, astrocytes and oligodendrocytes is referred to as 'gliogenesis' [313]. Prior to neurogenesis, neuroepithelial cells (NEC) of the developing neocortex, which are found in the ventricular zone (VZ), divide symmetrically to generate radial glial cells (RGC) **(Figure 1.12)**. Both NEC and RGC are neural stem cells.

Neurogenesis occurs between early embryonic and early postnatal stages (E11-E16) whereas gliogenesis occurs during late embryogenesis (E17), continuing through postnatal stages [312,314-316] (**Figure 1.12**). In the mouse cerebral cortex, neurogenesis is initiated at E12, peaks around E15. Some studies suggest that mouse neurogenesis reaches its completion around birth [317]. On the contrary, other studies provide evidence of continued neurogenesis even after birth. In three restricted areas of the adult mouse brain, namely, hippocampus, lateral ventricle, and olfactory bulb, neural precursors continue to generate neurons in adult stages [318].

At the onset of neurogenesis, RGC undergo asymmetric cell division to generate one RGC and one differentiated neuron. Additionally, RGC give rise to intermediate progenitor cells (IP), which then migrate to the subventricular zone (SVZ) and further divide symmetrically to generate two neurons [319]. The generated neurons migrate to the cortical plate and finally undergo terminal differentiation and morphogenic changes into neuronal subtypes. In contrast, the radial glia-dependent gliogenesis occurs around E17, with a second wave of cortical gliogenesis happening during the first postnatal week [320-322]. During this time, RGC divide to generate glial cell types, both astrocytes, and oligodendrocytes.
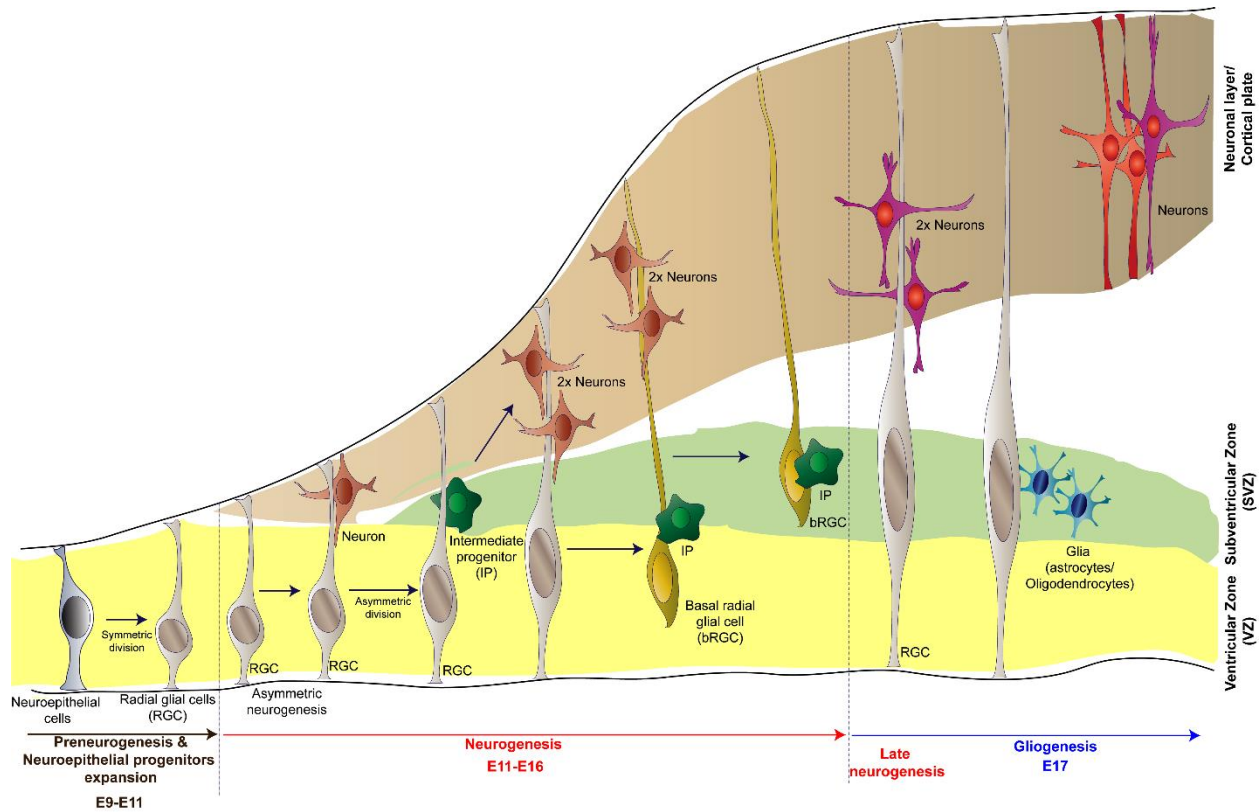
Figure 1.12 Mouse neurogenesis and gliogenesis

The illustration represents the processes of mouse neurogenesis, which spans E11 to E16 and gliogenesis occurring after E17. Layers of the mouse forebrain, namely, VZ, SVZ and cortical plate neuronal layer are also shown.

Information extracted and designed based on [314,323,324].

NSC differentiation model: The multipotent nature of NSC can be exploited to differentiate them into neurons and glial cells under *in vitro* conditions. The developmental stage at which neural stem cells are isolated for differentiation has been shown to influence the lineage output greatly. For instance, NSC harvested around E10 (during the time of neurogenesis) predominantly differentiate to neurons whereas, NSC isolated at E14.5 are capable of differentiating into neurons, astrocytes, and oligodendrocytes [317]. NSC differentiation can be directed by the addition of

exogenous factors such as platelet-derived growth factor (PDGF) for neuronal differentiation, ciliary neurotrophic factor (CNTF) for astrocyte differentiation and thyroid hormone T3 for oligodendrocyte differentiation [325,326]. NSC differentiation can also be induced by mitogen withdrawal, followed by addition of serum [327,328]. The latter technique is used in our lab to differentiate NSC into neurons and astrocytes. NSC differentiation *in vitro* mimics many of the characteristics of *in vivo* neurogenesis and gliogenesis and therefore, is an ideal system to analyze the regulation of neuronal TFs such as MeCP2. This model has been used in our lab to study MEIS1 homeoprotein transcription factor, and we have demonstrated the dynamic expression of *Meis1*/MEIS1 during NSC differentiation [329]. More importantly, we have used the NSC differentiation model to demonstrate the ability of custom *MECP2* isoform-specific gene therapy vectors to rescue dendritic maturation of neurons in an *ex vivo* model of RTT [107]. Moreover, retroviral transduction of NSC isolated from *Mecp2^{tm1.1Bird}+/−* female mice with *MECP2* isoform-specific gene therapy vectors showed that these NSC could maintain long-term reporter gene expression. This has several implications for future therapeutic strategies since it demonstrates that NSC transduced with *MECP2* isoform-specific gene therapy vectors can be used to deliver individual *MECP2* isoforms to different brain regions of animal models of MeCP2-deficiency and potentially to patients. Collectively, our previous studies using a NSC differentiation model demonstrate its versatility in studying the expression as well as functions of brain TFs.

1.5.2 Primary neuronal and glial cell models

Primary cultures of neuronal and glial cells provide a relatively homogenous system to understand the expression and function of a particular TF in a cell-type specific manner. In our lab, primary neurons and astrocytes isolated from E18 mouse brain cortex are used in studying

expression, regulation, and functions of proteins that are important in brain development and function. For instance, these primary cell types were used to investigate expression and localization patterns of MEIS1 [329]. More importantly, we have used them to study MeCP2, which is the gene of interest in this thesis. We reported the detection levels of total MeCP2 and MeCP2E1 in neurons and astrocytes along with their localization to the nuclei of these cell types [120]. Moreover, *rRNA* was recognized as a neuronal MeCP2 target gene, and the consequences of *MECP2* isoform-specific overexpression were investigated recently in our lab [330]. Therefore, these two primary cell models may be ideal systems to investigate cell type-specific regulatory mechanisms of *Mecp2* isoforms.

1.6 Rationale, hypotheses, and objectives

1.6.1 Rationale

MeCP2 is a multifunctional epigenetic regulator of the brain. The two *Mecp2/*MeCP2 isoforms are generated by alternative splicing and have differential expression and functions in the brain. Deficiency and overexpression of *MECP2*/MeCP2 are associated with RTT, MDS, ASD, and alcohol (ethanol)-mediated neurological damage in FASD animal and cellular models. The X-linked nature of the *Mecp2/MECP2* could contribute to the sex-bias observed for these disorders. Currently, there is no cure for any of them. The notion of 'too much'-'too little'-'too bad' represents the health concerns caused by increased MeCP2 levels ('too much'), decreased MeCP2 levels ('too little') and no cure for these disorders ('too bad') **(Figure 1.13)**.

Normal   **Too Much**   **Too Little**   **Too Bad**

Eg.
- *MECP2* Duplication Syndrome (MDS)
- Austim Spectrum Disorders (ASD)
- Alcohol-related disorders

Eg.
- Rett Syndrome (RTT)
- ASD
- Alcohol-related disorders

No Cure

Understanding of *Mecp2*/*MECP2* regulation in brain cell types will identify methods for therapy
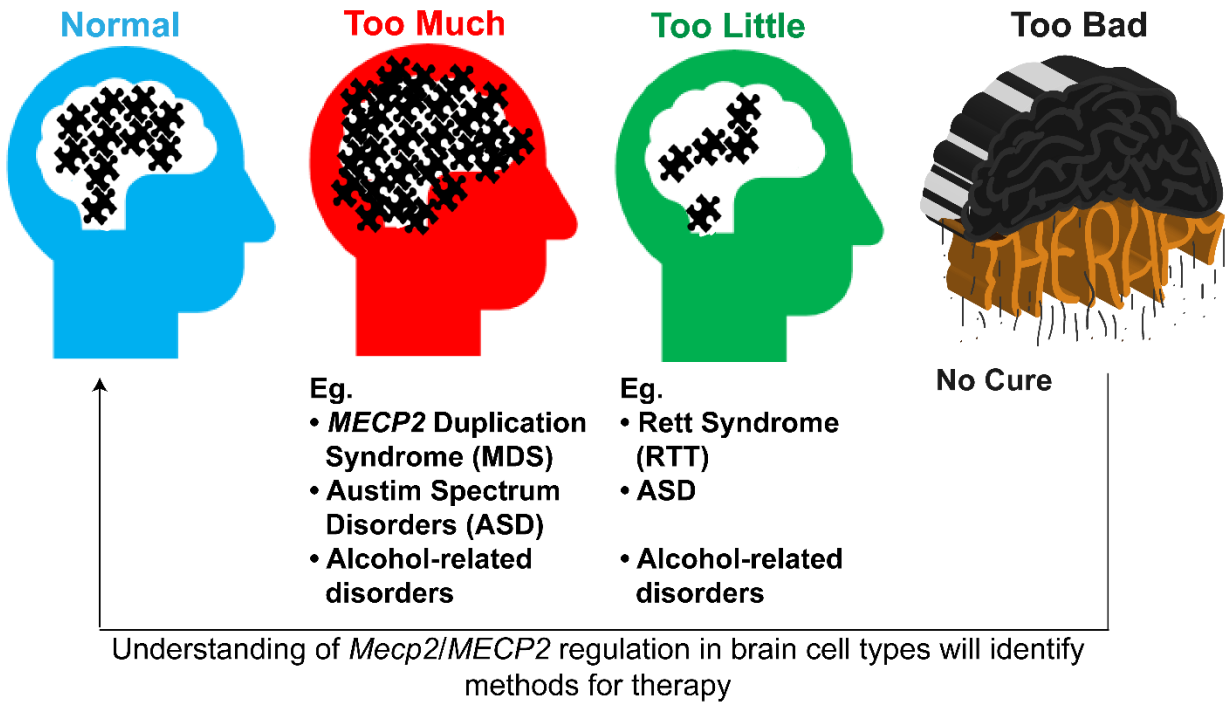
Figure 1.13 The representation of the notion of 'too much'-'too little'-'too bad' for MeCP2-associated neurological disorders.

The importance of studying regulatory mechanisms of *MECP2/Mecp2*/MeCP2 expression in brain cell types is to gather significant insights regarding how these regulatory mechanisms can be used to restore *MECP2/Mecp2*/MeCP2 expression deficits in MeCP2-associated neurological disorders.

As *MECP2/Mecp2*/MeCP2 expression deficits lead to neurological symptoms, recapitulation of normal *MECP2/Mecp2*/MeCP2 levels in the brain could provide a potential avenue for therapeutic strategies of these disorders. Therefore, understanding the regulatory mechanisms of *MECP2/Mecp2*/MeCP2 expression in diverse brain cell types will be a stepping stone for designing future therapeutic strategies based on *MECP2/Mecp2*/MeCP2 expression. The primary objective of my thesis work is to explore the role of DNA methylation in the regulation of *Mecp2e1* and *Mecp2e2*, the two transcript isoforms of *Mecp2* in *in vitro* mouse brain cellular models.

1.6.2 Hypotheses

DNA methylation patterns of the *Mecp2* gene differentially regulate *Mecp2* isoforms during neural stem cell differentiation under normal conditions and in response to ethanol exposure. Differences in transcript expression and DNA methylation patterns may correlate with a higher expression of *Mecp2* isoforms in neurons as compared to astrocytes.

1.6.3 Objectives

To determine the epigenetic and transcriptional mechanisms regulating production of *Mecp2e1* and *Mecp2e2* transcripts (*Mecp2* isoforms) in brain cell types; differentiating NSC, and differentiated neurons and astrocytes.

Aim 1. Determine the role of DNA methylation at the *Mecp2* REs at the *Mecp2* promoter and intron 1 in regulating *Mecp2* isoforms during NSC differentiation.

Aim 2. Investigate the role of DNA methylation at the *Mecp2* REs in mediating *Mecp2* misregulation by ethanol exposure and withdrawal during NSC differentiation.

Aim 3. Investigate cell type-specific regulation of *Mecp2e1* and *Mecp2e2*.

1.7 References

1. Riethoven J-JM (2010) Regulatory regions in DNA: promoters, enhancers, silencers, and insulators. Computational Biology of Transcription Factor Binding: 33-42.

2. Levine M, Tjian R (2003) Transcription regulation and animal diversity. Nature 424: 147-151.

3. Fussner E, Ching RW, Bazett-Jones DP (2011) Living without 30nm chromatin fibers. Trends Biochem Sci 36: 1-6.

4. Fussner E, Strauss M, Djuric U, Li R, Ahmed K, Hart M, Ellis J, Bazett-Jones DP (2012) Open and closed domains in the mouse genome are configured as 10-nm chromatin fibres. EMBO Rep 13: 992-996.

5. Liyanage VRB, Zachariah RM, Delcuve GP, Davie JR, Rastegar M (2012) New Developments in Chromatin Research: An Epigenetic Perspective. In: Simpson NM, Stewart VJ, editors. New Developments in Chromatin Research: Nova Science Publishers pp. 29-58.

6. Liyanage VR, Jarmasz JS, Murugeshan N, Del Bigio MR, Rastegar M, Davie JR (2014) DNA modifications: function and applications in normal and disease States. Biology (Basel) 3: 670-723.

7. Segal E, Widom J (2009) What controls nucleosome positions? Trends Genet 25: 335-343.

8. Jiang C, Pugh BF (2009) Nucleosome positioning and gene regulation: advances through genomics. Nat Rev Genet 10: 161-172.

9. Burgess RJ, Zhang Z (2010) Histones, histone chaperones and nucleosome assembly. Protein & cell 1: 607-612.

10. Smale ST, Kadonaga JT (2003) The RNA polymerase II core promoter. Annual review of biochemistry 72: 449-479.

11. Sandelin A, Carninci P, Lenhard B, Ponjavic J, Hayashizaki Y, Hume DA (2007) Mammalian RNA polymerase II core promoters: insights from genome-wide studies. Nat Rev Genet 8: 424-436.

12. Yang C, Bolotin E, Jiang T, Sladek FM, Martinez E (2007) Prevalence of the Initiator over the TATA box in human and yeast genes and identification of DNA motifs enriched in human TATA-less core promoters. Gene 389: 52-65.

13. Joughin B, Cheung E, Krishna R, Murthy Karuturi S-RJ, Lauffenburger D, Liu E (2009) Cellular Regulatory Networks. Systems Biomedicine: Concepts and Perspectives: 57-108.

14. Maston GA, Evans SK, Green MR (2006) Transcriptional regulatory elements in the human genome. Annu Rev Genomics Hum Genet 7: 29-59.

15. Smale ST, Baltimore D (1989) The "initiator" as a transcription control element. Cell 57: 103-113.

16. Xi H, Yu Y, Fu Y, Foley J, Halees A, Weng Z (2007) Analysis of overrepresented motifs in human core promoters reveals dual regulatory roles of YY1. Genome research 17: 798-806.

17. Calhoun VC, Stathopoulos A, Levine M (2002) Promoter-proximal tethering elements regulate enhancer-promoter specificity in the Drosophila Antennapedia complex. Proceedings of the National Academy of Sciences 99: 9243-9247.

18. Yella VR, Bansal M (2015) In silico Identification of Eukaryotic Promoters. Systems and synthetic biology: Springer. pp. 63-75.

19. Maston GA, Evans SK, Green MR (2006) Transcriptional regulatory elements in the human genome. Annu Rev Genomics Hum Genet 7: 29-59.

20. Gershenzon NI, Ioshikhes IP (2004) Synergy of human Pol II core promoter elements revealed by statistical sequence analysis. Bioinformatics 21: 1295-1300.

21. Jin VX, Singer GA, Agosto-Pérez FJ, Liyanarachchi S, Davuluri RV (2006) Genome-wide analysis of core promoter elements from conserved human and mouse orthologous pairs. BMC bioinformatics 7: 114.

22. Bajic VB, Seah SH (2003) Dragon gene start finder: an advanced system for finding approximate locations of the start of gene transcriptional units. Genome research 13: 1923-1929.

23. Trinklein ND, Aldred SJF, Saldanha AJ, Myers RM (2003) Identification and functional analysis of human transcriptional promoters. Genome research 13: 308-312.

24. Kutach AK, Kadonaga JT (2000) The downstream promoter element DPE appears to be as widely used as the TATA box in Drosophila core promoters. Molecular and cellular biology 20: 4754-4764.

25. Birney E, Stamatoyannopoulos JA, Dutta A, Guigó R, Gingeras TR, Margulies EH, Weng Z, Snyder M, Dermitzakis ET, et al. (2007) Identification and analysis of functional elements in 1% of the human genome by the ENCODE pilot project. Nature 447: 799-816.

26. Lieberman-Aiden E, Van Berkum NL, Williams L, Imakaev M, Ragoczy T, Telling A, Amit I, Lajoie BR, Sabo PJ, et al. (2009) Comprehensive mapping of long-range interactions reveals folding principles of the human genome. science 326: 289-293.

27. OGBOURNE S, ANTALIS TM (1998) Transcriptional control and the role of silencers in transcriptional regulation in eukaryotes. Biochemical Journal 331: 1-14.

28. Bell AC, West AG, Felsenfeld G (1999) The protein CTCF is required for the enhancer blocking activity of vertebrate insulators. Cell 98: 387-396.

29. Barkess G, West AG (2012) Chromatin insulator elements: establishing barriers to set heterochromatin boundaries. Epigenomics 4: 67-80.

30. Sammeth M, Foissac S, Guigó R (2008) A general definition and nomenclature for alternative splicing events. PLoS Comput Biol 4: e1000147.

31. Matlin AJ, Clark F, Smith CW (2005) Understanding alternative splicing: towards a cellular code. Nature reviews Molecular cell biology 6: 386-398.

32. Das R, Yu J, Zhang Z, Gygi MP, Krainer AR, Gygi SP, Reed R (2007) SR proteins function in coupling RNAP II transcription to pre-mRNA splicing. Molecular cell 26: 867-881.

33. Kornblihtt AR (2012) CTCF: from insulators to alternative splicing regulation. Cell research 22: 450-452.

34. Ayoubi T, Van De Ven W (1996) Regulation of gene expression by alternative promoters. The FASEB Journal 10: 453-460.

35. Tian B, Manley JL (2013) Alternative cleavage and polyadenylation: the long and short of it. Trends in biochemical sciences 38: 312-320.

36. Allfrey VG, Faulkner R, Mirsky AE (1964) Acetylation and Methylation of Histones and Their Possible Role in the Regulation of Rna Synthesis. Proc Natl Acad Sci U S A 51: 786-794.

37. Kouzarides T (2007) Chromatin modifications and their function. Cell 128: 693-705.

38. LaSalle JM, Powell WT, Yasui DH (2013) Epigenetic layers and players underlying neurodevelopment. Trends Neurosci 36: 460-470.

39. Yun M, Wu J, Workman JL, Li B (2011) Readers of histone modifications. Cell Research 21: 564-578.

40. Henikoff S (2005) Histone modifications: Combinatorial complexity or cumulative simplicity? Proceedings of the National Academy of Sciences of the United States of America 102: 5308-5309.

41. Delcuve GP, Rastegar M, Davie JR (2009) Epigenetic control. Journal of cellular physiology 219: 243-250.

42. Hotchkiss RD (1948) The quantitative separation of purines, pyrimidines, and nucleosides by paper chromatography. J Biol Chem 175: 315-332.

43. Srinivasan P (1962) Kinetics of incorporation of 5-methylcytosine in HeLa cells. Biochimica et Biophysica Acta (BBA)-Specialized Section on Nucleic Acids and Related Subjects 55: 553-556.

44. Wyatt GR (1951) Recognition and estimation of 5-methylcytosine in nucleic acids. Biochem J 48: 581-584.

45. Wyatt GR (1950) Occurrence of 5-methylcytosine in nucleic acids. Nature 166: 237-238.

46. Creusot F, Acs G, Christman JK (1982) Inhibition of DNA methyltransferase and induction of Friend erythroleukemia cell differentiation by 5-azacytidine and 5-aza-2'-deoxycytidine. J Biol Chem 257: 2041-2048.

47. Auclair G, Weber M (2012) Mechanisms of DNA methylation and demethylation in mammals. Biochimie 94: 2202-2211.

48. Jones PA, Liang G (2009) Rethinking how DNA methylation patterns are maintained. Nat Rev Genet 10: 805-811.

49. Kohli RM, Zhang Y (2013) TET enzymes, TDG and the dynamics of DNA demethylation. Nature 502: 472-479.

50. Klungland A, Robertson AB (2017) Oxidized C5-methyl cytosine bases in DNA: 5-Hydroxymethylcytosine; 5-formylcytosine; and 5-carboxycytosine. Free Radical Biology and Medicine 107: 62-68.

51. Kass SU, Pruss D, Wolffe AP (1997) How does DNA methylation repress transcription? Trends in Genetics 13: 444-449.

52. Liyanage V, Zachariah R, Delcuve G, Davie J, Rastegar M (2012) New developments in chromatin research: an epigenetic perspective. New developments in chromatin research 1.

53. Mellen M, Ayata P, Dewell S, Kriaucionis S, Heintz N (2012) MeCP2 binds to 5hmC enriched within active genes and accessible chromatin in the nervous system. Cell 151: 1417-1430.

54. Cartron PF, Nadaradjane A, Lepape F, Lalier L, Gardie B, Vallette FM (2013) Identification of TET1 Partners That Control Its DNA-Demethylating Function. Genes Cancer 4: 235-241.

55. Zhubi A, Chen Y, Dong E, Cook EH, Guidotti A, Grayson DR (2014) Increased binding of MeCP2 to the GAD1 and RELN promoters may be mediated by an enrichment of 5-hmC in autism spectrum disorder (ASD) cerebellum. Transl Psychiatry 4: e349.

56. Pinney SE (2014) Mammalian Non-CpG Methylation: Stem Cells and Beyond. Biology (Basel) 3: 739-751.

57. Guo JU, Su Y, Shin JH, Shin J, Li H, Xie B, Zhong C, Hu S, Le T, et al. (2014) Distribution, recognition and regulation of non-CpG methylation in the adult mammalian brain. Nat Neurosci 17: 215-222.

58. Guo JU, Su Y, Shin JH, Shin J, Li H, Xie B, Zhong C, Hu S, Le T, et al. (2014) Distribution, recognition and regulation of non-CpG methylation in the adult mammalian brain. Nature neuroscience 17: 215-222.

59. Sharma A, Klein SS, Barboza L, Lohdi N, Toth M (2016) Principles Governing DNA Methylation during Neuronal Lineage and Subtype Specification. The Journal of Neuroscience 36: 1711-1722.

60. Yokochi T, Robertson KD (2002) Preferential methylation of unmethylated DNA by Mammalian de novo DNA methyltransferase Dnmt3a. J Biol Chem 277: 11735-11745.

61. Yoder JA, Soman NS, Verdine GL, Bestor TH (1997) DNA (cytosine-5)-methyltransferases in mouse cells and tissues. Studies with a mechanism-based probe. J Mol Biol 270: 385-395.

62. Kinde B, Gabel HW, Gilbert CS, Griffith EC, Greenberg ME (2015) Reading the unique DNA methylation landscape of the brain: non-CpG methylation, hydroxymethylation, and MeCP2. Proceedings of the National Academy of Sciences 112: 6800-6806.

63. Huang Y, Pastor WA, Shen Y, Tahiliani M, Liu DR, Rao A (2010) The behaviour of 5-hydroxymethylcytosine in bisulfite sequencing. PLoS One 5: e8888.

64. Nestor C, Ruzov A, Meehan R, Dunican D (2010) Enzymatic approaches and bisulfite sequencing cannot distinguish between 5-methylcytosine and 5-hydroxymethylcytosine in DNA. Biotechniques 48: 317-319.

65. Booth MJ, Branco MR, Ficz G, Oxley D, Krueger F, Reik W, Balasubramanian S (2012) Quantitative sequencing of 5-methylcytosine and 5-hydroxymethylcytosine at single-base resolution. Science 336: 934-937.

66. Yu M, Hon GC, Szulwach KE, Song CX, Zhang L, Kim A, Li X, Dai Q, Shen Y, et al. (2012) Base-resolution analysis of 5-hydroxymethylcytosine in the mammalian genome. Cell 149: 1368-1380.

67. Weber M, Davies JJ, Wittig D, Oakeley EJ, Haase M, Lam WL, Schubeler D (2005) Chromosome-wide and promoter-specific analyses identify sites of differential DNA methylation in normal and transformed human cells. Nat Genet 37: 853-862.

68. Nestor CE, Meehan RR (2014) Hydroxymethylated DNA immunoprecipitation (hmeDIP). Methods Mol Biol 1094: 259-267.

69. Glisovic T, Bachorik JL, Yong J, Dreyfuss G (2008) RNA-binding proteins and post-transcriptional gene regulation. FEBS Lett 582: 1977-1986.

70. Proudfoot NJ, Furger A, Dye MJ (2002) Integrating mRNA processing with transcription. Cell 108: 501-512.

71. Zhao BS, Roundtree IA, He C (2017) Post-transcriptional gene regulation by mRNA modifications. Nat Rev Mol Cell Biol 18: 31-42.

72. Liyanage VRB (2016) Role of RNA Methylation and Non-Coding RNAs in Pathobiology of Autism Spectrum Disorders. Biomedical Sciences 2: 24-33.

73. Palazzo AF, Lee ES (2015) Non-coding RNA: what is functional and what is junk? Frontiers in genetics 6: 2.

74. Bian S, Sun T (2011) Functions of noncoding RNAs in neural development and neurological diseases. Mol Neurobiol 44: 359-373.

75. Cech Thomas R, Steitz Joan A (2014) The Noncoding RNA Revolution - Trashing Old Rules to Forge New Ones. Cell 157: 77-94.

76. Bethune J, Artus-Revel CG, Filipowicz W (2012) Kinetic analysis reveals successive steps leading to miRNA-mediated silencing in mammalian cells. EMBO Rep 13: 716-723.

77. Latos PA, Pauler FM, Koerner MV, Şenergin HB, Hudson QJ, Stocsits RR, Allhoff W, Stricker SH, Klement RM, et al. (2012) Airn transcriptional overlap, but not its lncRNA products, induces imprinted Igf2r silencing. Science 338: 1469-1472.

78. Brockdorff N, Ashworth A, Kay GF, McCabe VM, Norris DP, Cooper PJ, Swift S, Rastan S (1992) The product of the mouse Xist gene is a 15 kb inactive X-specific transcript containing no conserved ORF and located in the nucleus. Cell 71: 515-526.

79. Tsai M-C, Manor O, Wan Y, Mosammaparast N, Wang JK, Lan F, Shi Y, Segal E, Chang HY (2010) Long noncoding RNA as modular scaffold of histone modification complexes. Science 329: 689-693.

80. Espinoza CA, Allen TA, Hieb AR, Kugel JF, Goodrich JA (2004) B2 RNA binds directly to RNA polymerase II to repress transcript synthesis. Nature structural & molecular biology 11: 822-829.

81. Li W, Notani D, Rosenfeld MG (2016) Enhancers as non-coding RNA transcription units: recent insights and future perspectives. Nat Rev Genet 17: 207-223.

82. Lasda E, Parker R (2014) Circular RNAs: diversity of form and function. RNA 20: 1829-1842.

83. Delcuve GP, Rastegar M, Davie JR (2009) Epigenetic control. J Cell Physiol 219: 243-250.

84. Lewis JD, Meehan RR, Henzel WJ, Maurer-Fogy I, Jeppesen P, Klein F, Bird A (1992) Purification, sequence, and cellular localization of a novel chromosomal protein that binds to methylated DNA. Cell 69: 905-914.

85. Bottomley MJ (2004) Structures of protein domains that create or recognize histone modifications. EMBO Reports 5: 464-469.

86. Christman JK (2002) 5-Azacytidine and 5-aza-2 [variant prime]-deoxycytidine as inhibitors of DNA methylation: mechanistic studies and their implications for cancer therapy. Oncogene 21: 5483.

87. Vacca M, Ragione FD, Tripathi KP, Scalabrì F, D'Esposito M (2015) MECP2: A Multifunctional Protein Supporting Brain Complexity. In: Zazzu V, Ferraro MB,

Guarracino MR, editors. Mathematical Models in Biology: Bringing Mathematics to Life. Cham: Springer International Publishing. pp. 109-117.

88. Liyanage VR, Rastegar M (2014) Rett syndrome and MeCP2. Neuromolecular Med 16: 231-264.

89. Hung MS, Shen CK (2003) Eukaryotic methyl-CpG-binding domain proteins and chromatin modification. Eukaryot Cell 2: 841-846.

90. Singh J, Saxena A, Christodoulou J, Ravine D (2008) MECP2 genomic structure and function: insights from ENCODE. Nucleic Acids Res 36: 6035-6047.

91. Saito M, Ishikawa F (2002) The mCpG-binding domain of human MBD3 does not bind to mCpG but interacts with NuRD/Mi2 components HDAC1 and MTA2. J Biol Chem 277: 35434-35439.

92. Zachariah RM, Rastegar M (2012) Linking epigenetics to human disease and Rett syndrome: the emerging novel and challenging concepts in MeCP2 research. Neural Plast 2012: 415825.

93. Adams VH, McBryant SJ, Wade PA, Woodcock CL, Hansen JC (2007) Intrinsic disorder and autonomous domain function in the multifunctional nuclear protein, MeCP2. Journal of Biological Chemistry 282: 15057-15064.

94. Chao HT, Zoghbi HY, Rosenmund C (2007) MeCP2 controls excitatory synaptic strength by regulating glutamatergic synapse number. Neuron 56: 58-65.

95. Qiu Z, Sylwestrak EL, Lieberman DN, Zhang Y, Liu XY, Ghosh A (2012) The Rett syndrome protein MeCP2 regulates synaptic scaling. J Neurosci 32: 989-994.

96. Na ES, Nelson ED, Kavalali ET, Monteggia LM (2013) The impact of MeCP2 loss- or gain-of-function on synaptic plasticity. Neuropsychopharmacology 38: 212-219.

97. Zhong X, Li H, Chang Q (2012) MeCP2 phosphorylation is required for modulating synaptic scaling through mGluR5. J Neurosci 32: 12841-12847.

98. Na ES, Nelson ED, Adachi M, Autry AE, Mahgoub MA, Kavalali ET, Monteggia LM (2012) A mouse model for MeCP2 duplication syndrome: MeCP2 overexpression impairs learning and memory and synaptic transmission. J Neurosci 32: 3109-3117.

99. Matarazzo V, Cohen D, Palmer AM, Simpson PJ, Khokhar B, Pan SJ, Ronnett GV (2004) The transcriptional repressor Mecp2 regulates terminal neuronal differentiation. Mol Cell Neurosci 27: 44-58.

100. Tsujimura K, Abematsu M, Kohyama J, Namihira M, Nakashima K (2009) Neuronal differentiation of neural precursor cells is promoted by the methyl-CpG-binding protein MeCP2. Exp Neurol 219: 104-111.

101. Kishi N, Macklis JD (2004) MECP2 is progressively expressed in post-migratory neurons and is involved in neuronal maturation rather than cell fate decisions. Mol Cell Neurosci 27: 306-321.

102. Fukuda T, Itoh M, Ichikawa T, Washiyama K, Goto Y (2005) Delayed maturation of neuronal architecture and synaptogenesis in cerebral cortex of Mecp2-deficient mice. J Neuropathol Exp Neurol 64: 537-544.

103. Kishi N, Macklis JD (2010) MeCP2 functions largely cell-autonomously, but also non-cell-autonomously, in neuronal maturation and dendritic arborization of cortical pyramidal neurons. Exp Neurol 222: 51-58.

104. Ballas N, Lioy DT, Grunseich C, Mandel G (2009) Non-cell autonomous influence of MeCP2-deficient glia on neuronal dendritic morphology. Nat Neurosci 12: 311-317.

105. Belichenko PV, Wright EE, Belichenko NP, Masliah E, Li HH, Mobley WC, Francke U (2009) Widespread changes in dendritic and axonal morphology in Mecp2-mutant mouse models of Rett syndrome: evidence for disruption of neuronal networks. J Comp Neurol 514: 240-258.

106. Wang IT, Reyes AR, Zhou Z (2013) Neuronal morphology in MeCP2 mouse models is intrinsically variable and depends on age, cell type, and Mecp2 mutation. Neurobiol Dis 58C: 3-12.

107. Rastegar M, Hotta A, Pasceri P, Makarem M, Cheung AY, Elliott S, Park KJ, Adachi M, Jones FS, et al. (2009) MECP2 isoform-specific vectors with regulated expression for Rett syndrome gene therapy. PLoS One 4: e6810.

108. Belichenko NP, Belichenko PV, Mobley WC (2009) Evidence for both neuronal cell autonomous and nonautonomous effects of methyl-CpG-binding protein 2 in the cerebral cortex of female mice with Mecp2 mutation. Neurobiol Dis 34: 71-77.

109. Larimore JL, Chapleau CA, Kudo S, Theibert A, Percy AK, Pozzo-Miller L (2009) Bdnf overexpression in hippocampal neurons prevents dendritic atrophy caused by Rett-associated MECP2 mutations. Neurobiol Dis 34: 199-211.

110. Li Y, Wang H, Muffat J, Cheng AW, Orlando DA, Loven J, Kwok SM, Feldman DA, Bateup HS, et al. (2013) Global transcriptional and translational repression in human-embryonic-stem-cell-derived rett syndrome neurons. Cell Stem Cell 13: 446-458.

111. Ricciardi S, Boggio EM, Grosso S, Lonetti G, Forlani G, Stefanelli G, Calcagno E, Morello N, Landsberger N, et al. (2011) Reduced AKT/mTOR signaling and protein synthesis dysregulation in a Rett syndrome animal model. Hum Mol Genet 20: 1182-1196.

112. Della Ragione F, Filosa S, Scalabri F, D'Esposito M (2012) MeCP2 as a genome-wide modulator: the renewal of an old story. Front Genet 3: 181.

113. Horike S, Cai S, Miyano M, Cheng JF, Kohwi-Shigematsu T (2005) Loss of silent-chromatin looping and impaired imprinting of DLX5 in Rett syndrome. Nat Genet 37: 31-40.

114. Zlatanova J (2005) MeCP2: the chromatin connection and beyond. Biochem Cell Biol 83: 251-262.

115. Chadwick LH, Wade PA (2007) MeCP2 in Rett syndrome: transcriptional repressor or chromatin architectural protein? Curr Opin Genet Dev 17: 121-125.

116. Georgel PT, Horowitz-Scherer RA, Adkins N, Woodcock CL, Wade PA, Hansen JC (2003) Chromatin compaction by human MeCP2. Assembly of novel secondary chromatin structures in the absence of DNA methylation. J Biol Chem 278: 32181-32188.

117. Nikitina T, Shi X, Ghosh RP, Horowitz-Scherer RA, Hansen JC, Woodcock CL (2007) Multiple modes of interaction between the methylated DNA binding protein MeCP2 and chromatin. Mol Cell Biol 27: 864-877.

118. Yasui DH, Peddada S, Bieda MC, Vallero RO, Hogart A, Nagarajan RP, Thatcher KN, Farnham PJ, Lasalle JM (2007) Integrated epigenomic analyses of neuronal MeCP2 reveal a role for long-range interaction with active genes. Proc Natl Acad Sci U S A 104: 19416-19421.

119. Olson CO, Zachariah RM, Ezeonwuka CD, Liyanage VR, Rastegar M (2014) Brain region-specific expression of MeCP2 isoforms correlates with DNA methylation within Mecp2 regulatory elements. PLoS One 9: e90645.

120. Zachariah RM, Olson CO, Ezeonwuka C, Rastegar M (2012) Novel MeCP2 isoform-specific antibody reveals the endogenous MeCP2E1 expression in murine brain, primary neurons and astrocytes. PLoS One 7: e49763.

121. Yasui DH, Gonzales ML, Aflatooni JO, Crary FK, Hu DJ, Gavino BJ, Golub MS, Vincent JB, Carolyn Schanen N, et al. (2014) Mice with an isoform-ablating Mecp2 exon 1 mutation recapitulate the neurologic deficits of Rett syndrome. Hum Mol Genet 23: 2447-2458.

122. Nikitina T, Ghosh RP, Horowitz-Scherer RA, Hansen JC, Grigoryev SA, Woodcock CL (2007) MeCP2-chromatin interactions include the formation of chromatosome-like structures and are altered in mutations causing Rett syndrome. J Biol Chem 282: 28237-28245.

123. Agarwal N, Becker A, Jost KL, Haase S, Thakur BK, Brero A, Hardt T, Kudo S, Leonhardt H, et al. (2011) MeCP2 Rett mutations affect large scale chromatin organization. Hum Mol Genet 20: 4187-4195.

124. Kumar A, Kamboj S, Malone BM, Kudo S, Twiss JL, Czymmek KJ, LaSalle JM, Schanen NC (2008) Analysis of protein domains and Rett syndrome mutations indicate that

multiple regions influence chromatin-binding dynamics of the chromatin-associated protein MECP2 in vivo. J Cell Sci 121: 1128-1137.

125. Brero A, Easwaran HP, Nowak D, Grunewald I, Cremer T, Leonhardt H, Cardoso MC (2005) Methyl CpG-binding proteins induce large-scale chromatin reorganization during terminal differentiation. J Cell Biol 169: 733-743.

126. Maunakea AK, Chepelev I, Cui K, Zhao K (2013) Intragenic DNA methylation modulates alternative splicing by recruiting MeCP2 to promote exon recognition. Cell Res 10.1038/cr.2013.110.

127. Young JI, Hong EP, Castle JC, Crespo-Barreto J, Bowman AB, Rose MF, Kang D, Richman R, Johnson JM, et al. (2005) Regulation of RNA splicing by the methylation-dependent transcriptional repressor methyl-CpG binding protein 2. Proc Natl Acad Sci U S A 102: 17551-17558.

128. Nomura T, Kimura M, Horii T, Morita S, Soejima H, Kudo S, Hatada I (2008) MeCP2-dependent repression of an imprinted miR-184 released by depolarization. Hum Mol Genet 17: 1192-1199.

129. Cheng T-L, Wang Z, Liao Q, Zhu Y, Zhou W-H, Xu W, Qiu Z MeCP2 Suppresses Nuclear MicroRNA Processing and Dendritic Growth by Regulating the DGCR8/Drosha Complex. Developmental Cell 28: 547-560.

130. Urdinguio RG, Fernandez AF, Lopez-Nieva P, Rossi S, Huertas D, Kulis M, Liu CG, Croce CM, Calin GA, et al. (2010) Disrupted microRNA expression caused by Mecp2 loss in a mouse model of Rett syndrome. Epigenetics 5: 656-663.

131. Wu H, Tao J, Chen PJ, Shahab A, Ge W, Hart RP, Ruan X, Ruan Y, Sun YE (2010) Genome-wide analysis reveals methyl-CpG-binding protein 2-dependent regulation of microRNAs in a mouse model of Rett syndrome. Proc Natl Acad Sci U S A 107: 18161-18166.

132. Mnatzakanian GN, Lohi H, Munteanu I, Alfred SE, Yamada T, MacLeod PJ, Jones JR, Scherer SW, Schanen NC, et al. (2004) A previously unidentified MECP2 open reading frame defines a new protein isoform relevant to Rett syndrome. Nat Genet 36: 339-341.

133. Kriaucionis S, Bird A (2004) The major form of MeCP2 has a novel N-terminus generated by alternative splicing. Nucleic Acids Res 32: 1818-1823.

134. Adachi M, Keefer EW, Jones FS (2005) A segment of the Mecp2 promoter is sufficient to drive expression in neurons. Hum Mol Genet 14: 3709-3722.

135. Shahbazian MD, Antalffy B, Armstrong DL, Zoghbi HY (2002) Insight into Rett syndrome: MeCP2 levels display tissue- and cell-specific differences and correlate with neuronal maturation. Hum Mol Genet 11: 115-124.

136. Ross PD, Guy J, Selfridge J, Kamal B, Bahey N, Tanner E, Gillingwater TH, Jones RA, Loughrey CM, et al. (2016) Exclusive expression of MeCP2 in the nervous system distinguishes between brain and peripheral Rett syndrome-like phenotypes. Human Molecular Genetics: ddw269.

137. Guideri F, Acampa M (2005) Sudden death and cardiac arrhythmias in Rett syndrome. Pediatr Cardiol 26: 111.

138. Ogier M, Katz DM (2008) Breathing dysfunction in Rett syndrome: understanding epigenetic regulation of the respiratory network. Respir Physiol Neurobiol 164: 55-63.

139. Nomura Y, Segawa M (1992) Motor symptoms of the Rett syndrome: abnormal muscle tone, posture, locomotion and stereotyped movement. Brain Dev 14 Suppl: S21-28.

140. Isaacs JS, Murdock M, Lane J, Percy AK (2003) Eating difficulties in girls with Rett syndrome compared with other developmental disabilities. J Am Diet Assoc 103: 224-230.

141. Ezeonwuka C, Rastegar M (2014) MeCP2-Related Diseases and Animal Models. Diseases 2: 45-70.

142. Miyake K, Nagai K (2007) Phosphorylation of methyl-CpG binding protein 2 (MeCP2) regulates the intracellular localization during neuronal cell differentiation. Neurochem Int 50: 264-270.

143. Shahbazian MD, Antalffy B, Armstrong DL, Zoghbi HY (2002) Insight into Rett syndrome: MeCP2 levels display tissue-and cell-specific differences and correlate with neuronal maturation. Human molecular genetics 11: 115-124.

144. Wither RG, Lang M, Zhang L, Eubanks JH (2013) Regional MeCP2 expression levels in the female MeCP2-deficient mouse brain correlate with specific behavioral impairments. Exp Neurol 239: 49-59.

145. Gemelli T, Berton O, Nelson ED, Perrotti LI, Jaenisch R, Monteggia LM (2006) Postnatal loss of methyl-CpG binding protein 2 in the forebrain is sufficient to mediate behavioral aspects of Rett syndrome in mice. Biol Psychiatry 59: 468-476.

146. Chen RZ, Akbarian S, Tudor M, Jaenisch R (2001) Deficiency of methyl-CpG binding protein-2 in CNS neurons results in a Rett-like phenotype in mice. Nat Genet 27: 327-331.

147. Chao HT, Chen H, Samaco RC, Xue M, Chahrour M, Yoo J, Neul JL, Gong S, Lu HC, et al. (2010) Dysfunction in GABA signalling mediates autism-like stereotypies and Rett syndrome phenotypes. Nature 468: 263-269.

148. Adachi M, Autry AE, Covington HE, 3rd, Monteggia LM (2009) MeCP2-mediated transcription repression in the basolateral amygdala may underlie heightened anxiety in a mouse model of Rett syndrome. J Neurosci 29: 4218-4227.

149. Wu SH, Camarena V (2009) MeCP2 function in the basolateral amygdala in Rett syndrome. J Neurosci 29: 9941-9942.

150. Dragich JM, Kim YH, Arnold AP, Schanen NC (2007) Differential distribution of the MeCP2 splice variants in the postnatal mouse brain. J Comp Neurol 501: 526-542.

151. Squillaro T, Alessio N, Cipollaro M, Melone MAB, Hayek G, Renieri A, Giordano A, Galderisi U (2012) Reduced expression of MECP2 affects cell commitment and maintenance in neurons by triggering senescence: new perspective for Rett syndrome. Molecular Biology of the Cell 23: 1435-1445.

152. Maezawa I, Swanberg S, Harvey D, LaSalle JM, Jin LW (2009) Rett syndrome astrocytes are abnormal and spread MeCP2 deficiency through gap junctions. J Neurosci 29: 5051-5061.

153. Okabe Y, Takahashi T, Mitsumasu C, Kosai K, Tanaka E, Matsuishi T (2012) Alterations of gene expression and glutamate clearance in astrocytes derived from an MeCP2-null mouse model of Rett syndrome. PLoS One 7: e35354.

154. Lioy DT, Garg SK, Monaghan CE, Raber J, Foust KD, Kaspar BK, Hirrlinger PG, Kirchhoff F, Bissonnette JM, et al. (2011) A role for glia in the progression of Rett's syndrome. Nature 475: 497-500.

155. Derecki NC, Cronk JC, Lu Z, Xu E, Abbott SB, Guyenet PG, Kipnis J (2012) Wild-type microglia arrest pathology in a mouse model of Rett syndrome. Nature 484: 105-109.

156. Luikenhuis S, Giacometti E, Beard CF, Jaenisch R (2004) Expression of MeCP2 in postmitotic neurons rescues Rett syndrome in mice. Proc Natl Acad Sci U S A 101: 6033-6038.

157. Nagarajan RP, Hogart AR, Gwye Y, Martin MR, LaSalle JM (2006) Reduced MeCP2 expression is frequent in autism frontal cortex and correlates with aberrant MECP2 promoter methylation. Epigenetics 1: e1-11.

158. Franklin TB, Russig H, Weiss IC, Graff J, Linder N, Michalon A, Vizi S, Mansuy IM (2010) Epigenetic transmission of the impact of early stress across generations. Biol Psychiatry 68: 408-415.

159. Nagarajan RP, Patzel KA, Martin M, Yasui DH, Swanberg SE, Hertz-Picciotto I, Hansen RL, Van de Water J, Pessah IN, et al. (2008) MECP2 promoter methylation and X chromosome inactivation in autism. Autism Res 1: 169-178.

160. Shukla S, Kavak E, Gregory M, Imashimizu M, Shutinoski B, Kashlev M, Oberdoerffer P, Sandberg R, Oberdoerffer S (2011) CTCF-promoted RNA polymerase II pausing links DNA methylation to splicing. Nature 479: 74-79.

161. Liu J, Francke U (2006) Identification of cis-regulatory elements for MECP2 expression. Hum Mol Genet 15: 1769-1782.

162. Vitezic M, Bertin N, Andersson R, Lipovich L, Kawaji H, Lassmann T, Sandelin A, Heutink P, Goldowitz D, et al. (2014) CAGE-defined promoter regions of the genes implicated in Rett Syndrome. BMC Genomics 15: 1177.

163. Coy JF, Sedlacek Z, Bachner D, Delius H, Poustka A (1999) A complex pattern of evolutionary conservation and alternative polyadenylation within the long 3"-untranslated region of the methyl-CpG-binding protein 2 gene (MeCP2) suggests a regulatory role in gene expression. Hum Mol Genet 8: 1253-1262.

164. Pelka GJ, Watson CM, Christodoulou J, Tam PP (2005) Distinct expression profiles of Mecp2 transcripts with different lengths of 3'UTR in the brain and visceral organs during mouse development. Genomics 85: 441-452.

165. Reichwald K, Thiesen J, Wiehe T, Weitzel J, Poustka WA, Rosenthal A, Platzer M, Stratling WH, Kioschis P (2000) Comparative sequence analysis of the MECP2-locus in human and mouse reveals new transcribed regions. Mamm Genome 11: 182-190.

166. Han K, Gennarino VA, Lee Y, Pang K, Hashimoto-Torii K, Choufani S, Raju CS, Oldham MC, Weksberg R, et al. (2013) Human-specific regulation of MeCP2 levels in fetal brains by microRNA miR-483-5p. Genes Dev 27: 485-490.

167. Kuhn DE, Nuovo GJ, Terry AV, Jr., Martin MM, Malana GE, Sansom SE, Pleister AP, Beck WD, Head E, et al. (2010) Chromosome 21-derived microRNAs provide an etiological basis for aberrant protein expression in human Down syndrome brains. J Biol Chem 285: 1529-1543.

168. Klein ME, Lioy DT, Ma L, Impey S, Mandel G, Goodman RH (2007) Homeostatic regulation of MeCP2 expression by a CREB-induced microRNA. Nat Neurosci 10: 1513-1514.

169. Gennarino VA, Alcott CE, Chen CA, Chaudhury A, Gillentine MA, Rosenfeld JA, Parikh S, Wheless JW, Roeder ER, et al. (2015) NUDT21-spanning CNVs lead to neuropsychiatric disease and altered MeCP2 abundance via alternative polyadenylation. Elife 4.

170. Balmer D, Goldstine J, Rao YM, LaSalle JM (2003) Elevated methyl-CpG-binding protein 2 expression is acquired during postnatal human brain development and is correlated with alternative polyadenylation. J Mol Med (Berl) 81: 61-68.

171. Newnham CM, Hall-Pogar T, Liang S, Wu J, Tian B, Hu J, Lutz CS (2010) Alternative polyadenylation of MeCP2: Influence of cis-acting elements and trans-acting factors. RNA Biol 7: 361-372.

172. Rodrigues DC, Kim DS, Yang G, Zaslavsky K, Ha KC, Mok RS, Ross PJ, Zhao M, Piekna A, et al. (2016) MECP2 Is Post-transcriptionally Regulated during Human Neurodevelopment by Combinatorial Action of RNA-Binding Proteins and miRNAs. Cell Rep 17: 720-734.

173. Zhang Y, Chen M, Qiu Z, Hu K, McGee W, Chen X, Liu J, Zhu L, Wu JY (2016) MiR-130a regulates neurite outgrowth and dendritic spine density by targeting MeCP2. Protein Cell 7: 489-500.

174. Su M, Hong J, Zhao Y, Liu S, Xue X (2015) MeCP2 controls hippocampal brain-derived neurotrophic factor expression via homeostatic interactions with microRNA132 in rats with depression. Mol Med Rep 12: 5399-5406.

175. Guo Y, Chen Y, Carreon S, Qiang M (2012) Chronic intermittent ethanol exposure and its removal induce a different miRNA expression pattern in primary cortical neuronal cultures. Alcohol Clin Exp Res 36: 1058-1066.

176. Yan B, Hu Z, Yao W, Le Q, Xu B, Liu X, Ma L (2017) MiR-218 targets MeCP2 and inhibits heroin seeking behavior. Sci Rep 7: 40413.

177. Berletch JB, Yang F, Xu J, Carrel L, Disteche CM (2011) Genes that escape from X inactivation. Hum Genet 130: 237-245.

178. Berletch JB, Yang F, Disteche CM (2010) Escape from X inactivation in mice and humans. Genome Biol 11: 213.

179. Zhao J, Sun BK, Erwin JA, Song JJ, Lee JT (2008) Polycomb proteins targeted by a short repeat RNA to the mouse X chromosome. Science 322: 750-756.

180. Heard E, Disteche CM (2006) Dosage compensation in mammals: fine-tuning the expression of the X chromosome. Genes Dev 20: 1848-1867.

181. Brown CJ, Hendrich BD, Rupert JL, Lafreniere RG, Xing Y, Lawrence J, Willard HF (1992) The human XIST gene: analysis of a 17 kb inactive X-specific RNA that contains conserved repeats and is highly localized within the nucleus. Cell 71: 527-542.

182. Brockdorff N, Ashworth A, Kay GF, McCabe VM, Norris DP, Cooper PJ, Swift S, Rastan S (1992) The product of the mouse Xist gene is a 15 kb inactive X-specific transcript containing no conserved ORF and located in the nucleus. Cell 71: 515-526.

183. Brown CJ, Ballabio A, Rupert JL, Lafreniere RG, Grompe M, Tonlorenzi R, Willard HF (1991) A gene from the region of the human X inactivation centre is expressed exclusively from the inactive X chromosome. Nature 349: 38-44.

184. Prothero KE, Stahl JM, Carrel L (2009) Dosage compensation and gene expression on the mammalian X chromosome: one plus one does not always equal two. Chromosome research 17: 637-648.

185. Deng X, Berletch JB, Nguyen DK, Disteche CM (2014) X chromosome regulation: diverse patterns in development, tissues and disease. Nature Reviews Genetics 15: 367-378.

186. Nguyen DK, Disteche CM (2006) High expression of the mammalian X chromosome in brain. Brain Res 1126: 46-49.

187. Zechner U, Wilda M, Kehrer-Sawatzki H, Vogel W, Fundele R, Hameister H (2001) A high density of X-linked genes for general cognitive ability: a run-away process shaping human evolution? Trends Genet 17: 697-701.

188. Ropers HH (2010) Genetics of early onset cognitive impairment. Annu Rev Genomics Hum Genet 11: 161-187.

189. Skuse DH (2005) X-linked genes and mental functioning. Hum Mol Genet 14 Spec No 1: R27-32.

190. Patrat C, Okamoto I, Diabangouaya P, Vialon V, Le Baccon P, Chow J, Heard E (2009) Dynamic changes in paternal X-chromosome activity during imprinted X-chromosome inactivation in mice. Proceedings of the National Academy of Sciences 106: 5198-5203.

191. Deng X, Berletch JB, Nguyen DK, Disteche CM (2014) X chromosome regulation: diverse patterns in development, tissues and disease. Nat Rev Genet 15: 367-378.

192. Ezeonwuka CD, Rastegar M (2014) MeCP2-Related Diseases and Animal Models. Diseases 2: 45-70.

193. Zoll B, Huppke P, Wessel A, Bartels I, Laccone F (2004) Fetal alcohol syndrome in association with Rett syndrome. Genet Couns 15: 207-212.

194. Wan M, Lee SS, Zhang X, Houwink-Manville I, Song HR, Amir RE, Budden S, Naidu S, Pereira JL, et al. (1999) Rett syndrome and beyond: recurrent spontaneous and familial MECP2 mutations at CpG hotspots. Am J Hum Genet 65: 1520-1529.

195. CDC (2016) Autism Spectrum Disorder (ASD): Data & Statistics. https://www.cdc.gov/ncbddd/autism/data.html

196. Liyanage VR, Curtis K, Zachariah RM, Chudley AE, Rastegar M (2017) Overview of the Genetic Basis and Epigenetic Mechanisms that Contribute to FASD Pathobiology. Curr Top Med Chem 17: 808-828.

197. Renieri A, Meloni I, Longo I, Ariani F, Mari F, Pescucci C, Cambi F (2003) Rett syndrome: the complex nature of a monogenic disease. J Mol Med (Berl) 81: 346-354.

198. Ramocki MB, Tavyev YJ, Peters SU (2010) The MECP2 duplication syndrome. Am J Med Genet A 152A: 1079-1088.

199. Petel-Galil Y, Benteer B, Galil YP, Zeev BB, Greenbaum I, Vecsler M, Goldman B, Lohi H, Minassian BA, et al. (2006) Comprehensive diagnosis of Rett's syndrome relying on genetic, epigenetic and expression evidence of deficiency of the methyl-CpG-binding protein 2 gene: study of a cohort of Israeli patients. J Med Genet 43: e56.

200. Samaco RC, Nagarajan RP, Braunschweig D, LaSalle JM (2004) Multiple pathways regulate MeCP2 expression in normal brain development and exhibit defects in autism-spectrum disorders. Hum Mol Genet 13: 629-639.

201. Kim P, Choi CS, Park JH, Joo SH, Kim SY, Ko HM, Kim KC, Jeon SJ, Park SH, et al. (2014) Chronic exposure to ethanol of male mice before mating produces attention deficit hyperactivity disorder-like phenotype along with epigenetic dysregulation of dopamine transporter expression in mouse offspring. J Neurosci Res 92: 658-670.

202. Subbanna S, Nagre NN, Shivakumar M, Umapathy NS, Psychoyos D, Basavarajappa BS (2014) Ethanol induced acetylation of histone at G9a exon1 and G9a-mediated histone H3 dimethylation leads to neurodegeneration in neonatal mice. Neuroscience 258: 422-432.

203. Tunc-Ozcan E, Ullmann TM, Shukla PK, Redei EE (2013) Low-dose thyroxine attenuates autism-associated adverse effects of fetal alcohol in male offspring's social behavior and hippocampal gene expression. Alcohol Clin Exp Res 37: 1986-1995.

204. Gangisetty O, Bekdash R, Maglakelidze G, Sarkar DK (2014) Fetal Alcohol Exposure Alters Proopiomelanocortin Gene Expression and Hypothalamic-Pituitary-Adrenal Axis Function via Increasing MeCP2 Expression in the Hypothalamus. PLoS One 9: e113228.

205. Perkins A, Lehmann C, Lawrence RC, Kelly SJ (2013) Alcohol exposure during development: Impact on the epigenome. Int J Dev Neurosci 31: 391-397.

206. Bekdash RA, Zhang C, Sarkar DK (2013) Gestational choline supplementation normalized fetal alcohol-induced alterations in histone modifications, DNA methylation, and proopiomelanocortin (POMC) gene expression in beta-endorphin-producing POMC neurons of the hypothalamus. Alcohol Clin Exp Res 37: 1133-1142.

207. Kim P, Park JH, Choi CS, Choi I, Joo SH, Kim MK, Kim SY, Kim KC, Park SH, et al. (2013) Effects of ethanol exposure during early pregnancy in hyperactive, inattentive and impulsive behaviors and MeCP2 expression in rodent offspring. Neurochem Res 38: 620-631.

208. Chen Y, Ozturk NC, Zhou FC (2013) DNA methylation program in developing hippocampus and its alteration by alcohol. PLoS One 8: e60503.

209. Chunshu Y, Endoh K, Soutome M, Kawamura R, Kubota T (2006) A patient with classic Rett syndrome with a novel mutation in MECP2 exon 1. Clin Genet 70: 530-531.

210. Quenard A, Yilmaz S, Fontaine H, Bienvenu T, Moncla A, des Portes V, Rivier F, Mathieu M, Raux G, et al. (2006) Deleterious mutations in exon 1 of MECP2 in Rett syndrome. Eur J Med Genet 49: 313-322.

211. Saxena A, de Lagarde D, Leonard H, Williamson SL, Vasudevan V, Christodoulou J, Thompson E, MacLeod P, Ravine D (2006) Lost in translation: translational interference from a recurrent mutation in exon 1 of MECP2. J Med Genet 43: 470-477.

212. Sheikh TI, Mittal K, Willis MJ, Vincent JB (2013) A synonymous change, p.Gly16Gly in MECP2 Exon 1, causes a cryptic splice event in a Rett syndrome patient. Orphanet J Rare Dis 8: 108.

213. Hoffbuhr KC, Moses LM, Jerdonek MA, Naidu S, Hoffman EP (2002) Associations between MeCP2 mutations, X-chromosome inactivation, and phenotype. Ment Retard Dev Disabil Res Rev 8: 99-105.

214. Van Esch H (1993) MECP2 Duplication Syndrome. In: Pagon RA, Adam MP, Ardinger HH, Wallace SE, Amemiya A et al., editors. GeneReviews(R). Seattle (WA).

215. Liyanage VR, Zachariah RM, Davie JR, Rastegar M (2015) Ethanol deregulates Mecp2/MeCP2 in differentiating neural stem cells via interplay between 5-methylcytosine and 5-hydroxymethylcytosine at the Mecp2 regulatory elements. Exp Neurol 265: 102-117.

216. Lombardi LM, Baker SA, Zoghbi HY (2015) MECP2 disorders: from the clinic to mice and back. J Clin Invest 125: 2914-2923.

217. Hagberg B, Aicardi J, Dias K, Ramos O (1983) A progressive syndrome of autism, dementia, ataxia, and loss of purposeful hand use in girls: Rett's syndrome: report of 35 cases. Ann Neurol 14: 471-479.

218. Neul JL, Kaufmann WE, Glaze DG, Christodoulou J, Clarke AJ, Bahi-Buisson N, Leonard H, Bailey ME, Schanen NC, et al. (2010) Rett syndrome: revised diagnostic criteria and nomenclature. Ann Neurol 68: 944-950.

219. Kaufmann WE, Stallworth JL, Everman DB, Skinner SA (2016) Neurobiologically-based treatments in Rett syndrome: opportunities and challenges. Expert Opin Orphan Drugs 4: 1043-1055.

220. Amir RE, Van den Veyver IB, Wan M, Tran CQ, Francke U, Zoghbi HY (1999) Rett syndrome is caused by mutations in X-linked MECP2, encoding methyl-CpG-binding protein 2. Nat Genet 23: 185-188.

221. Cheadle JP, Gill H, Fleming N, Maynard J, Kerr A, Leonard H, Krawczak M, Cooper DN, Lynch S, et al. (2000) Long-read sequence analysis of the MECP2 gene in Rett syndrome patients: correlation of disease severity with mutation type and location. Hum Mol Genet 9: 1119-1129.

222. Saunders CJ, Minassian BE, Chow EW, Zhao W, Vincent JB (2009) Novel exon 1 mutations in MECP2 implicate isoform MeCP2_e1 in classical Rett syndrome. Am J Med Genet A 149A: 1019-1023.

223. Bartholdi D, Klein A, Weissert M, Koenig N, Baumer A, Boltshauser E, Schinzel A, Berger W, Matyas G (2006) Clinical profiles of four patients with Rett syndrome carrying a novel exon 1 mutation or genomic rearrangement in the MECP2 gene. Clin Genet 69: 319-326.

224. Ravn K, Nielsen JB, Schwartz M (2005) Mutations found within exon 1 of MECP2 in Danish patients with Rett syndrome. Clin Genet 67: 532-533.

225. Amir RE, Fang P, Yu Z, Glaze DG, Percy AK, Zoghbi HY, Roa BB, Van den Veyver IB (2005) Mutations in exon 1 of MECP2 are a rare cause of Rett syndrome. J Med Genet 42: e15.

226. Evans JC, Archer HL, Whatley SD, Kerr A, Clarke A, Butler R (2005) Variation in exon 1 coding region and promoter of MECP2 in Rett syndrome and controls. Eur J Hum Genet 13: 124-126.

227. Itoh M, Tahimic CG, Ide S, Otsuki A, Sasaoka T, Noguchi S, Oshimura M, Goto Y, Kurimasa A (2012) Methyl CpG-binding protein isoform MeCP2_e2 is dispensable for Rett syndrome phenotypes but essential for embryo viability and placenta development. J Biol Chem 287: 13859-13867.

228. Petel-Galil Y, Benteev B, Galil YP, Zeev BB, Greenbaum I, Vecsler M, Goldman B, Lohi H, Minassian BA, et al. (2006) Comprehensive diagnosis of Rett's syndrome relying on genetic, epigenetic and expression evidence of deficiency of the methyl-CpG-binding protein 2 gene: study of a cohort of Israeli patients. Journal of Medical Genetics 43: e56-e56.

229. Fichou Y, Nectoux J, Bahi-Buisson N, Rosas-Vargas H, Girard B, Chelly J, Bienvenu T (2008) The first missense mutation causing Rett syndrome specifically affecting the MeCP2_e1 isoform. neurogenetics 10: 127.

230. Sheikh TI, Mittal K, Willis MJ, Vincent JB (2013) A synonymous change, p.Gly16Gly in MECP2 Exon 1, causes a cryptic splice event in a Rett syndrome patient. Orphanet Journal of Rare Diseases 8: 108.

231. Pitcher MR, Herrera JA, Buffington SA, Kochukov MY, Merritt JK, Fisher AR, Schanen NC, Costa-Mattioli M, Neul JL (2015) Rett syndrome like phenotypes in the R255X

Mecp2 mutant mouse are rescued by MECP2 transgene. Human Molecular Genetics 24: 2662-2672.

232. Vieira JP, Lopes F, Silva-Fernandes A, Sousa MV, Moura S, Sousa S, Costa BM, Barbosa M, Ylstra B, et al. (2015) Variant Rett syndrome in a girl with a pericentric X-chromosome inversion leading to epigenetic changes and overexpression of the MECP2 gene. Int J Dev Neurosci 46: 82-87.

233. Miyake K, Yang C, Minakuchi Y, Ohori K, Soutome M, Hirasawa T, Kazuki Y, Adachi N, Suzuki S, et al. (2013) Comparison of Genomic and Epigenomic Expression in Monozygotic Twins Discordant for Rett Syndrome. PLoS One 8: e66729.

234. Nino-Soto M, Nuber UA, Basrur P, Ropers H-H, King W (2005) Differences in the pattern of X-linked gene expression between fetal bovine muscle and fibroblast cultures derived from the same muscle biopsies. Cytogenetic and genome research 111: 57-64.

235. Villard L, Levy N, Xiang F, Kpebe A, Labelle V, Chevillard C, Zhang Z, Schwartz CE, Tardieu M, et al. (2001) Segregation of a totally skewed pattern of X chromosome inactivation in four familial cases of Rett syndrome without MECP2 mutation: implications for the disease. J Med Genet 38: 435-442.

236. Sirianni N, Naidu S, Pereira J, Pillotto RF, Hoffman EP (1998) Rett syndrome: confirmation of X-linked dominant inheritance, and localization of the gene to Xq28. Am J Hum Genet 63: 1552-1558.

237. Schanen NC, Dahle EJ, Capozzoli F, Holm VA, Zoghbi HY, Francke U (1997) A new Rett syndrome family consistent with X-linked inheritance expands the X chromosome exclusion map. Am J Hum Genet 61: 634-641.

238. Weaving LS, Williamson SL, Bennetts B, Davis M, Ellaway CJ, Leonard H, Thong MK, Delatycki M, Thompson EM, et al. (2003) Effects of MECP2 mutation type, location and X-inactivation in modulating Rett syndrome phenotype. Am J Med Genet A 118A: 103-114.

239. Krepischi AC, Kok F, Otto PG (1998) X chromosome-inactivation patterns in patients with Rett syndrome. Hum Genet 102: 319-321.

240. Camus P, Abbadi N, Perrier MC, Chery M, Gilgenkrantz S (1996) X chromosome inactivation in 30 girls with Rett syndrome: analysis using the probe. Hum Genet 97: 247-250.

241. Kerr B, Soto CJ, Saez M, Abrams A, Walz K, Young JI (2012) Transgenic complementation of MeCP2 deficiency: phenotypic rescue of Mecp2-null mice by isoform-specific transgenes. Eur J Hum Genet 20: 69-76.

242. Guy J, Gan J, Selfridge J, Cobb S, Bird A (2007) Reversal of neurological defects in a mouse model of Rett syndrome. Science 315: 1143-1147.

243. Jugloff DG, Vandamme K, Logan R, Visanji NP, Brotchie JM, Eubanks JH (2008) Targeted delivery of an Mecp2 transgene to forebrain neurons improves the behavior of female Mecp2-deficient mice. Hum Mol Genet 17: 1386-1396.

244. Giacometti E, Luikenhuis S, Beard C, Jaenisch R (2007) Partial rescue of MeCP2 deficiency by postnatal activation of MeCP2. Proc Natl Acad Sci U S A 104: 1931-1936.

245. Brendel C, Klahold E, Gartner J, Huppke P (2009) Suppression of nonsense mutations in Rett syndrome by aminoglycoside antibiotics. Pediatr Res 65: 520-523.

246. Brendel C, Belakhov V, Werner H, Wegener E, Gartner J, Nudelman I, Baasov T, Huppke P (2011) Readthrough of nonsense mutations in Rett syndrome: evaluation of novel aminoglycosides and generation of a new mouse model. J Mol Med (Berl) 89: 389-398.

247. Popescu AC, Sidorova E, Zhang G, Eubanks JH (2010) Aminoglycoside-mediated partial suppression of MECP2 nonsense mutations responsible for Rett syndrome in vitro. J Neurosci Res 88: 2316-2324.

248. Vecsler M, Ben Zeev B, Nudelman I, Anikster Y, Simon AJ, Amariglio N, Rechavi G, Baasov T, Gak E (2011) Ex vivo treatment with a novel synthetic aminoglycoside NB54 in primary fibroblasts from Rett syndrome patients suppresses MECP2 nonsense mutations. PLoS One 6: e20733.

249. Yu D, Sakurai F, Corey DR (2011) Clonal Rett Syndrome cell lines to test compounds for activation of wild-type MeCP2 expression. Bioorg Med Chem Lett 21: 5202-5205.

250. Ben-Zeev B, Aharoni R, Nissenkorn A, Arnon R (2011) Glatiramer acetate (GA, Copolymer-1) an hypothetical treatment option for Rett syndrome. Med Hypotheses 76: 190-193.

251. Kline DD, Ogier M, Kunze DL, Katz DM (2010) Exogenous brain-derived neurotrophic factor rescues synaptic dysfunction in Mecp2-null mice. J Neurosci 30: 5303-5310.

252. Tropea D, Giacometti E, Wilson NR, Beard C, McCurry C, Fu DD, Flannery R, Jaenisch R, Sur M (2009) Partial reversal of Rett Syndrome-like symptoms in MeCP2 mutant mice. Proc Natl Acad Sci U S A 106: 2029-2034.

253. Pini G, Scusa MF, Congiu L, Benincasa A, Morescalchi P, Bottiglioni I, Di Marco P, Borelli P, Bonuccelli U, et al. (2012) IGF1 as a Potential Treatment for Rett Syndrome: Safety Assessment in Six Rett Patients. Autism Res Treat 2012: 679801.

254. Marchetto MC, Carromeu C, Acab A, Yu D, Yeo GW, Mu Y, Chen G, Gage FH, Muotri AR (2010) A model for neural development and treatment of Rett syndrome using human induced pluripotent stem cells. Cell 143: 527-539.

255. Nag N, Mellott TJ, Berger-Sweeney JE (2008) Effects of postnatal dietary choline supplementation on motor regional brain volume and growth factor expression in a mouse model of Rett syndrome. Brain Res 1237: 101-109.

256. Hagebeuk EE, Koelman JH, Duran M, Abeling NG, Vyth A, Poll-The BT (2011) Clinical and electroencephalographic effects of folinic acid treatment in Rett syndrome patients. J Child Neurol 26: 718-723.

257. Schaevitz LR, Nicolai R, Lopez CM, D'Iddio S, Iannoni E, Berger-Sweeney JE (2012) Acetyl-L-carnitine improves behavior and dendritic morphology in a mouse model of Rett syndrome. PLoS One 7: e51586.

258. De Felice C, Signorini C, Durand T, Ciccoli L, Leoncini S, D'Esposito M, Filosa S, Oger C, Guy A, et al. (2012) Partial rescue of Rett syndrome by omega-3 polyunsaturated fatty acids (PUFAs) oil. Genes Nutr 7: 447-458.

259. Kondo M, Gray LJ, Pelka GJ, Christodoulou J, Tam PP, Hannan AJ (2008) Environmental enrichment ameliorates a motor coordination deficit in a mouse model of Rett syndrome-- Mecp2 gene dosage effects and BDNF expression. Eur J Neurosci 27: 3342-3350.

260. Lonetti G, Angelucci A, Morando L, Boggio EM, Giustetto M, Pizzorusso T (2010) Early environmental enrichment moderates the behavioral and synaptic phenotype of MeCP2 null mice. Biol Psychiatry 67: 657-665.

261. Kerr B, Silva PA, Walz K, Young JI (2010) Unconventional transcriptional response to environmental enrichment in a mouse model of Rett syndrome. PLoS One 5: e11534.

262. Vignoli A, Borgatti R, Peron A, Zucca C, Ballarati L, Bonaglia C, Bellini M, Giordano L, Romaniello R, et al. (2012) Electroclinical pattern in MECP2 duplication syndrome: eight new reported cases and review of literature. Epilepsia 53: 1146-1155.

263. Friez MJ, Jones JR, Clarkson K, Lubs H, Abuelo D, Bier JA, Pai S, Simensen R, Williams C, et al. (2006) Recurrent infections, hypotonia, and mental retardation caused by duplication of MECP2 and adjacent region in Xq28. Pediatrics 118: e1687-1695.

264. Van Esch H, Bauters M, Ignatius J, Jansen M, Raynaud M, Hollanders K, Lugtenberg D, Bienvenu T, Jensen LR, et al. (2005) Duplication of the MECP2 region is a frequent cause of severe mental retardation and progressive neurological symptoms in males. Am J Hum Genet 77: 442-453.

265. Ramocki MB, Tavyev YJ, Peters SU (2010) The MECP2 duplication syndrome. American journal of medical genetics Part A 152: 1079-1088.

266. Ramocki MB, Tavyev YJ, Peters SU (2010) The MECP2 Duplication Syndrome. American journal of medical genetics Part A 152A: 1079-1088.

267. Hanchard NA, Carvalho CMB, Bader P, Thome A, Omo-Griffith L, del Gaudio D, Pehlivan D, Fang P, Schaaf CP, et al. (2012) A partial MECP2 duplication in a mildly affected adult male: a putative role for the 3' untranslated region in the MECP2 duplication phenotype. BMC Medical Genetics 13: 71-71.

268. Novara F, Simonati A, Sicca F, Battini R, Fiori S, Contaldo A, Criscuolo L, Zuffardi O, Ciccone R (2014) MECP2 duplication phenotype in symptomatic females: report of three further cases. Molecular Cytogenetics 7: 10-10.

269. Shimada S, Okamoto N, Ito M, Arai Y, Momosaki K, Togawa M, Maegaki Y, Sugawara M, Shimojima K, et al. (2013) MECP2 duplication syndrome in both genders. Brain Dev 35: 411-419.

270. Sztainberg Y, Chen HM, Swann JW, Hao S, Tang B, Wu Z, Tang J, Wan YW, Liu Z, et al. (2015) Reversal of phenotypes in MECP2 duplication mice using genetic rescue or antisense oligonucleotides. Nature 528: 123-126.

271. Disorders NOoR (2013) MECP2 Duplication Syndrome.

272. Nascimento FA, Faghfoury H, Krings T, Ali A, Fridhandler JD, Lozano A, Wennberg R, Andrade DM (2014) Deep brain stimulation for the management of seizures in MECP2 duplication syndrome. Seizure 23: 405-407.

273. Nonkin Avchen R, Bhasin TK, van naarden braun K, Yeargin-Allsopp M (2006) Public Health Impact: Metropolitan Atlanta Developmental Disabilities Surveillance Program*. International Review of Research in Mental Retardation: Academic Press. pp. 149-190.

274. Speaks A (2013) DSM-5 diagnostic criteria. Retrieved August 12: 2013.

275. Geschwind DH (2008) Autism: Many Genes, Common Pathways? Cell 135: 391-395.

276. Hu-Lince D, Craig DW, Huentelman MJ, Stephan DA (2005) The Autism Genome Project. American Journal of Pharmacogenomics 5: 233-246.

277. Rangasamy S, D'Mello SR, Narayanan V (2013) Epigenetics, autism spectrum, and neurodevelopmental disorders. Neurotherapeutics 10: 742-756.

278. Voineagu I (2012) Gene expression studies in autism: moving from the genome to the transcriptome and beyond. Neurobiology of disease 45: 69-75.

279. Zhubi A, Chen Y, Dong E, Cook EH, Guidotti A, Grayson DR (2014) Increased binding of MeCP2 to the GAD1 and RELN promoters may be mediated by an enrichment of 5-hmC in autism spectrum disorder (ASD) cerebellum. Translational Psychiatry 4: e349.

280. Peters SU, Hundley RJ, Wilson AK, Warren Z, Vehorn A, Carvalho C, Lupski JR, Ramocki MB (2013) The behavioral phenotype in MECP2 duplication syndrome: a comparison with idiopathic autism. Autism Research 6: 42-50.

281. Cukier HN, Lee JM, Ma D, Young JI, Mayo V, Butler BL, Ramsook SS, Rantus JA, Abrams AJ, et al. (2012) The expanding role of MBD genes in autism: identification of a MECP2 duplication and novel alterations in MBD5, MBD6, and SETDB1. Autism Research 5: 385-397.

282. Tantra M, Hammer C, Kastner A, Dahm L, Begemann M, Bodda C, Hammerschmidt K, Giegling I, Stepniak B, et al. (2014) Mild expression differences of MECP2 influencing aggressive social behavior. EMBO Mol Med 6: 662-684.

283. Bodda C, Tantra M, Mollajew R, Arunachalam JP, Laccone FA, Can K, Rosenberger A, Mironov SL, Ehrenreich H, et al. (2013) Mild overexpression of Mecp2 in mice causes a higher susceptibility toward seizures. Am J Pathol 183: 195-210.

284. Taylor MM, Doshi S (2012) Insights into the cellular and molecular contributions of MeCP2 overexpression to disease pathophysiology. J Neurosci 32: 9451-9453.

285. Shibayama A, Cook EH, Jr., Feng J, Glanzmann C, Yan J, Craddock N, Jones IR, Goldman D, Heston LL, et al. (2004) MECP2 structural and 3'-UTR variants in schizophrenia, autism and other psychiatric diseases: a possible association with autism. Am J Med Genet B Neuropsychiatr Genet 128B: 50-53.

286. Coutinho AM, Oliveira G, Katz C, Feng J, Yan J, Yang C, Marques C, Ataide A, Miguel TS, et al. (2007) MECP2 coding sequence and 3'UTR variation in 172 unrelated autistic patients. Am J Med Genet B Neuropsychiatr Genet 144B: 475-483.

287. Matoulkova E, Michalova E, Vojtesek B, Hrstka R (2012) The role of the 3'untranslated region in post-transcriptional regulation of protein expression in mammalian cells. RNA biology 9: 563-576.

288. Shibayama A, Cook EH, Feng J, Glanzmann C, Yan J, Craddock N, Jones IR, Goldman D, Heston LL, et al. (2004) MECP2 structural and 3′-UTR variants in schizophrenia, autism and other psychiatric diseases: A possible association with autism. American Journal of Medical Genetics Part B: Neuropsychiatric Genetics 128B: 50-53.

289. Coutinho AM, Oliveira G, Katz C, Feng J, Yan J, Yang C, Marques C, Ataíde A, Miguel TS, et al. (2007) MECP2 coding sequence and 3′UTR variation in 172 unrelated autistic patients. American Journal of Medical Genetics Part B: Neuropsychiatric Genetics 144B: 475-483.

290. Xi CY, Ma HW, Lu Y, Zhao YJ, Hua TY, Zhao Y, Ji YH (2007) MeCP2 gene mutation analysis in autistic boys with developmental regression. Psychiatr Genet 17: 113-116.

291. Vourc'h P, Bienvenu T, Beldjord C, Chelly J, Barthelemy C, Muh JP, Andres C (2001) No mutations in the coding region of the Rett syndrome gene MECP2 in 59 autistic patients. Eur J Hum Genet 9: 556-558.

292. Zappella M, Meloni I, Longo I, Canitano R, Hayek G, Rosaia L, Mari F, Renieri A (2003) Study of MECP2 gene in Rett syndrome variants and autistic girls. Am J Med Genet B Neuropsychiatr Genet 119B: 102-107.

293. Myers SM, Johnson CP (2007) Management of children with autism spectrum disorders. Pediatrics 120: 1162-1182.

294. Ameis SH, Daskalakis ZJ, Blumberger DM, Desarkar P, Drmic I, Mabbott DJ, Lai M-C, Croarkin PE, Szatmari P (2017) Repetitive Transcranial Magnetic Stimulation for the Treatment of Executive Function Deficits in Autism Spectrum Disorder: Clinical Trial Approach. Journal of Child and Adolescent Psychopharmacology.

295. Enticott PG, Fitzgibbon BM, Kennedy HA, Arnold SL, Elliot D, Peachey A, Zangen A, Fitzgerald PB (2014) A double-blind, randomized trial of deep repetitive transcranial magnetic stimulation (rTMS) for autism spectrum disorder. Brain Stimul 7: 206-211.

296. Baruth JM, Casanova MF, El-Baz A, Horrell T, Mathai G, Sears L, Sokhadze E (2010) Low-Frequency Repetitive Transcranial Magnetic Stimulation (rTMS) Modulates Evoked-Gamma Frequency Oscillations in Autism Spectrum Disorder (ASD). J Neurother 14: 179-194.

297. Hendren RL, James SJ, Widjaja F, Lawton B, Rosenblatt A, Bent S (2016) Randomized, Placebo-Controlled Trial of Methyl B12 for Children with Autism. J Child Adolesc Psychopharmacol 26: 774-783.

298. FASlink (2010) The FASlink Collection.

299. Chudley AE, Conry J, Cook JL, Loock C, Rosales T, LeBlanc N (2005) Fetal alcohol spectrum disorder: Canadian guidelines for diagnosis. CMAJ : Canadian Medical Association Journal 172: S1-S21.

300. Govorko D, Bekdash RA, Zhang C, Sarkar DK (2012) Male germline transmits fetal alcohol adverse effect on hypothalamic proopiomelanocortin gene across generations. Biol Psychiatry 72: 378-388.

301. Muralidharan P, Sarmah S, Marrs JA (2015) Zebrafish retinal defects induced by ethanol exposure are rescued by retinoic acid and folic acid supplement. Alcohol 49: 149-163.

302. Karch SB (2007) Drug abuse handbook. Boca Raton: CRC Press/Taylor & Francis. 1267 p. p.

303. Haycock PC (2009) Fetal alcohol spectrum disorders: the epigenetic perspective. Biol Reprod 81: 607-617.

304. Lee BY, Park SY, Ryu HM, Shin CY, Ko KN, Han JY, Koren G, Cho YH (2015) Changes in the methylation status of DAT, SERT, and MeCP2 gene promoters in the blood cell in

Chapter 1

families exposed to alcohol during the periconceptional period. Alcohol Clin Exp Res 39: 239-250.

305. Repunte-Canonigo V, Chen J, Lefebvre C, Kawamura T, Kreifeldt M, Basson O, Roberts AJ, Sanna PP (2014) MeCP2 regulates ethanol sensitivity and intake. Addict Biol 19: 791-799.

306. Hunihan L, Brown J, Cacace A, Fernandes A, Weston A (2017) Generation of a clonal induced pluripotent stem cell (iPSC) line expressing the mutant MECP2 allele from a Rett Syndrome patient fibroblast line. Stem Cell Res 20: 67-69.

307. Larimore J, Ryder PV, Kim KY, Ambrose LA, Chapleau C, Calfa G, Gross C, Bassell GJ, Pozzo-Miller L, et al. (2013) MeCP2 regulates the synaptic expression of a Dysbindin-BLOC-1 network component in mouse brain and human induced pluripotent stem cell-derived neurons. PLoS One 8: e65069.

308. Bertulat B, De Bonis ML, Della Ragione F, Lehmkuhl A, Milden M, Storm C, Jost KL, Scala S, Hendrich B, et al. (2012) MeCP2 dependent heterochromatin reorganization during neural differentiation of a novel Mecp2-deficient embryonic stem cell reporter line. PLoS One 7: e47848.

309. Olynik BM, Rastegar M (2012) The genetic and epigenetic journey of embryonic stem cells into mature neural cells. Front Genet 3: 81.

310. Mitalipov S, Wolf D (2009) Totipotency, pluripotency and nuclear reprogramming. Adv Biochem Eng Biotechnol 114: 185-199.

311. Binder MD, Hirokawa N, Windhorst U (2009) Encyclopedia of neuroscience: Springer Berlin, Heidelberg.

312. Urban N, Guillemot F (2014) Neurogenesis in the embryonic and adult brain: same regulators, different roles. Front Cell Neurosci 8: 396.

313. Urbán N, Guillemot F (2014) Neurogenesis in the embryonic and adult brain: same regulators, different roles. Frontiers in Cellular Neuroscience 8: 396.

314. Paridaen JT, Huttner WB (2014) Neurogenesis during development of the vertebrate central nervous system. EMBO Rep 15: 351-364.

315. Rowitch DH, Kriegstein AR (2010) Developmental genetics of vertebrate glial-cell specification. Nature 468: 214-222.

316. Gotz M, Huttner WB (2005) The cell biology of neurogenesis. Nat Rev Mol Cell Biol 6: 777-788.

317. Qian X, Shen Q, Goderie SK, He W, Capela A, Davis AA, Temple S (2000) Timing of CNS cell generation: a programmed sequence of neuron and glial cell production from isolated murine cortical stem cells. Neuron 28: 69-80.

318. Ming G-l, Song H (2011) Adult Neurogenesis in the Mammalian Brain: Significant Answers and Significant Questions. Neuron 70: 687-702.

319. Paridaen JT, Huttner WB (2014) Neurogenesis during development of the vertebrate central nervous system. EMBO reports 15: 351-364.

320. Ge WP, Miyawaki A, Gage FH, Jan YN, Jan LY (2012) Local generation of glia is a major astrocyte source in postnatal cortex. Nature 484: 376-380.

321. Pinto L, Gotz M (2007) Radial glial cell heterogeneity--the source of diverse progeny in the CNS. Prog Neurobiol 83: 2-23.

322. Malatesta P, Hack MA, Hartfuss E, Kettenmann H, Klinkert W, Kirchhoff F, Gotz M (2003) Neuronal or glial progeny: regional differences in radial glia fate. Neuron 37: 751-764.

323. Kwan KY The generation and migration of neocortical projection neurons. https://sites.google.com/a/umich.edu/kwanlab/background

324. Van Den Ameele J, Tiberi L, Vanderhaeghen P, Espuny-Camacho I (2014) Thinking out of the dish: what to learn about cortical development using pluripotent stem cells. Trends in neurosciences 37: 334-342.

325. Johe KK, Hazel TG, Muller T, Dugich-Djordjevic MM, McKay RD (1996) Single factors direct the differentiation of stem cells from the fetal and adult central nervous system. Genes Dev 10: 3129-3140.

326. Hermanson O, Jepsen K, Rosenfeld MG (2002) N-CoR controls differentiation of neural stem cells into astrocytes. Nature 419: 934-939.

327. Doering LC (2010) Protocols for neural cell culture: Springer.

328. Barber BA (2012) A study of primary neural stem cell differentiation in vitro, focusing on the Three Amino acid Loop Extension (TALE) homeobox transcription factors: University of Manitoba.

329. Barber BA, Liyanage VR, Zachariah RM, Olson CO, Bailey MA, Rastegar M (2013) Dynamic expression of MEIS1 homeoprotein in E14.5 forebrain and differentiated forebrain-derived neural stem cells. Ann Anat 195: 431-440.

330. Zachariah R (2017) Investigating MeCP2 isoform-specific expression and function: University of Manitoba.

CHAPTER 2. MATERIALS AND METHODS

2.1 Ethics

All experiments were performed in agreement with the standards of the Canadian Council on animal care with the approval of the office of research ethics at the University of Manitoba, and according to the peer-reviewed and approved animal protocols (protocol numbers: 09-020/1/2, 12-031, 12-031/1/2, 12-031/1/2/3).

2.2 Experimental biological replicates

The biological and technical replicates were determined based on previously known definitions. "Biological replicates are biologically distinct samples (e.g., the same type of organism treated or grown in the same conditions), which show biological variation." [1]. "A technical replicate consists of repeating the analysis of the same sample several times. Such an approach allows for the evaluation of the variability inherent to the technique being applied." [2].

All experiments were performed in primary cells (NSC, neurons or astrocytes) isolated from 2-3 separate pregnant mice, and were tested for reproducibility multiple times, unless in few cases that are stated in the thesis (e.g., qRT-PCR for female neurons Chapter 5). In most cases, the final results represent data from multiple biological replicates that were processed simultaneously. Unless stated otherwise, a minimum of three biological replicates was collected simultaneously to perform all required analyses from the same batch of harvested primary cells. NSC, neuronal and astrocytic cultures from the embryos collected from each pregnant mouse were carried out separately and collected separately according to the definition of biological replicates. Experiments conducted on the same day (e.g., cell culture) from individual mice were considered independent as the mice were coming from a larger breeding colony [3].

2.3 NSC differentiation

NSC isolated from the forebrain of E14.5 CD1 mice were cultured as previously described [4,5]. A schematic of the NSC differentiation and treatments used in this thesis is shown in **Figure 2.1**. Dr. Mojgan Rastegar carried out isolation, culture, and differentiation of primary brain-derived neural stem cells.
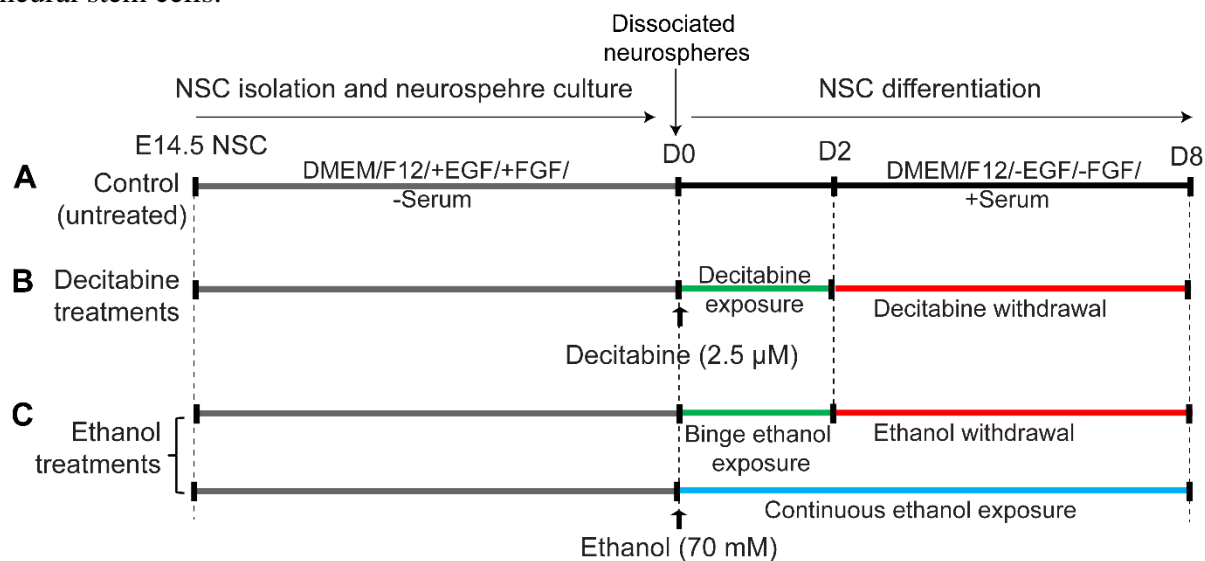
Figure 2.1 Differentiation of NSC and decitabine or ethanol treatments.

A) Schematic representation of isolation of NSC from the forebrains of E14.5, culturing them to generate neurospheres and differentiation of dissociated neurosphere cells into neurons, astrocytes, and oligodendrocytes. Differentiating NSC without any treatment were used as control experiments. **B)** Schematic of decitabine treatment to study the effect of DNA demethylation. Decitabine (2.5 µM) was added to the cells (dissociated neurosphere cells: D0) at the beginning of NSC differentiation for two days, and samples were collected at D2 to study the effect of decitabine exposure. Cells were cultured in media with serum and continued to differentiate till D8 for decitabine withdrawal. **C)** Binge ethanol exposure was modeled by adding 70 mM of ethanol to dissociated neurospheres at D0 for two days until D2. Ethanol withdrawal was modeled by removal of ethanol at D2, and cells were differentiated for extra six days till D8. Continuous ethanol exposure was modeled by treating differentiating NSC with ethanol continuously for eight days. Media was refreshed every other day.

Figure modified from [6,7].

In brief, dissected forebrain tissues were dissociated into single cells in NSC media: Dulbecco's modified eagle medium: nutrient mixture F-12 1:1 (DMEM/F12; Wisent) containing 4-(2-hydroxyethyl)-1-piperazineethanesulfonic acid (HEPES), glutamine, antibiotic/antimycotic, glucose, recombinant human epidermal growth factor (rhEGF; Sigma, 20 ng/ml), basic fibroblast growth factor (bFGF; 20 ng/ml), heparin (Sigma, 2 µg/ml) and hormone mix [glucose (0.6%), insulin (0.25 mg/ml), transferrin (1 mg/ml), progesterone (0.2 µM), putrescine (0.097 mg/ml), sodium selenite (0.3µM)] and plated at a density of 10^5 cells/cm^2 in serum-free full NSC media. Cells were cultured for seven days to generate primary neurospheres. Dissociated neurospheres were plated in growth factor-reduced matrigel coated-plates (BD Biosciences) at a density of 10^5 cells/cm^2 in DMEM media (GIBCO) containing 10% fetal bovine serum (FBS, Invitrogen) in the absence of rhEGF and bFGF. Cells were differentiated for eight days under these conditions, reported to be sufficient for both neuronal and glial differentiation [4,5].

2.4 Decitabine treatment during NSC differentiation

NSC differentiation was done as described in section 2.3. Decitabine, which is a known DNA demethylating agent [8,9] was used to investigate the role of DNA methylation in regulation of *Mecp2* expression. Concentration was chosen based on a gradient experiment consisting of 1, 2.5 and 5 µM decitabine. As 2.5 µM showed least cellular toxicity, it was chosen for further experiments. At the beginning of NSC differentiation, which is herein referred to as D0, dissociated NSC were treated with 2.5 µM decitabine for 48 h **(Figure 2.1B)**. After two days (D2), media was replaced with fresh media every other day for an extra six days (until D8). This set of experiments was considered as decitabine withdrawal. Control cells were cultured under similar experimental conditions, in the absence of decitabine **(Figure 2.1A)**. Cell pellets were collected at

D0, D2, and D8 for RNA, DNA and protein extractions. Neurospheres were collected for mounting, sectioning, and immunohistochemistry experiments. Cells were grown on coverslips in 24-well plates for fixation and immunocytochemistry.

2.5 Ethanol treatments during NSC differentiation

Ethanol treatments were carried out to study the effects of alcohol exposure on gene expression and *Mecp2* deregulation during NSC differentiation. These experiments were designed for obtaining insights regarding the influence of alcohol (ethanol) on embryonic brain cells, that might provide further understanding of FASD or alcohol-related neurological disorders. Ethanol concentration was chosen based on a dose-response experiment of 35, 70, 105 mM. The 70-mM concentration was chosen as it caused minimal cell death. Moreover, the selected concentration of ethanol was in agreement with previous research studies reporting, a) the blood alcohol levels detected in alcoholics (30-100 mM) [10], b) the effects of ethanol on isolated NSC from human fetal brain (20-100 mM) [11], and c) conditions which show minimal effects on cell proliferation and survival of cultured NSC (22-70 mM) [12].

Neurospheres were dissociated to obtain single cells that were cultured for differentiation as described in section 2.3. Cells were treated at D0 (onset of NSC differentiation) with 100% ethanol (Commercial alcohols) at a final concentration of 70 mM **(Figure 2.1C)**. Based on this concentration, 40.90 µl (in 10 ml media) and 4.09 µl (in 1 ml media) of ethanol were added to 10 cm^2 plates and 24-well plates, respectively. To study binge ethanol exposure, ethanol treatment was done only once at D0 for 48 h and cells were collected at D2. This can also be considered as an acute ethanol exposure. For modeling continuous ethanol exposure or chronic ethanol exposure, cells were treated with ethanol starting at D0 for eight days continuously. The media with ethanol

was refreshed every other day. To study the effect of ethanol withdrawal, after binge ethanol exposure for 48 h, culture media with ethanol was exchanged with fresh media without ethanol. Cells were kept in culture for an extra six days, and the media was refreshed every other day. Control cells were cultured under similar experimental conditions, in the absence of ethanol **(Figure 2.1A)**. Cells were harvested at D0, D2, and D8 for DNA, RNA and protein extractions, and immunocytochemistry experiments.

2.6 Primary culture of cortical neurons

Primary neurons from the cortex of E18.5 CD-1 mice were cultured as previously described [4,5,13]. The embryos were separated based on their sex. In brief, dissected cortices were dissociated using papain and trituration using a pasteur pipette. Dissociated cells were resuspended in neurobasal media supplemented with B27 and plated at a density of 1.2×10^5 cells/ml in poly-lysine coated dishes. Half of the media was replaced 72 h following initial seeding and replenished every 48 h thereon. Cells were collected after eight days. Isolation and culture of primary cortical neurons were carried out by a former Ph.D. student in our lab, Dr. Robby Zachariah and Dr. Mojgan Rastegar.

2.7 Primary astrocyte culture

Primary astrocytes from the cortex of E18.5 CD-1 mice were cultured as previously described [4,5,13]. The embryos were separated based on the sex. In brief, dissected cortices were further dissociated using papain enzyme and triturated with pasteur pipette. Cells were subsequently resuspended in minimum essential medium (MEM, Thermo Scientific) with 10% FBS. Cells were then seeded at a density of 2×10^5 cells/ml in poly-lysine coated dishes. Media

was replaced every 48 h until the day of collection. Cells were collected after 15 days. Isolation and culture of primary astrocytes were carried out by Dr. Robby Zachariah (former student), and Dr. Mojgan Rastegar.

2.8 Culturing of sex-specific neurons and astrocytes

To study the expression and regulation of *Mecp2* isoforms in a sex-specific manner, we modified our neuronal and astrocyte culture protocols slightly to separate the two sexes. We used one visual-based technique (completed by our lab technician Mr. Carl Olson), and two molecular techniques were used for sex determination and confirmation.

2.8.1 Identification and culture of sex-specific primary cell types

Pregnant mice at E18.5 were sacrificed according to animal ethics guidelines. Embryos were examined under a dissecting microscope for their genital organs. Male embryos were identified by visualization of a pair of testis on either side of the bladder. If no testis was found to be present adjacent to the bladder, the embryos were further examined for the presence of fallopian tubes, which are present leading towards the kidneys and ovaries, which are visible as small tissue masses adjacent to kidneys. Separated male and female embryos were then dissected to isolate the cortex for isolation and culture of primary neurons and astrocytes as described in sections 2.6 and 2.7. Embryonic collections, sex separation of individual embryos, and forebrain dissections were done by Mr. Carl Olson.

2.8.2 Molecular confirmation of cultured sex-specific cell types

I used a qRT-PCR-based method for identification of female cells and a PCR-based method for identification of male cells to confirm the sexes of cultured cells. The molecular tests that I used in the identification of sexes were also utilized in the studies included in Chapters 3 and 4 of this thesis to study sex ratio in control and treated cells [6,7].

2.8.2.1 Xist-based female confirmation

Neurons and astrocytes isolated from male and female mouse embryos identified visually were cultured as described in sections 2.6 and 2.7. RNA was extracted from the neurons at day 8 and astrocytes at day 15. For neurons and astrocytes originating from male embryos, trizol extraction method following manufacturer's instructions was used to extract RNA. The extracted RNA was treated with DNase to remove any DNA contamination, which will be discussed in detail in section 2.9.2. In the case of neurons and astrocytes originating from female embryos, mirVana RNA extraction kit was used for RNA extraction. RNA extracted by mirVana RNA extraction kit was run through a DNA removing column and thus did not require DNase I treatments. The cDNA synthesis and qRT-PCR were performed as described in our previous reports [5,14]. To identify female cells, I used *Xist*, which is a lncRNA expressed from the X chromosome that is being silenced and binds to the same X chromosome during XCI [15]. I did quantitative qRT-PCR for *Xist* transcripts to identify and differentiate female cell types as previously described [16], using the primers listed in **Table 3.2**. The PCR program used was: 95°C for 5 min, 35 cycles of 95°C for 30 s, 53°C for 30 s, 72°C for 30 s and 78°C for 30 s, followed by a melt curve.

2.8.2.2 Sry-based male confirmation

Neurons and astrocytes isolated from visually identified male and female mouse embryos were cultured as described in sections 2.4 and 2.5. Genomic DNA from cultured neurons and astrocytes was extracted using the DNeasy blood and tissue kit (Qiagen, Ontario, Toronto, Canada), as per the manufacturer's instructions [17]. Semi-quantitative PCR-based amplification of two genes was used in this assay. First one was Sex-determining region protein gene on the Y chromosome or the mammalian Y-chromosomal testis-determining gene (*Sry*), which is specific for males. It is involved in male sex determination through induction of Sertoli cell differentiation and subsequent testis formation [18]. The second gene is Interleukin 3 (*Il3*) or colony-stimulating factor, which is localized on chromosome 5 and therefore detected in both male and female cell types. It is involved in differentiation of hematopoietic stem cells [19]. In the duplex PCR reaction, *Il3* is also considered as an internal control [20]. **Table 3.1** lists the primers utilized for the assay. *PCR*: The PCR reaction utilized platinum *Pfx* DNA polymerase (Invitrogen, 11708-013). The reaction was prepared as per manufacturer's instructions [21]; amplification buffer (5 µl), 10 mM dNTP mixture (1.5 µl), 50 mM MgSO$_4$ (1 µl), 0.2µM *Sry* primers (1 µl), 0.12µM *Il3* primers (0.6 µl), template DNA (100 ng), platinum™ Pfx DNA polymerase (0.4 µl) and ultrapure water to a final volume of 50 µl. The components of the PCR mix were added to a sterile microcentrifuge tube at room temperature (RT). After mixing, tubes were spun down briefly. The PCR program for *Sry/Il3* amplification is as follows: initial denaturation at 95°C for 4.5 min, 33 cycles of 95°C for 35 s, 50°C for 1 min, 72°C for 1 min, and final extension at 72°C for 5 min. The PCR products were run on an agarose gel (1.5%), visualized using ethidium bromide staining and identified based on their respective sizes (**Table 3.1**).

Agarose gel electrophoresis: Agarose gel electrophoresis for identification of *Sry/Il3* bands was carried out using Sub-Cell GT agarose gel electrophoresis systems (Bio-Rad) as per manufacturer's guidelines [22]. I used 2% agarose gel in 1X tris-acetate-EDTA (TAE) buffer. The working TAE solution was prepared by diluting a 50X stock solution, which was prepared by mixing 242 g of tris base, 57.1 ml of glacial acid and 100 ml of 0.5 M EDTA (pH 8.0). The agarose plus TAE solution was boiled in a microwave oven until all the agarose was melted. A gel tray was set up securely on a gel caster with an appropriate comb. The boiled agarose solution was added to the gel tray to solidify for 30 min. Once the gel was solidified properly, the gel tray was kept in the electrophoresis tank filled with 1XTAE. PCR DNA samples were prepared for loading by mixing 1.5 µl of loading buffer and 10 µl of sample. The prepared sample (10 µl) was added to each well. A 100 bp bench top ladder was used as a DNA size marker. The gel was run for 45 - 60 min followed by soaking the gel in TAE buffer containing 10 µl of ethidium bromide. The stained gel was imaged using a Gel Doc.

2.9 Quantitative RT-PCR (qRT-PCR)

2.9.1 RNA extraction

RNA extraction using RNeasy mini kit: RNA extraction from neural stem cell samples shown in Chapters 3 and 4 was carried out using the RNeasy mini kit (Qiagen, 74106) as per manufacturer's protocols [23]. Prior to starting the experiment, 10 µl of β-mercaptoethanol was added to each 1 ml buffer RLT inside a fume hood. Frozen NSC cell pellets were thawed slowly on ice. For smaller pellets with approximately $<5 \times 10^6$ cells, 350 µl of RLT buffer (+ β-mercaptoethanol) was added while for larger pellets with 5×10^6 - 1×10^7 cells, 600 µl of RLT buffer was used. Cells were then lysed and homogenized by mixing (pulse vortexing) for 1 min. Once the cell pellets were

homogenized, one volume of 70% ethanol was added to each cell lysate and mixed well. RNeasy spin columns were placed inside 2 ml collection tubes, and 700 μl of cell lysate (+ ethanol) was transferred to the RNeasy spin columns and centrifuged for 30 s at 13000 rpm at RT. The flow-through was discarded. The rest of the cell lysate (in case sample volume was higher than 700 μl) was centrifuged in the next round in the same tube. This was followed by addition of buffer RW1 (700 μl) onto the RNeasy spin column, which now has the RNA attached to the filter membrane. The tubes were centrifuged for 30 s at 13000 rpm at RT. RNeasy spin columns were removed carefully from the collection tubes and filled with 500 μl buffer RPE for washing the membrane-absorbed RNA. This was followed by centrifugation for 30 s at 13000 rpm at RT. The flow-through was discarded. Another round of buffer RPE (500 μl) was added to the spin columns and centrifuged for 2 min at 13000 rpm at RT to ensure removal of residual ethanol from the membrane. RNeasy spin columns were placed on new 2 ml collection tubes and centrifuged for 1 min at 13000 rpm at RT to fully remove residual ethanol and carryover of buffer RPE, and dry the membrane. Finally, RNeasy spin columns were placed inside labeled 1.5 ml eppendorf tubes and 30-50 μl RNase-free water or ultrapure water was carefully added directly onto the membrane. The volume of water added was determined based on the starting pellet size. If the pellet was small, 30 μl of water was used to increase the RNA concentration upon collection, and the tubes were centrifuged for 1 min at 13000 rpm to elute RNA. To increase RNA yield, this step was repeated with less water for a second RNA elution. The RNA was quantified and stored in -20℃.

RNA extraction using trizol RNA extraction protocol: Trizol RNA extraction protocol (Life Technologies Inc. 15596-026) was used to extract RNA from male neurons and astrocytes discussed in Chapter 5 as per manufacturer's guidelines, by Mr. Carl Olson [24]. RNA was quantified and stored in -80°C.

RNA extraction using mirVana RNA extraction kit: RNA extraction from female neurons and astrocytes were done using mirVana RNA extraction kit (Thermo Scientific, AM1560) following the user manual [25]. Frozen cell pellets were thawed. The amount of lysis/binding solution to be added was decided based on the number of cells. For hundreds of cells, 300 μl, and for thousands to millions of cells, 600 μl of lysis solution was used. Upon addition of the lysis solution, the tubes were mixed by vortexing vigorously for 15 s for complete cell lysis and homogenization. This was followed by addition of 1/10 volume of miRNA homogenate additive to the cell lysate and mixed for few seconds. The tubes were kept on ice for 10 min. The experimental set up was moved to a chemical fume hood and one volume of acid-phenol: chloroform was added to each tube. It was ensured to obtain acid-phenol: chloroform from the lower phase of the bottle. The mix was vortexed carefully for 60 s, followed by centrifugation in a microcentrifuge at 13000 rpm for 5 min at RT. As now the two phases have separated, the tubes were taken out of the microcentrifuge without disturbing the phases (top: aqueous and bottom: organic). The tubes were opened carefully in a fume hood, without disturbing the interphase and the top aqueous phase was transferred to a new tube. The volume obtained was noted down. To each tube with the aqueous phase, 1.25 volumes of 100% ethanol were added. Filter cartridges were placed inside labeled collection tubes, and 700 μl of lysate/ethanol mixture was added to each filter cartridge. If the sample volume was larger than 700 μl, the rest was added to the same filter in the second round. The tubes were centrifuged for 30 s at 10000 rpm so that the RNA attaches to the filter. The flow-through was discarded. Filter cartridges were kept back inside the collection tubes and 700 μl miRNA wash solution 1 was added to each filter for washing. The tubes were centrifuged for 30 s at 10000 rpm, and the flow-through was discarded. Filters were washed twice with wash solution 2/3 (500 μl) similar to the previous washing step. After the two washes, empty filter cartridges were placed

back in the collection tubes and centrifuged for 1 min (10000 rpm) to remove any residual washing solution. While the washes were going on, the elution solution or nuclease-free water was boiled to 95°C. To elute total RNA (which also includes miRNA), 100 µl of pre-warmed elution solution was added directly onto the filter cartridges, which were now placed in fresh eppendorf tubes. The tubes were centrifuged for 30 s at 13000 rpm at RT. Eluted RNA was quantified and stored in -20°C.

2.9.2 DNase treatment of trizol-extracted RNA

RNA extracted using trizol treatment for male neurons, and male astrocytes samples were treated with DNase to remove genomic DNA contaminations. RNA extracted using the RNeasy mini kit and mirVana RNA extraction kit did not require DNase treatment as they contain DNA removing columns. DNase treatment was done using Ambion® TURBO DNA-free™ DNase treatment and removal reagents by modifying manufacturer's protocol to fit the initial RNA amount used [26]. The routine DNase treatment protocol was used, which is suitable for DNase treatment for samples with ≤200 µg nucleic acid per ml. Briefly, 1.5 µl of the 10X TURBO DNase buffer was added to 1 µl of TURBO DNase enzyme, and approximately 1 µg of RNA was diluted to 10.5 µl final volume with sterile water, mixed gently and kept in 37°C water bath for 30 min. DNase inactivation (2 µl) reagent was added and mixed gently. As the inactivation reagent is a white slurry with high density, the vial was mixed carefully by flicking to obtain the accurate volume of the inactivation reagent, incubated for 5 min at RT with occasional mixing by flicking the tubes (every 1 min). Tubes were centrifuged at 13000 rpm for 1.5 min. The supernatants containing DNA-free RNA was transferred into a new sterile tube and quantified.

2.9.3 cDNA synthesis

RNA was converted to cDNA with a reaction set up containing Superscript III reverse transcriptase (Invitrogen) using previously described methods [27,28]. The cDNA synthesis mix was prepared as follows: 1 µl of dNTPs, 0.1 µl of random primers, and 400-500 ng of RNA diluted up to 13 µl of final volume with sterile water. The cDNA synthesis mix was mixed gently by pipetting and incubated for 5 min in a 65°C (in a heat block). The tubes were transferred to ice and kept on ice for 1-2 min, followed by a brief spin. The master mix was prepared as follows: 4 µl of 5x first strand buffer, 1 µl of 0.1 M DTT, 1 µl of RNaseOUT and 1 µl of Superscript III RT. The cDNA synthesis mix (13 µl) was mixed with 7 µl of master mix, followed by incubation for 5 min at 25°C (RT). They were transferred on to a 50°C-heat block in which samples were incubated for 60 min. After 60 min, the samples were transferred to the 70°C-heat block and kept for 15 min. Finally, the samples were transferred onto ice, spun briefly and stored in -20°C until used.

2.9.4 qRT-PCR

Quantitative RT-PCR was performed as described previously in our studies [5,14]. Transcript levels of a selected set of genes were examined. The primers used for these genes are listed in **Tables 3.2** and **4.1**, and qPCR conditions are listed in section 2.9.5. The primers for *Mecp2e1* [NM_001081979.1] and *Mecp2e2* [NM_010788.3] identification and relative quantification were obtained from a previous study [29]. **Figure 2.2** illustrates the location of primers that differentiate *Mecp2* isoforms. Additionally, transcript levels of *Mecp2* (total), cell type-specific gene markers for neurons [*Tubulin III (Tub III)*, *NEUronal Nuclei (NeuN)*], astrocytes [*Glial fibrillary acidic protein (Gfap)*, *S100 calcium-binding protein B (S100b)*] and oligodendrocytes [*2',3'-Cyclic-nucleotide-3'-phosphodiesterase (Cnpase)*, *Myelin basic protein*

(Mbp)] were determined. For determination of transcript levels of *Dnmt1, Dnmt3a,* and *Dnmt3b-* specific primers were used.
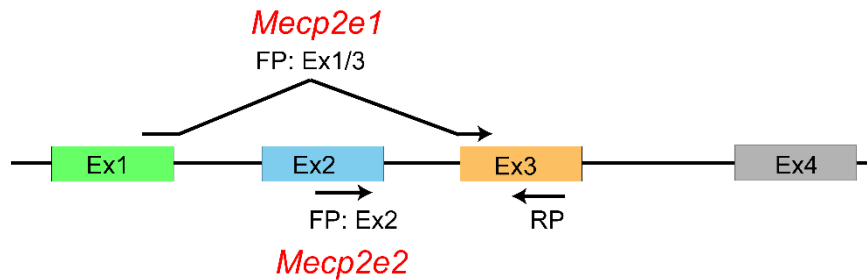
Figure 2.2 Location of qRT-PCR primers for detection of *Mecp2* isoforms.
Mecp2e1 isoform is recognized using a forward primer spanning the exons 1/3 boundary while *Mecp2e2* is recognized by a forward primer located in the exon 2. Both isoforms use the same reverse primer located in the exon 3. FP: forward primer; RP: reverse primer; Ex: exon.

QRT-PCR was performed in a fast 7500 real-time PCR machine (Applied Biosystems) using SYBR Green-based RT^2 qPCR master mix (Applied Biosystems) and MicroAmp® fast optical 96-well reaction plate with barcode. The primers used in qRT-PCR were reconstituted with ultrapure water to obtain 100 μM stock solution as described in the IDT website (https://www.idtdna.com/Calc/resuspension/). For individual reactions, a 10 μM concentration mix of forward and reverse primers was prepared by using 10 μl forward primer (100 μM stock), 10 μl reverse primer (100 μM stock) and 80 μl ultrapure water.

The qRT-PCR reaction mix was prepared on ice as follows: 1 μl primer mix, 10-20 ng template, 10 μl SYBR Green and ultra pure water for a final volume of 21 μl. The reaction mix (10 μl) was added to each well of the 96-well plate in duplicates. The reaction plate was covered with an adhesive film and centrifuged using a plate rotor for 1 min at 2000 rpm to remove air bubbles. In case the reaction could not be run immediately, the plate was covered in aluminum foil

and stored in 4°C no longer than few hours. Experimental conditions for comparative C_T ($\Delta\Delta C_T$) experiments were programmed onto the computer connected to the RT-PCR machine as described in the manual [30]. The $\Delta\Delta C_T$ method was used to measure relative expression of target genes with respect to an endogenous control (e.g., *Gapdh* or *Actin*), with reference to a control sample. This is applicable when there are multiple experimental conditions such as control and treated samples.

2.9.5 qRT-PCR conditions

Total Mecp2, Mecp2e1, Mecp2e2, Gapdh, Tub III, Gfap: 95°C for 3 min, 35 cycles of 95°C for 1 min, 60°C for 30 s, 72°C for 45 s and 72°C for 10 min, followed by a melt curve. The continuous melt curve conditions were 95°C for 15 s, 60°C for 1 min, 95°C for 30 s and 60°C for 15 s.

S100b, NeuN: 50°C for 2 min and 95°C for 10 min, 40 cycles of 95°C for 15 s, 60°C for 1 min, followed by a melt curve.

Cnpase, Mbp: 95°C for 10 min, 30 cycles of 95°C for 15 s, 60°C for 1 min, followed by a melt curve.

Dnmt1, Dnmt3a, Dnmt3b: 95°C for 10 min, 45 cycles of 95°C for 30 s, 60°C for 30 s, 72°C for 30 s and 95°C for 15 s, followed by a melt curve.

Xist: 95°C for 5 min, 35 cycles of 95°C for 30 s, 53°C for 30 s, 72°C for 30 s and 78°C for 30 s, followed by a melt curve.

2.9.6 Calculation of relative expression values and fold change

After qRT-PCR experiments, the baseline and the threshold for each gene were adjusted for consistent analysis settings between samples for the same gene as described in Applied Biosystems 7500/7500 fast RT-PCR system manual [30]. The threshold for all the samples was adjusted to be

in the exponential phase of the amplification curve in ΔRn vs. cycle setting. The Ct values were exported in the form of an excel file, and Ct values for all genes were normalized with reference to the housekeeping gene *Gapdh* to obtain ΔCt values for each sample (equation 1). Relative expression of each gene was determined by calculating $2^{-\Delta Ct}$ within each sample (equation 2). Fold change was calculated using equation 3. All calculations were done in Microsoft Excel 2010 as we have done previously [5,14].

$$\Delta Ct = Ct_{(Gene\ of\ Interest)} - Ct_{(Gapdh)} \ldots\ldots\ldots\ldots\ldots\ldots\text{(Equation 1)}$$

$$Relative\ expression = 2^{-\Delta Ct} \ldots\ldots\ldots\ldots\ldots\ldots\text{(Equation 2)}$$

$$Fold\ change = \frac{[2^{-\Delta Ct}]treatment}{[2^{-\Delta Ct}]control} \ldots\ldots\ldots\ldots\ldots\ldots\ldots\ldots\ldots\text{(Equation 3)}$$

2.10 Sodium dodecyl sulfate-polyacrylamide gel electrophoresis (SDS-PAGE) and western blot (WB)

In Chapters 3 and 4, to determine specific protein expression levels, SDS-PAGE and WB were performed as previously described [5,13,31].

2.10.1 Nuclear and cytoplasmic protein extractions

Nuclear and cytoplasmic protein extractions from D2 and D8 NSC (control and ethanol- or decitabine-treated) were carried out using the NE-PER nuclear and cytoplasmic extraction kit (Thermo Scientific, 78833), as per manufacturer's instructions [32].

Protein Extraction: Briefly, the kit consisted of three buffers cytoplasmic extraction reagent I (CER I), cytoplasmic extraction reagent II (CER II) and nuclear extraction reagent (NER). Immediately before use, protease inhibitors were added to CER I and NER. The volumes of each

reagent were decided based on the initial packed cell volume (PCV) as described in the manual [32]. As NSC cell pellets were small, either 10 µl or 20 µl PCV was used. For 10 µl PCV, 100 µl CER I, 5.5 µl CER II and 50 µl NER were used. For 20 µl PCV, 200 µl CER I, 11 µl CER II and 100 µl NER were used (CER I: CER II: NER ratio 200:11:100 µl). NSC cell pellets were resuspended in ice-cold CER I, mixing vigorously (by pulse-vortexing) on the highest setting for 15 s and kept on ice for 10 min. Ice-cold CER II was added to cell lysates, mixed vigorously using a vortex for 5 s, and incubated on ice for 1 min. They were centrifuged for 5 min at 16000g (maximum speed) at 4°C. The supernatants with cytoplasmic proteins were transferred to another tube and aliquoted for storage. The pellet containing the nuclear proteins was resuspended in NER by vigorous mixing for 15 sec. The tubes were kept on ice for 40 min and mixed by vortexing for 15 s, every 10 min. After 40 min, the nuclear protein suspension was centrifuged at 16000g for 10 min at 4°C. The supernatants containing the nuclear protein extracts were transferred to pre-chilled tubes, aliquoted, quantified and stored at -80°C until use.

Quantification of protein concentration: Bradford assay using the Bio-Rad protein assay dye reagents was used for protein quantification as per manufacturer's instructions [33]. Bradford assay dye reagent was prepared by diluting 1 in 5 in distilled water, followed by filtering through a Whatman #1 filter. A protein standard dilution series in the linear range of 0.2 to 0.9 mg/ml was prepared using bovine serum albumin (BSA). A dilution series of 1:5, 1:10 or 1:20 of the unknown protein samples was prepared. 5µl of the standard dilution series and the unknown protein samples were added to a 96-well plate in triplicate. The dye reagent (500 µl) was added to each well and mixed carefully but thoroughly without making any air bubbles. The 96-well plate with samples was kept in a spectrophotometer (SpectraMax M2e, Molecular Devices) using, which the

absorbance values were captured at a wavelength of 595 nm. The standard curve was used to calculate the concentrations of unknown samples using the Softmax Pro 5.3 software.

2.10.2 SDS-PAGE

All experiments were carried out with 10-30 µg of nuclear or cytoplasmic extracts. SDS-PAGE gel consisted of a resolving gel and a stacking gel prepared as follows:

Resolving gel: 10% polyacrylamide; 0.375M tris-HCl (pH 8.8); 0.1% SDS; 0.1% ammonium-persulfate; 0.0004% tetramethylethylenediamine (TEMED)

Stacking gel: 4% polyacrylamide; 0.125M tris-HCl (pH 6.8); 0.1% SDS; 0.05% ammonium-persulfate; 0.001% TEMED

The SDS-PAGE gel was prepared in a Bio-Rad mini protean 3 apparatus. The nuclear and cytoplasmic protein extracts of 10-30 µg were resuspended in a loading buffer that contains 10% glycerol, 12.5 mM EDTA, 50 mM tris-HCl pH 8.0, 2% SDS, and 0.02% bromophenol blue. β-mercaptoethanol (1%) was added inside a chemical fume hood to each tube mixed thoroughly and boiled at 100°C for 5 min for denaturation of the proteins. After 5 min, samples were quickly transferred onto ice and spun briefly to bring down the condensed liquid. Samples (30-40 µl) were loaded into each well. Empty lanes were filled with an equal volume of 1X loading buffer. A prestained protein ladder was used to determine the protein size. The gel was placed in running apparatus with running buffer (25 mM tris, 192 mM glycine, 0.1% SDS, pH 8.3) and run in the cold room (4°C) at 100 V.

2.10.3 Western blot

Transfer: After the gel was run to the expected size range, the gel transfer was set up using mini Trans-Blot® electrophoretic transfer cell as per manufacturer's instructions [34]. The transfer buffer, which consisted of 192 mM glycine, 25 mM tris, 0.05% SDS, 20% methanol was prepared before the transfer began and kept in 4°C to improve heat dissipation. The membrane, filter papers, and fiber pads were soaked in transfer buffer. The gel sandwich was prepared in the following order on the cassette: the black side of the cassette - fiber pad - two filter papers - gel - membrane - two filter papers - fiber pad - the white side of the cassette. The locked cassettes were kept in the tank along with an ice pack and followed by filling the tank with the transfer buffer. The transfer was carried out for 1 h at 100 V.

Blotting: After transfer, the membranes were blocked for 1-3 h at RT using 2% non-fat skim milk in tris-buffered saline (TBS) with 0.2% tween 20 (TBST). The blocking period and milk concentration were optimized for each protein or the antibody. The membranes were incubated with the corresponding primary antibodies either overnight at 4°C or RT for 2 h. The primary antibodies and their conditions are listed in **Table 3.3** and **4.2**. Beta ACTIN or GAPDH was used as a loading control. The membrane was rinsed twice with TBST followed by three 20 min-washes with TBST. Subsequently, the membranes were incubated with the appropriate secondary antibodies, which are peroxidase-conjugated, and this reaction was carried out at RT for 1 h. The secondary antibodies used in this thesis are listed in **Table 3.4** and **4.3**. The membranes were rinsed twice and washed three times with TBST, each wash being 20-min.

Development: To develop the membrane, an enhanced chemiluminescence method - Immobilon western chemiluminescent HRP substrate solution (EMD Millipore™) containing luminol and peroxide was used as per manufacturer's instructions [35]. HRP substrate was prepared by mixing

equal volumes of luminol reagent and peroxide solution and was added onto the membrane for 5 min ensuring full membrane coverage by the solution. After 5 min, the membrane was covered with a clean plastic wrap and exposed to an X-ray film inside the WB developing-dark room. Different exposures of the membrane were captured on X-ray films. Some of the developing X-ray films were blue in color, and they were converted into gray scale before quantification and assembly of the figures. Note that the brightness or contrast of the bands was not adjusted.

Quantification: Quantification of WB bands was done semi-quantitatively with Adobe Photoshop CS5 software and normalized to ACTIN or GAPDH signals as described previously [7,14]. MeCP2 expression in decitabine-treated or ethanol-treated samples was compared to corresponding control untreated cells within the same biological replicate. Note that exposure times were not the same for different experiments. The X-ray films were scanned and opened in Adobe Photoshop CS5. Using the 'image>adjust>invert' command, the image of the bands was inverted for the purpose of quantification. Using the marquee tool, a box was drawn around the biggest band, as the box was the same size throughout the analysis. Mean pixels were noted down using the histogram option (image>histogram). The same analysis was repeated for all the bands of MeCP2 and loading controls. Finally, the box was dragged onto the background to measure the mean pixel value for the background. Background values were subtracted from the main band values. The limitations of using X-ray film-based quantification will be discussed in Chapter 6.

2.11 Immunocytochemistry, imaging and quantification

2.11.1 Fixation of coverslips with cells

Differentiating NSC treated with decitabine, ethanol or untreated control NSC were cultured and fixed onto the coverslips in 24-well plates as we have done before [5,13]. Briefly, 24-well

plates were kept on ice; media was aspirated and rinsed twice with ice-cold 1X phosphate-buffered saline (PBS). A 4% paraformaldehyde [PFA (Electron Microscopy Sciences)] prepared by diluting 16% PFA in ice-cold PBS was added to coverslips for 10 min for fixation. Subsequently, PFA was aspirated carefully, and the coverslips with cells were rinsed twice with 1 ml of PBS. This was followed by washing the coverslips with ice-cold PBS (1 ml) three times, at intervals of 5 min. After the final washing, 1 ml of ice-cold PBS was added to each well of the 24-well plate, which was sealed with parafilm and stored in at 4°C until further use.

2.11.2 Immunocytochemistry for proteins

PBS used in storage of coverslips was aspirated, and the coverslips were rinsed once with 1 ml of ice-cold PBS. The fixed cells were permeabilized by addition of 250 µl of 2% NP-40 in PBS for 10 min. NP-40 was briefly rinsed off by two rounds of PBS addition. The coverslips were blocked with 10% (v/v) normal goat serum (NGS, Jackson Immunoresearch Laboratories, 005-000-121) in PBS for 1 h at RT. During this time, primary antibodies that are listed in **Table 3.3** and **4.2** were prepared in PBS with 10% NGS. After 1 h blocking, primary antibodies were added to the coverslips, and the plate was covered in Parafilm and incubated at 4°C overnight. The next day, primary antibody solutions were removed, and coverslips were rinsed twice with PBS. Subsequently, three PBS (1 ml) washes were done at 5 min intervals. Secondary antibodies **(Table 3.4** and **4.3)** were prepared in 10% NGS and added onto coverslips for 1h and kept at RT. Coverslips were rinsed twice, followed by three 5-min PBS washes. Prolong-gold antifade (Molecular Probes, P36930) containing 2 µg/ml 4′,6-diamidino-2-phenylindole (DAPI) (Calbiochem, EMD Millipore, 268298) counter-stain was prepared. The DAPI-antifade solution

(6 µl) was added to a clean glass slide, and the coverslip was placed inverted on the DAPI-antifade solution. The coverslip was secured onto the glass slide with nail polish.

2.11.3 Immunocytochemistry for 5mC

Immunocytochemistry for 5mC detection was done as reported in a previous study [13] and was developed based on another report [36]. Briefly, control and decitabine-treated NSC fixed onto coverslips were treated with 2% NP40 in PBS for 10 min. After a quick rinse, cells were exposed to 4N HCl for 10 min, followed by neutralization of HCl using 100 mM tris-HCl (pH 8.5) for 15 min. The coverslips were rinsed three times with ice-cold PBS. The blocking step of the protocol was done by incubating the coverslips with 10% NGS in PBS for 1 h. Primary antibody 5mC was added in 1:200 dilution in PBS onto the coverslips and incubated overnight at 4°C. Next day, the antibody solution was removed, and coverslips were rinsed twice with ice-cold PBS. They were washed thrice with 1 ml of ice-cold PBS at 5 min intervals. This was followed by incubation of the cells with the appropriate secondary antibody in 10% NGS, for 1 h at RT. After three PBS washes, the coverslips were mounted on glass slides with antifade containing 2 µg/ml DAPI.

2.11.4 Immunohistochemistry for sectioned neurospheres

Fixation and sectioning: Neurosphere fixation and sectioning were completed by Mr. Carl Olson, as described in our previous studies [4,5]. Briefly, neurospheres were rinsed in PBS. A solution of PFA prepared by mixing 0.16 M sodium phosphate buffer, pH7.4 and 2% PFA was added to the tube containing the neurospheres to fix them for 20 min at RT. They were rinsed with a cryoprotectant containing 25 mM sodium phosphate buffer, pH 7.4, 10% sucrose and 0.04% NaN_3 and incubated for 24 h at 4°C in the same cryoprotectant solution. Subsequently, cells were

mounted onto optimal cutting temperature compound (OCT). This was followed by sectioning them to obtain 8-10 µm thick cryosections, which were adhered to gelatinized slides, and stored at -20°C until further use.

Immunohistochemistry: I conducted IHC for MeCP2 and NESTIN in fixed and sectioned neurospheres, as described in previous studies [5,13,14]. Slides with sectioned-neurospheres were air dried under an electric fan for 20 min and kept in a tank filled with 0.3% Triton X-100 (tr), TBS and NaCl for 20 min at RT. This step removed excess fixation solution and cell permeabilization. The slides were taken out of the bath, and excess solution was drained for few seconds and wiped around the neurosphere section carefully with a tissue paper. They were kept on a humidity chamber-box designed for IHC experiments, and the pre-blocking solution that contains 10% NGS in TBS-tr was added onto the neurosphere for 1h at RT. A PAP pen was used to draw a line around the neurosphere section, thereby creating a hydrophobic barrier around the neurosphere section. Primary antibodies listed in **Table 3.3** were prepared by diluting them in 10% NGS and TBS-tr. Blocking solution was drained from the slides to add the primary antibodies (250 µl), which were secured by the PAP pen barrier on the slide. The primary antibody incubation occurred at 4°C overnight. Next day, the primary antibodies were drained from the slides, and the slides were kept in a tank containing TBS-tr for washing. I did three 20-min washes. The slides were taken out of the tank; excess washing solution was drained and wiped carefully with a tissue paper. They were kept on the humidity chamber-box. The secondary antibodies listed in **Table 3.3** were prepared by diluting the antibodies in 10% NGS in TBS-tr and added onto the neurospheres. This incubation occurred for 1 h at RT in the dark, as the secondary antibodies are sensitive to light. The slides were washed three times (each 20 min) with TBS-tr and twice (each 20-min) with tris-HCl (50 mM) buffer, pH 7.4. During the washing steps, the tank was covered with aluminum

Chapter 2

foil to avoid light. Finally, an antifade Gold solution containing 2 µg/ml DAPI was added onto each slide covering the neurospheres. A coverslip was added carefully to cover the neurospheres. Coverslips were secured onto the glass slides with nail polish. The slides were stored in -20°C until used for imaging. I used primary antibody omission as a negative control for these experiments.

2.11.5 Fluorescent inverted microscopy

ICC and IHC images were captured using Axio Observer Z1 inverted microscope (Carl Zeiss) as per manufacturer's instruction manual [37], and we described previously [5,13,14]. Images were captured using either 10X lens [numerical aperture (NA) =0.3)], 40X lens (NA = 0.95) or 63X oil-immersion lens (NA=1.4). For cell population quantification, neuronal and glial morphological quantification images were taken using 40X lens and 63X lens. The captured images were observed and analyzed using Zen Blue 2011/2012 (Carl Zeiss Canada Ltd.) software. The images were exported and adjusted for size and resolution (300 dpi) using Adobe Photoshop C5. Finally, figures were assembled using Adobe Illustrator C5.

2.11.6 Confocal microscopy

Confocal microscopy for Chapter 3 was done by Mr. Robby Zachariah. An LSM710 confocal microscope (Carl Zeiss Canada Ltd.) with 63X oil-immersion lens (NA=1.4) was used. The captured images were observed and analyzed using Zen Black 2011 software. The images were exported and adjusted for size and resolution (300 dpi) using Adobe Photoshop C5. Finally, figures were assembled using Adobe Illustrator C5.

Chapter 2

2.11.7 Cell quantification

In Chapters 3 and 4, cell quantifications were done to determine the population of specific cell types in differentiating NSC and to assess the effect of decitabine or ethanol on NSC fate commitment. Cell quantification was done as we have reported previously [5,7] using ImageJ program. From D2 of NSC differentiation, 250 DAPI$^+$ cells and from D8, 400-500 DAPI$^+$ cells from 3 biological replicates were collectively chosen for quantification. Approximately 10 random microscopic fields were selected for quantification based on the channel showing the DAPI$^+$ cells. As per ImageJ program manual [38], 'cell counter' plugin was used. The images were loaded onto the ImageJ program, and different colors/counters for specific markers (channels) were chosen. The ImageJ program cell counter recorded the number of counted cells for each color, which were recorded in an Excel file for calculating averages and standard deviations. The graphs were prepared using GraphPad Prism.

2.11.8 Neuronal morphology quantification

In Chapter 4 studies with ethanol treatment, I determined the effect of ethanol on neurite branching. Neurons were labeled with TUB III, which were detected by Axio Observer Z1 inverted microscope, and images were obtained by Zen 2011 as described in section 2.10.5. To accurately capture all neurites, signal intensity was adjusted and superimposed Z-stacked images were taken at 0.32 µm sections. Images were loaded onto ImageJ program, and neurites were quantified using the cell counter plugin based on a previous study [4]. Approximately 20 TUB III$^+$ neurons from each biological replicate were imaged for three biological replicates.

2.11.9 Glial morphology/size quantification

In Chapter 4 ethanol studies, the effect of ethanol on glial cell size or morphology was determined. ICC experiments were done to label GFAP in astrocytes. Axio Observer Z1 inverted microscope and Zen 2011 software were used in imaging. Superimposed Z-stacked images of GFAP$^+$ cells were taken at 0.32 µm sections. The image intensity was adjusted to see all the cellular processes and cell margins. The spline contour tool within the Zen 2011 software was used to quantify the surface area of GFAP$^+$ astrocytes as shown in a previous study [39]. Spline contour tool was used to mark the outer margin of each cell carefully, and Zen 2011 software directly provided the area in µm^2. From each biological replicate, at least 20 GFAP$^+$ astrocytes were measured in three biological replicates.

2.12 DNA methylation analysis by bisulfite pyrosequencing

Bisulfite pyrosequencing analysis was done for extracted DNA from NSC treated with decitabine (Chapter 3) or ethanol (Chapter 4), and male neurons and astrocytes (Chapter 5).

2.12.1 Identification and design of Mecp2 REs for DNA methylation analysis

Initially, to determine *Mecp2* REs, I did a literature survey on *MECP2/Mecp2* regulation by *cis*-regulatory elements and *trans*-regulatory factors [40-42]. The previous studies of DNA methylation analysis on *MECP2* promoter were also taken into consideration [43,44]. As most reports were related to the *MECP2* (human) gene regulation, I performed a sequence similarity analysis of human *MECP2* and mouse *Mecp2* genes by Emboss Needle sequence similarity tool (http://www.ebi.ac.uk/Tools/services/web_emboss_needle) **(Figure 2.3A)**. The similarity of

known positive and negative regulatory regions reported for *MECP2* gene [42] was mapped on to *Mecp2* gene, and sequence similarity was determined as shown in **Figure 2.3B**.

A

Sequence similarity between *Mecp2* and *MECP2* gene regions								
Genomic region	Promoter	Exon 1	Intron 1	Exon 2	Intron 2	Exon 3	Intron 3	Exon 4
Mecp2	797 bp	77 bp	5477 bp	123 bp	42578 bp	351 bp	487 bp	9673 bp
MECP2	793 bp	62 bp	5295 bp	123 bp	59634 bp	351 bp	757 bp	9639 bp
Similarity	64.6%	80.5%	59.8%	100%	40.1%	88%	43.5%	72.1%

B

C

Regions suggested for DNA methylation analysis and finalized REs
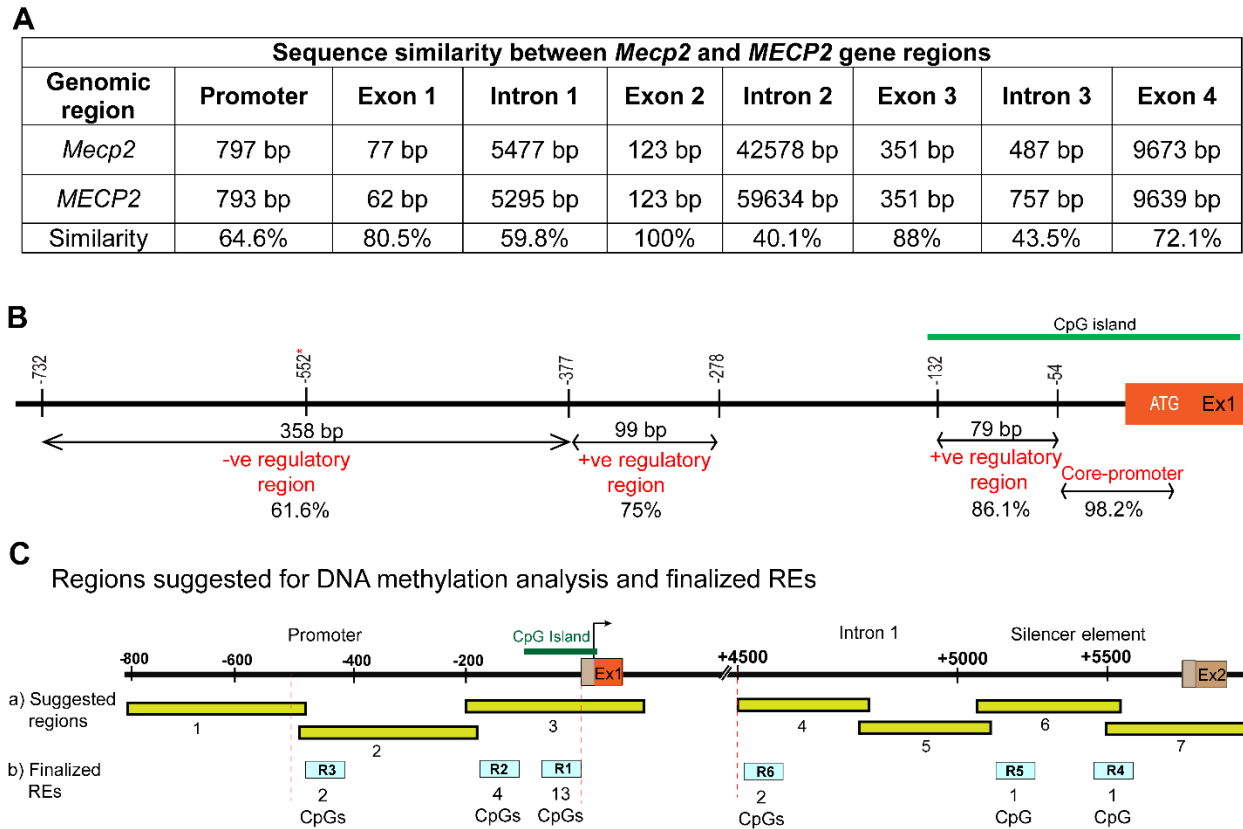
Figure 2.3 Selection of *Mecp2* gene regions for DNA methylation analysis.

A) *Mecp2* and *MECP2* gene sequence similarity analysis. Comparison of size and sequence similarity of the *Mecp2* gene in mouse and human. Gene sequences were obtained from http://genome.ucsc.edu. Sequence similarity for each coding and non-coding region was calculated by Emboss Needle sequence similarity tool, which is shown as percentages. **B)** Known regulatory sequences of *MECP2* promoter assigned to the *Mecp2* promoter. The figure illustrates the sequences in the *Mecp2* gene that correspond to the regulatory sequences reported for *MECP2* [42] and the % similarity to human sequences. CpG island was obtained from UCSC genome browser. The red star marks a highly methylated region in autistic patients reported previously [43,44]. **C)** **a**) The initial design of the *Mecp2* promoter and intron 1 regulatory regions (7 regions) to be analyzed. **b**) These 7 regions were later narrowed down and finalized to six REs for DNA methylation analysis. Three REs within the promoter R1-R3 and three REs within the intron 1

silencer element R4-R6 were finalized. The number of CpGs within each RE is indicated under each RE.

The *Mecp2* promoter was chosen for analysis with the hypothesis that DNA methylation at the promoter may regulate the expression of both *Mecp2* isoforms. The intron 1 silencer element reported in a previous study [42], which is immediately upstream of the exon 2 was chosen based on the hypothesis that DNA methylation at this region may impact *Mecp2e2*. This region was shown to have activity in reporter assays performed with non-neuronal cell types (NIH3T3 and HepG2) [42]. Initially, I designed seven regulatory regions for DNA methylation analysis **(Figure 2.3C:a)**. Within the *Mecp2* promoter, three regions were designed. Regions 1 and 2 included two negative and positive regulatory elements shown in **Figure 2.3B** and regions corresponding to highly methylated regions in autism patients [40-42]. A region overlapping the exon1 and downstream of exon 1 was also considered for analysis (Region 3). The *Mecp2* intron 1 regions chosen for analysis showed 55.2% similarity to the human silencer element [42]. This was divided into regions 4-6. Exon 2 and a part of intron 2 were included in the suggested region 7.

These regulatory regions were provided to the Hospital for Sick Children (SickKids hospital) sequencing service and were narrowed down to feasible regions for analysis by bisulfite pyrosequencing. Combining their expertise in DNA methylation analysis and our hypotheses on *Mecp2* isoform-specific regulation, we finally concluded three regions within the *Mecp2* promoter and three regions within the *Mecp2* intron 1 silencer element as illustrated in **Figure 2.3C:b**. The promoter R1 overlaps with the CpG island and the core promoter of *Mecp2* that contains 13 CpG sites. The promoter R2 contains 4 CpG sites and this region contains binding sites for regulatory proteins including RNA Pol II, TAF1, and SP1 [40,42], and overlaps with a positive RE. The

promoter R3, which overlaps an upstream negative RE and contains 2 CpG sites. On the other hand, intron 1 R4 and R4 have 1 CpG site each and R2 contains 2 CpG sites.

2.12.2 DNA extraction

Genomic DNA was isolated using the DNeasy blood and tissue kit (Qiagen, 69506) as per manufacturer's instructions [45]. The cell pellets were resuspended in 200 µl PBS to which, 20 µl proteinase K was added. Buffer AL (200 µl) was added to the cell suspension and mixed thoroughly (pulse-vortexing) for 5-10 s. The tubes containing cell suspensions were incubated at 56°C (heat block) for 10 min. The tubes were taken out of the heat block, 200 µl ethanol (96-100%) was added and mixed (pulse-vortexing) until a homogenous solution was obtained. The mix was transferred into the DNeasy mini spin column placed in a collection tube, which was the centrifuged using a microcentrifuge at RT at 8000 rpm for 1 min. The flow through was discarded. The DNeasy mini spin column was placed in a new collection tube, and 500 µl of the buffer AW1 was added to each column. They were centrifuged at 8000 rpm for 1 min after which the flow through was discarded. Buffer AW2 (500 µl) was added to each tube and centrifuged at 14000 rpm for 3 min until the membrane of the column was dried off. To ensure no carry over of ethanol occurred, the columns were kept in new empty collection tubes and centrifuged at 14000 rpm for 1 min. DNeasy mini spin columns were kept in new 1.5 ml microcentrifuge tubes and 100-200 µl buffer AE or water was directly onto the DNeasy membrane, incubated at RT for 1 min and centrifuged at 8000 rpm for 1 min to elute DNA. A second and third rounds of elution were done with less elution buffer or water (50-75 µl) in new tubes. DNA was quantified and stored in -20°C.

2.12.3 Bisulfite pyrosequencing

The *Mecp2* REs for DNA methylation analysis were chosen as described in Section 2.12.1. Primer design and bisulfite pyrosequencing experiments were conducted as a service by SickKids hospital, Toronto, Canada, as reported elsewhere [46], using the primers listed in **Table 3.5** and **4.4**. The regions analyzed for the methylation patterns are shown in **Figure 2.3C:b**.

2.12.4 Data analyses and interpretation

SickKids hospital bisulfite sequencing facility provided us with two sets of files, one set of Excel files containing the three biological replicates of the percentage methylation levels at individual CpG sites at different *Mecp2* REs. The second set of files included pdf files with the calculation of percentage methylation with the sequences showing the CpG sites analyzed. They labelled *Mecp2* promoter Res as follows: *Mecp2-s1* = R1; *Mecp2s1-v2* = R2; *Mecp2-s1v3* = R3. The intron 1 REs were, *Mecp2-s2v3* = R4; *Mecp2-s2v2* = R5; *Mecp2-s2v1* = R6. First, I compared the CpG sites shown in the Pdf files and Excel files and ensured the represented percentage methylation was accurate. The percentage methylation values shown in excel files report whether the quality of each PCR has 'passed,' 'check' or 'failed.' The failed PCR reactions were not included in the analysis. The 'check' reactions were compared with the other biological replicates, and if they were recognized to be non-outliers (determined by comparing the differences between the three values), they were included in the analysis. For each CpG sites, average percentage methylation from three biological replicates was determined. Additionally, for the regions that contained more than 1 CpG site (R1, R2, R3, and R6) average methylation over entire regions was calculated. In Chapter 5, *Mecp2* promoter REs were compared to the distribution of CpG island regions [CpG island, North (N) Shore, North (N) shelf, South (S) Shore and South (S) Shelf] based

on the distance and direction (north or south) from the CpG island. CpGs within the genome are not equally distributed. CpG islands are short regions with high CpG density and are associated with gene promoters, yet their methylation levels are low [47]. Recent DNA methylation analyses have identified further differentially methylated regions around CpG islands. Within 2 kb of CpG islands are CpG shores, which can be either N shore or S shore. Further 2 kb downstream and upstream of each CpG shore is where CpG shelves are located [48]. The rest of the CpG distributed within the genome are called 'open sea' [49].

2.12.5 Correlation analysis between DNA methylation at individual CpG sites and expression of Mecp2 isoforms

Correlation analysis between DNA methylation and gene expression is an established method to determine/predict the role of DNA methylation in gene expression regulation [14,50]. Therefore, Pearson's correlation analysis and linear regression were performed to determine correlations between DNA methylation at the *Mecp2* REs and expression of *Mecp2* isoforms in differentiating NSC (Chapter 3), and neurons and astrocytes (Chapter 5). For each CpG site, Pearson's correlation coefficient (*r*) was calculated against the relative expression of each *Mecp2* isoform. In Chapter 3, correlation analysis was also done for average methylation over entire regions. The strength of correlation was considered as follows: weak, $0 < r < 0.3$; moderate, $0.3 < r < 0.4$; strong, $0.4 < r < 0.7$; or very strong, $0.7 < r < 1.0$ [51]. It is assumed that a negative *r*-value might represent inverse/negative correlation and implies gene repression by DNA methylation. On the other hand, a positive *r*-value is assumed to represent direct/positive correlation, suggesting an active regulation by DNA methylation. Statistical significance was determined at $P < 0.05$.

2.13 DNA methylation analysis by MeDIP and hMeDIP

In Chapter 4, 5mC and 5hmC levels at the *Mecp2* REs were determined by MeDIP and hMeDIP, respectively.

2.13.1 Methylated DNA immunoprecipitation

DNA immunoprecipitation for 5mC enrichment was carried out using MeDIP kit (Abcam; ab117133) as per manufacturer's guidelines [52], using samples from 3-4 biological replicates. MeDIP was done only for D8 continuous ethanol exposure and ethanol withdrawal conditions using 1 µg of DNA per reaction.

Preparation of antibody-coated wells: Briefly, first strip wells (provided with the kit) in which immunoprecipitation was carrying out were kept on the plate frame, and 100 µl of the antibody buffer (antibody to buffer ratio was 1:100) was added to each well. Antibody (1 µl) was added to a set of wells while normal mouse IgG antibody (1 µl) was added to the negative control wells. This was followed by covering the strip wells with parafilm M and incubating the antibody in the well allowing it to bind to the wells at RT for 1 h.

Preparation of DNA samples: During the 1h incubation time, the sample DNA was prepared for shearing. DNA (1 µg) was mixed with 100 µl of the reaction buffer and sonicated inside the cold room. The sonication was done by 5 x 10 s pulses with 30 s intervals on ice in between each pulse. The sonication probe was 3 mm, and the amplitude was 30%. The sonicated DNA was denatured by boiling to 95°C for 2 min in a heat block, and the tubes were immediately transferred onto ice. A portion of the sonicated DNA was kept aside as input DNA for qPCR experiments.

Immunoprecipitation: After 1h, the antibody solution was discarded, and two washes of the strip wells were done, once with 150 µl of the antibody buffer and once with 150 µl of the wash buffer. Washing was done simply by slowly adding the solutions to the wells and pipetting them out.

Subsequently, 100 µl of the sonicated DNA was added to each strip well, and they were covered with parafilm M. The strip wells were secured onto the plate by more parafilm and was covered with aluminum foil. They were incubated for 90 min an orbital shaker (100 rpm) at RT. After the incubation period, the solutions were removed from the strip wells carefully, and three washes were done with 150 µl of the wash buffer. Each wash was done simply by pipetting the washing solution in and out of the well. After the last wash, 60 µl of the DNA release buffer (with proteinase K) was added to each well. The wells were covered with strip caps, and they were kept in a thermal cycler with a 48-well block, which was programmed for 60 min at 65ºC. After this 1h incubation, the elution reaction was set up as follows. Spin columns were kept inside 2 ml collection tubes, and 100 µl of the binding buffer was added directly to each column. The samples in strip wells were taken out and added to eppendorf tubes and mixed with 180 µl of 100% ethanol. The sample-ethanol mix was transferred to the columns with the binding buffer. The tubes were centrifuged for 30 s at 12000 rpm using a microcentrifuge. The flow through was discarded, and 200 µl of 90% ethanol was added to the spin column and centrifuged for 30 s at 12000 rpm. The same protocol of washing with 200 µl of 90% ethanol was repeated one more time.

Release and elution of DNA: Finally, the columns were kept in eppendorf tubes and 20 µl of the elution buffer was added directly onto the filter of the column. The tubes were centrifuged for 30 s at 12000 rpm to elute DNA from the column. The samples contained 5mC-immunoprecipitated DNA were stored in -20°C until used in qPCR experiments.

2.13.2 hMeDIP

DNA immunoprecipitation for 5hmC enrichment was carried out using MeDIP kit (Abcam; ab117134) as per manufacturer's guidelines [53]. hMeDIP was done for D2 binge ethanol

exposure, D8 ethanol withdrawal, and D8 continuous ethanol exposure. Due to limited sample availability, 100 ng of DNA per reaction was used for D2 binge ethanol condition. In contrast, 500 ng of DNA per reaction was used for all D8 conditions.

Preparation of antibody-coated wells: The strip wells required for the experiment were kept carefully on the plate frame (provided with the kit), and 100 µl of the antibody buffer was administered to each well. The strip wells were organized in a way that there were sample wells to which NSC DNA was to be added and a positive control well to which a positive control DNA sample (44 5hmC-CpG sites) provided within the kit was added. To both sample and positive control wells, 1 µl of non-immune IgG antibody (negative control) or 1 µl of 5hmC antibody was added and mixed carefully. The strip wells were covered with parafilm M and incubated for 60 min at RT.

Preparation of DNA samples: During this 1h, the sample DNA preparation was done. DNA was sonicated for 10 s pulses five times with 30 sec-interval on ice in between each pulse. The sonication probe was 3 mm in size, and the amplitude was 30%. These sonication conditions produced DNA fragments of 200-500 bp in size as determined by agarose gel electrophoresis. A portion of the sonicated DNA was kept aside as 'input DNA.' Once the incubation period was over, the antibody buffer was carefully removed from the wells, and they were washed twice with 200 µl of 1X wash buffer by pipetting in and out of the well at RT.

Preparation of hMeDIP reaction and immunoprecipitation: The samples were diluted to 10 ng/µl in hMeDIP solution as follows: 50 µl of sample DNA was mixed with 50 µl of the hMeDIP solution; 1 µl of positive control DNA was mixed with 99 µl of the hMeDIP solution. Subsequently, all the strip wells were covered with parafilm M and incubated for 90 min on an orbital shaker at 75 rpm at RT as described in section 2.15.1. After the incubation, the reaction

solution was pipetted out carefully and discarded. This was followed by five washes with 200 µl of the 1X wash buffer by pipetting the buffer in and out of the wells. A final wash was given with 200 µl of the DNA release buffer.

Release and elution of DNA: Subsequently, 40 µl of the DNA release buffer (with proteinase K) was administered into the strip wells. The wells were placed inside a thermal cycler with a 48-well block, which was programmed for the following reaction: 60°C for 15 min, 95°C for 3 min and 4°C for 5 min. The strip wells were sealed with an adhesive 8-well strip film, and the reaction was started. After the reaction, the wells were taken out and kept on the tray plate and spun them down briefly at RT in a plate rotor. The release buffer with the immunoprecipitated DNA was stored in -20°C until used for qPCR reactions.

2.13.3 qPCR for calculation of percentage input

Following the MeDIP and hMeDIP reactions, qPCR was done to analyze the immunoprecipitated DNA for the enrichment of 5mC and 5hmC at the *Mecp2* REs. The primers used in the qPCR reactions are listed in **Table 4.5**, the accuracy of which was determined by running the products on an agarose gel to confirm their sizes **(Figure 2.4)**. For each biological replicate of the MeDIP and hMeDIP reactions, 2-3 qPCRs were performed. The qPCR conditions used are as follows:

Mecp2 R1-R6: 95°C for 10 min; 50 cycles of 95°C for 15 s, 60°C for 1 min, followed by a melt curve

Positive control 5hmC DNA: 95°C for 7 min; 40 cycles of 95°C for 10 s, 55°C for 10 s and 72°C for 8 s; Final extension 72°C for1 min

Chapter 2

As a negative control for unmethylated DNA in both MeDIP and hMeDIP experiments, qPCR with *Gapdh* primers was done. Using the primers provided with the kit, qPCR for the positive control 5hmC-enriched DNA was carried out as well. As a positive control for 5mC methylated DNA, qPCR for *major satellite repeats* was conducted.
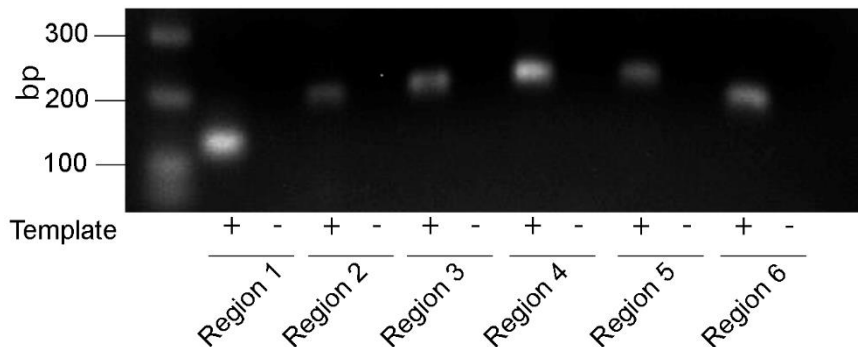
Figure 2.4 Agarose gel illustrating PCR product sizes for *Mecp2* REs

After qPCR experiments, the correct PCR product formation was evaluated by agarose gel (1.5%) electrophoresis. The corresponding product sizes are listed in Table 2.7. Regions 1-3 are *Mecp2* promoter REs, while Regions 4-6 are intron 1 REs.

Percentage input for the Ct values obtained from each qPCR was calculated relative to the Ct value of the input DNA used. The difference in Ct values for the *Mecp2* REs between sample immunoprecipitated with 5hmC, 5mC or IgG and input DNA was calculated using the following equations.

$$\Delta Ct = Ct_{(immunoprecipatated)} - Ct_{(input)} \ldots\ldots\ldots\ldots\ldots\ldots \text{Equation 1}$$

$$\text{Percentage input} = 2^{\Delta Ct} \, x \, 100 \ldots\ldots\ldots\ldots\ldots\ldots \text{Equation 2}$$

2.14 DNA dot blot

2.14.1 Performing DNA dot blot

DNA dot blot was performed using a previously described protocol [54], with minor modifications. This method was employed in studies shown in Chapters 3 and 4 with NSC treated with decitabine or ethanol.

Sample preparation: The sample DNA was prepared by mixing 200-250 ng NSC DNA, 0.4M NaOH and 10 mM EDTA to a final volume of 250µl. The tubes were sealed with parafilm and kept in a heat block to denature the DNA at 100°C for 10 min. The sample tubes were immediately transferred onto ice. The denatured DNA containing NaOH was neutralized with an equal volume (250µl) of ice-cold 2M ammonium acetate (pH 7.0), and the tubes were spun briefly using a benchtop Dr. Spin personal centrifuge to bring down the evaporated liquid.

Transferring DNA onto membrane: Zeta-probe GT blotting membrane (Bio-Rad) was cut into the size of the bio-dot microfiltration apparatus. The transfer of DNA onto the zeta-probe membranes was carried out as per manufacturer's instructions for bio-dot microfiltration apparatus [55] and zeta-probe membrane [56]. The membrane was immersed in ultrapure water for 10 min. The microfiltration apparatus was cleaned up thoroughly and set up with the membrane inside as instructed in the manual. Throughout the process, the membrane should not be allowed to dry. DNA sample (500 µl) was added to each well, and the rest of the wells were filled with ultra-pure water. Vacuum was applied until the wells were just emptied (but not dried up). Vacuum was closed, and 500 µl of 0.4M NaOH was added to all sample wells. Vacuum was applied to remove NaOH from the wells. The microfiltration apparatus was disassembled, and the membrane was taken out, and the wells were marked carefully. The membrane was rinsed for few seconds with 100 ml of 2X saline-sodium citrate (SSC) buffer. Subsequently, the membrane was air dried on a

clean filter paper.

Blotting: The membrane was kept inside a UV cross-linker with the DNA side of the membrane up. Using maximum crosslink DNA was cross-linked on the membrane. The membrane was wet with ultrapure water and blocked with 5% milk for 5hmC or 3% milk for 5mC in PBST (PBS with 0.2% tween20) for 3 h at RT. Appropriate primary antibody (5mC or 5hmC) suspended in 5% or 3% milk in PBST (**Table 3.3** and **4.2**) was added onto the membrane and incubated overnight (16-20 h) at 4°C. Next day, the membrane was rinsed quickly with PBST, followed by three 20 min-washes with PBST at RT. After washes, appropriate secondary antibodies, which are peroxidase-conjugated **(Table 3.4** and **4.3)** were added onto the membrane and incubated for 1 h at RT. This was followed by two rinses and three 20-min washes with PBST.

Development: Immobilon western chemiluminescent HRP substrate solution (EMD Millipore™) containing luminol and peroxide was used in the development of dot blot as per manufacturer's instructions [35].

2.14.2 Measurement of total DNA content

5mC and 5hmC levels detected in each dot of DNA were normalized to the amount of total DNA loaded on the membrane*s*. This was done by methylene blue (MB) staining as described previously [57]. The membrane was washed twice with PBST for 20 min. 0.02% MB in 0.3 μM sodium acetate (pH 5.2) solution was added enough to cover the membrane. The MB staining was carried out for 10-15 min at RT on a shaker. After MB was removed from the membrane, it was rinsed with distilled water three times, each for 5-10 s, making sure all the wells are stained blue (against the white/blue background). The membrane was dried and imaged using a camera.

2.14.3 Quantification and data analyses

Dot blot signal quantification was done with Adobe Photoshop CS5 software and normalized to the signals from MB total DNA signals. Briefly, the X-ray films containing the dot blot 5mC or 5hmC signals and images with MB signals were scanned and loaded to Adobe Photoshop CS5. Images of the dots were inverted. A box was drawn around a dot using the marquee tool, and mean pixels were obtained using histogram. The same box was used to quantify mean signals from all the dots and the background signals. The mean signals from the background were subtracted from the 5mC or 5hmC values. The 5mC and 5hmC values were normalized to MB signals and represented as arbitrary units.

2.15 *In silico* analysis of ChIPseq data from CistromeDB

Mouse *Mecp2*: ChIPseq data available through CistromeDB data portal (cistrome.org/db/) were extracted as described elsewhere [58] to identify the enrichment of selected hPTMs and TFs at the *Mecp2* promoter. ChIPseq data were assembled using UCSC genome browser on mouse Dec. 2011 (GRCm38/mm10) assembly. For determination of active nature of the *Mecp2* promoter in neurons, ChIPseq data for H3K27ac, H4K16ac, and H3K4me2 were extracted from [59] and neuronal transcription activator MEF2A from [60]. For comparison purpose, ChIPseq data for H3K27ac were extracted from [61].

Human *MECP2*: To determine the enrichment of hPTMs and TFs on the human *MECP2* promoter, I used ChIPseq data available through ENCODE consortium project (http://genome.ucsc.edu/ENCODE/) for human Neurons (SK-N-SH_RA) differentiated using retinoic acid (RA) and human astrocytes (NH-A-Brain) (**Table 2.1**). ChIPseq data were assembled using UCSC genome browser on human Feb. 2009 (GRCh37/hg19) assembly.

Table 2.1 Histone PTMs and TFs used to determine expression status of *MECP2* in human neurons and astrocytes			
TFs or hPTMs	**Function**	**Neurons (SK-N-SH_RA)**	**Astrocytes (NH-A-Brain)**
EZH2	Partner of POLR2	✓	✓
H3K27me3	Inactive chromatin	✓	✓
H3K4me3	Active promoters	✓	✓
POLR2A	Transcription	✓	✗
H3K9ac	Active promoters	✗	✓
H3K27ac	Active promoters	✗	✓

2.16 Statistical analyses

All graphs were generated using GraphPad Prism software and represent the average of two to four independent experiments. Error bars indicate standard error of the mean (SEM). Statistical significance was calculated by *****P <0.0001, ***P <0.001, **P <0.01,* or **P <0.05*. For gene expression analysis involving ethanol and decitabine treatments, student's *t*-test was used to determine statistical significance. In accordance with previous studies, error bars were included for N=2 experiments, which had extremely low amount of samples in Chapters 3 and 4 [62,63]. For comparison of cell type-specific, sex-specific and isoform-specific expression of *Mecp2*, two-way ANOVA was used. For N=2 experiments in Chapter 5, error bars were not included, and individual values were represented as described in other studies [3]. DNA methylation analysis by bisulfite pyrosequencing, hMeDIP and MeDIP in between control and treated samples and in between cell types was evaluated statistically using two-way ANOVA. Cell number quantification, neurite branching, and glial cell size were also analyzed using two-way ANOVA.

Chapter 2

2.17 References

1. Bell G (2016) Replicates and repeats. BMC Biology 14: 28.

2. Langton PD (2012) Essential guide to reading biomedical papers: recognising and interpreting best practice: John Wiley & Sons.

3. Vaux DL (2012) Research methods: Know when your numbers are significant. Nature 492: 180-181.

4. Rastegar M, Hotta A, Pasceri P, Makarem M, Cheung AY, Elliott S, Park KJ, Adachi M, Jones FS, et al. (2009) MECP2 isoform-specific vectors with regulated expression for Rett syndrome gene therapy. PLoS One 4: e6810.

5. Barber BA, Liyanage VR, Zachariah RM, Olson CO, Bailey MA, Rastegar M (2013) Dynamic expression of MEIS1 homeoprotein in E14.5 forebrain and differentiated forebrain-derived neural stem cells. Ann Anat 195: 431-440.

6. Liyanage VR, Zachariah RM, Davie JR, Rastegar M (2015) Ethanol deregulates Mecp2/MeCP2 in differentiating neural stem cells via interplay between 5-methylcytosine and 5-hydroxymethylcytosine at the Mecp2 regulatory elements. Exp Neurol 265: 102-117.

7. Liyanage VR, Zachariah RM, Rastegar M (2013) Decitabine alters the expression of Mecp2 isoforms via dynamic DNA methylation at the Mecp2 regulatory elements in neural stem cells. Mol Autism 4: 46.

8. Ishimaru N, Fukuchi M, Hirai A, Chiba Y, Tamura T, Takahashi N, Tabuchi A, Tsuda M, Shiraishi M (2010) Differential epigenetic regulation of BDNF and NT-3 genes by trichostatin A and 5-aza-2'-deoxycytidine in Neuro-2a cells. Biochem Biophys Res Commun 394: 173-177.

9. Mossman D, Kim KT, Scott RJ (2010) Demethylation by 5-aza-2'-deoxycytidine in colorectal cancer cells targets genomic DNA whilst promoter CpG island methylation persists. BMC Cancer 10: 366.

10. Adachi J, Mizoi Y, Fukunaga T, Ogawa Y, Ueno Y, Imamichi H (1991) Degrees of alcohol intoxication in 117 hospitalized cases. J Stud Alcohol 52: 448-453.

11. Vangipuram SD, Lyman WD (2012) Ethanol affects differentiation-related pathways and suppresses Wnt signaling protein expression in human neural stem cells. Alcohol Clin Exp Res 36: 788-797.

12. Hicks SD, Middleton FA, Miller MW (2010) Ethanol-induced methylation of cell cycle genes in neural stem cells. J Neurochem 114: 1767-1780.

13. Zachariah RM, Olson CO, Ezeonwuka C, Rastegar M (2012) Novel MeCP2 isoform-specific antibody reveals the endogenous MeCP2E1 expression in murine brain, primary neurons and astrocytes. PLoS One 7: e49763.

14. Olson CO, Zachariah RM, Ezeonwuka CD, Liyanage VR, Rastegar M (2014) Brain region-specific expression of MeCP2 isoforms correlates with DNA methylation within Mecp2 regulatory elements. PLoS One 9: e90645.

15. Cerase A, Pintacuda G, Tattermusch A, Avner P (2015) Xist localization and function: new insights from multiple levels. Genome biology 16: 166.

16. Hartshorn C, Rice JE, Wangh LJ (2002) Developmentally-regulated changes of Xist RNA levels in single preimplantation mouse embryos, as revealed by quantitative real-time PCR. Mol Reprod Dev 61: 425-436.

17. QIAGEN (2006) DNeasy® Blood & Tissue Handbook.

18. Kashimada K, Koopman P (2010) Sry: the master switch in mammalian sex determination. Development 137: 3921-3930.

19. Yang Y-C, Ciarletta AB, Temple PA, Chung MP, Kovacic S, Witek-Giannotti JS, Leary AC, Kriz R, Donahue RE, et al. (1986) Human IL-3 (multi-CSF): identification by expression cloning of a novel hematopoietic growth factor related to murine IL-3. Cell 47: 3-10.

20. Lambert JF, Benoit BO, Colvin GA, Carlson J, Delville Y, Quesenberry PJ (2000) Quick sex determination of mouse fetuses. J Neurosci Methods 95: 127-132.

21. Invitrogen (2016) Platinum™ Pfx DNA Polymerase Product information. Invitrogen.https://tools.thermofisher.com/content/sfs/manuals/platinumpfx_pps.pdf

22. Manual I Sub-Cell® GT Agarose Gel Electrophoresis Systems.

23. QIAGEN (2012) RNeasy® Mini Handbook. In: 5, editor.

24. Invitrogen (2012) TRIzol™ Reagent User guide.

25. Ambion-Life-Technologies (2011) mirVana™ miRNA Isolation Kit.

26. Ambion-Life-Technologies (2012) Ambion® TURBO DNA-free™ DNase Treatment and Removal Reagents User Guide.

27. Kobrossy L, Rastegar M, Featherstone M (2006) Interplay between chromatin and trans-acting factors regulating the Hoxd4 promoter during neural differentiation. J Biol Chem 281: 25926-25939.

28. Rastegar M, Kobrossy L, Kovacs EN, Rambaldi I, Featherstone M (2004) Sequential histone modifications at Hoxd4 regulatory regions distinguish anterior from posterior embryonic compartments. Mol Cell Biol 24: 8090-8103.

29. Mnatzakanian GN, Lohi H, Munteanu I, Alfred SE, Yamada T, MacLeod PJ, Jones JR, Scherer SW, Schanen NC, et al. (2004) A previously unidentified MECP2 open reading frame defines a new protein isoform relevant to Rett syndrome. Nat Genet 36: 339-341.

30. Applied-Biosystems (2010) Applied Biosystems 7500/7500 Fast Real-Time PCR System - Relative Standard Curve and Comparative CT Experiments - Getting Started Guide.

31. Rastegar M, Rousseau GG, Lemaigre FP (2000) CCAAT/enhancer-binding protein-alpha is a component of the growth hormone-regulated network of liver transcription factors. Endocrinology 141: 1686-1692.

32. Thermo_Scientific (2013) NE-PER Nuclear and Cytoplasmic Extraction Reagents

33. Bio-Rad (1994) Bio-Rad Protein Assay.

34. Manual I Mini Trans-Blot® Electrophoretic Transfer Cell Instruction Manual.

35. Millipore User Guide for Immobilon™ Western Chemiluminescent HRP Substrate.

36. Yamaguchi S, Hong K, Liu R, Inoue A, Shen L, Zhang K, Zhang Y (2013) Dynamics of 5-methylcytosine and 5-hydroxymethylcytosine during germ cell reprogramming. Cell Res 23: 329-339.

37. Zeiss C (2006) Operating Manual Axio Observer Inverted microscope

38. Ferreira TA, Rasband W (2010) The ImageJ User Guide - Version 1.43.

39. Schade A, Delyagina E, Scharfenberg D, Skorska A, Lux C, David R, Steinhoff G (2013) Innovative Strategy for MicroRNA Delivery in Human Mesenchymal Stem Cells via Magnetic Nanoparticles. Int J Mol Sci 14: 10710-10726.

40. Adachi M, Keefer EW, Jones FS (2005) A segment of the Mecp2 promoter is sufficient to drive expression in neurons. Hum Mol Genet 14: 3709-3722.

41. Singh J, Saxena A, Christodoulou J, Ravine D (2008) MECP2 genomic structure and function: insights from ENCODE. Nucleic Acids Res 36: 6035-6047.

42. Liu J, Francke U (2006) Identification of cis-regulatory elements for MECP2 expression. Hum Mol Genet 15: 1769-1782.

43. Nagarajan RP, Patzel KA, Martin M, Yasui DH, Swanberg SE, Hertz-Picciotto I, Hansen RL, Van de Water J, Pessah IN, et al. (2008) MECP2 promoter methylation and X chromosome inactivation in autism. Autism Res 1: 169-178.

44. Nagarajan RP, Hogart AR, Gwye Y, Martin MR, LaSalle JM (2006) Reduced MeCP2 expression is frequent in autism frontal cortex and correlates with aberrant MECP2 promoter methylation. Epigenetics 1: e1-11.

45. QIAGEN (2006) DNeasy® Blood & Tissue Handbook.

46. Choufani S, Shapiro JS, Susiarjo M, Butcher DT, Grafodatskaya D, Lou Y, Ferreira JC, Pinto D, Scherer SW, et al. (2011) A novel approach identifies new differentially methylated regions (DMRs) associated with imprinted genes. Genome Res 21: 465-476.

47. Gardiner-Garden M, Frommer M (1987) CpG islands in vertebrate genomes. Journal of molecular biology 196: 261-282.

48. Bibikova M, Barnes B, Tsan C, Ho V, Klotzle B, Le JM, Delano D, Zhang L, Schroth GP, et al. (2011) High density DNA methylation array with single CpG site resolution. Genomics 98: 288-295.

49. Sandoval J, Heyn H, Moran S, Serra-Musach J, Pujana MA, Bibikova M, Esteller M (2011) Validation of a DNA methylation microarray for 450,000 CpG sites in the human genome. Epigenetics 6: 692-702.

50. Chen C, Zhang C, Cheng L, Reilly JL, Bishop JR, Sweeney JA, Chen H-y, Gershon ES, Liu C (2014) Correlation between DNA methylation and gene expression in the brains of patients with bipolar disorder and schizophrenia. Bipolar disorders 16: 790-799.

51. Ratner B The Correlation Coefficient: Definition. http://www.dmstat1.com/res/TheCorrelationCoefficientDefined.html

52. Abcam (2014) ab117133 –Methylated DNA Immunoprecipitation (MeDIP) Kit.

53. Abcam (2014) ab117134 – Hydroxymethylated DNA Immunoprecipitation (hMeDIP) ChIP Kit.

54. Ko M, Huang Y, Jankowska AM, Pape UJ, Tahiliani M, Bandukwala HS, An J, Lamperti ED, Koh KP, et al. (2010) Impaired hydroxylation of 5-methylcytosine in myeloid cancers with mutant TET2. Nature 468: 839-843.

55. Bio-Rad (2008) Dot Blot microfiltration apparatus- Instructions manual.

56. Bio-Rad Zeta-Probe® GT (Genomic Tested) Blotting Membranes Instruction Manual.

57. Ko M, Huang Y, Jankowska AM, Pape UJ, Tahiliani M, Bandukwala HS, An J, Lamperti ED, Koh KP, et al. (2010) Impaired hydroxylation of 5-methylcytosine in myeloid cancers with mutant TET2. Nature 468: 839-843.

58. Mei S, Qin Q, Wu Q, Sun H, Zheng R, Zang C, Zhu M, Wu J, Shi X, et al. (2017) Cistrome Data Browser: a data portal for ChIP-Seq and chromatin accessibility data in human and mouse. Nucleic Acids Research 45: D658-D662.

59. Telese F, Ma Q, Perez PM, Notani D, Oh S, Li W, Comoletti D, Ohgi KA, Taylor H, et al. (2015) LRP8-Reelin-Regulated Neuronal Enhancer Signature Underlying Learning and Memory Formation. Neuron 86: 696-710.

60. Akhtar MW, Kim M-S, Adachi M, Morris MJ, Qi X, Richardson JA, Bassel-Duby R, Olson EN, Kavalali ET, et al. (2012) In Vivo Analysis of MEF2 Transcription Factors in Synapse Regulation and Neuronal Survival. PLOS ONE 7: e34863.

61. Schick S, Fournier D, Thakurela S, Sahu SK, Garding A, Tiwari VK (2015) Dynamics of chromatin accessibility and epigenetic state in response to UV damage. J Cell Sci 128: 4380-4394.

62. GraphPad (2014) Frequently Asked Questions: Statistics with n=2. http://www.graphpad.com/support/faqid/591/

63. Portoso M, Ragazzini R, Brenčič Ž, Moiani A, Michaud A, Vassilev I, Wassef M, Servant N, Sargueil B, et al. (2017) PRC2 is dispensable for HOTAIR-mediated transcriptional repression. The EMBO journal: e201695335.

CHAPTER 3. DECITABINE ALTERS THE EXPRESSION OF *MECP2* ISOFORMS *VIA* DYNAMIC DNA METHYLATION AT THE *MECP2* REGULATORY ELEMENTS IN NEURAL STEM CELLS.

3.1 Foreword

In Chapter 1, I discussed the importance of studying the regulatory mechanisms of *Mecp2*/MeCP2 isoforms in brain cell types. Therefore, the first aim of my thesis is the determination of the role of DNA methylation at the *Mecp2* REs in the *Mecp2* promoter and intron 1 in regulating *Mecp2* isoforms during NSC differentiation.

This chapter presents the first evidence of the potential role of DNA methylation in regulating *Mecp2* isoforms during neural stem cell differentiation while suggesting a potential method to modulate *Mecp2*/MeCP2 expression using a DNA demethylating drug called decitabine. The results included in this chapter are a direct reprint of my first-authored article published in Molecular Autism [1]. I have obtained copyright permission to reprint this article as a part of my thesis (see page xxi). The modifications made to the text included in this chapter are as follows;

1) The figure and table numbers have been changed to comply with the chapter formatting. Eg. Figure 1 to Figure 3.1 or Table 1 to Table 3.1.

2) The supplementary figures have been placed within the body of text as they appear in the chapter and their figure numbers have also been changed to comply with the chapter formatting. Eg. Additional file 1: Figure S1 to Figure 3.S1.

3) The reference style of Molecular Autism was changed to PLoS formatting to comply with the overall thesis format.

4) The figure 1 of the article (Figure 3.1 of this chapter) was slightly modified to correct the exon 4.

Chapter 3: Aim 1

As the first author of the study, I have contributed the majority of the contents of the study, which included conception, design, performing experiments, data analyses, data interpretation and manuscript writing. Details of the author contributions are indicated below.

<u>Vichithra R.B. Liyanage:</u> Conceived and designed experiments; helped with maintenance of NSC cultures; decitabine treatments; assisted with sample collection; RNA extraction, cDNA synthesis and qRT-PCR; DNA extraction, selection of regions for DNA methylation analysis by bisulfite pyrosequencing, analysis of bisulfite pyrosequencing data (gene-specific probe selection, primer optimization, and bisulfite pyrosequencing were done as a paid service at SickKids hospital, Toronto); DNA dot blot; nuclear protein extractions and western blotting; fixation of cultured cells and immunocytochemistry, inverted microscopic imaging and cell number quantification; data collection, analyses and interpretation; preparation of figures; manuscript writing.

<u>Robby M. Zachariah:</u> Conceived and designed experiments; maintained NSC cultures; sample collection; initial PFA steps of cell fixation; conducted some of the immunocytochemistry experiments; confocal imaging; reading and approving the final manuscript.

<u>Dr. Mojgan Rastegar:</u> Conceived and designed experiments; embryonic forebrain dissections; isolation and culture of primary NSC; neurosphere collections, cellular dissociations, and differentiation of NSC; provided research support; contributed reagents/materials/analysis tools; data analyses and interpretation, manuscript writing, final approval, and submission.

3.2 Author information

Vichithra R. B. Liyanage, Robby M. Zachariah, Mojgan Rastegar*

Regenerative Medicine Program, Department of Biochemistry and Medical Genetics, Faculty of Medicine, University of Manitoba, Rm. 627, Basic Medical Sciences Bldg., 745 Bannatyne Avenue, Winnipeg, Manitoba R3E 0J9, Canada

* Correspondence: rastegar@cc.umanitoba.ca

3.3 Author contributions

VRBL, RMZ, and MR conceived and designed experiments. MR performed neural stem cell isolation, culture, and differentiation. RMZ maintained neural stem cell cultures. VRBL performed qRT-PCR, dot blot, WB, IF and inverted microscopy imaging. RMZ performed IF and confocal imaging. VRBL and MR analyzed data. MR contributed reagents/materials/analysis tools. VRBL and MR wrote the paper. All authors read and approved the final manuscript.

3.4 Abstract

Background: Aberrant MeCP2 expression in the brain is associated with neurodevelopmental disorders including autism. In the brain of stressed mouse and autistic human patients, reduced MeCP2 expression is correlated with *Mecp2/MECP2* promoter hypermethylation. Altered expression of MeCP2 isoforms (MeCP2E1 and MeCP2E2) is associated with neurological disorders, highlighting the importance of proper regulation of both isoforms. While known regulatory elements (REs) within the *MECP2/Mecp2* promoter and intron 1 are involved in *MECP2/Mecp2* regulation, *Mecp2* isoform-specific regulatory mechanisms are unknown. We hypothesized that DNA methylation at these REs may impact the expression of *Mecp2* isoforms.

Methods: We used a previously characterized *in vitro* differentiating neural stem cell (NSC) system to investigate the interplay between *Mecp2* isoform-specific expression and DNA

methylation at the *Mecp2* REs. We studied altered expression of *Mecp2* isoforms, affected by global DNA demethylation and remethylation, induced by exposure and withdrawal of decitabine (5-aza-2′-deoxycytidine). Further, we performed correlation analysis between DNA methylation at the *Mecp2* REs and the expression of *Mecp2* isoforms after decitabine exposure and withdrawal.

Results: At different stages of NSC differentiation, *Mecp2* isoforms showed reciprocal expression patterns associated with minor, but significant changes in DNA methylation at the *Mecp2* REs. Decitabine treatment induced *Mecp2e1*/MeCP2E1 (but not *Mecp2e2*) expression at day (D) 2, associated with DNA demethylation at the *Mecp2* REs. In contrast, decitabine withdrawal downregulated both *Mecp2* isoforms to different extents at D8, without affecting DNA methylation at the *Mecp2* REs. NSC cell fate commitment was minimally affected by decitabine under tested conditions. Expression of both isoforms negatively correlated with methylation at specific regions of the *Mecp2* promoter, both at D2 and D8. The correlation between intron 1 methylation and *Mecp2e1* (but not *Mecp2e2*) varied depending on the stage of NSC differentiation (D2: negative; D8: positive).

Conclusions: Our results show the correlation between the expression of *Mecp2* isoforms and DNA methylation in differentiating NSC, providing insights on the potential role of DNA methylation at the *Mecp2* REs in *Mecp2* isoform-specific expression. The ability of decitabine to induce *Mecp2e1*/MeCP2E1, but not *Mecp2e2* suggests the differential sensitivity of *Mecp2* isoforms to decitabine and is important for future drug therapies for autism.

Keywords: Epigenetics, *Mecp2e1*, *Mecp2e2*, decitabine/5-aza-2′-deoxycytidine, DNA methylation, Autism

3.5 Background

Methyl CpG Binding Protein 2 (MeCP2) is a key transcriptional regulator in the brain [2]. *MECP2* mutations and expression deficits result in a broad range of neurodevelopmental disorders, including Rett syndrome (RTT) and Autism Spectrum Disorders [3,4]. In mice (*Mecp2*) and humans (*MECP2*), alternative splicing of a single gene leads to the generation of two protein isoforms MeCP2E1 and MeCP2E2 (mature transcripts for *Mecp2e1* and *Mecp2e2* are shown in **Figure 3.1A**) [5,6]. We and others have shown differential expression of the two *Mecp2*/MeCP2 isoforms in mouse brain [6-8]. Recent studies suggest that MeCP2E1 is the most relevant isoform for RTT pathology [9,10]. Moreover, overexpression of *Mecp2e2*, but not *Mecp2e1*, promotes neuronal cell death [11], implicating the importance of proper regulation of both *Mecp2* isoforms in the brain.
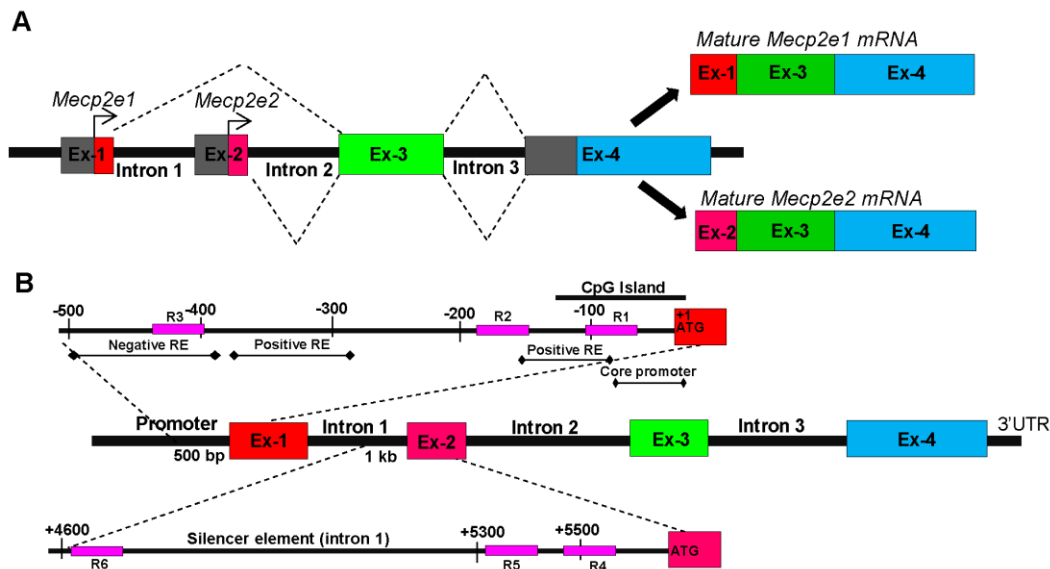
Figure 3.1. Schematics of the Methyl CpG binding protein 2 gene (*Mecp2*), *Mecp2e1/e2* transcripts, and known regulatory elements (REs).

A) Generation of MeCP2 isoforms by alternative splicing; mature *Mecp2e1* transcripts comprise of exons 1, 3, and 4. Mature *Mecp2e2* transcripts comprise of exons 2, 3, and 4 [adapted from [5,12]]. Exons are denoted as Ex. **B)** Regulatory elements of the *MECP2/Mecp2* gene. The

MECP2/Mecp2 gene is reported to be regulated by negative and positive REs within the promoter and a silencer element within intron 1 [information extracted from [13,14]]. For our studies, we selected a 500-bp region in the promoter upstream of exon 1 and a 1-kb region in intron 1 upstream of exon 2. Each sequence was divided into three regions, R1 to R3 in the *Mecp2* promoter and R4 to R6 in intron 1. Note that there are no CpG dinucleotides in the mouse genomic sequence between R5 and R6.

Figure modified and figure legend reprinted with permission from [1].

In RTT mouse models, transgenic expression of either *Mecp2* isoform can rescue RTT phenotypes to different extents [15,16]. However, gene therapy delivery of *MECP2* into the affected cells or drug therapies to induce *MECP2* expression has to be carried out with caution, as even mild overexpression of MeCP2 can lead to progressive neurological disorders [17,18]. Currently, limited knowledge exists on *MECP2/Mecp2* regulation, with no specific knowledge on possible differential *MECP2/Mecp2* isoform-specific regulatory mechanisms.

MECP2/Mecp2 gene expression is known to be regulated by regulatory elements (REs) within the promoter and a silencer element within the *Mecp2* intron 1 [13,14,19] (**Figure 3.1B**). Implying the role of DNA methylation in *MECP2* regulation, reduced *MECP2* expression in the brains of male autistic patients correlates with human *MECP2* promoter hypermethylation [3]. Moreover, reduced *Mecp*2 expression in the postnatal murine brain in response to early maternal separation and stress is associated with hypermethylation of the mouse *Mecp2* promoter [20]. However, the possible differential impact of DNA methylation on *MECP2*/*Mecp2* isoforms is currently unknown. DNA methylation is a major epigenetic modification that controls gene expression without affecting the underlying DNA sequences (reviewed in [21,22]). DNA methylation at the cytosine residues [5-methylcytosine (5mC)] of the CpG dinucleotides is carried out by DNA methyltransferases (DNMT) and is generally considered to be a repressive epigenetic

modification [2,23]. Conversely, 5-hydroxymethylcytosine (5hmC), which is generated by oxidation of 5mC by TET proteins, is generally considered to be an active epigenetic mark [24,25]. Promoter methylation (5mC) is mostly associated with gene silencing [26], while DNA methylation at both intronic and exonic regions are shown to correlate with isoform-specific transcription by alternative splicing or by utilizing alternate promoters [27,28].

Treatment with DNA demethylating agents or DNMT/*Dnmt* inhibitors such as decitabine (also called 5-aza-2′-deoxycytidine) is a commonly used method to study the role of DNA methylation in gene expression [29,30]. While exposure to decitabine results in DNA demethylation, its subsequent withdrawal causes remethylation or methylation reprogramming [30], providing an excellent platform to uncover the role of DNA methylation in gene expression.

In vitro differentiation of neural precursor cells/neural stem cells (NSC) into different brain cell types is utilized as an acceptable model system to mimic the *in vivo* neural development [31-36]. Previously, we used a similar *in vitro* NSC differentiation system to report the first preclinical *MECP2* isoform-specific gene therapy vectors, for future gene therapy applications in Rett syndrome [35]. Further, we introduced differentiating NSC as a suitable *in vitro* model to study the expression and function of developmentally important genes such as *Meis1* in neural development [37]. In the current study, we used this previously characterized system to study the expression and regulation of *Mecp2* isoforms during NSC differentiation.

Investigation of *MECP2*/MeCP2 expression and function in neurodevelopmental disorders has been the focus of intensive research. However, despite the critical importance of precisely controlled levels of MeCP2 expression in the brain, the underlying regulatory mechanisms have been understudied. Here, we report the correlation between the expression of *Mecp2* isoforms and DNA methylation patterns at the *Mecp2* REs at different stages of NSC differentiation. Further,

we demonstrate the effect of dynamic changes in DNA methylation induced by exposure and withdrawal of decitabine on the expression of *Mecp2/*MeCP2 isoforms.

3.6 Methods

3.6.1 Ethics statement

All experiments were performed in accordance with the standards of the Canadian Council on Animal Care with the approval of the Office of Research Ethics of the University of Manitoba. All experimental procedures were reviewed and approved (protocol number 12-031) by the University of Manitoba Bannatyne Campus Protocol Management and Review Committee.

3.6.2 Neural stem cell isolation, culture, and differentiation

Embryonic mouse forebrain-derived NSC were isolated from the forebrains of CD-1 mice at embryonic day (E) 14.5 and were cultured according to previously described methods [35,37]. Briefly, dissected forebrain tissues were mechanically homogenized in NSC media DMEM/F12 1:1 (Wisent, Quebec, Canada) containing HEPES, glutamine, antibiotic/antimycotic, glucose, recombinant human epidermal growth factor (rhEGF) (Sigma Aldrich, Oakville, Ontario, Canada, 20 ng/ml), basic fibroblast growth factor (bFGF) (Upstate (Millipore), Billerica, MA, USA, 20 ng/ml), heparin (Sigma Aldrich, Oakville, Ontario, Canada, 2 µg/ml) and hormone mix. Dissociated single cells were plated at a density of 10^5 cells/cm^2 in NSC media. The media was refreshed every 48 h and cells were cultured under these conditions for 7 days to generate neurospheres. Primary neurospheres were gently dissociated to single cells by accutase treatment. Dissociated cells were plated on plates coated with growth factor-reduced matrigel (BD Biosciences, Mississauga, Ontario, Canada) at a density of 10^5 cells/cm^2 in DMEM (GIBCO, Life

Technologies Inc., Burlington, Ontario, Canada) and 10% Fetal Bovine Serum (Invitrogen, Life Technologies Inc., Burlington, Ontario, Canada) in the absence of rhEGF and bFGF. Cells were differentiated for 8 days, reported to be sufficient for differentiation of neuronal and glial cells [35,37], and media was changed every other day.

3.6.3 Decitabine treatment

At the onset of differentiation on day zero (D0), dissociated NSC were treated with 2.5 μM decitabine for 48 h. After two days (D2), the media was replaced with fresh media that were refreshed every other day for an extra 6 days (until D8). Control cells were cultured under similar experimental conditions, in the absence of decitabine.

3.6.4 Quantitative measurement of male/female contribution

Genomic DNA from NSC at D0, D2, D8 and decitabine-treated cells were extracted using the DNeasy Blood and Tissue kit (Qiagen, Ontario, Toronto, Canada), as per manufacturer's instructions. The contribution of male and female sexes was determined by semi-quantitative PCR-based amplification of *Sry* (sex-determining region protein gene on the Y chromosome) and *Il3* (autosomal gene as an internal control) genes, as described previously [38], using the primers listed in **Table 3.1**. The PCR program consisted of an initial denaturation at 95°C for 4.5 min, followed by 33 cycles of 95°C for 35 s, 50°C for 1 min, 72°C for 1 min, and a final extension step at 72°C for 5 min. The amplified products were run on 1.5% agarose gel, and the bands were visualized by ethidium bromide staining. The *Sry* and *Il3* PCR products were identified based on the corresponding sizes (*Sry:* 402 bp, and *Il3*: 544 bp). The intensity of the corresponding bands was quantified using Adobe Photoshop CS5 software. The contribution of either sex was further

determined by quantitative reverse transcription PCR (qRT-PCR) for *Xist* (X-inactive specific transcript) gene, as previously described, with minor modifications [39]. The PCR program for *Xist* included an initial denaturation at 95°C for 5 min; followed by 35 cycles of 95°C for 30 s, 53°C for 30 s, 72°C for 30 s, and 78°C for 30 s.

Table 3.1 List of primers used for PCR			
Gene	**Direction**	**Sequence**	**Reference**
Sry	Forward	5′-TGGGACTGGTGACAATTGTC-3′	[38]
	Reverse	5′-GAGTACAGGTGTGCAGCTCT-3′	
Il3	Forward	5′-GGGACTCCAAGCTTCAATCA-3′	
	Reverse	5′-GGAGGAGGAAGAAAAGCAA-3′	

3.6.5 Quantitative reverse transcription polymerase chain reaction

RNeasy Mini Kit (Qiagen, Ontario, Toronto, Canada) was used for RNA extraction as per the manufacturer's protocol. Preparation of cDNA and qRT-PCR were carried out as described previously [40-43]. Transcript levels of *Mecp2* (total), *Mecp2e1* [NCBI: NM_001081979.1], *Mecp2e2* [NCBI: NM_010788.3], *Dnmt* genes (*Dnmt1, Dnmt3a* and *Dnmt3b*), neuronal genes (*Tubulin III* (*Tub III*), *NeuN*), astrocytic genes (*Gfap*, *S100b*), and oligodendrocyte-specific genes (*Cnpase*, *Mbp*) were examined by using gene-specific primers **(Table 3.2)**, as described previously [37,43]. The relative expression and fold changes were calculated as described previously [37]. Two-way analysis of variance (ANOVA) and the Student *t*-test were used to calculate significant differences between untreated control and decitabine-treated samples.

Table 3.2 List of primers used for qRT-PCR			
Gene	**Direction**	**Sequence**	**Reference**
Mecp2 (**total**)	Forward	5′-GGTAAAACCCGTCCGGAAAATG-3′	[5]
	Reverse	5′-TTCAGTGGCTTGTCTCTGAG-3′	
Mecp2e1	Forward	5′-AGGAGAGACTGGAGGAAAAGT-3′	[6]
	Reverse	5′-CTTAAACTTCAGTGGCTTGTCTCTG-3′	
Mecp2e2	Forward	5′-CTCACCAGTTCCTGCTTTGATGT-3′	
	Reverse	5′-CTTAAACTTCAGTGGCTTGTCTCTG-3′	
Tubulin III (Tub III)	Forward	5′-TCAGCGATGAGCACGGCATA-3′	[37]
	Reverse	5'-CACTCTTTCCGCACGACATC-3′	
Gfap	Forward	5′-GCTCACAATACAAGTTGTCC-3′	
	Reverse	5′-ACCTAATTACACAGAGCCAGG-3′	
Gapdh	Forward	5′-AACGACCCCTTCATTGAC-3′	[43]
	Reverse	5′-TCCACGACATACTCAGCAC-3′	
NeuN	Forward	5′-GGCAATGGTGGGACTCAAAA-3′	[44]
	Reverse	5′-GGGACCCGCTCCTTCAAC-3′	
S100b	Forward	5′-GCTGACCACCATGCCCCTGTAG-3′	[45]
	Reverse	5'-CTGGCCATTCCCTCCTCTGTC-3′	
Mbp	Forward	5′-GGCACGCTTTCCAAAATCT-3′	[46]
	Reverse	5′-CCATGGGAGATCCAGAGC-3′	
Cnpase	Forward	5′-CATCCTCAGGAGCAAAGGAG-3′	[47]
	Reverse	5′-TGAATAGCGTCTTGCACTCG-3′	
Dnmt1	Forward	5′-AGGGAAAAGGGAAGGGCAAG-3′	[48]
	Reverse	5′-AGAAAACACATCCAGGGTCCG-3′	
Dnmt3a	Forward	5′-CAGCGTCACACAGAAGCATATCC-3′	
	Reverse	5′-GGTCCTCACTTTGCTGAACTTGG-3′	
Dnmt3b	Forward	5′-CCTGCTGAATTACTCACGCCCC-3′	
	Reverse	5′-GTCTGTGTAGTGCACAGGAAAA-3′	

Xist	Forward	5′-TTGTGGCTTGCTAATAAT-3′	[39]
	Reverse	5′-AAACCCCATCCTTTATG-3′	

3.6.6 Immunofluorescence experiments

Immunofluorescence (IF) experiments were performed according to previously described protocols [8,35,37]. Primary and secondary antibodies used for IF are listed in the **Tables 3.3 and 3.4**, respectively. Immunofluorescence signals were detected by an Axio Observer Z1 inverted microscope and LSM710 Confocal microscope from Carl Zeiss. Images were obtained with AxioVision 4.8 (Carl Zeiss Canada Ltd. Ontario, Toronto, Canada) and Zen 2009 software and assembled using Adobe Photoshop CS5 and Adobe Illustrator CS5. For quantification analysis in neurospheres, three neurospheres were randomly selected, and all cells within each neurosphere were counted based on 4',6-diamidino-2-phenylindole (DAPI) staining. For cell quantification of differentiating cells at D2 and D8, 8 to 10 random fields were selected under the microscope. Approximately 250 cells from the D2 population and 750 cells from the D8 population were counted based on DAPI labeling. The cell counting was done using the ImageJ program.

Table 3.3 Primary antibodies used

Primary antibody	Application and dilution	Description	Source
MeCP2 (C-terminal)	IF 1:200	Rabbit polyclonal	Millipore, Billerica, MA, USA, 07-013
MeCP2 (C-terminal)	WB 1:100 IF 1:200	Mouse monoclonal	Abcam, Ontario, Toronto, Canada, Ab50005
MeCP2E1	WB 1:100	Chicken polyclonal	Custom-made [7]
GFAP	IF 1:200	Mouse monoclonal	Invitrogen, Life Technologies Inc., Burlington, Ontario, Canada 421262
TUBULIN III (TUB III)	IF 1:200	Mouse monoclonal	Chemicon, Millipore, Billerica, MA, USA MAB1637
OLIG2	IF 1:200	Rabbit polyclonal	Millipore, Billerica, MA, USA, AB9610
NESTIN	IF 1:230	Rat monoclonal	Developmental Studies Hybridoma Bank, Rat-401c
S100B	IF 1:100	Mouse monoclonal	Abcam, Ontario, Toronto, Canada, ab4066
CNPase	IF 1:100	Mouse monoclonal	Covance, SMI-91R
MBP	IF 1:100	Rabbit polyclonal	Abcam, Ontario, Toronto, Canada, ab40390
NEUN	IF 1:200	Mouse monoclonal	Millipore, Billerica, MA, USA, Mab377
Ki67	IF 1:200	Rabbit polyclonal	Santa Cruz, Dallas, Texas, USA, sc-15402
5mC	Dot blot 1:1000 IF 1:200	Mouse monoclonal	Abcam, Ontario, Toronto, Canada, Ab73938
5hmC	Dot blot 1:1000	Rabbit polyclonal	Active Motif, Carlsbad, CA, 39769

MeCP2, Methyl CpG binding protein; GFAP, Glial fibrillary acidic protein; OLIG2, Oligodendrocyte lineage transcription factor; CNPase, 2',3'-Cyclic-nucleotide 3'-phosphodiesterase, MBP, Myelin basic protein; NEUN, NEUronal Nuclei; 5mC, 5-methylcytosine; 5hmc, 5-hydroxymethylcytosine; IF, Immunofluorescence; WB, Western blot.

Table 3.4 Secondary antibodies used		
Secondary antibody	Application and dilution	Source
FITC conjugated goat anti rabbit IgG	IF 1:400	Jackson Immunoresearch, PA, USA, 111-095-144
Rhodamine Red-X conjugated goat anti mouse IgG	IF 1:400	Jackson Immunoresearch, PA, USA, 115-259-146
Dylight 649 conjugated goat anti chicken IgY	IF 1:400	Jackson Immunoresearch, PA, USA, 103-485-155
Dylight 649 conjugated donkey anti goat IgG	IF 1:400	Jackson Immunoresearch, PA, USA, 705-494-147
Alexa Fluor 594 conjugated donkey anti mouse IgG	IF 1:1,000	Life Technologies Inc., Ontario, Canada, 987237
Alexa Fluor 448 conjugated donkey anti rabbit IgG	IF 1:1,000	Life Technologies Inc., Ontario, Canada 913921
Peroxidase-Affinipure Gt anti-mouse IgG	WB 1:7,500; Dot blot 1:7,500	Jackson ImmunoResearch, PA, USA, 115-035-174

IF, immunofluorescence; WB, western blot.

3.6.7 Nuclear extractions and western blotting

Nuclear extraction from D2 and D8 NSC were carried out using the NE-PER Nuclear and Cytoplasmic Extraction Kit (Thermo Scientific, Ontario, Toronto, Canada), as per the manufacturer's instructions. Western blot (WB) experiments were conducted according to

previously described protocols [49-51], and quantification of the signals was performed as reported [8]. ACTIN or glyceraldehyde-3-phosphate dehydrogenase (GAPDH) was used as a loading control. Student *t*-test was used to determine statistical significance between control and treated cells. Primary and secondary antibodies used for WB are listed in the **Tables 3.3 and 3.4**, respectively.

3.6.8 DNA dot blot assay for 5mC and 5hmC

Genomic DNA was isolated using the DNeasy Blood and Tissue kit (Qiagen, Ontario, Toronto, Canada). DNA dot blot was performed using a previously described protocol [52], with minor modifications. The DNA blotted membranes were probed with either 5mC or 5hmC antibody **(Tables 3.3 and 3.4)**. Total DNA levels were detected by staining the same membrane with 0.02% methylene blue (MB) in 0.3 μM sodium acetate (pH 5.2). Adobe Photoshop CS5 software was used to quantify dot blot signals.

3.6.9 Bisulfite pyrosequencing

Genomic DNA was isolated as described in the previous section. Primer design and bisulfite pyrosequencing experiments were conducted as a service by the Hospital for Sick Children (SickKids), Toronto, Canada, as reported elsewhere [53], using the primers listed in **Table 3.5**. The regions analyzed for the methylation patterns are shown in **Figure 3.1B**. Specific CpG dinucleotides that are analyzed within each region are shown in **Figure 3.S1**.

Table 3.5 Primers used in bisulfite pyrosequencing	
Mecp2 region	Sequence
Region 1	F: 5'-TGGGTTTTATAATTAATGAAGGGTAA-3'
	R: 5'- CGCCAGGGTTTTCCCAGTCACGACATTTTACCACAACCCTCTCT-3'
	S: 5'-AGGTGTAGTAGTATATAGG-3'
Region 2	F: 5'-AGTTTGGGTTTTATAATTAATGAAGGG-3'
	R: 5'- CGCCAGGGTTTTCCCAGTCACGACATTTTACCACAACCCTCTCT-3'
	S: 5'-AAGGGTAATTTAGATAAAGAGTAAG-3'
Region 3	F: 5'- GGTGAATTATTTAGTAGGGAGGTTTTAA -3'
	R: 5'- CGCCAGGGTTTTCCCAGTCACGACAAAAAAAAAAACCAACCCCATTC AACTAC -3'
	S: 5'- AGTAGGGAGGTTTTAATAG -3'
Region 4	F: 5'- GTTTTAAAAAGTTTTGGGAAAAGGTGTAGT -3'
	R:5'- CGCCAGGGTTTTCCCAGTCACGACCTAAACCCTAACATCCCAACTA CCAT-3'
	S: 5'- AGTTTAATGGGGATTTTTAATT -3'
Region 5	F: 5'- AGTAGAAGTTATTATTTGTGGTGTGTAT -3'
	R: 5'- CGCCAGGGTTTTCCCAGTCACGACACTATATTACTTCCCAACTCAA CTAATT -3'
	S: 5'- AGAGGTGTAAGGATTTT -3'
Region 6	F: 5'- GAAGTAGGAAGAATTGAGTTTGAGGATAG -3'
	R: 5'- CGCCAGGGTTTTCCCAGTCACGACATCTATACACTACCCACATATA ATACC -3'
	S: 5'- GTTTGAGGATAGTTTGAAT -3'

F: Forward PCR primer, R: Reverse PCR primer (Biotinylated), S: Sequencing primer

3.6.10 Correlation analysis

The correlation between DNA methylation at the *Mecp2* REs and expression of *Mecp2* isoforms was determined using the Pearson's correlation analysis and linear regression. The

Pearson's correlation coefficient (*r*) was calculated for average methylation against each *Mecp2* isoform, over entire regions and for individual CpG sites within each region. The strength of correlation was considered as follows: weak, 0 <*r* <0.3; moderate, 0.3 <*r* <0.4; strong, 0.4 <*r* <0.7; or very strong, 0.7 <*r* <1.0. A negative *r*-value indicates an inverse/negative correlation whereas a positive *r*-value indicates direct/positive correlation. Statistical significance was determined at *P* <0.05.

3.7 Results

3.7.1 Dynamic expression of Mecp2 isoforms during NSC differentiation and DNA methylation patterns at the Mecp2 regulatory elements

Primary neural stem cells were isolated from the embryonic forebrain at E14.5 and were cultured in the presence of growth factors to generate primary neurospheres. After 7 days in culture, primary neurospheres were dissociated and cultured under differentiation conditions for 8 days, reported to be sufficient for differentiation of both neuronal and glial cells [35,37] **(Figure 3.2A)**. In agreement with our previous report [37], the proliferating primary neurospheres expressed NESTIN and KI67 **(Figure 3.2B)**. Similar to our previous reports [35,37] differentiated NSC at D8 consisted of a mixed population of neurons, astrocytes, and oligodendrocytes **(Figure 3.2C)**. The composition of the D8 population was determined by detection of cell type-specific markers [TUB III (4.7% ± 0.8, mean ± standard error of the mean (SEM)], Glial fibrillary acidic protein (GFAP) (54.4% ± 1.1), S100B (15.9% ± 2.7), 2',3'-Cyclic-nucleotide 3'-phosphodiesterase (CNPase) (1.6% ± 0.2), Myelin basic protein (MBP) (2.6% ± 0.42), Oligodendrocyte lineage transcription factor 2 (OLIG2) (36.2% ± 1.8) and Ki67 (92.4% ± 1.3) by immunofluorescence **(Figure 3.2C)**. Ki67 is not a cell type-specific marker, but rather reflects the fraction of cycling

cells within differentiating NSC. Indicating that the cells at an early stage of differentiation are actively dividing, expression of Ki67 (98.8% ± 0.8) was also detected in D2 cells **(Figure 3.S2)**. Our detection of Ki67 in the majority of cells at D8 indicates that although most differentiating NSC are actively dividing, fewer than 10% of cells are post-mitotic and may include neurons (TUB III$^+$) or non-proliferating cells committed towards neuronal cell fate. Taken together, this *in vitro* NSC differentiation system provided a suitable model system consisting of the three main neural cell types (neurons, astrocytes, and oligodendrocytes) in the brain to study *Mecp2*/MeCP2 isoforms during neural differentiation.

First, we confirmed MeCP2 expression in neurospheres at D0 and differentiated NSC at D8 by IF studies. We used an antibody that was raised against the MeCP2 C-terminus and recognizes both isoforms. Characteristic punctate nuclear expression of MeCP2 was detected in 41% ± 1.2 of neurosphere cells **(Figure 3.2D, a)**, which were positive for the NSC marker NESTIN **(Figure 3.2D, b)**. At D8 of NSC differentiation, MeCP2 protein was detected in all cell types in the D8 differentiated progenies, including neurons, astrocytes, and oligodendrocytes **(Figure 3.2E)**. Indicating the expression of MeCP2 in proliferating cells, we detected MeCP2 in Ki67$^+$ cells in the D8 population **(Figure 3.2E, g)**. The detected nuclear MeCP2 signals were enriched at the heterochromatin-rich regions of all three cell types. These observations are consistent with our previous reports on MeCP2 nuclear expression in *in vivo* differentiated primary neurons and astrocytes [8].
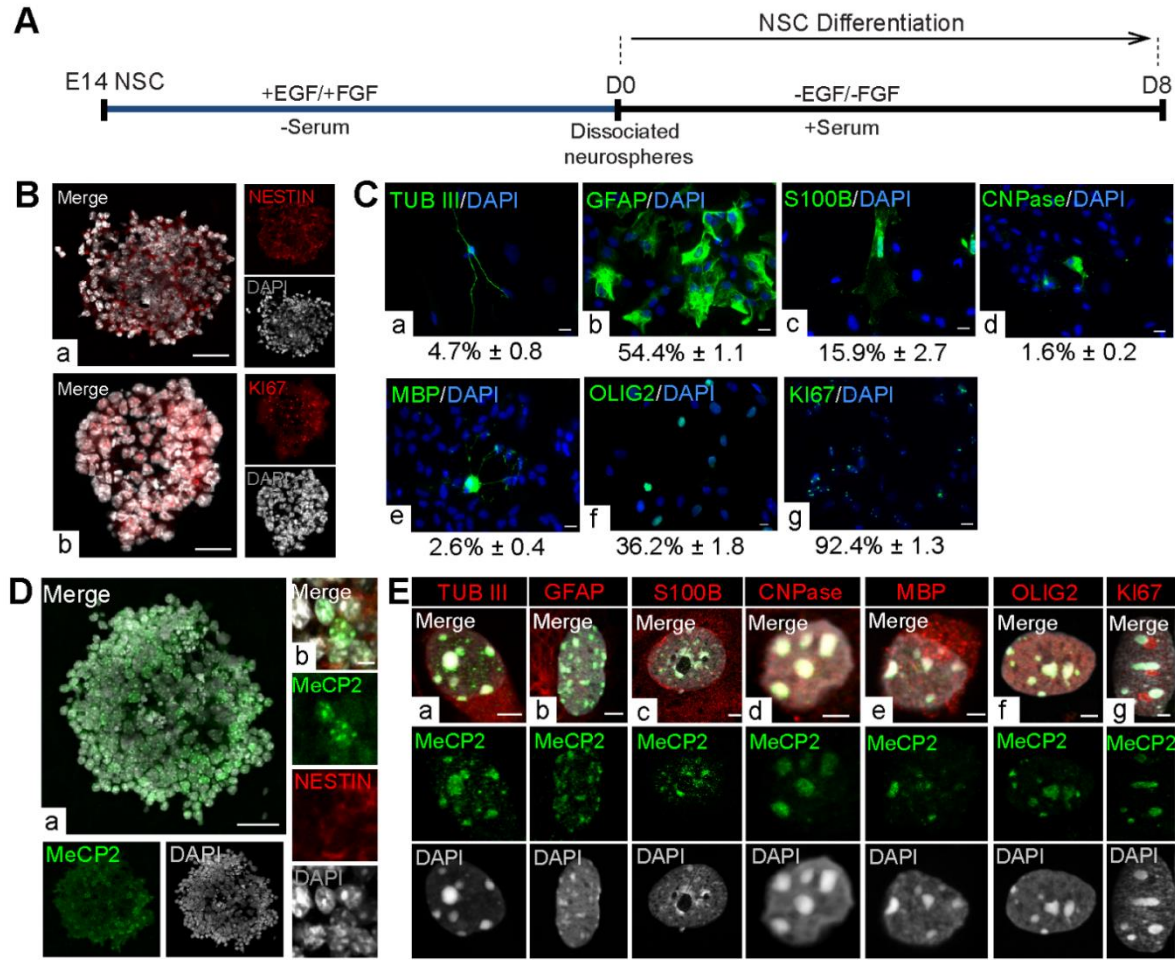
Figure 3.2 Characterizing *in vitro* neural stem cells to study Methyl CpG binding protein 2 (MeCP2) expression.

A) Schematic representation of *in vitro* neural stem cell (NSC) differentiation. **B)** Detection of (**a**) NESTIN$^+$ and (**b**) Ki67$^+$ cells in self-renewing neurospheres. Scale bars represent 20 μm. **C)** Immunofluorescent detection of different cell type markers in the day 8 (D8) population (**a**) TUBULIN III (TUB III): neurons, (**b**) Glial fibrillary acidic protein (GFAP): astrocytes, (**c**) S100B: mature astrocytes, (**d**) 2',3'-Cyclic-nucleotide 3'-phosphodiesterase (CNPase): oligodendrocytes, (**e**) Myelin basic protein (MBP): oligodendrocytes, (**f**) Oligodendrocyte lineage transcription factor 2 (OLIG2): early oligodendrocytes and progenitors, and (**g**) Ki67: proliferating cells. Scale bars represent 10 μm. The percentages represent average number of cells from three individual experiments [N = 3 ± standard error of the mean (SEM)]. **D)** (**a**) Immunofluorescent

detection of MeCP2 in a sectioned primary neurosphere. Scale bar represents 20 μm. (**b**) Double labeling of MeCP2 and NESTIN within primary neurosphere cells. Scale bar represents 5 μm. **E)** Immunofluorescent detection of MeCP2 in D8 cell types: (**a**) TUB III, (**b**) GFAP, (**c**) S100B, (**d**) CNPase, (**e**) MBP, (**f**) OLIG2, and (**g**) Ki67. Scale bars represent 2 μm.

Next, we investigated *Mecp2* isoform-specific transcript expression at three stages of NSC differentiation: undifferentiated cells (D0), cells at an early stage of differentiation (D2), and cells at a later stage of differentiation (D8). Distinct and mirror-like (reciprocal) transcript expression patterns for *Mecp2* isoforms were observed during NSC differentiation (D0, D2, and D8) **(Figure 3.3A)**, suggesting possible differential regulation of these isoforms during NSC differentiation. Expression of *Mecp2e1* was reduced from D0 to D2 (2.7-fold, P <0.001) and was slightly elevated from D2 to D8. In contrast, *Mecp2e2* expression increased from D0 to D2 (3.1-fold, P <0.05), but declined from D2 to D8 (4.2-fold, P <0.01). At each of these studied differentiation stages, the expression ratio between the two isoforms (*Mecp2e1/Mecp2e2*) varied significantly (D0, 5.99; D2, 0.69; D8, 4.62) **(Figure 3.S3)**. At D0 and D8, *Mecp2e1* expression was significantly higher than *Mecp2e2* (D0, P <0.01, and D8, P <0.05). In contrast at D2, *Mecp2e2* expression was significantly higher than *Mecp2e1* (D2, P <0.05). These observations imply differential regulation of *Mecp2* isoforms and possible changes in alternative splicing of *Mecp2* at different stages of NSC differentiation.
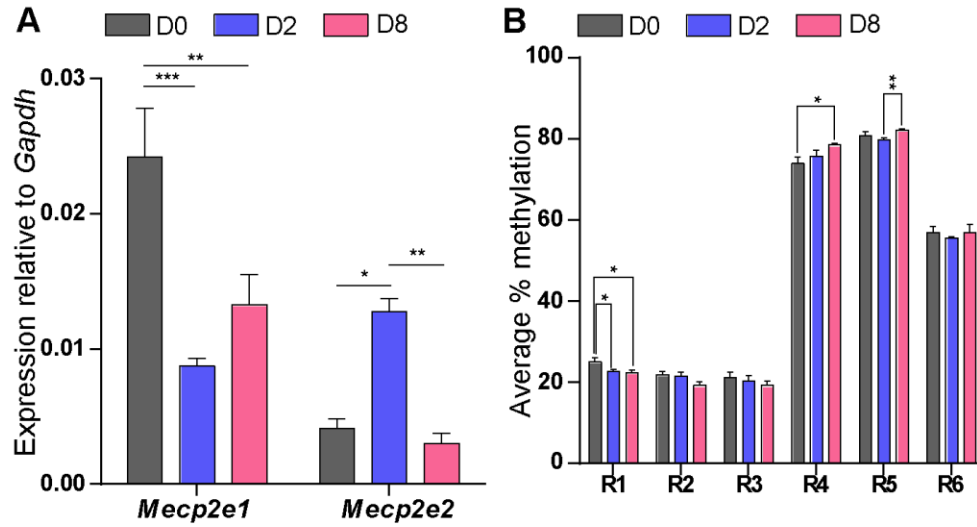
Figure 3.3 Methyl CpG binding protein 2 gene (*Mecp2*) isoform-specific transcript expression and DNA methylation at the *Mecp2* regulatory elements during neural stem cell (NSC) differentiation.

A) Analysis of *Mecp2e1* and *Mecp2e2* transcript levels during NSC differentiation: N = 3 ± SEM. Significant differences are indicated by ***P <0.001, **P <0.01 or *P <0.05. **B)** Average percentage methylation over *Mecp2* promoter and intron 1 regions at day 0 (D0), day 2 (D2) and day 8 (D8) during NSC differentiation. The regions are promoter regions R1, CpG island contains 13 CpG sites; R2, 4 CpG sites; R3, 2 CpG sites, and intron 1 regions R4, 1 CpG site; R5, 1 CpG site; and R6, 2 CpG sites; N = 3 ± SEM. Significant differences are indicated by **P <0.01 or *P <0.05. *Gapdh*, glyceraldehyde-3-phosphate dehydrogenase gene.

MECP2/*Mecp2* expression is known to be regulated by REs found within its promoter and intron 1. The altered MeCP2 expression in autistic patients and in mouse brains subjected to stress is correlated with increased *MECP2/Mecp2* promoter methylation [3,13,14,19,20,54]. Therefore, we hypothesized that DNA methylation at the *Mecp2* promoter and intron 1 might impact *Mecp2* isoform-specific expression. For DNA methylation analysis by bisulfite pyrosequencing, we selected three regions within the *Mecp2* promoter (named R1 to R3, hereafter) and three regions

within intron 1 (named R4 to R6, hereafter) **(Figure 3.1B)**. These regions harbored different numbers of CpG sites; promoter regions R1: CpG island contains 13 CpG sites; R2: 4 CpG sites; R3: 2 CpG sites, and intron 1 regions R4: 1 CpG site; R5: 1 CpG site; and R6: 2 CpG sites.

Pyrosequencing analysis of R1-R6 indicated that downregulation of *Mecp2e1* and upregulation of *Mecp2e2* from D0 to D2 were associated with slight, but significant demethylation of *Mecp2* promoter R1 (2.3%, P <0.05). Similarly, upregulation of *Mecp2e1* and downregulation of *Mecp2e2* from D2 to D8 were associated with hypermethylation of *Mecp2* intron 1 R5 (2.4%, P <0.01) **(Figure 3.3B)**. Detected expression changes in *Mecp2* isoforms from D0 to D8 were associated with demethylation of *Mecp2* promoter R1 (2.6%, P <0.05), and hypermethylation of *Mecp2* intron 1 R4 (4.6%, P <0.05). In all cases, the differences in average percentage methylation between D0, D2, and D8 were relatively small, but statistically significant and ranging between 2 to 5%. Previous reports have shown that an increase in the overall *MECP2* promoter methylation by approximately 2.0 to 2.5% in male autistic patients correlates with significantly reduced *MECP2* expression levels [3]. In mouse brain exposed to maternal separation and stress, DNA methylation changes that are as little as 2 to 5% at individual CpG sites of the *Mecp2* promoter are associated with significantly reduced MeCP2 expression [20]. As even slightly altered *MECP2/Mecp2* promoter methylation (2 to 5%) affects *MECP2/Mecp2* gene expression in the human and mouse brain, it is likely that the statistically significant changes detected in the present study might be biologically important for *Mecp2e1* and/or *Mecp2e2* expression.

As mentioned, the ratio of *Mecp2* splice variants was changed at different stages of NSC differentiation. Therefore, we performed Pearson correlation analysis between *Mecp2e1/Mecp2e2* expression ratio and DNA methylation at R1, R4, and R5 (the three regions that showed significant changes) during NSC differentiation. Pearson's correlation coefficient (r) represents the strength

of the correlation, with negative *r* indicating inverse correlation, and positive *r* indicating a direct correlation between DNA methylation and the *Mecp2e1/Mecp2e2* splice ratio. We detected a statistically significant positive correlation ($r > 0.9$, $P < 0.01$) between *Mecp2e1/Mecp2e2* splice ratio at D2 and DNA methylation at intron 1 R4 **(Figure 3.S3)**. Although it is possible that intron 1 (R4) may play a role in alternative splicing of *Mecp2*, further investigations are required to establish the involvement of DNA methylation in *Mecp2* splicing.

As *MECP2*/*Mecp2* is an X-linked gene, it is possible that the observed changes in *Mecp2* expression are due to a shift in the number of cells derived from male and female embryos. To exclude such a possibility, we determined the contribution of the male/female embryonic cells during NSC differentiation using a semi-quantitative PCR-based method. Genomic DNA was extracted from each differentiation stage and subjected to PCR analysis for the presence of the *Sry* gene found on the Y chromosome. The autosomal gene *Il3* was used an internal control. The adult male brain cortex was used as a positive control for the presence of the male genomic DNA **(Figure 3.S4A)**. We did not observe statistically significant changes in the ratio of *Sry/Il3* in the cells collected at different stages of differentiation, indicating that the ratio of male/female differentiating NSC were unchanged **(Figure 3.S4B)**. To further confirm the contribution from the male/female sex, we tested the transcript levels of *Xist* gene (the gene is involved in X-chromosome inactivation) by qRT-PCR. We did not detect any significant change in *Xist* gene expression at different stages of NSC differentiation **(Figure 3.S4C)**. These results indicate that our observed changes in *Mecp2* expression are not due to altered contribution of male and female cells. Taken together, our results suggest a possible link between the *Mecp2* isoform-specific expression and DNA methylation at the *Mecp2* REs within the *Mecp2* promoter and intron 1 during NSC differentiation.

3.7.2 Decitabine exposure leads to Mecp2e1 upregulation, but its withdrawal downregulates both Mecp2 isoforms to different extents

To further study the impact of DNA demethylation/remethylation in *Mecp2* isoform-specific expression, we treated dissociated neurosphere cells with 2.5 μM decitabine for 48 h, at the onset of NSC differentiation (D0) **(Figure 3.4A)**. At D2, decitabine was withdrawn from the media and cells were kept in culture for another 6 days until D8, to study the effect of DNA remethylation **(Figure 3.4A)**. First, as a proof of principle, we verified whether decitabine acted as a DNA demethylating agent in our system. Global change in DNA methylation was determined by IF for 5mC and DNA dot blot assay for both 5mC and 5hmC. As expected, IF experiments showed that 5mC nuclear signals were noticeably lower in decitabine-treated NSC compared to D2 control untreated cells **(Figure 3.4B)**. DNA dot blot assays indicated that decitabine treatment resulted in reduced 5mC levels (3.79-fold, $P < 0.05$), with a slight but statistically insignificant increase in 5hmC levels **(Figure 3.4C-D)**. In contrast, decitabine withdrawal led to re-establishment of global DNA methylation (5mC) at D8 as detected by IF **(Figure 3.4F)**. Furthermore, DNA dot blot assay showed DNA methylation reprogramming upon decitabine withdrawal, with elevated 5mC levels (1.5-fold, $P < 0.05$), and relatively unchanged 5hmC levels in decitabine-treated NSC compared to controls **(Figure 3.4G-H)**. Although globally altered 5mC levels were expected following decitabine treatment in agreement with previous studies [55,56], the observed effect of decitabine to slightly increase 5hmC levels was novel and might be biologically important.

DNA demethylating agents can function as cytosine analogues and/or as *Dnmt*/DNMT inhibitors [57]. Therefore, we investigated *Dnmt* expression levels in decitabine-treated differentiating NSC by qRT-PCR. In accordance with reduced DNA methylation levels at D2, decitabine treatment caused significant inhibition of transcript levels of all three DNA

methyltransferases (*Dnmt1*, 1.7-fold, *P* <0.05; *Dnmt3a*, 1.5-fold, *P* <0.05 and *Dnmt3b*, 2.5-fold, *P* <0.01; **Figure 3.4E**). Even though we anticipated that decitabine withdrawal would restore *Dnmt* levels, only *Dnmt1* levels were elevated (2.2-fold, *P* <0.05), whereas both *Dnmt3a* (1.4-fold, *P* <0.05) and *Dnmt3b* (1.8-fold, *P* = 0.06) levels remained inhibited **(Figure 3.4I)**. In summary, these results indicate that decitabine functions as a DNA demethylating agent in differentiating NSC and globally affects DNA methyl marks. Additionally, our data indicate that decitabine withdrawal would lead to DNA methylation reprogramming in differentiating NSC.
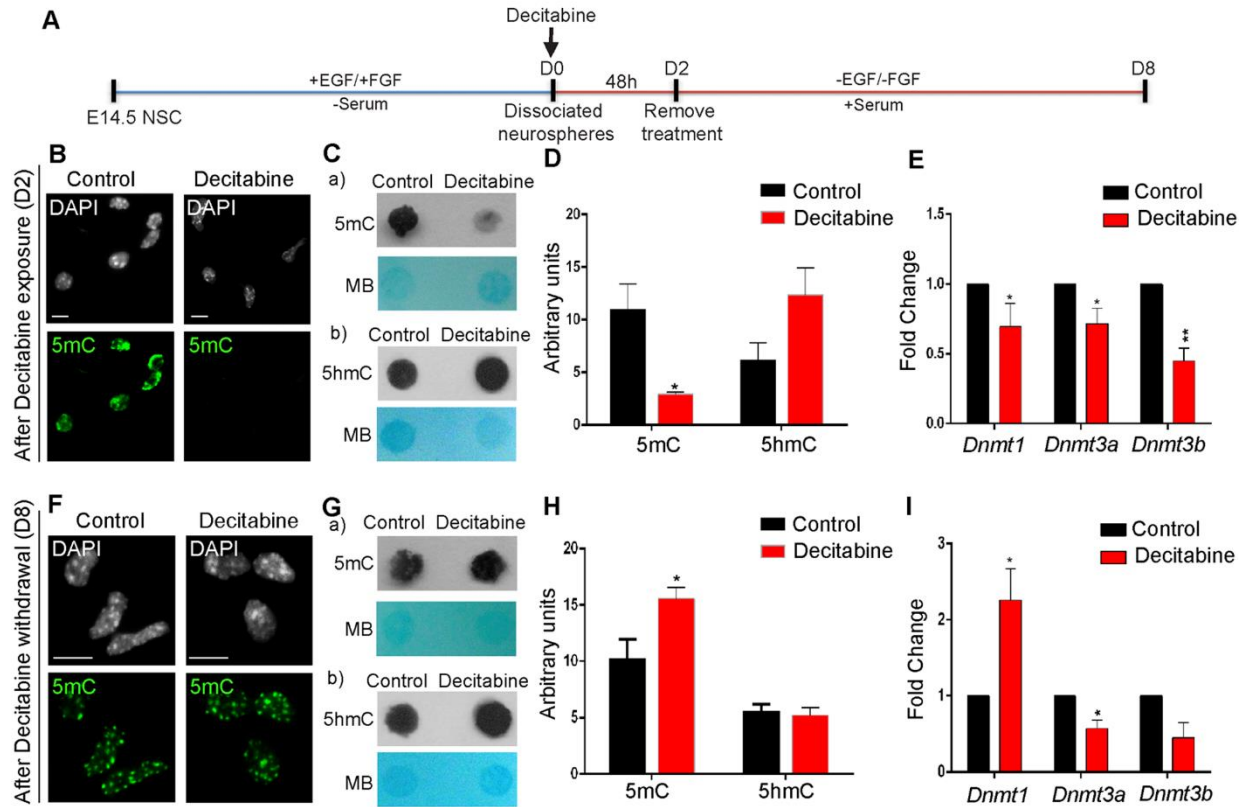
Figure 3.4 Effect of decitabine on global DNA methylation (5mC and 5hmC) and *Dnmt* genes in differentiating neural stem cells (NSC).

A) Schematic representation of decitabine treatment. Briefly, 2.5 μM of decitabine was added to dissociated neurospheres on day 0 (D0) at the onset of NSC differentiation for 48 h, and the treatment was withdrawn at D2. Cells were kept in culture till D8. Top panel (B-E), after exposure to decitabine at D2. **B)** Immunofluorescent detection of DNA methylation using 5-methylcytosine (5mC) antibody. Decitabine caused reduced levels of DNA methylation, note the presence of 4',6-diamidino-2-phenylindole (DAPI) signals in decitabine-treated cells with no 5mC signal. Scale bars represent 5 μm. **C)** Detection of overall DNA methylation levels by DNA dot blot with antibodies specific for (**a**) 5mC, (**b**) 5-hydroxymethylcytosine (5hmC). MB refers to Methylene Blue for visualizing total DNA. **D)** Quantification of 5mC and 5hmC levels after decitabine exposure. **E)** Detection of *Dnmt* transcript levels by qRT-PCR. Bottom panel (F-I), after withdrawal of decitabine at D8. **F)** DNA methylation detection by immunofluorescence using 5mC antibody. Scale bars represent 5 μm. **G)** Detection of global DNA methylation levels by DNA dot blot, (**a**) 5mC, (**b**) 5hmC. **H)** Quantification of 5mC and 5hmC levels after withdrawal of

decitabine. **I)** Detection of *Dnmt* transcript levels by qRT-PCR. Fold changes are calculated relative to transcript levels at D2 or D8 control; N = 3 ± SEM. Significant differences from control are indicated by **P <0.01* or *P <0.05*. MB, methylene blue (used for visualizing total DNA).

Next, we investigated possible changes in *Mecp2*/MeCP2 expression induced by decitabine. Quantitative RT-PCR experiments indicated that decitabine treatment at D2 caused slight but statistically significant upregulation of *Mecp2e1* (1.41-fold, *P* <0.05), with minimal and insignificant increased levels of the total *Mecp2* (1.2-fold, *P* = 0.5), and unchanged levels of *Mecp2e2* **(Figure 3.5A)**. Analysis of protein levels by WB showed that decitabine upregulated total MeCP2 (2.5-fold, *P* <0.05), and MeCP2E1 (3.1-fold, *P* <0.05) protein expression **(Figure 3.5B-C)**. However, the lack of an antibody specific for MeCP2E2 at the time of this study limited our investigation of MeCP2E2 protein levels. Correlation analysis of transcript and protein levels of *Mecp2*/MeCP2 at D2 indicated significant correlation between the detected transcript and protein expression (*Mecp2*/MeCP2 (r = 0.97, *P* <0.05) and *Mecp2e1*/MeCP2E1 (r = 0.98, *P* <0.01); **Figure 3.5G**).

In contrast to D2, withdrawal of decitabine at D8 significantly downregulated the transcript expression levels of *Mecp2e1* (1.92-fold, *P* <0.001), *Mecp2e2* (1.39-fold, *P* <0.05) and the total *Mecp2* (1.52-fold, *P* <0.01) **(Figure 3.5D)**. Similar to the transcript levels, decitabine withdrawal resulted in downregulation of total MeCP2 (3.2-fold, *P* <0.001), and MeCP2E1 (4.3-fold, *P* <0.05) protein expression levels **(Figure 3.5E-F)**. A similar correlation analysis between transcript and protein levels of *Mecp2*/MeCP2 at D8 did not show any statistically significant correlation (*Mecp2*/MeCP2 (r = 0.6, *P* = 0.2), and *Mecp2e1*/MeCP2E1 (r = 0.6, *P* = 0.3); **Figure 3.5H**). These observations emphasize that even minor change in *Mecp2* transcript levels are biologically important and can result in significantly altered MeCP2 protein expression levels.

Next, we aimed to study whether the detected changes in *Mecp2*/MeCP2 expression were due to changes in cell population in response to decitabine treatment. Therefore, we studied the effect of decitabine on cell fate commitment of differentiating NSC at D2 and D8. After decitabine exposure at D2, we examined the expression of cell type-specific markers (neurons: *Tub III*, *NeuN*; astrocytes: *Gfap*, *S100b*; oligodendrocytes: *Cnpase*, *Mbp*) at the transcript levels by qRT-PCR. Comparing the control and decitabine-treated cells, we did not detect any statistically significant change in these cell type-specific genes, except for significant downregulation of *Cnpase* (9-fold, $P < 0.01$) **(Figure 3.5I)**. In order to determine whether any of these detected changes in transcript levels are represented in the number of cells expressing each corresponding cell type-specific marker, we performed IF experiments with specific antibodies against these markers **(Figure 3.5J)**. IF experiments showed that there was no significant change in the number of TUB III$^+$, GFAP$^+$, CNPase$^+$, or MBP$^+$ cells. However, we did not find any NEUN$^+$, or S100B$^+$ cells in the control or decitabine-treated populations at D2, probably because these cells are still in the early stages of differentiation **(Figure 3.5J)**.
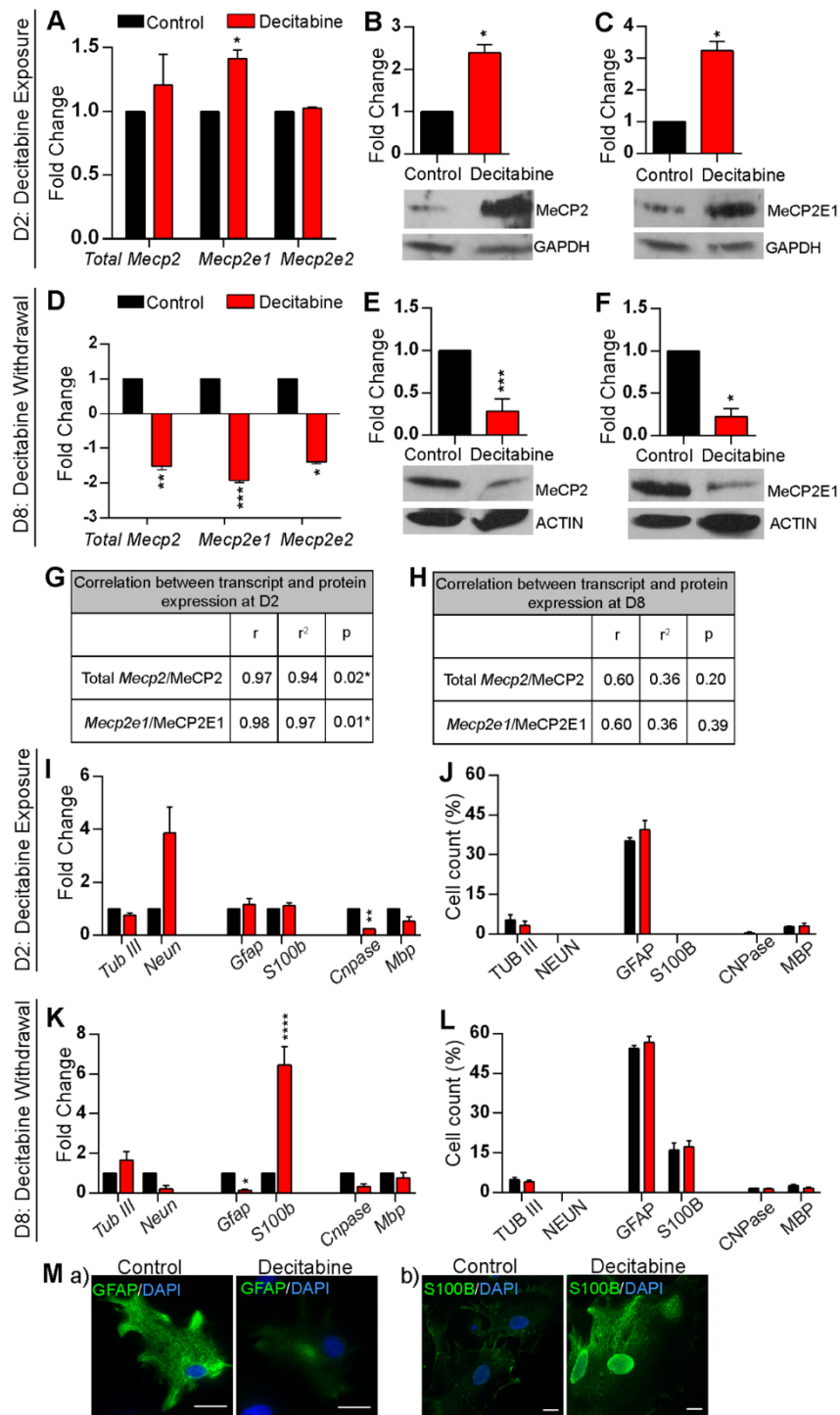
Figure 3.5 Effect of decitabine exposure and withdrawal on Methyl CpG binding protein gene (*Mecp2*/MeCP2) expression.

(**A**-**C**), After exposure to decitabine at D2. **A)** Analysis of *Mecp2* (total), *Mecp2e1* and *Mecp2e2* transcript levels by qRT-PCR. **B)** Detection of MeCP2 (total) protein expression levels by western blot; N = 2 ± SEM. **C)** Detection of MeCP2E1 protein expression levels by western blot; N = 2 ± SEM. (**D**-**F**), After the withdrawal of decitabine at day 8 (D8). **D)** Analysis of total *Mecp2*, *Mecp2e1* and *Mecp2e2* transcript levels by qRT-PCR. **E)** Detection of MeCP2 (total) protein expression levels by western blot. **F)** Detection of MeCP2E1 protein expression levels by western blot. (**G**-**H**) Pearson correlation analysis of the relation between *Mecp2* transcript levels and MeCP2 protein levels at D2 (**G**) and D8 (**H**); *r* = Pearson's correlation coefficient, r^2 = coefficient of determination. **I)** Transcript detection of cell type-specific markers for neurons (*Tub III*, *NeuN*); astrocytes (*Gfap*, *S100b*); oligodendrocytes (*Cnpase*, *Mbp*) by qRT-PCR in D2 control and decitabine-treated cells. **J)** Quantification of neurons, astrocytes, and oligodendrocytes using cell type-specific markers by immunofluorescence in D2 control and decitabine-treated cells. **K)** Transcript detection of cell type-specific markers for neurons (*Tub III*, *NeuN*); astrocytes (*Gfap*, *S100b*); oligodendrocytes (*Cnpase*, *Mbp*) by qRT-PCR in D8 control and decitabine-treated cells. **L)** Quantification of neurons, astrocytes, and oligodendrocytes using cell type-specific markers in D8 control and decitabine-treated cells. **M)** Comparison of immunofluorescent detection of (**a**) Glial fibrillary acidic protein (GFAP) and (**b**) S100B between control and decitabine-treated cells. Images were taken at the same exposure time. Scale bars represent 20 μm. For all the panels, fold changes are calculated relative to expression levels at D2 or D8 controls. Significant differences from controls are indicated by ****P <0.001*, ***P <0.01 or *P <0.05*; N = 3 ± SEM, unless specifically mentioned.

In the D8 population, decitabine treatment led to insignificant changes in the transcript levels for all neuronal and oligodendrocyte markers compared to control untreated cells. Additionally, *Gfap* expression in decitabine-treated cells was downregulated 5.5-fold, whereas *S100b* expression was upregulated to a similar extent (6-fold) (**Figure 3.5K**). Quantification of differentiated neurons, astrocytes and oligodendrocytes at D8 by IF did not show any significant change in the cell-fate commitment of these cells (**Figure 3.5L**). However, reduced *Gfap* expression in

decitabine-treated cells without any changes in the number of GFAP$^+$ cells might be explained by the reduced intensity of GFAP staining relative to the control astrocytes, since the images were taken at the same exposure level **(Figure 3.5M, a)**. Similarly, the significant upregulation of *S100b* transcript levels by decitabine with no change in the number of S100B$^+$ cells could be explained by the increased intensity of S100B in decitabine-treated cells, when the images were taken at the same exposure time **(Figure 3.5M, b)**. Taken together, these results suggest that decitabine has minimal effect on the differentiated number of neurons, astrocytes, and oligodendrocytes under the described conditions. They further suggest that the detected changes in *Mecp2* expression are not likely due to altered population of differentiating cell types.

Next, we investigated whether the observed altered *Mecp2*/MeCP2 expression was due to changes in the number of cells deriving from male and female embryos. Detection of *Sry* and *Il3* by PCR indicated that the ratio of *Sry/Il3* was relatively similar in D2 control and decitabine-treated populations **(Figure 3.S4D)**. Similar PCR analysis at D8 also showed no significant differences in the ratio of *Sry/Il3* between D8 control and decitabine-treated cells **(Figure 3.S4E)**. Furthermore, qRT-PCR analysis of the *Xist* gene expression in both D2 and D8 populations with and without decitabine treatment showed no significant change in *Xist* transcript expression levels between the control and decitabine-treated cells **(Figure 3.S4F-G)**. Therefore, these results indicate that the observed changes in *Mecp2*/MeCP2 expression in response to decitabine exposure and withdrawal are not due to a shift in the number of cells deriving from male/female embryos.

Taken together, our data so far indicate that a single administration of decitabine for 48 h induces *Mecp2e1*/MeCP2E1, MeCP2 (total) expression, whereas its withdrawal downregulates *Mecp2* (total)*/*MeCP2 (total), *Mecp2e1*/MeCP2E1, and *Mecp2e2* expression with minimal change in NSC differentiation.

3.7.3 Decitabine mediates altered DNA methylation patterns at the Mecp2 regulatory elements

As mentioned earlier, DNA methylation changes at the overall *MECP2* promoter and individual CpG sites within the *MECP2/Mecp2* promoter are associated with altered *MECP2/Mecp2* expression [3,20,54]. Therefore, we investigated whether altered expression of *Mecp2* isoforms in our NSC system is associated with change in DNA methylation at the *Mecp2* REs found within the *Mecp2* promoter and intron 1. Bisulfite pyrosequencing analysis showed that decitabine treatment (D2) caused no significant change in the percentage DNA methylation at the *Mecp2* promoter R1 and R3 (**Figure 3.6A, a, c**). However, decitabine caused demethylation of all individual CpG dinucleotides at the R2 (CpG1, 3.5%; CpG2, 4.4%; CpG3, 3.1%; CpG4, 4.28%) (**Figure 3.6A, b**), as well as the average R2 percentage DNA methylation (3.83%, $P <0.05$) (**Figure 3.6B, a**). Similarly, decitabine caused demethylation of individual CpG sites at the intron 1 R4 (15.8%, $P <0.05$), R5 (13.08%, $P <0.05$), and R6 (CpG1, 8.01%, $P <0.01$; CpG2, 3.8%, $P = 0.4$) (**Figure 3.6A, d-f**), with significant demethylation at the entire intron 1 (10.37%, $P <0.05$) (**Figure 3.6B, b**). These results indicated that decitabine induced significant DNA demethylation at both the *Mecp2* promoter and intron 1, at individual CpG sites and the overall DNA methylation. As mentioned earlier, this detected DNA demethylation was associated with significant upregulation of *Mecp2e1* isoform, but not *Mecp2e2*. Therefore, it is possible that the observed changes in DNA methylation at the studied REs contribute to the upregulation of *Mecp2e1*.
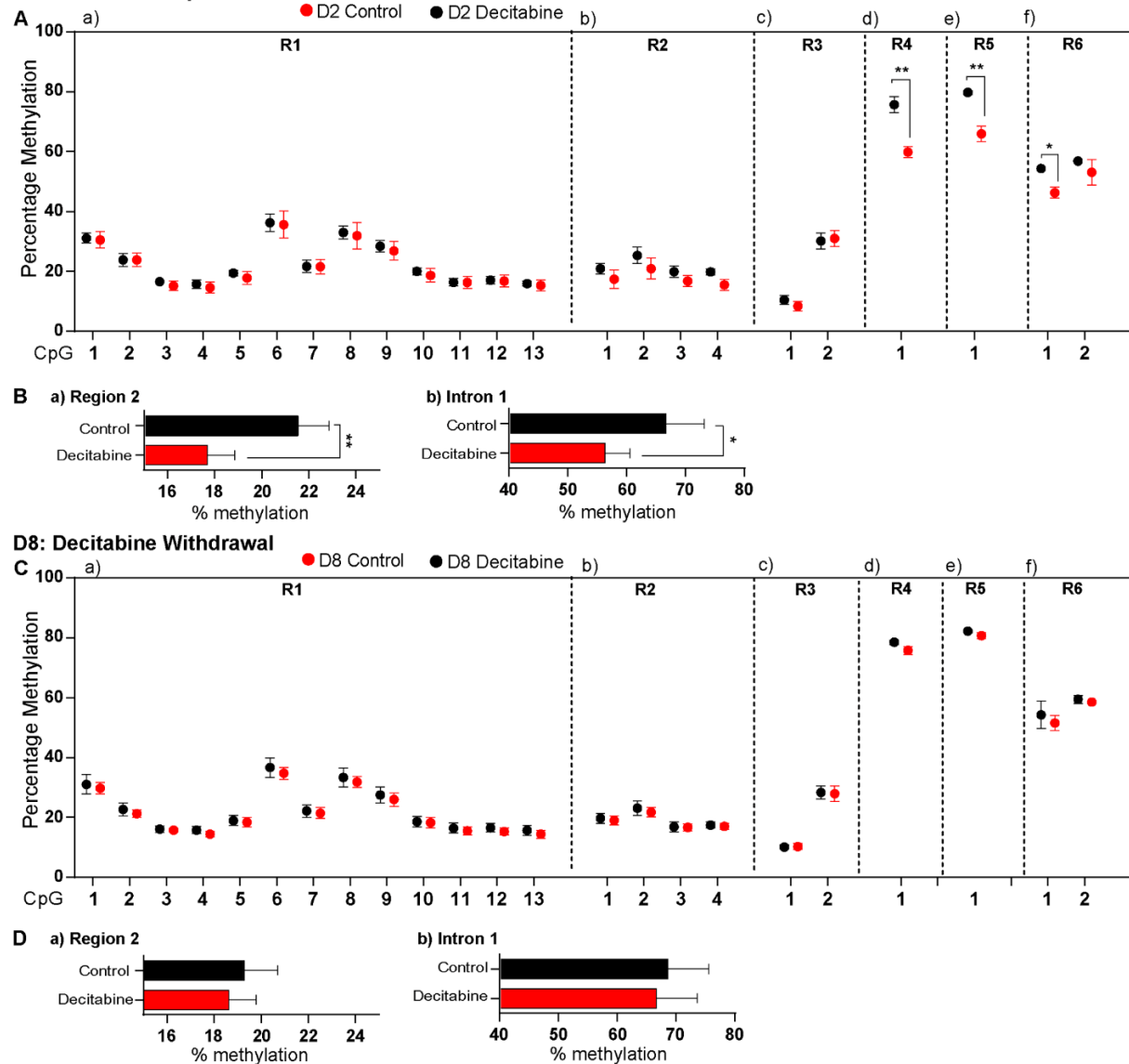
Figure 3.6 Bisulfite pyrosequencing analysis of DNA methylation at the Methyl CpG binding protein 2 gene (*Mecp2*) regulatory elements after decitabine treatment.

A) Effect of decitabine exposure at D2 on the percentage DNA methylation of *Mecp2* regulatory regions. The three promoter regions are (**a**) R1, (**b**) R2, (**c**) R3, and the three intron 1 regions are (**d**) R4, (**e**) R5, and (**f**) R6. **B)** Effect of decitabine exposure on average methylation over the entire region 2 (R2) (**a**), and intron 1 (R4 to R6) (**b**). Significant differences from controls are indicated by $**P < 0.01$ or $*P < 0.05$; $N = 3 \pm$ SEM. **C)** Effect of decitabine withdrawal at D8 on percentage methylation of *Mecp2* regulatory regions. The regions are promoter regions (**a**) R1, (**b**) R2 and (**c**)

R3, and intron 1 regions (**d**) R4, (**e**) R5 and (**f**) R6. **D)** Effect of decitabine withdrawal on average DNA methylation over entire region 2 (R2) (**a**), and intron 1 (R4 to R6) (**b**).

Similar bisulfite pyrosequencing analysis at D8 indicated that the three *Mecp2* promoter regions (R1 to R3) and intron 1 regions (R4 to R6) were remethylated and DNA methylation was almost re-established following decitabine withdrawal **(Figure 3.6C)**. Analyzing the average DNA methylation over the *Mecp2* promoter R2 and the entire intron 1 (which were demethylated at D2), we observed no significant differences in DNA methylation between D8 control and decitabine-treated cells **(Figure 3.6D)**. Despite the fact that DNA remethylation is expected to restore the gene expression levels, expression of both *Mecp2* isoforms were significantly downregulated. This observation implies that at D8, other regulatory mechanisms apart from promoter/intron 1 DNA methylation might be involved in downregulating *Mecp2* expression.

Taken together, these results show that the induced *Mecp2e1* (but not *Mecp2e2*) expression is associated with reduced DNA methylation at the *Mecp2* REs and decreased global 5mC DNA methylation. Hence, our findings implicate the possible role of *Mecp2* gene-specific DNA demethylation at the specific REs on the expression of *Mecp2e1*/MeCP2E1 and MeCP2 (total) at D2. Moreover, altered expression of *Mecp2* isoforms without any change in DNA methylation at the *Mecp2* REs at D8 implies that mechanisms other than DNA methylation could be involved in downregulating *Mecp2* isoforms.

3.7.4 Mecp2 isoform-specific expression correlates with DNA methylation at the Mecp2 regulatory elements

In order to establish a link between *Mecp2* isoform-specific expression and DNA methylation, we performed Pearson correlation analysis by comparing normalized (log2)

163

expression of *Mecp2* in each data set to the respective average percentage methylation levels over entire regions, as well as methylation at individual CpG sites (from both control and decitabine-treated cells).

First, we tested whether average DNA methylation of the entire *Mecp2* promoter (R1 to R3) and intron 1 (R4 to R6) regions correlate with *Mecp2e1* and *Mecp2e2* expression at D2 in control and decitabine-treated cells. We observed a significant negative correlation between *Mecp2e1* expression and the average methylation at R1, R3, and R5 ($r > -0.9$, $P < 0.05$). Correlation between *Mecp2e1* upregulation and significant demethylation at R5, induced by decitabine at D2, suggests a possible contribution of R5 in upregulating *Mecp2e1*. On the other hand, *Mecp2e2* showed significant negative correlation only with R3 methylation ($r > -0.9$, $P < 0.05$) **(Figure 3.7A, a)**, that remained unchanged at D2, and this could explain the unaffected *Mecp2e2* expression at D2.
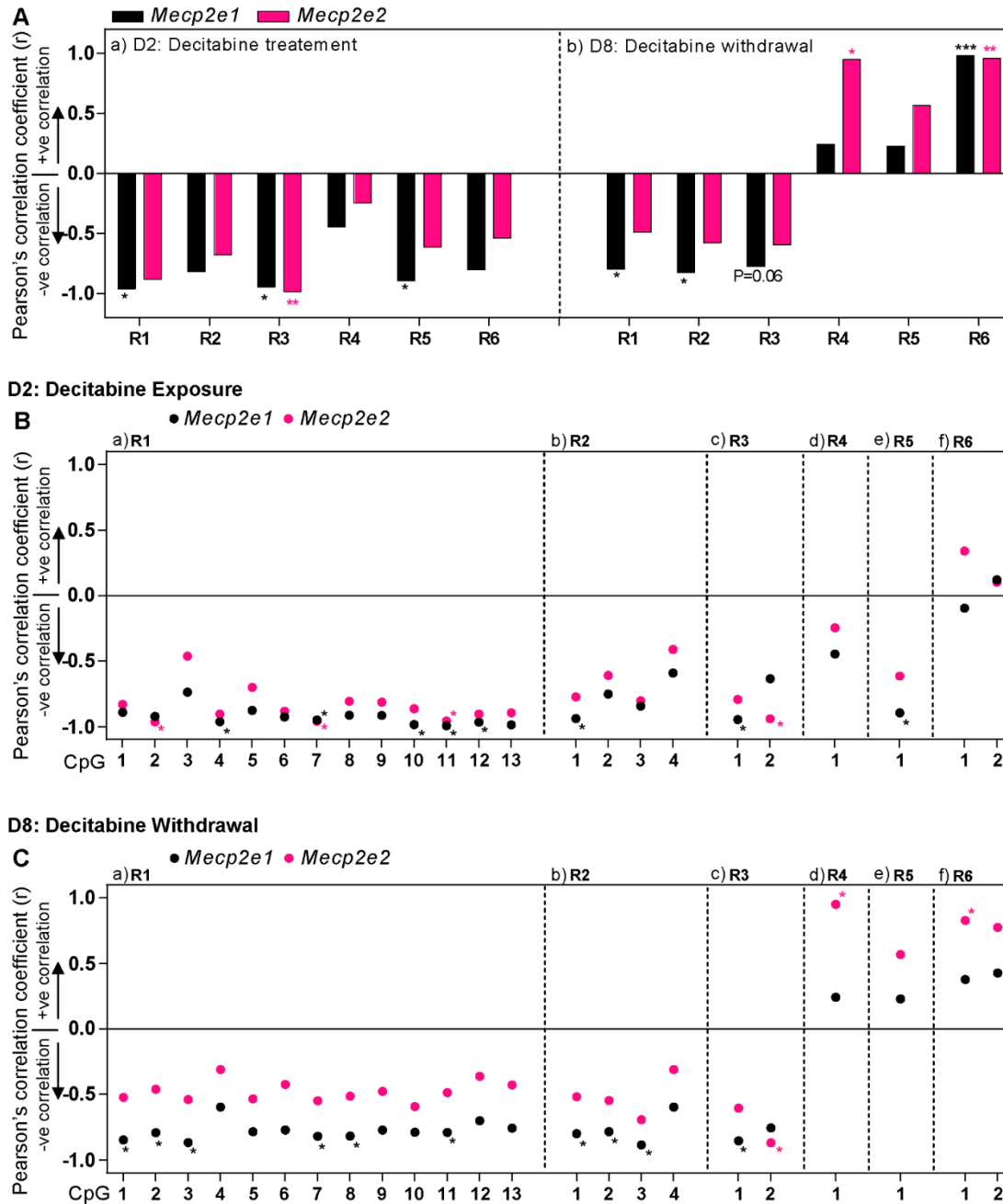
Figure 3.7 Correlation analysis between DNA methylation at the Methyl CpG binding protein 2 gene (*Mecp2*) regulatory elements and *Mecp2* expression after decitabine treatment (day 2) and decitabine withdrawal (day 8).

All graphs represent the Pearson correlation coefficient (*r*) for *Mecp2e1* (black), and *Mecp2e2* (pink): statistical significance indicated by ***P <0.001, **P <0.01 or *P <0.05*; N = 3. **A)** Correlation coefficients for the relation between *Mecp2* expression and average methylation over

entire regions in *Mecp2* promoter (region (R)1 to R3) and intron 1 (R4 to R6) after decitabine exposure on day 2 (D2) (**a**), and after decitabine withdrawal on D8 (**b**). **B)** After decitabine exposure: correlation coefficients for *Mecp2e1* (black), and *Mecp2e2* (pink) with individual CpG methylation at the promoter regions (**a**) R1, (**b**) R2 and (**c**) R3, and intron 1 regions (**d**) R4, (**e**) R5 and (**f**) R6. **C)** After decitabine withdrawal: correlation coefficients for *Mecp2e1* (black), and *Mecp2e2* (pink) with individual CpG methylation at promoter regions (**a**) R1, (**b**) R2 and (**c**) R3, and intron 1 regions (**d**) R4, (**e**) R5 and (**f**) R6. Statistical significance indicated by *$P <0.05$*; N = 3.

Similar correlation analysis at D8 (in control D8 and Decitabine-treated cells), indicated that *Mecp2e1* shows a significant negative correlation with average DNA methylation at the promoter R1 ($r > -0.7$, $P <0.05$), R2 ($r > -0.8$, $P <0.05$) and R3 ($r > -0.7$, $P = 0.06$, close to significant) and a significant positive correlation with the average DNA methylation at the intron 1 R6 ($r >0.9$, $P <0.001$) (**Figure 3.7A, b**). In contrast, *Mecp2e2* did not show any significant correlation with any of the promoter regions (R1 to R3) but showed a significant positive correlation with the average methylation at intron 1 R4 ($r >0.9$, $P <0.05$) and R6 ($r >0.9$, $P <0.01$). This divergence in the correlation patterns (negative and positive depending on the stage of differentiation), might imply a potential dynamic role of DNA methylation in regulating *Mecp2* isoforms at different stages of NSC differentiation.

Last, we investigated whether individual CpG sites within the studied regions (R1 to R6) showed specific correlation with either *Mecp2* isoform (**Figure 3.7B-C).** Implicating the possible role of promoter R1 and R2 in mainly regulating *Mecp2e1* (major isoform) at both D2 and D8, we observed a negative correlation between CpG methylation and *Mecp2e1* expression at several CpG sites ($r > -0.8$, $P <0.05$) (**Figure 3.7B, a, and 7C, a**). At D2, unlike other REs, the average methylation over R3 showed an equally strong negative correlation with both *Mecp2e1* ($r = -0.94$,

P <0.05) and *Mecp2e2* (*r* = -0.98, *P* <0.01) **(Figure 3.7A, a)**. Therefore, we studied the two individual CpG sites located within R3 far apart from each other, which were differentially methylated (CpG1, approximately 10% and CpG2, approximately 30%) **(Figure 3.6A, c)**. Interestingly, CpG1 showed a significant negative correlation with *Mecp2e1* (*r* = -0.9, P <0.05), while CpG2 showed a significant negative correlation with *Mecp2e2* (r = −0.9, *P* <0.01) **(Figure 3.7B, c)**. Further confirming the potential role of these two CpG sites within R3 in *Mecp2* isoform-specific expression, a similar correlation (CpG1: *Mecp2e1*, *r* = −0.85, *P* <0.05; CpG2: *Mecp2e2*, *r* = -0.87, *P* <0.05) was observed at D8 **(Figure 3.7C, c)**. The studied intron 1 regions seemed to have preferential correlation with individual isoforms. For instance, at D2, the only CpG site within R5 showed negative, significant correlation with *Mecp2e1* (*r* > -0.8, *P* <0.05) **(Figure 3.7B, e)**. Interestingly, at D8 intron 1 R4 and R6 showed positive, significant correlation with the *Mecp2e2* isoform (*r* >0.8, *P* <0.05) **(Figure 3.7C, d-f)**. The observed correlations for all REs are represented in **Figure 3.7B-C** and are summarized in **Figure 3.8**.
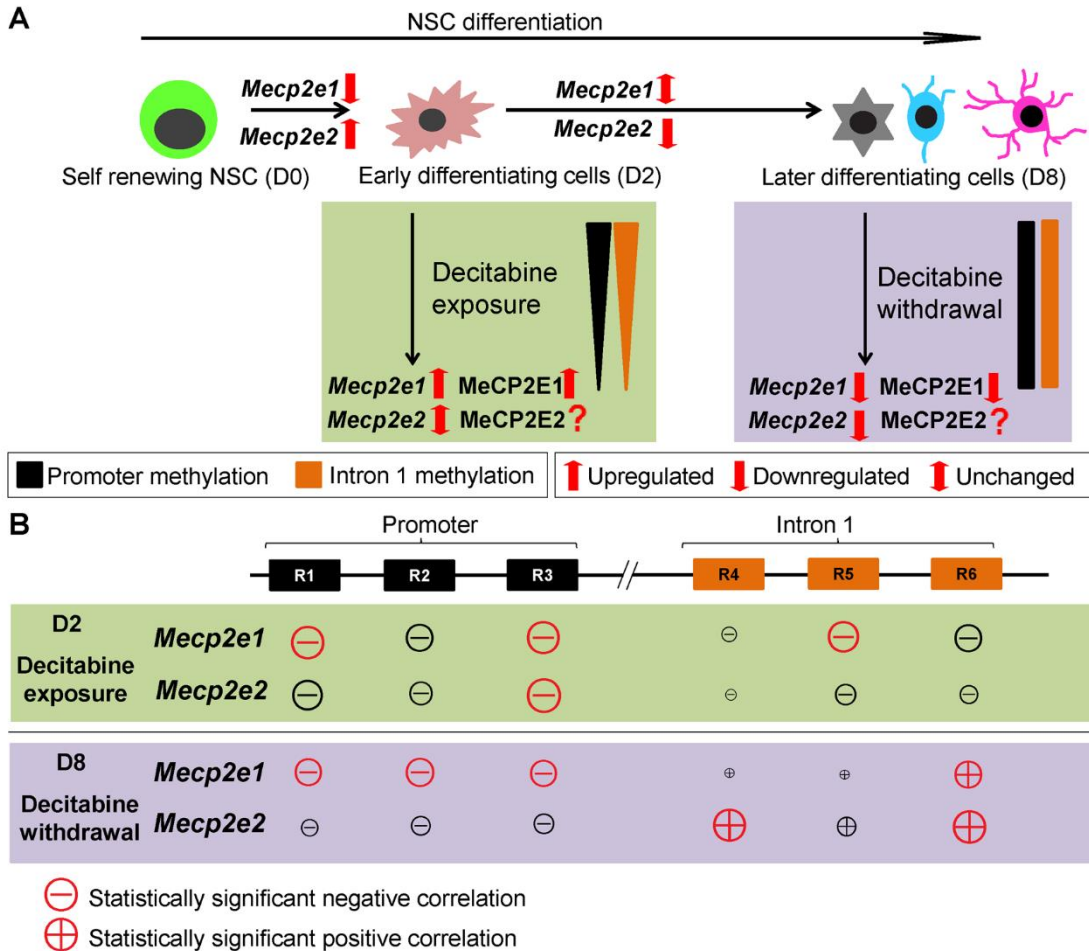
Figure 3.8 Summary of the correlations between the expression of Methyl CpG binding protein 2 gene (*Mecp2*) isoforms and DNA methylation at the *Mecp2* regulatory elements.

A) Dynamic changes in the expression of *Mecp2* isoforms (*Mecp2e1* and *Mecp2e2*) at different time points of neural stem cell (NSC) differentiation at day 0 (D0), D2 and D8. Decitabine caused upregulation of *Mecp2e1*/MeCP2E1 but not *Mecp2e2* at D2. Decitabine effect on MeCP2E2 at the protein levels is unknown. Decitabine withdrawal by D8 downregulated *Mecp2e1*/MeCP2E1, and *Mecp2e2/*MeCP2E2 (unknown) to different extents. **B)** Schematic representation of the correlation between *Mecp2* isoform-specific expression and DNA methylation at the *Mecp2* promoter regions (R1 to R3), and intron 1 regions (R4 to R6). The size of the signs, plus (+), and minus (-) represents the relative degree of correlation with either *Mecp2* isoform. The statistically significant correlations are represented in red (red-circled plus, red-circled minus). After decitabine exposure *Mecp2e1* expression negatively correlated with promoter R1 and R3, and intron 1 R5. *Mecp2e2* isoform negatively correlates with promoter R3. In contrast, after decitabine withdrawal, *Mecp2e1*

expression negatively correlated with promoter R1, R2, and R3, and positively correlated with intron 1 R6. Hence, the correlation between *Mecp2e1* and DNA methylation at REs changed depending on the stage of NSC differentiation. *Mecp2e2* isoform positively correlated with intron 1 R4 and R6.

Taken together, these results show a strong ($r > 0.8$, $P < 0.05$) and dynamic (positive or negative) relationship between DNA methylation at the *Mecp2* REs and expression of *Mecp2* isoforms depending on the different stages of NSC differentiation. Therefore, these results implicate a possible dynamic role of DNA methylation at the *Mecp2* REs in regulating *Mecp2* isoform-specific regulation.

3.8 Discussion

In the brain, precisely controlled *MECP2*/MeCP2 transcript and protein expression levels are critical, as even slightly altered expression is associated with severe neurological symptoms [3,17,58-61]. However, so far little is known about how MeCP2 expression is regulated in the developing brain. MeCP2 is a major epigenetic regulator in the brain, and its reduced expression in the autistic brain is associated with *MECP2* promoter hypermethylation [3]. Surprisingly, the role of DNA methylation in MeCP2 expression during brain development is unclear. Currently, most diseases that are associated with aberrant MeCP2 function or expression deficits, including autism and Rett syndrome, have no cure or effective treatment. This underscores an urgent need for investigating how MeCP2 expression is regulated in the brain. Such knowledge for addressing this gap is essential for designing possible future therapeutic strategies. DNA methylation is a reversible epigenetic modification [22], which can be targeted by existing Food and Drug Administration (FDA)-approved drugs, including decitabine, which is suggested for use in autism

[62,63]. Therefore, investigating the effect of such epigenetic drugs on MeCP2 expression is important. Therapeutic approaches such as gene therapy or restoring MeCP2 expression by genetic engineering have been suggested as possible therapeutic strategies for MeCP2-associated disorders [15,16,35]. However, even mild MeCP2 overexpression can lead to severe neurological complications, highlighting the importance of understanding MeCP2 regulatory mechanisms. Since both MeCP2 isoforms have been implicated in severe neurological disorders, investigating MeCP2 regulation is equally important for individual isoforms. The present study is the first report on the potential role of DNA methylation at the *Mecp2* REs and the impact on the expression of *Mecp2* isoforms.

We observed globally altered DNA methylation upon decitabine exposure and withdrawal. Since DNA methylation is a major epigenetic mechanism that is involved in modulating gene expression and chromatin architecture [22], these observed changes in 5mC levels may possibly lead to altered chromatin structure and genome-wide changes in gene expression. Furthermore, the presented findings highlight that exposure to drugs that disturb the epigenetic marks during differentiation of brain cells may lead to aberrant DNA methylation profiles. Our observations at D8 indicate that, even after the disturbance factor is withdrawn from the system, an epigenetic memory for this disturbance may be associated throughout cellular differentiation of brain cells. Thus, our findings highlight the biological importance of maintaining proper regulation of epigenetic factors/modifications during brain development with a clear focus on DNA methylation and MeCP2.

Our results show that decitabine alters *Mecp2*/MeCP2 expression at both the transcript and protein levels. Importantly, even minor changes in *Mecp2* transcript expression led to nearly 2- to 3-fold altered protein expression, highlighting the biological significance of proper regulation of

Mecp2 expression at the transcript levels. The observed correlation between the *Mecp2*/MeCP2 (total) and *Mecp2e1*/MeCP2E1 transcript and protein expression at D2 reinforces the concept that potential changes in *Mecp2* transcript levels may reflect possible changes at the protein levels. However, the non-correlated *Mecp2*/MeCP2 (total) and *Mecp2e1*/MeCP2E1 transcript/protein expression at D8 indicates that decitabine withdrawal causes not only transcriptional but also, post-transcriptional regulation of MeCP2 expression, leading to reduced expression of MeCP2 (total)/MeCP2E1. One such post-transcriptional regulatory mechanism could be the action of microRNAs such as *miR132*, expression of which has been shown to be increased by 5-aza-2′-deoxycytidine/decitabine [64] and has the ability to repress MeCP2 expression [65].

Increased promoter methylation of autistic candidate genes such as *RORA*, *BCL2,* and *MECP2* are shown to be associated with reduced expression of these genes in autistic patients [3,54,63]. Treatment with decitabine was shown to demethylate promoters and restore/induce the expression of the silenced *RORA* and *BCL2* in autistic and patients with fragile X syndrome and hence, the use of DNA demethylating agents in drug therapy for autism and fragile X syndrome has been suggested [62,63]. A similar strategy to restore/induce MeCP2 expression might be extended to treat such diseases associated with reduced MeCP2 expression, including autism and RTT. Providing insights on such therapeutic strategies, the application of epigenetic drug therapy to induce non-mutated copy of *MECP2* expression in Rett syndrome cell lines has been suggested and attempted previously [66]. Therefore, our findings on the ability of decitabine to induce MeCP2 expression in differentiating NSC provide further insights on designing possible drug therapies for autism. Even though the exposure of RTT cell lines (fibroblasts) to lower doses of decitabine for a longer period did not activate *MECP2* expression [66], our results indicate that moderate dose of decitabine can induce *Mecp2*/MeCP2 expression within a shorter period.

However, inhibition of MeCP2 by the withdrawal of decitabine as well as other observed changes in DNA methyl marks implies that such drug therapy should be administrated with great caution.

Our findings on the changes in DNA methylation at the *Mecp2* REs are in agreement with the previous reports on *MECP2* promoter methylation, which demonstrated that an approximate difference of 2.0 to 2.5% overall methylation over a region -233 to -531 upstream of the *MECP2* promoter is correlated with reduced *MECP2* expression in autistic male brains. The authors report that within the 15 CpG sites found in this *MECP2* promoter region, two CpG sites are specifically altered in the autistic males [54]. Furthermore, our results are in agreement with a previous report on significantly reduced MeCP2 expression in the postnatal mouse brain (under stress), which is associated with 2 to 5% increased methylation at the individual CpG sites within a 164-bp region of the *Mecp2* promoter [20]. Supporting these observations, studies have also shown minor differences, such as 2 to 5% DNA methylation causing significant changes in the expression of other genes, such as *RASSF* in the human brain [67], *AMOTL2* in human heart [68], and *PGC1α* in human muscles [31]. Therefore, although the detected DNA methylation changes in this current study are not considerably high (they varied between 2 to 15%), they were statistically significant for average DNA methylation (within R1, R3 and R5) during NSC differentiation, and for several specific CpG dinucleotides subsequent to decitabine treatment (within R2, R4, R5, and R6), and are likely to be biologically important.

The *Mecp2* promoter CpG island studied by Franklin *et al.* [20] overlaps with the R1 and R2 of the *Mecp2* promoter that we studied here. The significantly methylated CpGs reported in their study coincides with the R2 CpGs, where we observed changes at individual CpG sites as well as average methylation upon decitabine treatment. However, in our study, we did not see any significant change in the R1 CpG sites (both D2 and D8), where Franklin *et al.* reported DNA

methylation changes. Importantly, the results we obtained for one of the promoter regions studied (R2) are in agreement with this previous report, which showed a biological and functional importance of the methylation changes in regulating MeCP2 expression in response to stress *in vivo*. Therefore, it is likely that the detected changes we observed in the *Mecp2* REs in our study also have biological importance. The hypermethylation of this R2 region in mouse brain was associated with MeCP2 downregulation [20], and hence it is possible that the hypomethylation/demethylation of the same R2 region causes *Mecp2/*MeCP2 upregulation.

Our results on the ability of 2.5 μM decitabine to upregulate *Mecp2e1* (but not *Mecp2e2*) suggest that the two isoforms may have different sensitivities to drugs/chemicals. This observation is in agreement with the previous report on the higher sensitivity of *Mecp2e1* than *Mecp2e2* to Bisphenol A [69]. These observations further suggest that the differential sensitivity to drugs might be used to specifically induce only one *Mecp2* isoform. This is also important because overexpression of *Mecp2e2,* but not *Mecp2e1* causes neuronal cell death [11]. Hence, our study provides a functional relevance of DNA demethylation at the *Mecp2* REs by decitabine causing upregulation of *Mecp2e1*, but not *Mecp2e2*.

The observed negative correlation between the expression of both *Mecp2* isoforms and *Mecp2* promoter elements are novel and are in accordance with previous correlation studies on the human *MECP2* expression and promoter DNA methylation [3,54]. Furthermore, our study is novel in demonstrating a dynamic (positive/negative) correlation between intronic DNA methylation and expression of *Mecp2* isoforms in differentiating brain cells. It is possible that the promoter regions analyzed in our study (which also overlap with the core *Mecp2* promoter [13]) might be shared by both *Mecp2* isoforms, whereas depending on the stage of neural differentiation, intron 1 regions may add another layer of regulation for *Mecp2* isoform-specific expression. Supporting our

findings, the role of intronic DNA methylation in regulating gene expression of other genes has been previously reported [70,71]. Several other reports also show evidence that gene expression negatively correlates with promoter methylation and positively correlates with gene-body methylation [68,72].

Intronic DNA methylation is reported to be involved in regulating alternative splicing [27,28]. Although, it is known that *Mecp2* isoforms are generated by alternative splicing [5,6], the underlying molecular mechanisms are still unclear. We observed that the expression ratio of *Mecp2e1/Mecp2e2* changed during NSC differentiation. The observed correlation between the splice ratio and intron 1 R4 DNA methylation in differentiating NSC at D2 would provide insights on the potential importance of this region in *Mecp2* alternative splicing.

The intron 1 regions analyzed in this study were designated as part of a silencer element, which has been previously proposed to regulate *MECP2* alternative splicing and tissue-specific expression [14]. Our findings are in agreement with possible involvement of these regions in *Mecp2* isoform-specific expression. Although the link between DNA methylation and *Mecp2* expression is supported by our results in the NSC system, the contribution of other epigenetic modifications such as histone acetylation and histone methylation should not be excluded [73,74].

3.9 Conclusion

The summary of the findings presented in our study is illustrated in **Figure 3.8**. First, expression of *Mecp2* isoforms was significantly and reciprocally changed at different stages of NSC differentiation, in association with minor but significant changes in DNA methylation at selected *Mecp2* REs, suggesting the possible involvement of these regions in *Mecp2* regulation. Second, treatment of differentiating NSC with decitabine for 48 h led to demethylation of specific

Mecp2 REs (promoter R2 and all intron 1 regions) and subsequent upregulation of *Mecp2e1/*MeCP2E1 (but not *Mecp2e2*), implying the differential sensitivity of the two *Mecp2* isoforms to decitabine. Such differential sensitivity of *Mecp2* isoforms to decitabine might be useful for future drug therapies to specifically activate one isoform but not the other. Furthermore, the ability of decitabine to induce *Mecp2e1*/MeCP2E1 at both transcript and protein levels provide insights for future therapeutic strategies for MeCP2 deficiency-related neurodevelopmental disorders such as autism and Rett syndrome. Finally, the significant and dynamic (positive or negative) correlation between the expression of *Mecp2* isoforms and DNA methylation implies the potential contribution of these REs in regulating *Mecp2* isoforms at different stages of neural differentiation. Collectively, our study contributes to the understanding of expression and regulation of *Mecp2* isoforms during neural development and provides important insights for future therapeutic applications of decitabine for MeCP2-related neurological disorders.

3.10 Competing interests

The authors have declared that no competing interests exist.

3.11 Acknowledgements

Chapter 3: Aim 1

Developmental Studies Hybridoma Bank, developed under the auspices of the NICHD and
maintained by The University of Iowa, Department of Biology, Iowa City, IA 52242.

3.12 References

1. Liyanage VR, Zachariah RM, Rastegar M (2013) Decitabine alters the expression of Mecp2
    isoforms via dynamic DNA methylation at the Mecp2 regulatory elements in neural stem
    cells. Mol Autism 4: 46.

2. Zachariah RM, Rastegar M (2012) Linking epigenetics to human disease and Rett syndrome:
    the emerging novel and challenging concepts in MeCP2 research. Neural Plast 2012:
    415825.

3. Nagarajan RP, Hogart AR, Gwye Y, Martin MR, LaSalle JM (2006) Reduced MeCP2
    expression is frequent in autism frontal cortex and correlates with aberrant MECP2
    promoter methylation. Epigenetics 1: e1-11.

4. Amir RE, Van den Veyver IB, Wan M, Tran CQ, Francke U, Zoghbi HY (1999) Rett
    syndrome is caused by mutations in X-linked MECP2, encoding methyl-CpG-binding
    protein 2. Nat Genet 23: 185-188.

5. Kriaucionis S, Bird A (2004) The major form of MeCP2 has a novel N-terminus generated by
    alternative splicing. Nucleic Acids Res 32: 1818-1823.

6. Mnatzakanian GN, Lohi H, Munteanu I, Alfred SE, Yamada T, MacLeod PJ, Jones JR,
    Scherer SW, Schanen NC, et al. (2004) A previously unidentified MECP2 open reading
    frame defines a new protein isoform relevant to Rett syndrome. Nat Genet 36: 339-341.

7. Dragich JM, Kim YH, Arnold AP, Schanen NC (2007) Differential distribution of the MeCP2
    splice variants in the postnatal mouse brain. J Comp Neurol 501: 526-542.

8. Zachariah RM, Olson CO, Ezeonwuka C, Rastegar M (2012) Novel MeCP2 isoform-specific
    antibody reveals the endogenous MeCP2E1 expression in murine brain, primary neurons
    and astrocytes. PLoS One 7: e49763.

9. Saunders CJ, Minassian BE, Chow EW, Zhao W, Vincent JB (2009) Novel exon 1 mutations
    in MECP2 implicate isoform MeCP2_e1 in classical Rett syndrome. Am J Med Genet A
    149A: 1019-1023.

10. Fichou Y, Nectoux J, Bahi-Buisson N, Rosas-Vargas H, Girard B, Chelly J, Bienvenu T
    (2009) The first missense mutation causing Rett syndrome specifically affecting the
    MeCP2_e1 isoform. Neurogenetics 10: 127-133.

11. Dastidar SG, Bardai FH, Ma C, Price V, Rawat V, Verma P, Narayanan V, D'Mello SR (2012) Isoform-specific toxicity of Mecp2 in postmitotic neurons: suppression of neurotoxicity by FoxG1. J Neurosci 32: 2846-2855.

12. Williamson SL, Christodoulou J (2006) Rett syndrome: new clinical and molecular insights. Eur J Hum Genet 14: 896-903.

13. Adachi M, Keefer EW, Jones FS (2005) A segment of the Mecp2 promoter is sufficient to drive expression in neurons. Hum Mol Genet 14: 3709-3722.

14. Liu J, Francke U (2006) Identification of cis-regulatory elements for MECP2 expression. Hum Mol Genet 15: 1769-1782.

15. Jugloff DG, Vandamme K, Logan R, Visanji NP, Brotchie JM, Eubanks JH (2008) Targeted delivery of an Mecp2 transgene to forebrain neurons improves the behavior of female Mecp2-deficient mice. Hum Mol Genet 17: 1386-1396.

16. Kerr B, Soto CJ, Saez M, Abrams A, Walz K, Young JI (2012) Transgenic complementation of MeCP2 deficiency: phenotypic rescue of Mecp2-null mice by isoform-specific transgenes. Eur J Hum Genet 20: 69-76.

17. Collins AL, Levenson JM, Vilaythong AP, Richman R, Armstrong DL, Noebels JL, David Sweatt J, Zoghbi HY (2004) Mild overexpression of MeCP2 causes a progressive neurological disorder in mice. Hum Mol Genet 13: 2679-2689.

18. Luikenhuis S, Giacometti E, Beard CF, Jaenisch R (2004) Expression of MeCP2 in postmitotic neurons rescues Rett syndrome in mice. Proc Natl Acad Sci U S A 101: 6033-6038.

19. Singh J, Saxena A, Christodoulou J, Ravine D (2008) MECP2 genomic structure and function: insights from ENCODE. Nucleic Acids Res 36: 6035-6047.

20. Franklin TB, Russig H, Weiss IC, Graff J, Linder N, Michalon A, Vizi S, Mansuy IM (2010) Epigenetic transmission of the impact of early stress across generations. Biol Psychiatry 68: 408-415.

21. Delcuve GP, Rastegar M, Davie JR (2009) Epigenetic control. J Cell Physiol 219: 243-250.

22. Liyanage VRB, Zachariah RM, Delcuve GP, Davie JR, Rastegar M (2012) New Developments in Chromatin Research: An Epigenetic Perspective. In: Simpson NM, Stewart VJ, editors. New Developments in Chromatin Research: Nova Science Publishers pp. 29-58.

23. Jeltsch A (2002) Beyond Watson and Crick: DNA methylation and molecular enzymology of DNA methyltransferases. Chembiochem 3: 274-293.

24. Kriaucionis S, Heintz N (2009) The nuclear DNA base 5-hydroxymethylcytosine is present in Purkinje neurons and the brain. Science 324: 929-930.

25. Tahiliani M, Koh KP, Shen Y, Pastor WA, Bandukwala H, Brudno Y, Agarwal S, Iyer LM, Liu DR, et al. (2009) Conversion of 5-methylcytosine to 5-hydroxymethylcytosine in mammalian DNA by MLL partner TET1. Science 324: 930-935.

26. Elango N, Yi SV (2008) DNA methylation and structural and functional bimodality of vertebrate promoters. Mol Biol Evol 25: 1602-1608.

27. Flores K, Wolschin F, Corneveaux JJ, Allen AN, Huentelman MJ, Amdam GV (2012) Genome-wide association between DNA methylation and alternative splicing in an invertebrate. BMC Genomics 13: 480.

28. Shukla S, Kavak E, Gregory M, Imashimizu M, Shutinoski B, Kashlev M, Oberdoerffer P, Sandberg R, Oberdoerffer S (2011) CTCF-promoted RNA polymerase II pausing links DNA methylation to splicing. Nature 479: 74-79.

29. Ishimaru N, Fukuchi M, Hirai A, Chiba Y, Tamura T, Takahashi N, Tabuchi A, Tsuda M, Shiraishi M (2010) Differential epigenetic regulation of BDNF and NT-3 genes by trichostatin A and 5-aza-2'-deoxycytidine in Neuro-2a cells. Biochem Biophys Res Commun 394: 173-177.

30. Mossman D, Kim KT, Scott RJ (2010) Demethylation by 5-aza-2'-deoxycytidine in colorectal cancer cells targets genomic DNA whilst promoter CpG island methylation persists. BMC Cancer 10: 366.

31. Barres R, Osler ME, Yan J, Rune A, Fritz T, Caidahl K, Krook A, Zierath JR (2009) Non-CpG methylation of the PGC-1alpha promoter through DNMT3B controls mitochondrial density. Cell Metab 10: 189-198.

32. Bazan E, Alonso FJ, Redondo C, Lopez-Toledano MA, Alfaro JM, Reimers D, Herranz AS, Paino CL, Serrano AB, et al. (2004) In vitro and in vivo characterization of neural stem cells. Histol Histopathol 19: 1261-1275.

33. Kishi N, Macklis JD (2004) MECP2 is progressively expressed in post-migratory neurons and is involved in neuronal maturation rather than cell fate decisions. Mol Cell Neurosci 27: 306-321.

34. Olynik BM, Rastegar M (2012) The genetic and epigenetic journey of embryonic stem cells into mature neural cells. Front Genet 3: 81.

35. Rastegar M, Hotta A, Pasceri P, Makarem M, Cheung AY, Elliott S, Park KJ, Adachi M, Jones FS, et al. (2009) MECP2 isoform-specific vectors with regulated expression for Rett syndrome gene therapy. PLoS One 4: e6810.

36. Tropepe V, Sibilia M, Ciruna BG, Rossant J, Wagner EF, van der Kooy D (1999) Distinct neural stem cells proliferate in response to EGF and FGF in the developing mouse telencephalon. Dev Biol 208: 166-188.

37. Barber BA, Liyanage VR, Zachariah RM, Olson CO, Bailey MA, Rastegar M (2013) Dynamic expression of MEIS1 homeoprotein in E14.5 forebrain and differentiated forebrain-derived neural stem cells. Ann Anat 10.1016/j.aanat.2013.04.005.

38. Lambert JF, Benoit BO, Colvin GA, Carlson J, Delville Y, Quesenberry PJ (2000) Quick sex determination of mouse fetuses. J Neurosci Methods 95: 127-132.

39. Hartshorn C, Rice JE, Wangh LJ (2002) Developmentally-regulated changes of Xist RNA levels in single preimplantation mouse embryos, as revealed by quantitative real-time PCR. Mol Reprod Dev 61: 425-436.

40. Huang H, Rastegar M, Bodner C, Goh SL, Rambaldi I, Featherstone M (2005) MEIS C termini harbor transcriptional activation domains that respond to cell signaling. J Biol Chem 280: 10119-10127.

41. Kobrossy L, Rastegar M, Featherstone M (2006) Interplay between chromatin and trans-acting factors regulating the Hoxd4 promoter during neural differentiation. J Biol Chem 281: 25926-25939.

42. Nolte C, Rastegar M, Amores A, Bouchard M, Grote D, Maas R, Kovacs EN, Postlethwait J, Rambaldi I, et al. (2006) Stereospecificity and PAX6 function direct Hoxd4 neural enhancer activity along the antero-posterior axis. Dev Biol 299: 582-593.

43. Rastegar M, Kobrossy L, Kovacs EN, Rambaldi I, Featherstone M (2004) Sequential histone modifications at Hoxd4 regulatory regions distinguish anterior from posterior embryonic compartments. Mol Cell Biol 24: 8090-8103.

44. Manczak M, Mao P, Nakamura K, Bebbington C, Park B, Reddy PH (2009) Neutralization of granulocyte macrophage colony-stimulating factor decreases amyloid beta 1-42 and suppresses microglial activity in a transgenic mouse model of Alzheimer's disease. Hum Mol Genet 18: 3876-3893.

45. Tsoporis JN, Marks A, Haddad A, Dawood F, Liu PP, Parker TG (2005) S100B expression modulates left ventricular remodeling after myocardial infarction in mice. Circulation 111: 598-606.

46. Schneider L, d'Adda di Fagagna F (2012) Neural stem cells exposed to BrdU lose their global DNA methylation and undergo astrocytic differentiation. Nucleic Acids Res 40: 5332-5342.

47. Mack JT, Beljanski V, Soulika AM, Townsend DM, Brown CB, Davis W, Tew KD (2007) "Skittish" Abca2 knockout mice display tremor, hyperactivity, and abnormal myelin ultrastructure in the central nervous system. Mol Cell Biol 27: 44-53.

48. Ghoshal K, Datta J, Majumder S, Bai S, Kutay H, Motiwala T, Jacob ST (2005) 5-Aza-deoxycytidine induces selective degradation of DNA methyltransferase 1 by a proteasomal pathway that requires the KEN box, bromo-adjacent homology domain, and nuclear localization signal. Mol Cell Biol 25: 4727-4741.

49. Rastegar M, Rousseau GG, Lemaigre FP (2000) CCAAT/enhancer-binding protein-alpha is a component of the growth hormone-regulated network of liver transcription factors. Endocrinology 141: 1686-1692.

50. Wu CH, Rastegar M, Gordon J, Safa AR (2001) beta(2)-microglobulin induces apoptosis in HL-60 human leukemia cell line and its multidrug resistant variants overexpressing MRP1 but lacking Bax or overexpressing P-glycoprotein. Oncogene 20: 7006-7020.

51. Gordon J, Wu CH, Rastegar M, Safa AR (2003) Beta2-microglobulin induces caspase-dependent apoptosis in the CCRF-HSB-2 human leukemia cell line independently of the caspase-3, -8 and -9 pathways but through increased reactive oxygen species. Int J Cancer 103: 316-327.

52. Ko M, Huang Y, Jankowska AM, Pape UJ, Tahiliani M, Bandukwala HS, An J, Lamperti ED, Koh KP, et al. (2010) Impaired hydroxylation of 5-methylcytosine in myeloid cancers with mutant TET2. Nature 468: 839-843.

53. Choufani S, Shapiro JS, Susiarjo M, Butcher DT, Grafodatskaya D, Lou Y, Ferreira JC, Pinto D, Scherer SW, et al. (2011) A novel approach identifies new differentially methylated regions (DMRs) associated with imprinted genes. Genome Res 21: 465-476.

54. Nagarajan RP, Patzel KA, Martin M, Yasui DH, Swanberg SE, Hertz-Picciotto I, Hansen RL, Van de Water J, Pessah IN, et al. (2008) MECP2 promoter methylation and X chromosome inactivation in autism. Autism Res 1: 169-178.

55. Nandakumar V, Vaid M, Katiyar SK (2011) (-)-Epigallocatechin-3-gallate reactivates silenced tumor suppressor genes, Cip1/p21 and p16INK4a, by reducing DNA methylation and increasing histones acetylation in human skin cancer cells. Carcinogenesis 32: 537-544.

56. Liu Q, Yang L, Gong C, Tao G, Huang H, Liu J, Zhang H, Wu D, Xia B, et al. (2011) Effects of long-term low-dose formaldehyde exposure on global genomic hypomethylation in 16HBE cells. Toxicol Lett 205: 235-240.

57. Christman JK (2002) 5-Azacytidine and 5-aza-2'-deoxycytidine as inhibitors of DNA methylation: mechanistic studies and their implications for cancer therapy. Oncogene 21: 5483-5495.

58. Squillaro T, Alessio N, Cipollaro M, Melone MA, Hayek G, Renieri A, Giordano A, Galderisi U (2012) Reduced expression of MECP2 affects cell commitment and maintenance in neurons by triggering senescence: new perspective for Rett syndrome. Mol Biol Cell 23: 1435-1445.

59. Smrt RD, Eaves-Egenes J, Barkho BZ, Santistevan NJ, Zhao C, Aimone JB, Gage FH, Zhao X (2007) Mecp2 deficiency leads to delayed maturation and altered gene expression in hippocampal neurons. Neurobiol Dis 27: 77-89.

60. Bodda C, Tantra M, Mollajew R, Arunachalam JP, Laccone FA, Can K, Rosenberger A, Mironov SL, Ehrenreich H, et al. (2013) Mild Overexpression of Mecp2 in Mice Causes a Higher Susceptibility toward Seizures. Am J Pathol 183: 195-210.

61. Na ES, Nelson ED, Adachi M, Autry AE, Mahgoub MA, Kavalali ET, Monteggia LM (2012) A mouse model for MeCP2 duplication syndrome: MeCP2 overexpression impairs learning and memory and synaptic transmission. J Neurosci 32: 3109-3117.

62. Chiurazzi P, Pomponi MG, Willemsen R, Oostra BA, Neri G (1998) In vitro reactivation of the FMR1 gene involved in fragile X syndrome. Hum Mol Genet 7: 109-113.

63. Nguyen A, Rauch TA, Pfeifer GP, Hu VW (2010) Global methylation profiling of lymphoblastoid cell lines reveals epigenetic contributions to autism spectrum disorders and a novel autism candidate gene, RORA, whose protein product is reduced in autistic brain. FASEB J 24: 3036-3051.

64. Im HI, Hollander JA, Bali P, Kenny PJ (2010) MeCP2 controls BDNF expression and cocaine intake through homeostatic interactions with microRNA-212. Nat Neurosci 13: 1120-1127.

65. Feng J, Nestler EJ (2010) MeCP2 and drug addiction. Nat Neurosci 13: 1039-1041.

66. Yu D, Sakurai F, Corey DR (2011) Clonal Rett Syndrome cell lines to test compounds for activation of wild-type MeCP2 expression. Bioorg Med Chem Lett 21: 5202-5205.

67. Mill J, Tang T, Kaminsky Z, Khare T, Yazdanpanah S, Bouchard L, Jia P, Assadzadeh A, Flanagan J, et al. (2008) Epigenomic profiling reveals DNA-methylation changes associated with major psychosis. Am J Hum Genet 82: 696-711.

68. Movassagh M, Choy MK, Goddard M, Bennett MR, Down TA, Foo RS (2010) Differential DNA methylation correlates with differential expression of angiogenic factors in human heart failure. PLoS One 5: e8564.

69. Warita K, Mitsuhashi T, Ohta K, Suzuki S, Hoshi N, Miki T, Takeuchi Y (2013) Gene expression of epigenetic regulatory factors related to primary silencing mechanism is less susceptible to lower doses of bisphenol A in embryonic hypothalamic cells. J Toxicol Sci 38: 285-289.

70. Jowaed A, Schmitt I, Kaut O, Wullner U (2010) Methylation regulates alpha-synuclein expression and is decreased in Parkinson's disease patients' brains. J Neurosci 30: 6355-6359.

71. Zhang X, Wu M, Xiao H, Lee MT, Levin L, Leung YK, Ho SM (2010) Methylation of a single intronic CpG mediates expression silencing of the PMP24 gene in prostate cancer. Prostate 70: 765-776.

72. Ball MP, Li JB, Gao Y, Lee JH, LeProust EM, Park IH, Xie B, Daley GQ, Church GM (2009) Targeted and genome-scale strategies reveal gene-body methylation signatures in human cells. Nat Biotechnol 27: 361-368.

73. Takebayashi S, Nakao M, Fujita N, Sado T, Tanaka M, Taguchi H, Okumura K (2001) 5-Aza-2'-deoxycytidine induces histone hyperacetylation of mouse centromeric heterochromatin by a mechanism independent of DNA demethylation. Biochem Biophys Res Commun 288: 921-926.

74. Nguyen CT, Weisenberger DJ, Velicescu M, Gonzales FA, Lin JC, Liang G, Jones PA (2002) Histone H3-lysine 9 methylation is associated with aberrant gene silencing in cancer cells and is rapidly reversed by 5-aza-2'-deoxycytidine. Cancer Res 62: 6456-6461.

3.13 Supplementary figures

CpG sites within Region 1

```
MECP2  CAAGAGGGCGGGGCGCGACGTCGGCCGTGCGGGGTCCCGGCGTCGGCGGCGCGCGCG
Mecp2  CGGGAGGGCGGGGCGCGACGTCTGCCGTGCGGGGTCCCGGCATCGGTTGCGCGCGCG
```

CpG sites within Region 2

```
MECP2  CGCGGGCGCG
Mecp2  CGCGGGCGCG
```

CpG sites within Region 3

```
MECP2  CGTCCCAAGCCTAGGCCTTCACTTGCC
Mecp2  CGCCAAGAGCCTAGACTTCCTTAAGCG
```

CpG sites within Region 4

```
MECP2  TACAAT
Mecp2  TACGAT
```

CpG sites within Region 5

```
MECP2  TGTTGATTC
Mecp2  TGACGCTTC
```

CpG sites within Region 6

```
MECP2  CCCTTC-TTCTGGGTTTGATTACA---TGAG--TAATTGTGTGAAT
Mecp2  CCGGAAGAACTGAGTTTGAGGACAGCCTGAACTACATAACGAGACT
```

Figure 3.S1 Comparison of CpG sites in human Methyl CpG binding protein 2 gene (*MECP2*) and mouse Methyl CpG binding protein 2 gene (*Mecp2*) promoter and intron 1. CpG sites analyzed in the mouse *Mecp2* (black) are underlined. Conserved CpGs between mouse and human sequences are also underlined in human *MECP2* (red) sequence.
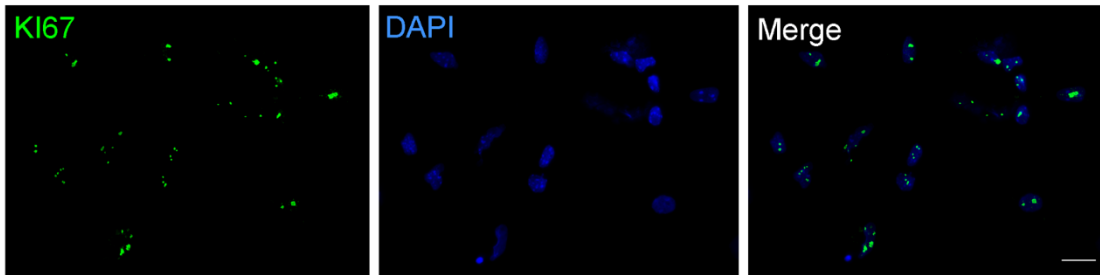
Figure 3.S2. Detection of Ki67 in day 2 (D2) control cells.

Ki67 was detected in (98.8% ± 0.8) of the D2 cell population, indicating that they were actively proliferating. Scale bars represent 20 μm.

Correlation between *Mecp2* splice ratio and DNA methylation					
	Mecp2e1/Mecp2e2		R1	R4	R5
D0	5.99 ± 0.52	r	0.9161	-0.994	-0.9964
		P value	0.2626	0.0699	0.0541
D2	0.69 ± 0.09	r	-0.988	0.9999	0.8895
		P value	0.0988	0.0087*	0.3022
D8	4.62 ± 0.46	r	-0.9959	0.5391	0.7949
		P value	0.0575	0.6375	0.415

Figure 3.S3 Relationship between the ratio of mouse Methyl CpG binding protein 2 gene (*Mecp2*) splice variants and DNA methylation at selected regulatory elements.

Pearson's correlation analysis between DNA methylation at the *Mecp2* regions R1, R4, and R5 and the *Mecp2e1/Mecp2e2* ratio at different stages of neural stem cell (NSC) differentiation. Significant differences: *P <0.05. The regions are, promoter regions R1: CpG island contains 13 CpG sites, intron 1 regions R4: 1 CpG site, and R5: 1 CpG site; N = 3 ± SEM.
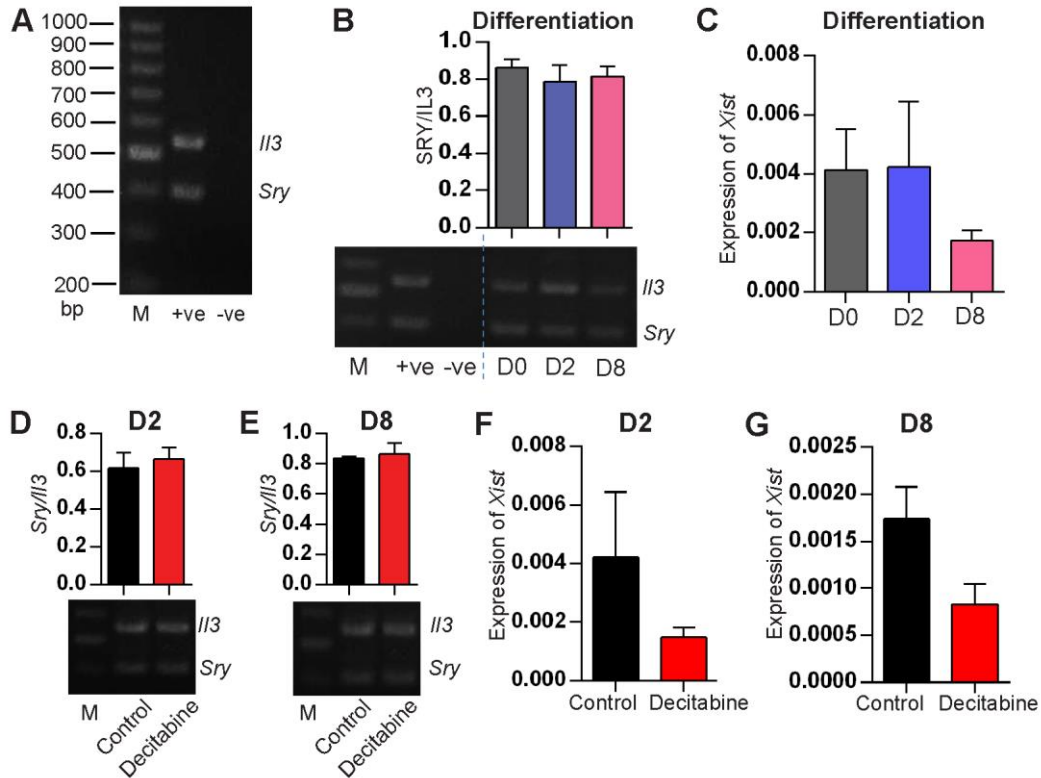
Figure 3.S4 Determination of the male/female contribution at different stages of neural stem cell (NSC) differentiation.

A) PCR amplification of *Sry* (402 bp) and *Il3* (544 bp) in the adult male cortex (positive control) and the absence of the signal in negative control PCR (no template). **B)** The detection of *Sry* and *Il3* in the positive and negative controls and during NSC differentiation (day 0 (D0), D2, D8). The graph represents the ratio of *Sry*/*Il3*; N = 3 ± SEM. **C)** Expression of *Xist* transcripts relative to *Gapdh* at different stages of NSC differentiation; N = 3 ± SEM. Significance was determined at *P <0.05. **D)** The ratio of *Sry*/*Il3* in D2 control and D2 decitabine-treated cells. **E)** The ratio of *Sry*/*Il3* in control and decitabine-treated cells at D8; N = 3 ± SEM. Expression of *Xist* transcripts relative to *Gapdh* at D2 after decitabine treatment **(F)**, and at D8 after decitabine withdrawal **(G)**; N = 3 ± SEM. Significance was determined at *P <0.05.

CHAPTER 4. ETHANOL DEREGULATES *MECP2*/MECP2 IN DIFFERENTIATING NEURAL STEM CELLS *VIA* INTERPLAY BETWEEN 5-METHYLCYTOSINE AND 5-HYDROXYMETHYLCYTOSINE AT THE *MECP2* REGULATORY ELEMENTS

4.1 Foreword

In Chapter 3, I included my first-authored research publication that reported the first evidence on the potential role of DNA methylation in regulating in *Mecp2* isoforms during NSC differentiation. In Chapter 1, I discussed that recent studies had suggested FASD as one of the MeCP2-related neurological disorders that have been linked to MeCP2 recently. The second aim of my thesis was to investigate the role of DNA methylation at *Mecp2* REs in mediating *Mecp2* misregulation by ethanol exposure and withdrawal during NSC differentiation. The results related to total *Mecp2* deregulation by ethanol was published in Experimental Neurology [1]. The results included in this chapter are a direct reprint of my first-authored article published in Experimental Neurology [1]. I have obtained copyright permission to reprint this article as a part of my thesis (License Number: 3933710063004) (also see page xxii). The modifications that have been done to the text to be included in this thesis chapter are as follows;

1. The figure and table numbers have been changed to comply with the chapter formatting. Eg. Fig.1 to Figure 4.1 or Table 1 to Table 4.1.

2. The supplementary figures have been placed within the body of text as they appear in the chapter, and their figure numbers have also been changed to comply with the chapter formatting. Eg. Supplementary Fig.S1 to Figure 4.S1.

3. The reference style of Experimental Neurology was changed to Plos formatting to comply with the overall thesis format.

As the first author, the majority of the contents of the study were conducted by myself, which included conception, design, performing the majority of the experiments, data analyses, interpretation and manuscript writing. Details of the author contributions are indicated below.

Vichithra R.B. Liyanage: Conceived and designed experiments; helped with maintenance of NSC cultures; ethanol treatments; assisted with sample collection; RNA extraction, cDNA synthesis and qRT-PCR; DNA extraction, analysis of bisulfite pyrosequencing data (gene-specific probe selection, primer optimization, and pyrosequencing were done as a paid service at the SickKids hospital, Toronto, Canada); hMeDIP and MeDIP; DNA dot blot; nuclear and cytoplasmic protein extractions and western blotting; fixation of cultured cells, immunocytochemistry and inverted microscopic imaging; quantification of cell numbers, neurite branching and glial cell size; nucleotide and amino acid sequence alignments of the four *Mbp*/MBP isoforms using CLUSTAL O(1.2.1); data collection, analyses and interpretation; preparation of figures; manuscript writing.

Robby M. Zachariah: Conceived and designed experiments; maintained NSC cultures; performed ethanol treatments, sample collection; initial paraformaldehyde steps of cell fixation, helped with immunocytochemistry experiments; reading and approving the final manuscript.

Dr. James R. Davie: Scientific input and discussions, as well as reading and approving the final manuscript.

Dr. Mojgan Rastegar: Conceived and designed experiments; embryonic forebrain dissections; isolation and culture of primary NSC; neurosphere collections, cellular dissociations, and differentiation of NSC; provided research support; contributed reagents/materials/analysis tools; data analyses and interpretation, manuscript writing, final approval, and submission.

Chapter 4. Aim 2

4.2 Author information

Vichithra Rasangi Batuwita Liyanage [a,b], Robby Mathew Zachariah [a,b], James Ronald Davie [b] and Mojgan Rastegar [a,b,*]

[a] Regenerative Medicine Program, [b] Department of Biochemistry and Medical Genetics, College of Medicine, Faculty of Health Sciences, University of Manitoba, 745 Bannatyne Avenue, Winnipeg, Manitoba R3E 0J9, Canada

* Corresponding Author

4.3 Author contributions

Vichithra R.B. Liyanage: Conception and design, collection and assembly of data, data analyses and interpretation, manuscript writing, final approval of manuscript

Robby M. Zachariah: Conception and design, collection and assembly of data, final approval of manuscript

James R. Davie: Scientific input, manuscript revisions, and final approval of manuscript

Mojgan Rastegar: Conception and design, contributed reagents/materials/analysis tools, data analyses, and interpretation, manuscript writing, final approval of manuscript

4.4 Highlights

- Ethanol exposure and withdrawal have opposing effects on *Mecp2*/MeCP2 expression.
- Ethanol deregulates *Mecp2* expression *via* DNA methylation at its regulatory elements.
- Provide insights on mechanisms of ethanol action and the effects on brain cells.
- Indicate contribution of epigenetic mechanisms in Fetal Alcohol Spectrum Disorders.

Chapter 4. Aim 2

4.5 Abstract

Methyl CpG Binding Protein 2 (MeCP2) is an important epigenetic factor in the brain. MeCP2 expression is affected by different environmental insults including alcohol exposure. Accumulating evidence supports the role of aberrant MeCP2 expression in ethanol exposure-induced neurological symptoms. However, the underlying molecular mechanisms of ethanol-induced MeCP2 deregulation remain elusive. To study the effect of ethanol on *Mecp2*/MeCP2 expression during neurodifferentiation, we established an *in vitro* model of ethanol exposure, using differentiating embryonic brain-derived neural stem cells (NSC). Previously, we demonstrated the impact of DNA methylation at the *Mecp2* regulatory elements (REs) on *Mecp2*/MeCP2 expression *in vitro* and *in vivo*. Here, we studied whether altered DNA methylation at these REs is associated with the *Mecp2*/MeCP2 misexpression induced by ethanol. Binge-like and continuous ethanol exposure upregulated *Mecp2*/MeCP2, while ethanol withdrawal downregulated its expression. DNA methylation analysis by methylated DNA immunoprecipitation indicated that increased 5-hydroxymethylcytosine (5hmC) and decreased 5-methylcytosine (5mC) enrichment at specific REs were associated with upregulated *Mecp2*/MeCP2 following continuous ethanol exposure. The reduced *Mecp2*/MeCP2 expression upon ethanol withdrawal was associated with reduced 5hmC and increased 5mC enrichment at these REs. Moreover, ethanol altered global DNA methylation (5mC and 5hmC). Under the tested conditions, ethanol had minimal effects on NSC cell fate commitment, but caused changes in neuronal morphology and glial cell size. Taken together, our data represent an epigenetic mechanism for ethanol-mediated misexpression of *Mecp2*/MeCP2 in differentiating embryonic brain cells. We also show the potential role of DNA methylation and MeCP2 in alcohol-related neurological disorders, specifically Fetal Alcohol Spectrum Disorders.

4.6 Introduction

Methyl CpG Binding Protein 2 (MeCP2) is a multifunctional epigenetic factor in the brain, which is involved in transcriptional regulation [2] and chromatin architecture [3,4]. *MECP2*/MeCP2 mutations or altered expression lead to a range of neurodevelopmental disorders including Autism Spectrum Disorders and Rett Syndrome (reviewed in [5]). MeCP2 also plays a role in substance abuse disorders such as drug addiction and alcoholism [6,7]. On the other hand, MeCP2 expression itself is sensitive to exposure to different environmental insults such as psychostimulants including cocaine and amphetamine, and alcohol (ethanol) (reviewed in [8]).

Ethanol is a typical teratogen, and prenatal exposure to ethanol leads to a wide range of developmental abnormalities known as Fetal Alcohol Spectrum Disorders (FASD) [9]. Recent studies also implicate the potential of preconception paternal alcohol consumption, which can lead to FASD [10,11]. Previous studies have shown the importance of both alcohol exposure and withdrawal (termination of alcohol consumption) in FASD pathogenesis [12], emphasizing the necessity to study the effect of both ethanol exposure and withdrawal on the central nervous system development [13,14]. During development, "binge-like" (single time) ethanol exposure, as well as continuous ethanol exposure, are reported to cause severe effects that contribute to FASD pathobiology [15].

Implicating the potential involvement of MeCP2 in FASD, a *MECP2* mutation (R270X) has been found in an FASD patient who showed overlapping phenotypes with both Rett Syndrome and FASD during development [16]. Additionally, both increased and decreased MeCP2 expression patterns have been reported in ethanol-fed rodent brain cells *in vivo* as well as in cultured cells *in vitro* (reviewed in [8]). The discrepancies in these studies regarding the effect of ethanol on MeCP2 expression could be attributed to multiple factors such as the model of study

(*in vivo* animal models or *in vitro* cultured cells), stage of embryonic development, specific brain region or cell type within a brain region, concentration and duration of ethanol treatment [11,17-24]. Further supporting the role of MeCP2 in alcoholism, a recent study demonstrated the regulatory effect of MeCP2 on sensitivity to ethanol and drinking ethanol [25]. Despite this increasingly evident link between changes in MeCP2 expression (increased or decreased) and ethanol exposure, the molecular mechanisms by which ethanol affects MeCP2 expression are understudied. Therefore, a detailed analysis of the effect of ethanol on MeCP2 expression and associated mechanisms is critical, which will be the primary focus of this current study.

DNA methylation is one of the most studied epigenetic mechanisms that are crucial in controlling gene expression during brain development [8,26-28]. Two major forms of DNA methylation are 5-methylcytosine (5mC) and 5-hydroxymethylcytosine (5hmC). While 5mC methylation of upstream promoter regions is considered to be a gene repressive mark, 5hmC has been detected in active gene regions [29,30]. MeCP2 has been shown to be the major protein, which binds to both 5mC and 5hmC in brain [31]. *MECP2* promoter hypermethylation is associated with *MECP2* downregulation in the autistic brain [32]. Increased *Mecp2* promoter methylation is also associated with reduced *Mecp2* expression in postnatal mouse brain in response to maternal separation and stress [33]. Apart from the regulatory elements (REs) found within the promoter, a silencer element within the *Mecp2* intron 1 is known to negatively regulate *Mecp2* expression [34]. Recently, we showed that DNA methylation at the REs found within the *Mecp2* promoter and intron 1 correlated with the dynamic expression of *Mecp2* in differentiating neural stem cells (NSC) and in response to a DNA demethylating drug decitabine (also called 5-aza-2'-deoxycytidine) [35]. Recently, our studies in adult murine brain regions demonstrated a correlation between the expression of *Mecp2* and DNA methylation at the *Mecp2* REs *in vivo* [36]. In this

current report, we studied whether DNA methylation at these reported *Mecp2* REs within the promoter and intron 1 contribute in deregulating *Mecp2* expression induced by ethanol.

Previously, we established a differentiating murine embryonic brain-derived NSC system to study the DNA methylation-mediated regulation of *Mecp2* [35]. We have used this NSC model to study the regulation of genes involved in neural development including *Mecp2* and *Meis1* [35,37,38]. We have successfully used the same NSC system to rescue the aberrant neuronal morphologies in *Mecp2*-deficient NSC by *MECP2* gene therapy strategies [37]. We also demonstrated the expression and regulation of *Mecp2*/MeCP2 by DNA methylation in a similar NSC model [35]. In this current study, we have modified this previously established NSC system to model binge-like and continuous ethanol exposure and ethanol withdrawal. We show that ethanol alters *Mecp2*/MeCP2 expression in association with an interplay between 5mC and 5hmC enrichment at the *Mecp2* regulatory elements.

4.7 Materials and methods

4.7.1 Ethics statement

All experiments were performed in agreement with the standards of the Canadian Council on Animal Care with the approval of the Office of Research Ethics at the University of Manitoba.

4.7.2 Neural stem cells isolation, culture, and differentiation

Neural stem cells isolated from the forebrains of embryonic day (E) 14.5 CD-1 mice were cultured as previously described [35,37,38]. In brief, dissected forebrain tissues were homogenized in NSC media Dulbecco's Modified Eagle Medium: Nutrient Mixture F-12 1:1 (DMEM/F12; Wisent) containing 4-(2-hydroxyethyl)-1-piperazineethanesulfonic acid (HEPES), glutamine,

antibiotic/antimycotic, glucose, recombinant human epidermal growth factor (rhEGF; Sigma, 20 ng/ml), basic fibroblast growth factor (bFGF; Upstate, 20 ng/ml), heparin (Sigma, 2 µg/ml) and hormone mix [DMEM:F12, glucose (0.6%), insulin (0.25 mg/ml), transferrin (1 mg/ml), progesterone (0.2 µM), putrescine (0.097 mg/ml), sodium selenite (0.3µM)] and plated at a density of 10^5 cells/cm^2 in serum-free full NSC media. Cells were cultured for 7 days to generate neurospheres. The dissociated neurosphere cells were plated in growth factor-reduced Matrigel coated-plates (BD Biosciences) at a density of 10^5 cells/cm^2 in DMEM media (GIBCO) containing 10% fetal bovine serum (FBS, Invitrogen) in the absence of rhEGF and bFGF. Cells were differentiated for 8 days under these conditions.

4.7.3 Ethanol treatment

Dissociated neurosphere cells were treated at the onset of differentiation at day 0 (D0) with ethanol (Commercial Alcohols) at a final concentration of 70 mM. To study binge ethanol exposure, ethanol treatment was done only once at D0 for 48 hours (h) and cells were collected at day 2 (D2). For continuous ethanol exposure, cells were treated with ethanol starting at D0 for 8 days continuously, and ethanol with media was refreshed every two days. To study the effect of ethanol withdrawal, the culture media was exchanged with fresh culture media after 48 h, and cells were kept in culture for an extra 6 days. The media was refreshed every other day. Control cells were cultured under similar experimental conditions in the absence of ethanol. Cells were harvested at day D2 and day 8 (D8).

4.7.4 Quantitative real-time polymerase chain reaction (qRT-PCR)

Total RNA was extracted using RNeasy Mini Kit (Qiagen). RNA was converted to cDNA with a reaction set up containing Superscript III Reverse Transcriptase (Invitrogen) using previously described methods [35,39-41]. Quantitative RT-PCR was performed using SYBR Green-based RT^2 qPCR Master Mix (Applied Biosystems) in a Fast 7500 Real-Time PCR machine (Applied Biosystems) as previously described [35,36,38]. Transcript levels of *Mecp2* and cell type-specific markers were examined using primers listed in **Table 4.1**. The Ct values (threshold cycle) for all genes were normalized with reference to the housekeeping gene glyceraldehyde 3-phosphate dehydrogenase (*Gapdh*) to obtain ΔCt values for each sample. Relative quantification analysis was carried out using Microsoft Excel 2010 by comparing the $2^{-\Delta Ct}$ of each sample to that of untreated control sample at D2 and D8 as described in our previous studies [35,36].

Table 4.1 The list of primers used for qRT-PCR experiments and their sources.			
Gene	**Direction**	**Sequence**	**Reference**
Mecp2	Forward	GGTAAAACCCGTCCGGAAAATG	[42]
	Reverse	TTCAGTGGCTTGTCTCTGAG	
β Tubulin III (Tub II)	Forward	TCAGCGATGAGCACGGCATA	[38]
	Reverse	CACTCTTTCCGCACGACATC	
Gfap	Forward	GCTCACAATACAAGTTGTCC	
	Reverse	ACCTAATTACACAGAGCCAGG	
Olig2	Forward	GTGGCTTCAAGTCATCTTCC	[35]
	Reverse	GTAGATCTCGCTACACAGTC	
Gapdh	Forward	AACGACCCCTTCATTGAC	[40]
	Reverse	TCCACGACATACTCAGCAC	

Mbp	Forward	GGCACGCTTTCCAAAATCT	[43]
	Reverse	CCATGGGAGATCCAGAGC	
Ki67	Forward	GCTGTCCTCAAGACAATCATCA	
	Reverse	GGCGTTATCCCAGGAGACT	
Nestin	Forward	CTGCAGGCCACTGAAAAGT	
	Reverse	TCTGACTCTGTAGACCCTGCTTC	

4.7.5 Immunocytochemistry (ICC)

Immunocytochemistry for cultured neural stem cells was carried out as described previously [35,37,44], using antibodies in **Tables 4.2** and **4.3**. Briefly, differentiated cells on coverslips were washed with phosphate buffered saline (PBS, GIBCO) and fixed in 4% paraformaldehyde. Cells were permeabilized with 2% NP40 in PBS for 10 min, followed by preblocking with 10% normal goat serum (NGS, Jackson Immunoresearch) in PBS for 1h. Appropriate primary antibodies were added and incubated overnight at 4°C followed by washes with PBS. This was followed by incubation with secondary antibodies that were diluted in 10% NGS [1h at room temperature (RT). Coverslips were mounted on glass slides with antifade containing 2 µg/ml DAPI. ICC signals were detected by an Axio Observer Z1 inverted microscope. Images were obtained using Zen 2009 software and assembled using Adobe Photoshop and Adobe Illustrator. For cell population determination, approximately 250 DAPI^{+} cells from D2 and 400-500 DAPI^{+} cells from D8 collectively from 3 biological replicates were counted using ImageJ program, as described previously [35].

Table 4.2 List of primary antibodies used in western blot and immunocytochemistry				
Primary Antibody	**Application and dilution**	**Molecular weight (kDa)**	**Description**	**Source**
MeCP2 (C-terminal)	WB 1:1000	72	Mouse monoclonal	Millipore, 07-013
Beta (β) ACTIN	WB: 1:2500	42	Mouse monoclonal	Sigma, A2228
GAPDH	WB: 1:500	37	Rabbit Polyclonal	Santa Cruz, Sc-25778
GFAP	IF 1:200	N/A	Mouse monoclonal	Invitrogen, 421262
Beta (β) TUBULIN III (TUB III)	IF 1:200	N/A	Mouse monoclonal	Chemicon, MAB1637
MBP	IF 1:100	N/A	Rabbit polyclonal	Abcam, ab40390
5mC	Dot Blot 1:1000	N/A	Mouse monoclonal	Abcam, Ab73938
5hmC	Dot Blot 1:1000	N/A	Rabbit polyclonal	Active Motif, 39769
NESTIN	IF 1:200	N/A	Rat polyclonal	Developmental Studies Hybridoma Bank, Rat-401c
Ki67	IF 1:200	N/A	Rabbit polyclonal	Sc-15402
OLIG2	IF 1:200	N/A	Rabbit polyclonal	Millipore, AB9610
RNA Polymerase (Pol) II	WB 1:1000	217	Mouse monoclonal	Abcam, Ab817

| HDAC2 | WB 1:1000 | 55 | Mouse monoclonal | Abcam, Ab12169 |
| Alpha (α) TUBULIN | WB 1:1000 | 50 | Mouse monoclonal | Sigma, T9026 |

Table 4.3 List of secondary antibodies used in western blot and immunocytochemistry		
Secondary Antibody	Application and dilution	Source
Alexa Fluor 488 conjugated goat anti-mouse IgG	IF 1:2000 or 1:3000	Invitrogen, A11017
Alexa Fluor 594 conjugated goat anti-rabbit IgG	IF 1:2000 or 1:3000	Invitrogen, A11037
Peroxidase-Affinipure Gt anti-mouse IgG	WB 1:7500, Dot blot 1:7500	Jackson ImmunoResearch 115-035-174
Peroxidase-AffiniPure donkey anti-rabbit IgG	WB 1:7500, Dot blot 1:7500	Jackson ImmunoResearch 711-035-152

4.7.6 Measurement of neurite branching and glial cell surface area

Immunofluorescence signals for glial fibrillary acidic protein positive (GFAP) and β Tubulin III (TUB III) were detected by an Axio Observer Z1 inverted microscope, and the images were obtained using Zen 2011 (Carl Zeiss). For quantification of the surface area of GFAP[+] astrocytes, superimposed Z-stacked images taken at 0.32 µm sections were analyzed. The surface area of GFAP[+] astrocytes was measured using the spline contour tool within Zen 2011 software, as shown in a previous study [45]. The signal intensity was adjusted to observe all the cellular processes of

GFAP$^+$ cells, and the outer margin of each cell was carefully marked using the spline contour tool, which directly provides the area in μm^2. At least 20 GFAP$^+$ astrocytes per biological replicate (three biological replicates) of control and ethanol-treated cells were measured. For the quantification of number of neurites, at least 20 TUB III$^+$ neurons per biological replicate (three biological replicates) were imaged, and neurites were marked and counted in ImageJ program as described in our previous study [37].

4.7.7 Western blot (WB)

Western blotting was performed as previously described [38,44,46,47]. NE-PER Nuclear and Cytoplasmic Extraction Kit (Thermo Scientific) was used to extract nuclear proteins as previously described [35,36]. Polyacrylamide gel electrophoresis was performed with 10-30 µg of nuclear extracts, and proteins were transferred to nitrocellulose membranes and blocked in 1-2% skim milk in TBS with tween20 (TBST: TBS+ 0.1% tween) for 1 h at RT. All primary antibody incubations were done overnight at 4°C. This was followed by three washes with TBST. Subsequently, we incubated the membranes with peroxidase-conjugated secondary antibody at RT for 1 h. Next, membranes were washed with TBST (three times). An enhanced chemiluminescence method was used to develop the membranes. The developing X-ray films were blue in color, and they were converted into gray color before quantification and assembly of the figures. Note that the brightness or contrast of the bands was not adjusted. RNA Pol II, HDAC2 (nuclear markers) and α-TUBULIN (mostly used as a cytoplasmic marker), ACTIN and GAPDH were tested to select the best endogenous loading control. ACTIN and GAPDH were chosen to be the most reliable and suitable loading controls (for further details see results). Quantification of WB bands was done with Adobe Photoshop CS5 software and normalized to ACTIN or GAPDH signals as described

previously [35,36]. MeCP2 expression in ethanol-treated samples was compared to the corresponding control untreated cells within the same biological replicate. Note that the exposure times were not the same for different experiments.

4.7.8 DNA dot blot assay for 5mC and 5hmC

DNA dot blot was performed using a previously described protocol [35]. Briefly, genomic DNA was isolated using the DNeasy Blood and Tissue kit (Qiagen) as per manufacturer's instructions. For each sample, 250 ng of DNA in 250µl final volume was heat denatured in 0.4 M sodium hydroxide (NaOH), 10 mM ethylenediaminetetraacetic acid (EDTA) at 100°C for 10 min and neutralized with an equal volume of ice-cold 2M ammonium acetate (pH 7.0) to obtain 500µl of final volume. Denatured DNA was loaded onto Zeta-Probe GT blotting membrane (Bio-Rad) set up in a dot blot apparatus (Bio-Rad). Wells were rinsed with 0.4 M NaOH to keep DNA denatured. The membrane was rinsed with 2X saline-sodium citrate (SSC), air-dried and UV cross-linked. Then the membrane was blocked with 3-5% skim milk in PBST (PBS+ 0.1% Tween) for 3h at RT followed by incubation in primary antibody [5mC or 5hmC (1:1000) in PBST] at 4°C overnight. After three washes with PBST, the membrane was incubated in secondary antibody for 1 h at RT. The signals were visualized by ECL chemiluminescence. Total DNA levels were detected by staining the same membrane with 0.02% methylene blue (MB) in 0.3 M sodium acetate (pH 5.2). Adobe Photoshop was used to quantify dot blot signals.

4.7.9 Bisulfite pyrosequencing

Bisulfite pyrosequencing was performed as a service at the Hospital for Sick Children, Toronto, Canada using previously described methods [35,36]. Genomic DNA was isolated as

described using the DNeasy Blood and Tissue kit (Qiagen) as per manufacturer's instructions. Three regions in the *Mecp2* promoter and three regions in *Mecp2* intron 1 were analyzed, which we have reported to impact *Mecp2* expression in differentiating NSC and adult mouse brain [35,36]. The primers used for pyrosequencing analysis are listed in **Table 4.4**. The control D2 methylation data were extracted from a recent report from our lab [35].

Table 4.4 List of primers used for bisulfite pyrosequencing	
***Mecp2* regions**	**Sequence**
R1	FP: 5'-TGGGTTTTATAATTAATGAAGGGTAA-3'
	RP: 5'- CGCCAGGGTTTTCCCAGTCACGACATTTTACCACAACCCTCTCT-3'
	SP: 5'-AGGTGTAGTAGTATATAGG-3'
R2	FP: 5'-AGTTTGGGTTTTATAATTAATGAAGGG-3'
	RR: 5'- CGCCAGGGTTTTCCCAGTCACGACATTTTACCACAACCCTCTCT-3'
	SR: 5'-AAGGGTAATTTAGATAAAGAGTAAG-3'
R3	FP: 5'- GGTGAATTATTTAGTAGGGAGGTTTTAA -3'
	RP: 5'- CGCCAGGGTTTTCCCAGTCACGACAAAAAAAAAAACCAACCCCATTCAACTAC -3'
	SP: 5'- AGTAGGGAGGTTTTAATAG -3'
R4	FP: 5'- GTTTTAAAAAGTTTTGGGAAAAGGTGTAGT -3'
	RP: 5'- CGCCAGGGTTTTCCCAGTCACGACCTAAACCCTAACATCCCAACTACCAT-3'
	SP: 5'- AGTTTAATGGGGATTTTTAATT -3'
R5	FP: 5'- AGTAGAAGTTATTATTTGTGGTGTGTAT -3'
	RP: 5'- CGCCAGGGTTTTCCCAGTCACGACACTATATTACTTCCCAACTCAACTAATT -3'
	SP: 5'- AGAGGTGTAAGGATTTT -3'
R6	FP: 5'- GAAGTAGGAAGAATTGAGTTTGAGGATAG -3'
	RP: 5'- CGCCAGGGTTTTCCCAGTCACGACATCTATACACTACCCACATA

	TAATACC -3'
	SP: 5'- GTTTGAGGATAGTTTGAAT -3'

FP: Forward PCR primer, RP: Reverse PCR primer (Biotinylated), SP: Sequencing primer, R: Region. Reference: [35]

4.7.10 Hydroxymethylated DNA immunoprecipitation (hMeDIP) and methylated DNA immunoprecipitation (MeDIP)

DNA immunoprecipitation was carried out using hMeDIP and MeDIP kits (Abcam) from 3-4 independent experimental replicates. For hMeDIP with D2 samples, 100 ng per reaction was used (due to the limited amount of the D2 samples), while for all D8 samples 500 ng per reaction was used. For MeDIP, 1 µg of DNA per reaction was used. The immunoprecipitated DNA was analyzed by qPCR using the primers specific for each *Mecp2* promoter or intron 1 region (**Table 4.5**). For each hMeDIP and MeDIP reaction, 2-3 qPCR technical replicates from 4 independent biological replicates were done to confirm the results. In order to confirm the specificity of the signals obtained from 5mC and 5hmC antibodies for both hMeDIP and MeDIP experiments, non-immunogenic IgG antibody was used. Quantitative PCR with *Gapdh* primers was used as an unmethylated negative control. For hMeDIP, a positive control DNA with 44 5hmC-CpG sites provided within the kit was used as a positive control for immunoprecipitation and was amplified using control primers provided within the kit. For MeDIP, primers specific for *Major Satellite Repeats* were used as a positive control for methylated DNA. The percentage input for the Ct values obtained from each qPCR was calculated relative to the Ct value of the input DNA used.

Table 4.5 List of primers used in qPCR for hMeDIP and MeDIP			
Mecp2 region (R)	**Direction**	**Sequence (5' to 3')**	**Reference**
R1	Forward	CAGGTGCAGCAGCACACAGGC	Designed in the lab
	Reverse	CGGACGGGTTTTACCACAGCC	
R2	Forward	GAACTCCACC AATCCGCAGC	
	Reverse	CCTGTGTGCTGCTGCACCTG	
R3	Forward	CAGGCTCCTCAACAGGCAAC	
	Reverse	GGCTGGTTTTGTGGGCAGCA	
R4	Forward	CTAGCTGAGCTGGGAAGTAAC	
	Reverse	GAGCTGGTCTACAGAAGCAAG	
R5	Forward	CTGTATAGTGTGGTGGAAGAAG	
	Reverse	GTTACTTCCCAGCTCAGCTAG	
R6	Forward	GAGTTTGAGGACAGCCTGAAC	
	Reverse	CTACCCACATGTAGTGCCTGC	

4.7.11 Statistical analysis

All graphs were generated using GraphPad Prism software and represent the average of two to four independent experiments. Error bars indicate standard error of mean (SEM). Student's *t*-test was used to determine statistical significance in gene expression. Two-way ANOVA was performed to determine statistical significance in percentage methylation (bisulfite pyrosequencing) and percentage input (hMeDIP and MeDIP) between control and ethanol-treated samples. Statistical significance was calculated using *****P* <0.0001, ****P* <0.001, ***P* <0.01 or **P* <0.05.

4.8 Results

4.8.1 A differentiating neural stem cell model was used to study the effect of ethanol on Mecp2/MeCP2 expression

To assess the impact of ethanol exposure on *Mecp2/*MeCP2 transcript and protein expression, we used a previously characterized embryonic NSC differentiation system [35,37,38]. Brain-derived neural stem cells were isolated from dissected forebrains of E14.5 mouse embryos and were cultured for 7 days in the presence of growth factors to generate neurospheres. Primary neurospheres were then dissociated, and single cells were differentiated for 8 days, as we have shown to be sufficient for generating neurons, astrocytes, and oligodendrocytes **(Figure 4.1A)** [35,37,38].
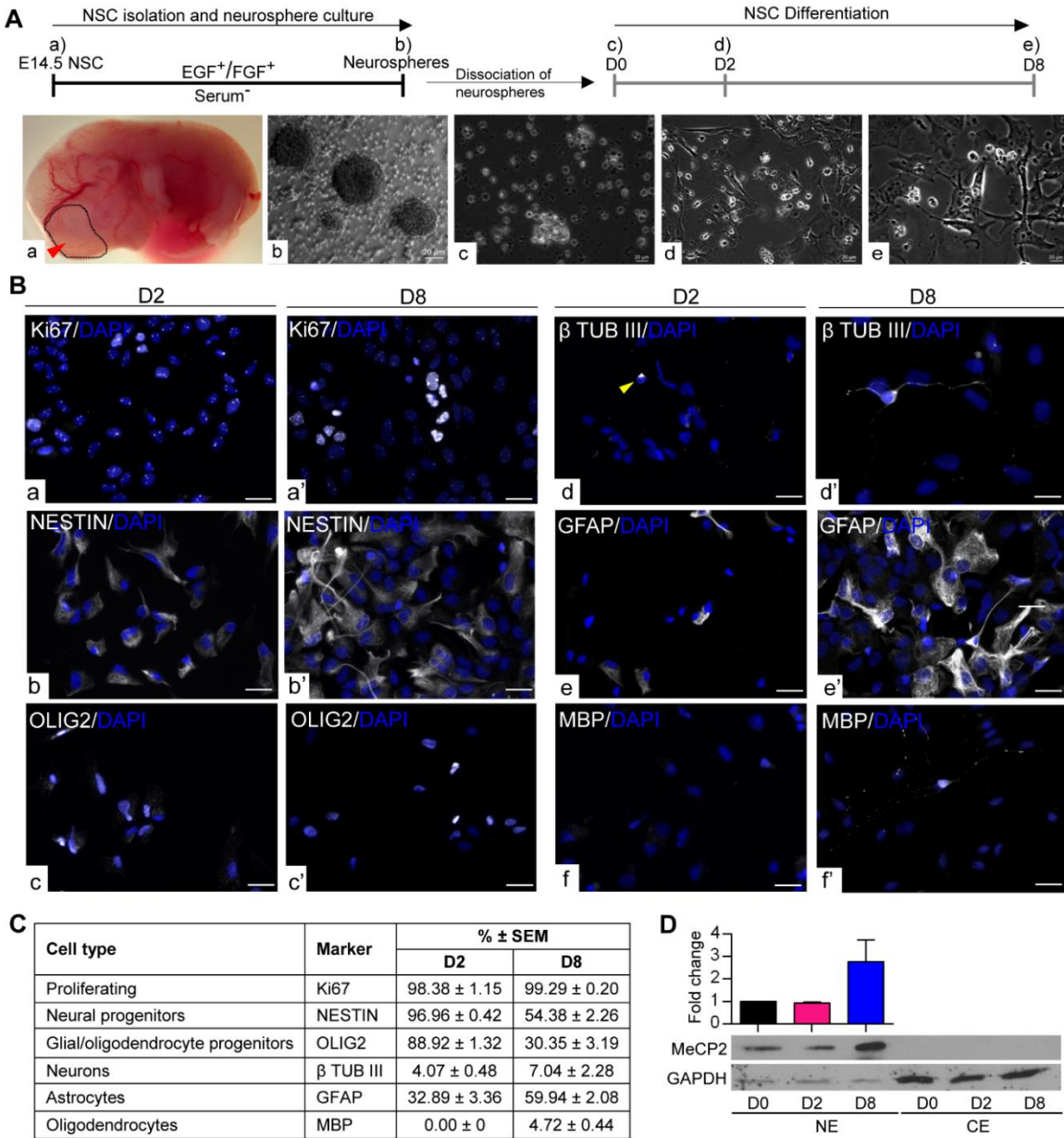
A) Schematic representation of NSC isolation, culture, and differentiation. NSC are isolated from Embryonic day (E) 14.5 forebrain (**a**) and cultured in the presence of growth factors (EGF and FGF) to generate neurospheres. (**b**) The neurospheres are dissociated at day zero (D0) (**c**) and differentiated for 8 days. Samples were collected at an early stage of differentiation at day (D)2 (**d**) and a later differentiation stage D8 (**e**). Scale bars represent 20 µm. **B)** Representative images of different cell types in D2 and D8 population. **a-a'**: Ki67, **b-b'**: NESTIN, **c-c'**: OLIG2, **d-d'**: β-

TUB III, **e-e'**: GFAP, **f-f'**: MBP. Note that no MBP+ cells were found at D2 (**f**). Scale bars represent 20 µm. **C)** Quantified percentages of the cellular composition of D2 and D8 differentiating populations. N=3 ± SEM. **D)** MeCP2 expression during NSC differentiation detected by Western blot. CE: Cytoplasmic extracts and NE: nuclear extracts. HDAC2 was used to show the purity of the nuclear extracts. GAPDH was used as the loading control. N=3 ± SEM.

We first determined the cellular composition of D2 and D8 differentiating cell populations by immunocytochemistry. All the images were captured in comparison to the exposure levels set using the primary omission negative control **(Figure 4.S1A)**. Representative images for each cell type-specific marker at D2 and D8 are shown in **Figure 4.1B,** and the quantifications for each cell type marker is shown in **Figure 4.1C**. We first studied Ki67 staining in D2, which marks proliferating cells. We observed two different patterns of Ki67, one that is localized to the nucleoli and another pattern with a diffused localization within the nucleus (extra-nucleolar) **(Figure 4.S1B)**.

Literature shows that both staining patterns are seen in proliferating cells, and the localization of Ki67 depends on the stage in the cell cycle [48,49]. Therefore, all cells with either diffused or nucleolar staining patterns were quantified, which resulted in 98.38 ± 1.15 Ki67+ cells **(Figure 4.1B: a; 1C)**. The D2 population was majorly composed of neural progenitor cells positive for NESTIN (96.96% ± 0.41) **(Figure 4.1B: b; 1C)**. D2 was also highly enriched for OLIG2 (88.91% ± 1.31) **(Figure 4.1B: c; 1C)**, which is a marker for glial/oligodendrocyte progenitor cells [50,51]. As differentiated cells at D2, we observed 4.07 ± 0.47 TUB III+ neurons and 32.89% ± 3.36 GFAP+ astrocytes **(Figure 4.1B: d-e; 1C)**. The quantification of TUB III+ neurons could presumably be an underestimate due to the very short nature of their neurites. Despite multiple efforts, we did not detect any MBP+ oligodendrocytes at D2. However, these cells were highly

enriched for the oligodendrocyte/glial progenitor marker OLIG2 (88.91% ± 1.31). Within the OLIG2^{+} progenitor population, two types of staining patterns were observed, one which is highly enriched at the nucleus and the second being nucleo-cytoplasmic **(Figure 4.S1C)**. In the literature, it has been shown that translocation of OLIG2 from the cytoplasm to nucleus is required for astrocyte differentiation [52]. Therefore, it is possible that the OLIG2^{+} cells in the D2 population are still in the process of committing towards oligodendrocyte/glial lineage.

In D8 population, we found 99.29% ± 0.20 Ki67^{+} proliferating cells **(Figure 4.1B: a'; 1C)**. At D8 differentiating cells, 54.38% ± 2.26 of cells showed NESTIN expression, indicating that they still carry their neural progenitor lineage signature **(Figure 4.1B: b'; 1C)**. As differentiated cell types at D8, we observed 7.03% ± 2.28 TUB III^{+} neurons, 59.94% ± 2.08 GFAP[+] astrocytes, and 4.72% ± 0.44 MBP[+] oligodendrocytes **(Figure 4.1B: d'-f'; 1C)**. This population still had 30.35% ± 3.19 OLIG2^{+} glial/oligodendrocyte progenitors **(Figure 4.1B:c'; 1C)**. In our previous study, we have shown the detection of MeCP2 in all these cell types [35].

Collectively, the number of differentiated cell types (TUB III[+], GFAP[+], and MBP[+]) increased from D2 to D8, as expected. The number of OLIG2^{+} glial/oligodendrocyte progenitor cells and neural progenitor cells (NESTIN[+]) decreased from D2 to D8. These observations confirmed that cells had undergone differentiation from D2 to D8. The number of proliferating cells (Ki67^{+}) more or less remained the same suggesting that D8 cells still are not terminally differentiated **(Figure 4.1C)**.

Next, we determined the expression levels of MeCP2 at different stages of NSC differentiation (D0, D2, and D8) by western blot. MeCP2 is a known nuclear protein, and yet some studies have reported the cytoplasmic expression of MeCP [53]. Therefore, we first confirmed

the expression pattern of MeCP2 in the nuclear and cytoplasmic fractions of D8 differentiated cells, which showed the detection of MeCP2 exclusively in nuclear fractions **(Figure 4.S2A)**.

In order to determine the most suitable endogenous control for our nuclear and cytoplasmic fractions, we screened known nuclear markers RNA Pol II and HDAC2, and α-Tubulin as a known cytoplasmic marker. Additionally, we used GAPDH and ACTIN loading controls, which were detected in both nuclear and cytoplasmic fractions **(Figure 4.S2A)**. As expected RNA Pol II was detected only in the nuclear fraction; while HDAC2 was highly enriched in the nuclear fraction. Alpha-Tubulin was enriched in the cytoplasmic fraction. Yet, it is known that α-Tubulin could also be detected in nuclear fraction [54,55]. As expected, ACTIN and GAPDH were detected in both fractions **(Figure 4.S2A)**. This is also in agreement with a previous report from our lab to detect GAPDH in both nuclear and cytoplasmic fractions of murine brain samples [36]. Re-probe of a membrane with lower levels of MeCP2 in ethanol- withdrawal samples (see next section), indicated a slight induction of RNA Pol II protein levels **(Figure 4.S2B)**, which suggested that perhaps RNA Pol II is not the best endogenous control to be used for quantification. Therefore, ACTIN, GAPDH, and HDAC2 were used as loading controls for the rest of the experiments and either ACTIN or GAPDH was used for western blot quantification.

Western blot experiments at D0, D2, and D8 (during differentiation) showed that MeCP2 protein levels are detected at all three stages **(Figure 4.1D; Figure 4.S3)**, which was in agreement with our previous study [35]. MeCP2 expression remained relatively the same from D0 to D2 but increased rapidly by D8 in three biological replicates. A representative blot for MeCP2 expression during NSC differentiation is shown in **Figure 4.1D**. MeCP2 was not detected in the cytoplasmic fractions at any tested differentiation stages **(Figure 4.1D)**.

4.8.2 Ethanol exposure and withdrawal show opposing effects on Mecp2/MeCP2 expression in differentiating neural stem cells
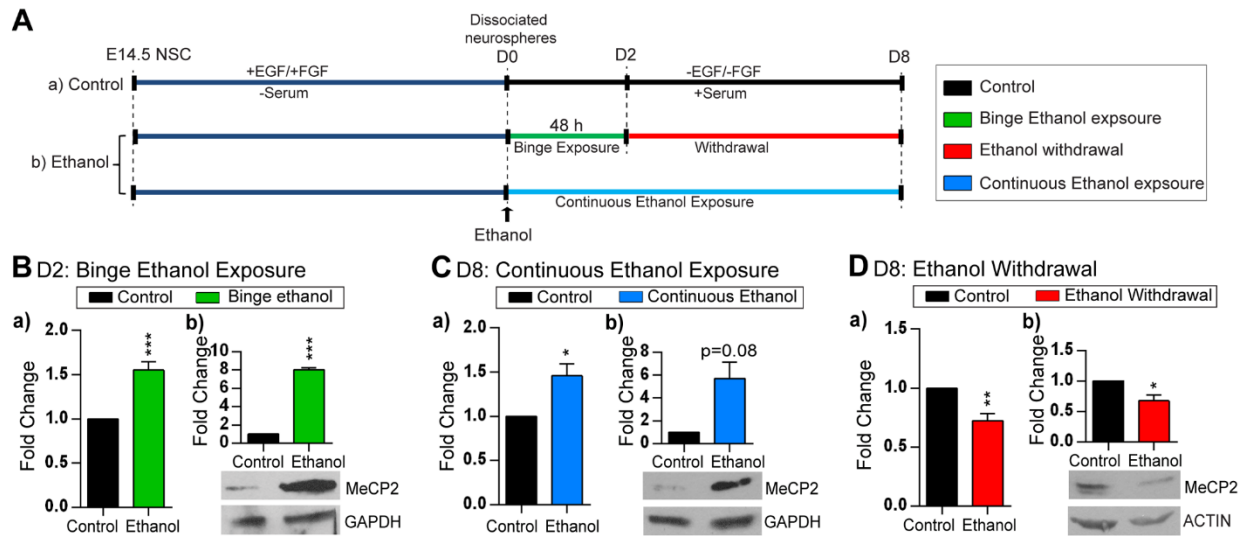
Figure 4.2 Effect of ethanol exposure and withdrawal on *Mecp2*/MeCP2 expression in differentiating neural stem cells (NSC).

A) Schematic representation of NSC differentiation and ethanol treatment. (**a**) Control experiment: NSC are isolated from embryonic day (E)14.5 forebrain and cultured in the presence of growth factors (EGF and FGF) to generate neurospheres. The primary neurospheres were dissociated (D0) and differentiated for 8 days. (**b**) To model binge ethanol exposure and withdrawal, 70 mM of ethanol was added at the onset of NSC differentiation (D0) to the media of cultured dissociated cells for 48 h and ethanol was withdrawn/removed at D2. To model continuous ethanol exposure, dissociated neural stem cells were treated with ethanol for continuously 8 days. Cells were kept in culture till D8 and media was refreshed every other day. **B)** Effect of binge ethanol exposure on the expression of (**a**) *Mecp2* transcript levels [N = 3 ± SEM], and (b) MeCP2 protein levels [N = 2 ± SEM]. **C)** Effect of continuous ethanol exposure on the expression of (a) *Mecp2* transcript levels [N = 3 ± SEM], and (**b**) MeCP2 protein levels [N = 2 ± SEM]. **D)** Effect of ethanol withdrawal on the expression of (**a**) *Mecp2* transcript expression [N = 3 ± SEM], and (**b**) MeCP2 protein levels [N = 2 ± SEM]. Fold changes are calculated relative to D2 and D8 untreated control cells. Significant differences from controls are indicated with ****P <0.001, **P <0.01 or *P <0.05.* The transcript expression values were normalized to *Gapdh* expression (endogenous

control). ACTIN or GAPDH was used as a loading control for Western blots. Note that exposure time for each western blot is different.

At the onset of differentiation (D0), cells were treated with 70 mM ethanol **(Figure 4.2A)**. The selected concentration of ethanol was chosen based on previous studies reporting, a) the blood alcohol levels detected in alcoholics (30-100 mM) [56], b) the effects of ethanol on isolated NSC from human fetal brain (20-100 mM) [57], c) conditions which show minimal effects on cell proliferation and survival of cultured NSC (22–69 mM) [58]. Control experiments were carried out without ethanol treatment. As established in previous similar studies [57,59,60], cells were treated once with ethanol for 48 h to study the effect of single time or binge-like alcohol exposure. To study the effects of continuous/chronic ethanol exposure, differentiating cells were treated with ethanol for 8 days (until D8). To study the effects of ethanol withdrawal, ethanol was removed from the cultures at D2, and the cells were kept in culture for extra 6 days until D8. Gene expression and DNA methylation analysis were performed after ethanol exposure at D2 and D8 and after ethanol withdrawal at D8 (6 days after ethanol removal) **(Figure 4.2A)**. Under each condition, *Mecp2*/MeCP2 expression levels in ethanol exposure or ethanol withdrawal conditions were compared to the untreated control cells in each biological replicate.

Next, we investigated *Mecp2* transcript and MeCP2 protein expression in response to ethanol treatments by qRT-PCR and WB. Following ethanol exposure at D2, we observed a slight, but significant induction of *Mecp2* transcript levels (1.55-fold, *P <0.001*) **(Figure 4.2B: a)**, which was translated into a significant induction of MeCP2 at the protein levels by 8-fold (*P <0.001*) **(Figure 4.2B: b)**. Similarly, continuous ethanol exposure upregulated *Mecp2* transcripts (1.46-fold, *P <0.05*), and MeCP2 protein levels (5.7-fold, P=0.08) **(Figure 4.2C)**. In contrast, ethanol withdrawal was associated with significantly reduced *Mecp2* transcript (1.38-fold, *P <0.01*) and

MeCP2 protein expression (1.48-fold, *P <0.05*) **(Figure 4.2D)**. Two biological replicates of western blots for each condition are shown in **Figure 4.S4**.

Comparison of the *Mecp2* transcript and MeCP2 protein levels indicated that even minor changes in *Mecp2* transcript levels can be translated into significant changes in MeCP2 protein. Previous reports on MeCP2 expression have shown that both mild overexpression (~2-fold) or slightly reduced MeCP2 levels may lead to severe neurological phenotypes [61,62]. Therefore, the detected alterations in MeCP2 protein levels (5.7-fold and 8-fold induction; and 1.48-fold inhibition) can biologically be important.

4.8.3 Changes to Mecp2/MeCP2 expression in response to ethanol exposure and withdrawal is associated with altered DNA methylation at the Mecp2 regulatory elements

It has been reported that altered gene expression in human alcoholics and alcohol-fed mice are associated with aberrant promoter DNA methylation [63,64]. In our recent studies, altered *Mecp2* expression by a DNA demethylating agent decitabine was correlated with DNA methylation at the *Mecp2* regulatory elements within its promoter and intron 1, in a similar differentiating NSC system. Moreover, *Mecp2* expression in adult murine brain regions *in vivo* was significantly correlated with DNA methylation at the same *Mecp2* REs [35,36]. This prompted us to investigate the DNA methylation status of the *Mecp2* REs upon ethanol exposure and withdrawal. To study whether the same REs are involved in the ethanol-mediated changes in *Mecp2* expression, we analyzed DNA methylation patterns of the previously reported three regions within the *Mecp2* promoter (R1-R3) and three regions within intron 1 (R4-R6) **(Figure 4.3A)** [35,36].

First, we performed bisulfite pyrosequencing to analyze DNA methylation at the individual CpG sites within these regions. After binge ethanol exposure at D2, DNA methylation levels at the individual CpG sites within the *Mecp2* promoter R1-R3 and intronic R4 and R5 were not significantly altered from the controls **(Figure 4.3B: a-e)**. However, R6: CpG-2 was slightly hypermethylated by 2.7% ($P <0.05$) **(Figure 4.3B: f)**. Further analysis of average percentage methylation over entire regions R1, R2, R3 and R6 (which contain multiple CpG sites) did not show any significant changes in the average DNA methylation by single ethanol exposure **(Figure 4.3B: g-j)**. A similar analysis after continuous ethanol exposure showed significant hypomethylation at both CpG sites within the intron 1 R6 (CpG1: 2.3%, p=0.06; CpG2: 7.5%, $P <0.05$) **(Figure 4.3C: f)**. Average methylation over the entire R6 also showed significant demethylation of the R6 (5%, $P <0.05$) by continuous ethanol exposure **(Figure 4.3C: j)**. However, no changes in DNA methylation at individual CpG sites or average methylation over the entire regions were observed in R1-R5 **(Figure 4.3C)**. Comparison of DNA methylation patterns in between D8 control and ethanol withdrawal conditions showed significant hypermethylation of the R6 CpG2 (4.5%, $P <0.05$) **(Figure 4.3D: f)** and no change in average DNA methylation of regions 1-6 **(Figure 4.3D: g-j)**.
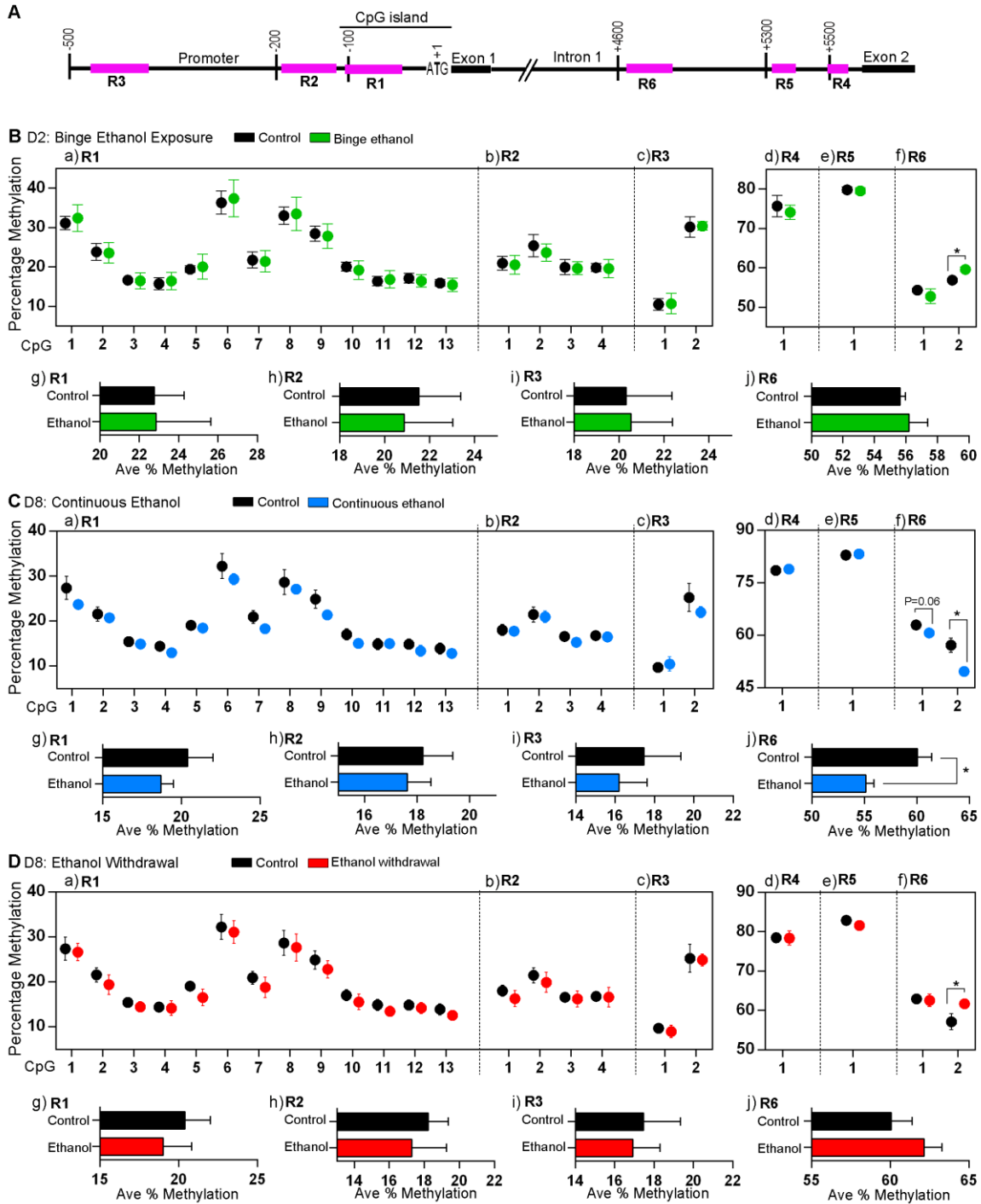
Figure 4.3 Bisulfite pyrosequencing analysis of the effect of ethanol on DNA methylation status at the *Mecp2* regulatory elements.

A) Schematic representation of the three regions (R1-R3) within the *Mecp2* promoter and three regions (R4-R6) within the *Mecp2* intron 1 (not drawn to scale). **B)** Effect of binge ethanol exposure at day (D) 2 on percentage DNA methylation of individual CpG sites within the *Mecp2* regulatory regions (**a**) R1, (**b**) R2, (**c**) R3, (**d**) R4, (**e**) R5, (**f**) R6; and the average percentage DNA methylation (Ave % Methylation) over (**g**) R1, (**h**) R2, (**i**) R3, (**j**) R6. **C)** Effect of continuous ethanol exposure at D8 on percentage DNA methylation of individual CpG sites within the *Mecp2* regulatory regions (**a**) R1, (**b**) R2, (**c**) R3, (**d**) R4, (**e**) R5, (**f**) R6; and the average percentage DNA methylation (Ave % Methylation) over (**g**) R1, (**h**) R2, (**i**) R3, (**j**) R6. **D)** Effect of ethanol withdrawal at D8 on percentage methylation of individual CpG sites within the *Mecp2* regulatory regions (**a**) R1, (**b**) R2, (**c**) R3, (**d**) R4, (**e**) R5, (**f**) R6; and the average percentage DNA methylation (Ave % Methylation) over (**g**) R1, (**h**) R2, (**i**) R3, (**j**) R6. Significant differences from controls are indicated with *P <0.05*. N = 3 ± SEM for all D2 samples, ethanol continuous and ethanol withdrawal samples and N = 6 ± SEM for D8 control samples. The control D2 DNA methylation data was extracted from our recent study [35], which was done at the same time and in parallel to this current study.

Previous studies have shown that 2-2.5% increase in average *MECP2/Mecp2* DNA promoter methylation is correlated with significantly reduced levels of MeCP2 in autistic patients and stressed mouse brain [32,33]. Our recent studies also showed that minor changes in percentage DNA methylation (2-5%) mediated by decitabine exposure correlated with significant changes in *Mecp2* expression [35]. This indicates that even minor changes in the DNA methylation at the *MECP2/Mecp2* REs might be associated with its altered expression. Therefore, it is likely that the detected changes in DNA methylation at the *Mecp2* REs are responsible for altered *Mecp2/*MeCP2 expression in differentiating NSC. However, bisulfite pyrosequencing does not differentiate between 5mC and 5hmC methyl marks [65] and might be reflecting cumulative changes in 5mC and 5hmC. Thus, further analysis of 5mC and 5hmC at these regions are required.

4.8.4 Ethanol causes interplay between 5mC and 5hmC enrichment at the Mecp2 regulatory elements

In order to differentiate between changes in 5mC and 5hmC at the *Mecp2* REs; we performed hMeDIP for 5hmC **(Figure 4.4)** and MeDIP for 5mC **(Figure 4.5)**.
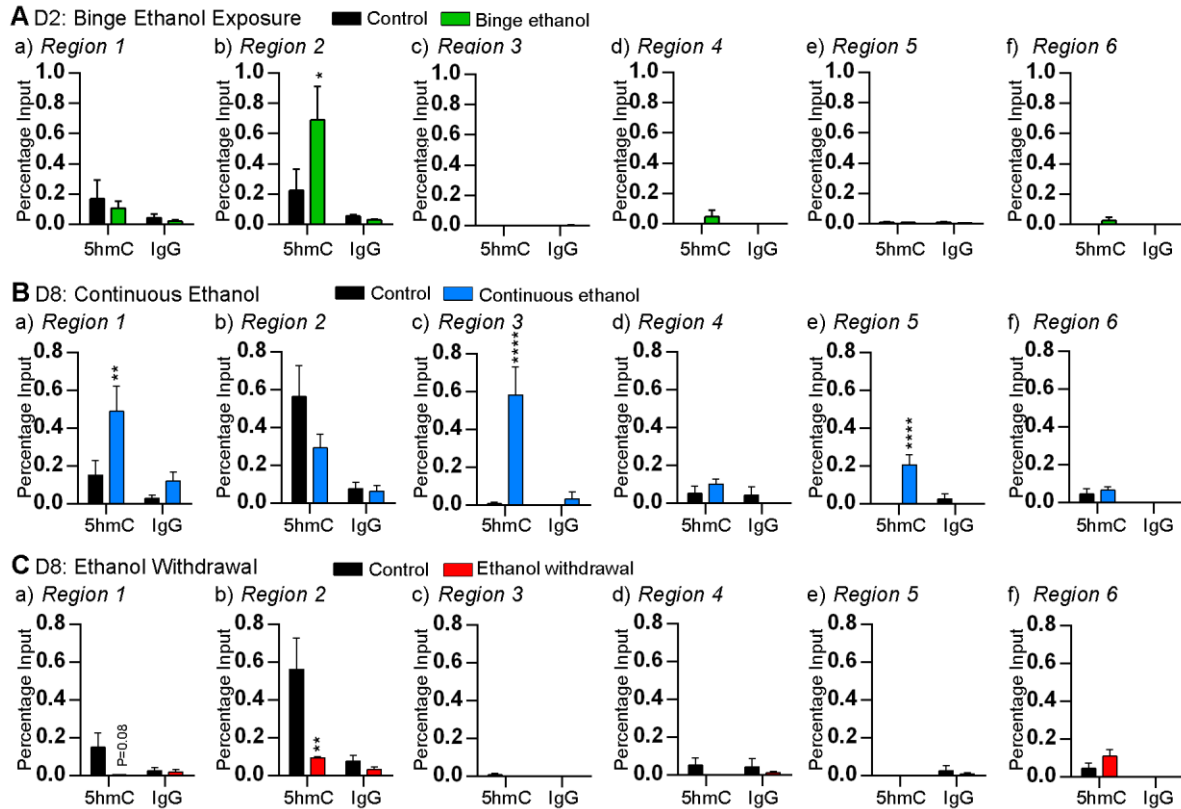
Figure 4.4 Effect of ethanol on the enrichment of 5hmC at the *Mecp2* regulatory elements. Enrichment of 5hmC and non-immunogenic IgG at the *Mecp2* promoter (**a**) region 1, (**b**) region 2, (**c**) region 3, and the *Mecp2* intron 1 (**d**) region 4, (**e**) region 5, (**f**) region 6; after **A)** binge ethanol exposure at day (D) 2, **B)** continuous ethanol exposure at D8, **C)** ethanol withdrawal at D8. Significant differences from controls are indicated with *****P <0.0001, **P <0.01 or *P <0.05*. N = 4 ± SEM.
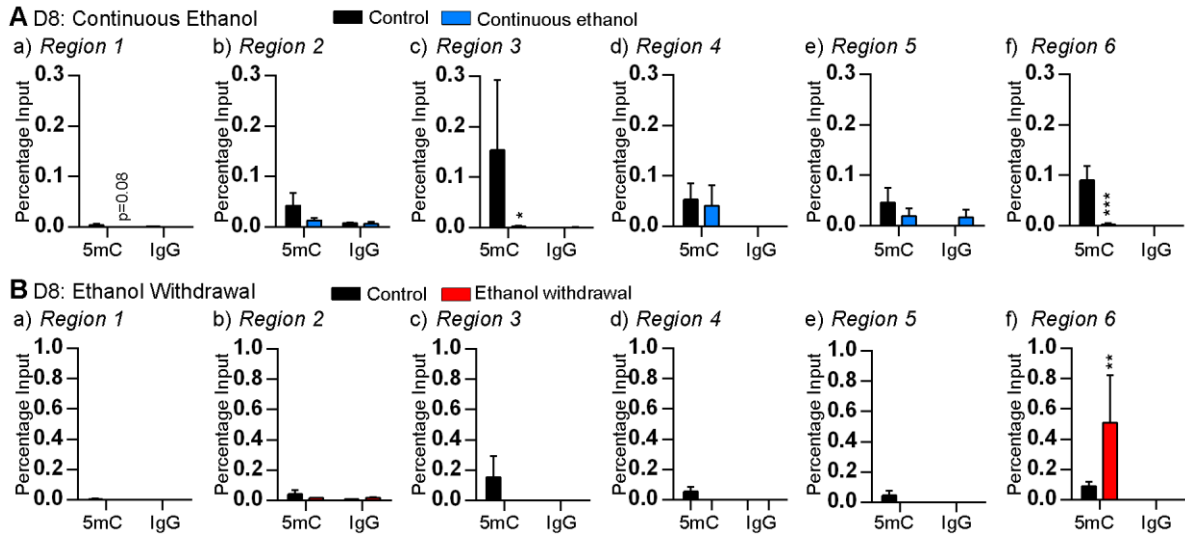
Figure 4.5 Effect of ethanol on the enrichment of 5mC at the *Mecp2* regulatory elements. Enrichment of 5mC and non-immunogenic IgG at the *Mecp2* promoter (**a**) region 1, (**b**) region 2, (**c**) region 3, and the *Mecp2* intron 1 (**d**) region 4, (**e**) region 5, (**f**) region 6; after **A)** continuous ethanol exposure at day (D) 8, **B)** ethanol withdrawal at D8. Significant differences from controls are indicated with ****P <0.001, **P <0.01 or *P <0.05*. N = 4 ± SEM.

Single ethanol exposure at D2 caused significant induction of 5hmC enrichment at the *Mecp2* promoter R2 (~3-fold, *P <0.05*) **(Figure 4.4A: b)**. The increased 5hmC levels at R2 were associated with upregulation of *Mecp2* transcript expression, suggesting that the increased 5hmC may contribute to *Mecp2* upregulation.

Since continuous ethanol exposure and ethanol withdrawal had opposing effects on *Mecp2* expression, we analyzed both 5mC and 5hmC enrichment at the *Mecp2* REs. In the case of continuous ethanol exposure (associated with increased *Mecp2* expression), significant 5hmC enrichment was observed at R1 (~3.2-fold, *P <0.01*), R3 (~65-fold, *P <0.0001*) and R5 (~69-fold, *P <0.0001*) **(Figure 4.4B)**. In contrast, reduced 5mC enrichment was observed at R3 (~77-fold, *P <0.05*) and R6 (~36.2-fold, *P <0.001*) upon continuous ethanol exposure **(Figure 4.5A)**. These

results suggest that the induced *Mecp2* expression by continuous ethanol exposure might be the result of increased 5hmC enrichment and reduced 5mC enrichment at specific *Mecp2* REs. Similar analysis after ethanol withdrawal (which caused downregulation of *Mecp2* expression) revealed reduced 5hmC enrichment at and increased 5mC at specific *Mecp2* REs. The 5hmC enrichment at the promoter R1 (~24-fold, P=0.08) and R2 (~6-fold, *P <0.01*) was reduced by ethanol withdrawal **(Figure 4.4C)**. In contrast, the 5mC enrichment at the intron 1 R6 was significantly induced by ~5.7-fold (*P <0.01*) **(Figure 4.5B)**. These results suggested that downregulation of *Mecp2* expression by ethanol withdrawal might be the result of reduced 5hmC and increased 5mC enrichment at specific *Mecp2* REs.

In all MeDIP and hMeDIP experiments, the specificity of the detected signals was confirmed by using a non-immunogenic IgG antibody, which showed negligible pull down **(Figure 4.4 and 4.5)**. For hMeDIP, we also used an internal control *Gapdh* as unmethylated negative control and a control DNA template (44 5hmC-CpGs) as a positive control, which was provided with the kit **(Figure 4.S5A)**. For MeDIP, the specificity of the detected signals was confirmed by using *Gapdh* and *Major Satellite Repeats* as negative and positive controls, respectively **(Figure 4.S5B)**.

Collectively, the changes we observed in *Mecp2*/MeCP2 expression after ethanol exposure and withdrawal are associated with dynamic changes in 5mC and 5hmC levels at specific regulatory elements. Overall, these changes in the 5hmc levels were independent of 5mC and *vice versa*, except for the R3 under continuous ethanol exposure conditions.

4.8.5 Ethanol changes global DNA methylation of differentiating neural stem cells

At the level of *Mecp2* gene, we observed dynamic changes in 5hmC and 5mC levels upon ethanol exposure and withdrawal. These observations prompted us to further investigate whether ethanol also causes globally changed levels of DNA methylation, as a control experiment for MeDIP and hMeDIP.
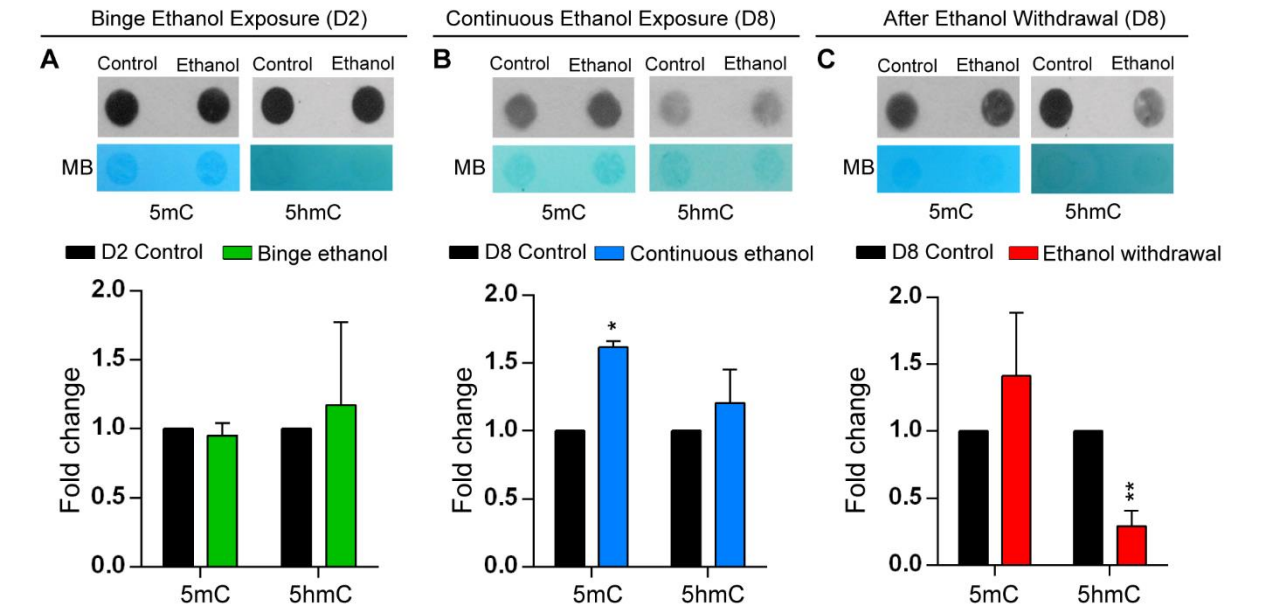
Figure 4.6 Effect of ethanol on global DNA methylation in differentiating neural stem cells (NSC).

DNA dot blot experiments to detect global DNA methylation levels for 5mC and 5hmC. MB refers to Methylene Blue staining for visualizing the total DNA. Quantification of the global 5mC and 5hmc levels normalized to the total DNA levels is also shown. Fold changes were calculated relative to day (D) 2 or D8 control untreated cells. N = 3 ± SEM. Significant differences from controls are indicated with **P <0.01 or *P <0.05*.

Quantitative DNA methylation analysis by DNA dot blot assay showed that binge ethanol exposure at D2 did not cause any significant alteration in the 5mC and 5hmC levels (**Figure 4.6A**). However, continuous ethanol exposure resulted in significant induction of 5mC levels (1.7-fold, *P*

<0.05) without significant effect on the 5hmC levels **(Figure 4.6B)**. In contrast, ethanol withdrawal significantly reduced 5hmC levels by 4-fold (*P <0.01*), with non-significant effects on 5mC levels **(Figure 4.6C)**. These findings indicate that effect of ethanol on global 5mC and 5hmC levels are dependent on the method of ethanol treatment (exposure or withdrawal) and the stage of neural stem cell differentiation. Moreover, the global changes in 5mC and 5hmC levels appear to be independent of each other.

4.8.6 Ethanol treatments have minimal effects on neural stem cell fate commitments but cause alterations in neuronal morphology and glial size

Next, we examined whether the observed changes in *Mecp2*/MeCP2 expression or the DNA methylation in response to ethanol treatments were associated with any changes in the cell population during NSC differentiation.

In order to determine the composition of both control and ethanol-treated populations, we studied the expression of cell type-specific markers that we analyzed in Figure 4.1 at the transcript level by qRT-PCR and the number of cells positive for these markers by IF. Binge ethanol exposure at D2 caused significant induction of *Mbp,* while changes of the rest of the cell type markers were not statistically significant **(Figure 4.S6A: a)**. Continuous ethanol exposure at D8 resulted in significant induction of *Nestin*, *Tub III,* and *Mbp*. Expression of other cell type-specific marker genes was relatively unaffected by continuous ethanol exposure **(Figure 4.S6B: a)**. Ethanol withdrawal did not result in significantly altered expression of any of the tested cell type-specific markers **(Figure 4.S6C: a)**.

Next, in order to determine whether the number of cells expressing these markers was changed by ethanol treatments, immunocytochemical experiments were carried out with the

antibodies specific for these markers. Binge ethanol exposure did not significantly change the number of cells positive for TUB III, GFAP, OLIG2, Ki67, and NESTIN. This observation suggested that binge ethanol exposure had minimal effects on cell population at D2 **(Figure 4.S6A: b)**. Since *Mbp* expression was upregulated at the transcript level and that was not represented in the number of MBP$^+$ oligodendrocytes determined by IF, we studied whether the presence of different isoforms of *Mbp*/MBP has affected our conclusion. Comparison of the mRNA sequence amplified by *Mbp*-specific primers **(Figure 4.S7A)** and the amino acid sequence used to generate the antibody for MBP **(Figure 4.S7B)** showed that the qRT-PCR primers, as well as MBP antibody, recognize similar sequences within all four isoforms (1, 2, 3 and 5) **(Figure 4.S7)**. Similar discordance between transcript and protein expression has also been reported for other genes [66].

Similar to binge ethanol exposure, continuous ethanol exposure, and ethanol withdrawal did not cause any significant change in the number of cells expressing each tested marker **(Figure 4.S6B: b; 4.S6C: b)**. In continuous ethanol-treated population, there was a slight but statistically non-significant increase in the number of MBP$^+$ cells, in accordance with the detected increase in *Mbp* transcript levels. This detected difference at the transcript levels and the number of cell counts could once again be due to the discordance between transcript and protein expression or changes in transcript expression within individual cells.

Taken together, these results confirmed that the balance between the numbers of differentiated cell types was not significantly affected under the tested conditions. Thus, the 70 mM ethanol treatments and withdrawal of ethanol had minimal impact on NSC cell fate commitment. Therefore, the observed changes in *Mecp2*/MeCP2 expression and global DNA methylation are not likely to be due to changes in cell fate commitment.

In ethanol-exposed neurons and glia, apart from the altered gene expression, alterations in the neuronal and glial morphology had been reported. Moreover, aberrant neurite outgrowth (both increased and decreased neurite outgrowth) and glial cell growth (mostly reduced glial cell growth) are associated with compromised central nervous system function and abnormal brain size (microcephaly) in FASD [67,68]. In agreement with these previous reports, we observed changes in neuronal morphology and glial size. As a measurement of glial size, we analyzed the surface area of GFAP^{+} cells, as other research groups have done to represent the size of glia [69,70]. Immunofluorescent labeling of binge ethanol-treated astrocytes at D2 showed reduced cellular size (~2.1-fold, *P* <0.0001) relative to the control untreated D2 cells **(Figure 4.7A)**. Unlike binge ethanol exposure, in the case of continuous ethanol exposure, approximately 1.5-fold (*P* <0.001) increase in glial size was observed relative to the untreated D8 control cells. No visible changes in glial size were observed between D8 control and ethanol withdrawal. We detected a 1.59-fold (*P* <0.0001) increase in the glial cell size in continuous ethanol exposure as compared to the ethanol withdrawal **(Figure 4.7C)**. These results suggest that glial size is affected by ethanol exposure but not by ethanol withdrawal. Also, in the case of ethanol exposure, the binge ethanol and continuous ethanol have opposing effects on the glial cell size.
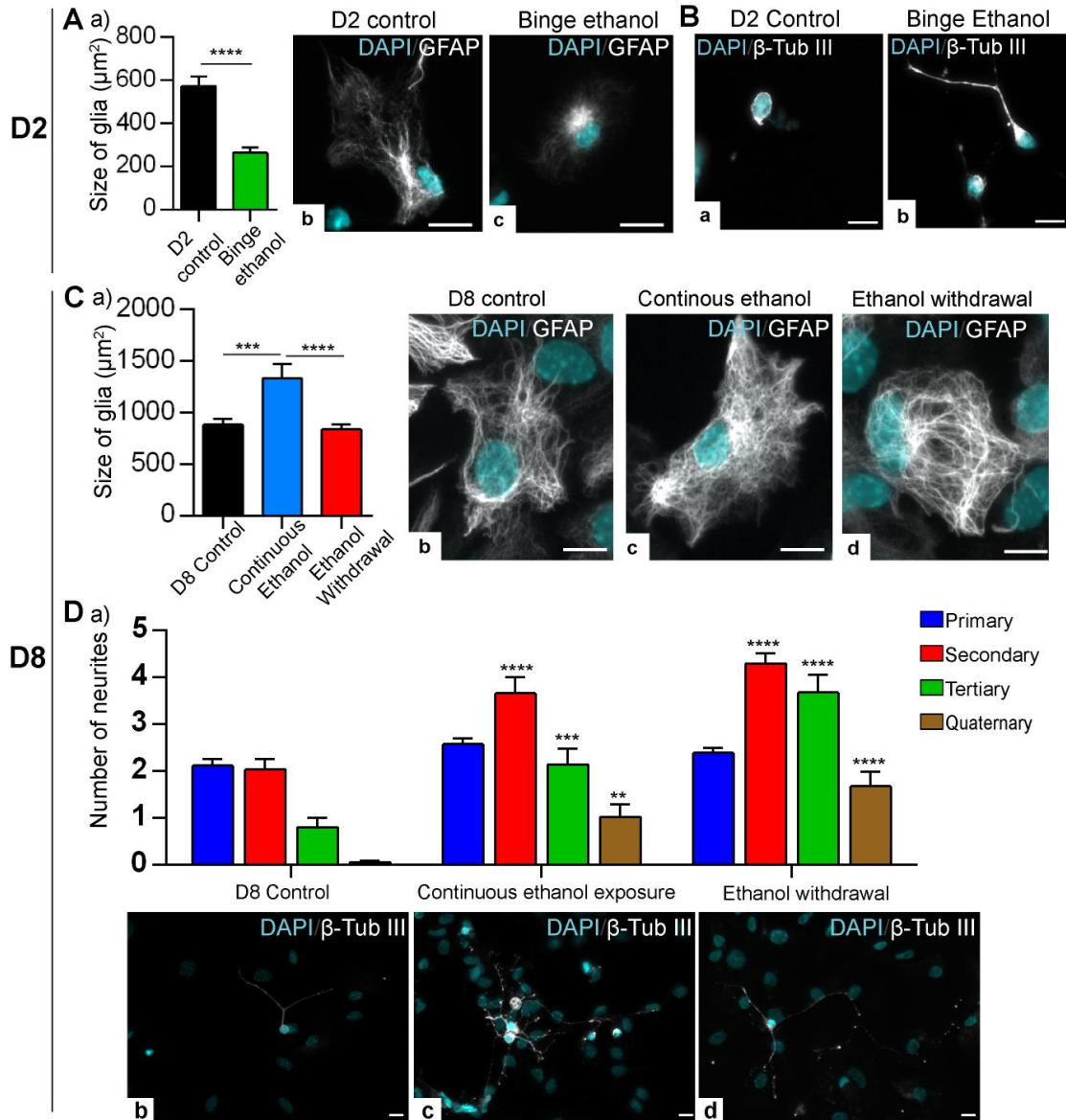
Figure 4.7 Effect of ethanol on the glial size and neuronal morphology.

A) Comparison of glial cell size in (μm^2) in day (D) 2 control and binge ethanol-treated conditions. (**a**) Graphical representation of the quantification of the glial cell size (μm^2). At least 20 GFAP$^+$ cells per biological replicate were quantified under each condition. N=3 ± SEM. Significant differences from controls are indicated with *****P <0.0001*. Representative images of (**b**) D2 control astrocyte, and (**c**) binge ethanol-exposed astrocyte. Scale bars represent 10 μm. **B)** Immunofluorescent staining of neurons with β Tubulin III in, (**a**) D2 control and (**b**) binge ethanol-treated cells. Scale bars represent 10 μm. **C)** Comparison of glial cell size in (μm^2) in D8 control,

continuous ethanol-treated and ethanol withdrawal conditions. **a**) Graphical representation of the quantification of the glial cell size (μm^2). At least 20 GFAP$^+$ cells per biological replicate were quantified under each condition. N=3 ± SEM. Significant differences from controls are indicated with ****P <0.0001 or ***P <0.001*. Representative images of (**b**) D8 control astrocyte, (**c**) continuous ethanol-exposed astrocyte and (**c**) ethanol-withdrawn astrocyte are shown. Scale bars represent 10 μm. **D)** Comparison of neuronal morphology in D8 control, continuous ethanol-treated and ethanol withdrawal conditions. (**a**) Quantification of number of neurites. At least 20 TUB III$^+$ neuronal cells per biological replicate were quantified under each condition. N=3 ± SEM. Significant differences from controls are indicated with ****P <0.0001, ***P <0.001 or **P <0.01*. Representative images of (**a**) D8 control neuron, (**b**) continuous ethanol-exposed neuron, and (**c**) ethanol-withdrawn neuron are shown. Scale bars represent 10 μm.

Interestingly, both ethanol exposure and ethanol withdrawal promoted neuronal neurite outgrowth and branching. Compared to the control D2 neurons, the binge ethanol-exposed neurons had induced neurite outgrowth. However, quantification of D2 neuronal branching was difficult due to the very short neurites observed in TUB III$^+$ neurons **(Figure 4.7B)**. Representative images of D2 neurons are shown in both **Figure 4.2B** and **Figure 4.7B**. Distinct changes in neuronal morphology were detected in continuous ethanol-exposed and ethanol withdrawal neurons as compared to D8 control neurons. Quantification of neuronal morphology in D8 control, continuous ethanol exposure, and ethanol withdrawal conditions showed that there is increased number of secondary, tertiary and quaternary neurites in both continuous ethanol-exposed neurons and ethanol-withdrawal neurons **(Figure 4.7D)**. Comparison of neurite branching between continuous ethanol exposure and ethanol withdrawal indicated a significant increase in tertiary neurites in ethanol withdrawal neurons. These observations suggest that exposure to ethanol at the beginning of neural differentiation, as well as its subsequent withdrawal, may recapitulate key features of ethanol-mediated neuro-glial morphological changes and also FASD.

4.9 Discussion

Among the epigenetic factors affected by alcohol, MeCP2 has become an emerging target [22,23,25], mostly due to its solid link with neurodevelopmental disorders [2]. These previous studies on the detrimental effects of ethanol on MeCP2 also suggest that MeCP2 expression is dependent on the dose and the duration of ethanol exposure. In this study, we demonstrate how *Mecp2*/MeCP2 expression is affected following a short time single exposure (binge), continuous exposure to ethanol as well as the withdrawal of ethanol during neuronal differentiation. We observed that ethanol exposure altered *Mecp2*/MeCP2 expression in association with altered DNA methylation at the *Mecp2* REs. Our results show the contribution of DNA methylation at the promoter and the intron 1 silencer element in deregulating *Mecp2*/MeCP2 expression upon ethanol exposure. The potential contribution of other mechanisms beyond DNA methylation such as histone acetylation or miRNA activities in deregulation of *Mecp2*/MeCP2 should not be excluded. In support of this concept, a study showed the association of changes in miRNAs (*miR-152*, *miR-199a-3p*, and *miR-685*) and downregulation of *Mecp2* expression followed by both ethanol (75 mM) exposure and withdrawal in E15 primary cortical neurons [24].

In our study, in almost all conditions (except for R3 in continuous ethanol exposure), 5hmC levels were changed without affecting the 5mC levels or *vice versa*. There are several explanations for such changes in DNA methylation patterns in our model. First, the DNA methylation patterns of continuous ethanol exposure and ethanol withdrawal were analyzed 6 days after binge ethanol exposure. During these 6 days, the neural stem cells were differentiating and proliferating with or without ethanol. In order to understand how the two methyl marks are changed gradually, DNA methylation patterns should be analyzed at shorter time points, perhaps every 12-24h. Secondly, the changes in 5hmC could also occur through either active or passive DNA demethylation [71].

It is unknown which pathways occur in our differentiating NSC model. In congruence with our observations on dynamics of 5mC and 5hmC, other studies suggest the possibility of 5hmC changes occurring independent of 5mC changes [72,73]. Even through, our study reports only 5hmC levels; there are other oxidative derivatives of 5mC, namely 5fC, and 5CaC, which could also contribute to the observed dynamics of 5mC and 5hmC [for review refer to [30]]. Further analysis is required to study whether altered DNA methylation (5mC and 5hmC) patterns at both *Mecp2* gene-specific regions and global levels are taking place gradually from binge ethanol exposure to continuous ethanol exposure or ethanol withdrawal.

In our study, bisulfite pyrosequencing of the studied regions did not reveal any considerable change in DNA methylation between control and ethanol-treated cells (except for intron 1-R6). However, analysis of 5mC and 5hmC enrichment at each region demonstrated significant changes in DNA methylation at these regions, representing a mechanism of DNA methylation-mediated regulation of *Mecp2*. These results also suggest the importance of investigating the enrichment of 5mC and 5hmC at the gene regulatory elements. This is especially important when no changes of DNA methylation are obtained through bisulfite pyrosequencing, which could be misleading to conclude that DNA methylation might not be involved in regulating certain genes.

Ethanol is known to alter global DNA methylation during neural development, and this has been suggested as a potential mechanism for FASD pathogenesis [23,74]. One single administration of ethanol at the onset of NSC differentiation did not alter the global 5mC and 5hmC levels. Continuous ethanol exposure induced 5mC levels whereas the withdrawal of ethanol reduced 5hmC levels. Therefore, it is possible that the effects of ethanol on global 5mC and 5hmC methylation is dependent on multiple factors such as the mode of ethanol treatment (binge ethanol, continuous ethanol exposure or ethanol withdrawal), duration of the treatment, stage of neural

differentiation and the type of DNA methylation (5mC or 5hmC). Since DNA methylation is a major player in maintaining chromatin architecture and regulating gene expression [29], altered 5mC and 5hmC levels, in turn, may alter chromatin structure and gene expression genome-wide. Our findings on ethanol-mediated altered global methylation patterns during NSC differentiation are supported by a recent study showing alteration of the progression of 5hmC marks by ethanol during neural development [23].

Neurological conditions caused by prenatal exposure to alcohol can also be considered as consequences of ethanol withdrawal because, during pregnancy, the fetus is exposed to alcohol and could be withdrawn from alcohol *in utero*, or after birth. Therefore, our observations on ethanol withdrawal downregulating *Mecp2*/MeCP2 expression is in agreement with several other reports where prenatal ethanol exposure, as well as preconception ethanol exposure (and subsequent withdrawal), led to decreased level of MeCP2 in a brain region-specific manner [11,20,22,23]. Comparing our data with previous reports that were earlier mentioned in the introduction [11,17-24], it is possible that the effect of ethanol on *Mecp2*/MeCP2 expression is influenced by multiple factors. This could include the type of ethanol treatment (binge exposure, continuous exposure and withdrawal), amount or concentration of ethanol, type of rodent model used in the study (mouse or rats), developmental stage (different embryonic time points or adult), brain regions and cell types within a certain brain region (specific neuronal subtype). For instance, in all previous reports the brain regions studied were either cortex, striatum or hippocampus whereas our studies were performed using NSC isolated from embryonic forebrain, which could also contribute to the differences observed in between the previous studies and our data. Moreover, in primary cortical neurons, exposure to ethanol and ethanol-withdrawal with similar concentration (75 mM as compared to 70 mM in our study) resulted in downregulation of *Mecp2*/MeCP2

expression [24]. In contrast, our study demonstrates that both binge and continuous ethanol exposure upregulate *Mecp2*/MeCP2 expression, while withdrawal of ethanol downregulates its expression. Ethanol exposure is considered as an environmental insult that may impact cell types or individuals differently. Additional factors to be considered may include maternal/paternal care, environmental conditions (light/dark, diet) of the rodent in terms of *in vivo* studies, and *in vitro* culture conditions.

As a key epigenetic factor in brain development and function, both deficiency and overexpression of MeCP2 lead to severe neurological disorders including autism [8]. FASD patients also show autistic symptoms [75,76]. Hence, our study provides insights on the possible involvement of MeCP2 in associated neurological symptoms in alcoholics and FASD patients. Studying the biological consequences of aberrant MeCP2 expression would be important for further understanding of MeCP2 involvement in ethanol-induced neurological symptoms. For instance, target genes of MeCP2 such as *NMDA* receptor subunits [77] are shown to be aberrantly expressed in alcohol-exposed neural cell types [78]. Therefore, altered MeCP2 expression, as well as altered binding of MeCP2 to its target genes, may contribute to ethanol teratogenesis. Moreover, it has been postulated that decreased levels of *Mecp2*/MeCP2 could contribute to the impulsive and hyperactive behaviors of offsprings exposed to ethanol prenatally (Kim et al., 2013). Previous studies show that even minor changes in MeCP2 expression may result in severe neurological conditions (reviewed in [8]). Therefore, it is logical to consider that the ethanol-induced changes in MeCP2 expression in our model are biologically relevant and may contribute to the adverse effects of ethanol on differentiating cells.

Differentiating neural stem cells are frequently used as *in vitro* models to study the underlying molecular mechanisms of ethanol teratogenesis and FASD pathogenesis [57,59,60].

Chapter 4. Aim 2

Alcohol-mediated neurological symptoms and microcephaly are usually associated with disrupted communications between neural cell types due to aberrant neurite outgrowth [79] and glial cell growth or morphology [80]. Our observations on the increased neurite outgrowth and changes in glial cellular size/surface area during NSC differentiation are in agreement with these previous reports. Several reports show the suppression of glial growth, glial proliferation as well as decreased expression of GFAP by ethanol [81-83]. In agreement with these reports, we observed reduced glial cell size after binge ethanol exposure. Similarly, our data on the increased glial size by continuous ethanol treatment is in agreement with the increase in glial size observed after chronic ethanol treatment *in vivo* in a rat FASD model [84]. Therefore, our ethanol-treated NSC model system recapitulates two of the cellular phenotypes seen in FASD patients, *in vivo* FASD models, and *in vitro* cellular models. This indicates that the differentiating neural stem cells model used in our studies represents a suitable system to study the effects of ethanol on gene expression changes, epigenetic mechanisms and molecular mechanisms of ethanol teratogenesis.

Interestingly, there is an overlap between the glial and neuronal cellular phenotypes observed in ethanol-treated conditions and MeCP2 overexpression/deficient-conditions. For example, ethanol exposure [85-87] and MeCP2 overexpression [37,88] have been shown to show similar patterns of increased neurite branching. However, ethanol exposure has also been shown to reduce the neurite outgrowth [89], similar to few studies on MeCP2-deficiency [37,90,91]. The reduced glial cell growth in ethanol-exposed astrocytes [80] is similar to the glial phenotypes seen in either MeCP2-deficient or MeCP2-overexpressed conditions [92,93]. The effects of ethanol on neuronal and glial morphologies/size seem to be influenced by many factors such as cell type, duration, and concentration of ethanol exposure. On the other hand, MeCP2 has been shown to either increase or decrease the neurite morphology. Neuronal morphology is also influenced by nearby glial cells

227

[94]. The absence of MeCP2 in adjacent glial cells has also been shown to be influencing the neuronal morphology [95]. In differentiating neural stem cells, both neurons and glia are present simultaneously. Thus any altered MeCP2 expression in glial cells could potentially influence the neuronal morphology. Moreover, MeCP2 expression is cell type-specific and presence of a mixed cell population might complicate the analysis. Therefore, analysis of pure populations might be beneficial in the future. However, the mixed nature of populations provides much resemblance to the *in vivo* conditions, where there are cell-to-cell communications and interactions similar to the developing brain. Additionally, ethanol-induced changes in the levels of neural growth factors have also been linked to the impaired neuronal morphology in response to ethanol treatment [96,97]. The MeCP2 target gene Brain-derived neurotrophic factor (*BDNF*) is also a key player in neuronal morphology [98]. Therefore, in addition to the more direct effects of ethanol on neurons and astrocytes, it is possible that MeCP2 and MeCP2-regulatory networks may presumably contribute to the altered neuronal and glial morphology observed in our study reported here.

Further investigations are required to elucidate the impact of 5mC and 5hmC at *Mecp2* regulatory elements (R1-R6), which could mediate *Mecp2*/MeCP2 deregulation by ethanol exposure *in vivo*.

4.10 Conclusion

In conclusion, this current study demonstrates deregulation of *Mecp2*/MeCP2 by binge-like, continuous ethanol exposure and ethanol withdrawal. We report an *in vitro* ethanol exposure- and withdrawal-model during differentiation of brain-derived neural stem cells, which recapitulates two key features of FASD brain (neuronal morphology and glial size changes) and have minimal effects on NSC cell fate commitments. We show that such altered *Mecp2*/MeCP2 expression is

correlated with dynamic changes of 5hmC and 5mC at the *Mecp2* regulatory elements. **Figure 4.8** illustrates a summary of the correlation between ethanol-induced changes in 5mC/5hmC enrichment at the *Mecp2* regulatory elements and *Mecp2*/MeCP2 expression. Based on our data, the increased 5hmC enrichment at R1, R2, R3 or R5 and decreased 5mC enrichment at R3 or R6 may contribute to the induction of *Mecp2*/MeCP2 expression. On the other hand, decreased 5hmC at R1 or R2 and increased 5mC enrichment at R6 seem to be contributing to the downregulation of *Mecp2*/MeCP2 expression. Furthermore, we show how ethanol impacts global DNA methylation at both 5mC and 5hmC levels. Collectively, our studies provide novel insights into the role of epigenetic mechanisms, specifically DNA methylation, and MeCP2 in ethanol-induced neurological symptoms during neural development and ethanol teratogenesis and ultimately on Fetal Alcohol Spectrum Disorders.
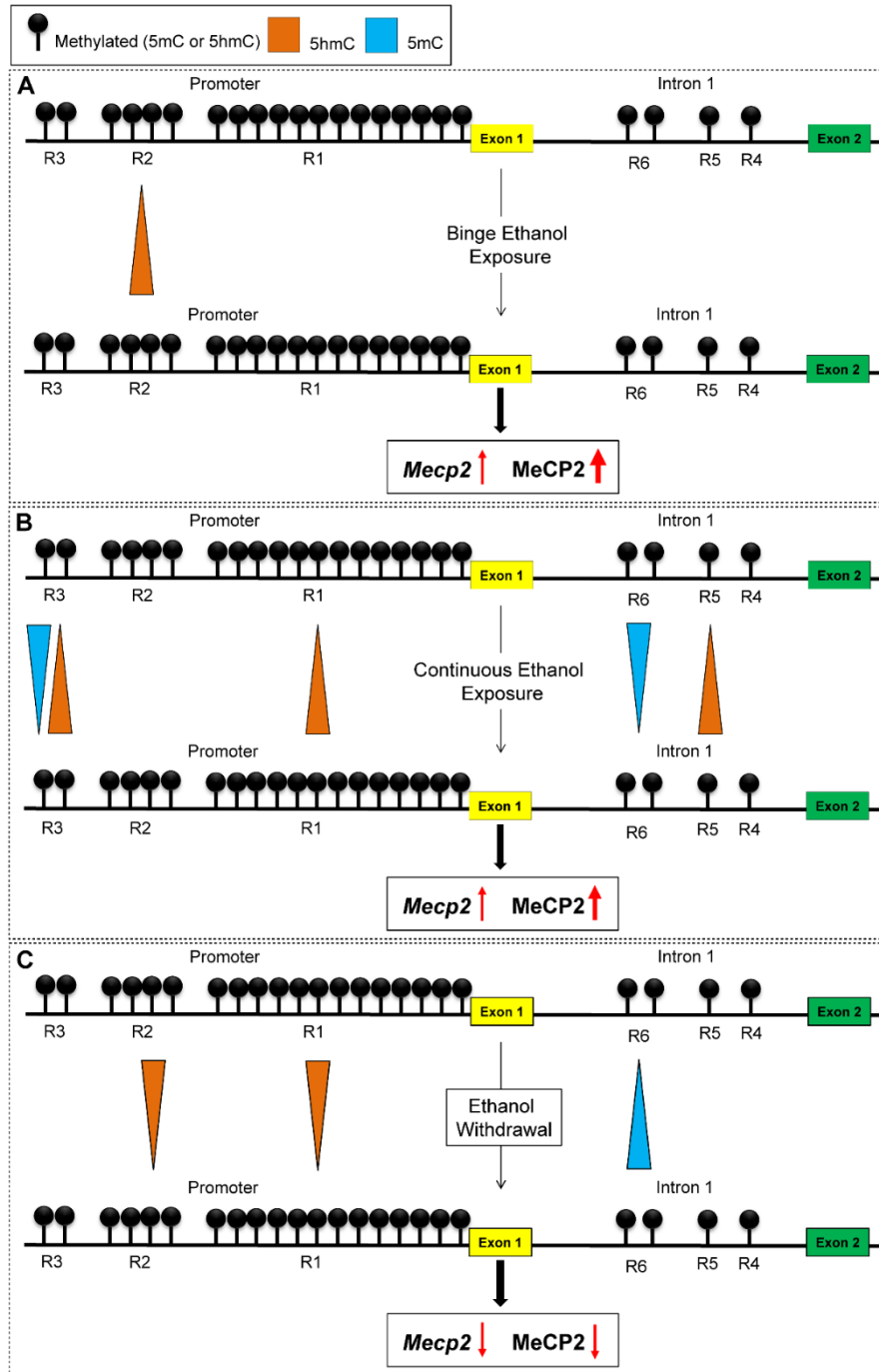
Figure 4.8 Summary of the results on DNA methylation and *Mecp2* expression in response to ethanol exposure and withdrawal during neural stem cells (NSC) differentiation.

The three promoter regions (R1-R3) and three intron 1 regions (R4-R6) within the *Mecp2* gene are shown (not to scale). **A)** Binge Ethanol exposure: increased enrichment of 5hmC at the R2 is associated with increased *Mecp2*/MeCP2. **B)** Continuous ethanol exposure: increased enrichment

of 5hmC at R1, R3, and R5 and decreased 5mC levels at R3 and R6 are associated with increased *Mecp2*/MeCP2. **C)** Ethanol withdrawal: increased enrichment of 5mC R6 and decreased 5hmC enrichment at R1 and R2 are associated with downregulated *Mecp2*/MeCP2.

4.11 Conflict of interest statement

None declared.

4.12 Acknowledgments

4.13 References

1. Liyanage VR, Zachariah RM, Davie JR, Rastegar M (2015) Ethanol deregulates Mecp2/MeCP2 in differentiating neural stem cells via interplay between 5-methylcytosine and 5-hydroxymethylcytosine at the Mecp2 regulatory elements. Exp Neurol 265: 102-117.

2. Zachariah RM, Rastegar M (2012) Linking epigenetics to human disease and Rett syndrome: the emerging novel and challenging concepts in MeCP2 research. Neural Plast 2012: 415825.

3. Stuss DP, Cheema M, Ng MK, Martinez de Paz A, Williamson B, Missiaen K, Cosman JD, McPhee D, Esteller M, et al. (2013) Impaired in vivo binding of MeCP2 to chromatin in the absence of its DNA methyl-binding domain. Nucleic Acids Res 41: 4888-4900.

4. Thambirajah AA, Ng MK, Frehlick LJ, Li A, Serpa JJ, Petrotchenko EV, Silva-Moreno B, Missiaen KK, Borchers CH, et al. (2012) MeCP2 binds to nucleosome free (linker DNA) regions and to H3K9/H3K27 methylated nucleosomes in the brain. Nucleic Acids Res 40: 2884-2897.

5. Ezeonwuka C, Rastegar M (2014) MeCP2-Related Diseases and Animal Models. Diseases 2: 45-70.

6. Feng J, Nestler EJ (2010) MeCP2 and drug addiction. Nat Neurosci 13: 1039-1041.

7. Repunte-Canonigo V, Chen J, Lefebvre C, Kawamura T, Kreifeldt M, Basson O, Roberts AJ, Sanna PP (2014) MeCP2 regulates ethanol sensitivity and intake. Addict Biol 19: 791-799.

8. Liyanage VR, Rastegar M (2014) Rett syndrome and MeCP2. Neuromolecular Med 16: 231-264.

9. Jones KL, Smith DW (1973) Recognition of the fetal alcohol syndrome in early infancy. Lancet 302: 999-1001.

10. Knezovich JG, Ramsay M (2012) The effect of preconception paternal alcohol exposure on epigenetic remodeling of the h19 and rasgrf1 imprinting control regions in mouse offspring. Front Genet 3: 10.

11. Kim P, Choi CS, Park JH, Joo SH, Kim SY, Ko HM, Kim KC, Jeon SJ, Park SH, et al. (2014) Chronic exposure to ethanol of male mice before mating produces attention deficit hyperactivity disorder-like phenotype along with epigenetic dysregulation of dopamine transporter expression in mouse offspring. J Neurosci Res 92: 658-670.

12. Carlson RW, Kumar NN, Wong-Mckinstry E, Ayyagari S, Puri N, Jackson FK, Shashikumar S (2012) Alcohol withdrawal syndrome. Crit Care Clin 28: 549-585.

13. Thomas JD, Riley EP (1998) Fetal alcohol syndrome: does alcohol withdrawal play a role? Alcohol Health Res World 22: 47-53.

14. Pierog S, Chandavasu O, Wexler I (1977) Withdrawal symptoms in infants with the fetal alcohol syndrome. J Pediatr 90: 630-633.

15. Flegel K, MacDonald N, Hebert PC (2011) Binge drinking: all too prevalent and hazardous. CMAJ 183: 411.

16. Zoll B, Huppke P, Wessel A, Bartels I, Laccone F (2004) Fetal alcohol syndrome in association with Rett syndrome. Genet Couns 15: 207-212.

17. Subbanna S, Nagre NN, Shivakumar M, Umapathy NS, Psychoyos D, Basavarajappa BS (2014) Ethanol induced acetylation of histone at G9a exon1 and G9a-mediated histone H3 dimethylation leads to neurodegeneration in neonatal mice. Neuroscience 258: 422-432.

18. Tunc-Ozcan E, Ullmann TM, Shukla PK, Redei EE (2013) Low-dose thyroxine attenuates autism-associated adverse effects of fetal alcohol in male offspring's social behavior and hippocampal gene expression. Alcohol Clin Exp Res 37: 1986-1995.

19. Gangisetty O, Bekdash R, Maglakelidze G, Sarkar DK (2014) Fetal Alcohol Exposure Alters Proopiomelanocortin Gene Expression and Hypothalamic-Pituitary-Adrenal Axis Function via Increasing MeCP2 Expression in the Hypothalamus. PLoS One 9: e113228.

20. Perkins A, Lehmann C, Lawrence RC, Kelly SJ (2013) Alcohol exposure during development: Impact on the epigenome. Int J Dev Neurosci 31: 391-397.

21. Bekdash RA, Zhang C, Sarkar DK (2013) Gestational choline supplementation normalized fetal alcohol-induced alterations in histone modifications, DNA methylation, and proopiomelanocortin (POMC) gene expression in beta-endorphin-producing POMC neurons of the hypothalamus. Alcohol Clin Exp Res 37: 1133-1142.

22. Kim P, Park JH, Choi CS, Choi I, Joo SH, Kim MK, Kim SY, Kim KC, Park SH, et al. (2013) Effects of ethanol exposure during early pregnancy in hyperactive, inattentive and impulsive behaviors and MeCP2 expression in rodent offspring. Neurochem Res 38: 620-631.

23. Chen Y, Ozturk NC, Zhou FC (2013) DNA methylation program in developing hippocampus and its alteration by alcohol. PLoS One 8: e60503.

24. Guo Y, Chen Y, Carreon S, Qiang M (2012) Chronic intermittent ethanol exposure and its removal induce a different miRNA expression pattern in primary cortical neuronal cultures. Alcohol Clin Exp Res 36: 1058-1066.

25. Repunte-Canonigo V, Chen J, Lefebvre C, Kawamura T, Kreifeldt M, Basson O, Roberts AJ, Sanna PP (2013) MeCP2 regulates ethanol sensitivity and intake. Addict Biol 10.1111/adb.12047.

26. Barber BA, Rastegar M (2010) Epigenetic control of Hox genes during neurogenesis, development, and disease. Ann Anat 192: 261-274.

27. Olynik BM, Rastegar M (2012) The genetic and epigenetic journey of embryonic stem cells into mature neural cells. Front Genet 3: 81.

28. Delcuve GP, Rastegar M, Davie JR (2009) Epigenetic control. J Cell Physiol 219: 243-250.

29. Liyanage VRB, Zachariah RM, Delcuve GP, Davie JR, Rastegar M (2012) New Developments in Chromatin Research: An Epigenetic Perspective. In: Simpson NM, Stewart VJ, editors. New Developments in Chromatin Research: Nova Science Publishers pp. 29-58.

30. Liyanage VR, Jarmasz JS, Murugeshan N, Del Bigio MR, Rastegar M, Davie JR (2014) DNA modifications: function and applications in normal and disease States. Biology (Basel) 3: 670-723.

31. Mellen M, Ayata P, Dewell S, Kriaucionis S, Heintz N (2012) MeCP2 binds to 5hmC enriched within active genes and accessible chromatin in the nervous system. Cell 151: 1417-1430.

32. Nagarajan RP, Hogart AR, Gwye Y, Martin MR, LaSalle JM (2006) Reduced MeCP2 expression is frequent in autism frontal cortex and correlates with aberrant MECP2 promoter methylation. Epigenetics 1: e1-11.

33. Franklin TB, Russig H, Weiss IC, Graff J, Linder N, Michalon A, Vizi S, Mansuy IM (2010) Epigenetic transmission of the impact of early stress across generations. Biol Psychiatry 68: 408-415.

34. Liu J, Francke U (2006) Identification of cis-regulatory elements for MECP2 expression. Hum Mol Genet 15: 1769-1782.

35. Liyanage VR, Zachariah RM, Rastegar M (2013) Decitabine alters the expression of Mecp2 isoforms via dynamic DNA methylation at the Mecp2 regulatory elements in neural stem cells. Mol Autism 4: 46.

36. Olson CO, Zachariah RM, Ezeonwuka CD, Liyanage VR, Rastegar M (2014) Brain region-specific expression of MeCP2 isoforms correlates with DNA methylation within Mecp2 regulatory elements. PLoS One 9: e90645.

37. Rastegar M, Hotta A, Pasceri P, Makarem M, Cheung AY, Elliott S, Park KJ, Adachi M, Jones FS, et al. (2009) MECP2 isoform-specific vectors with regulated expression for Rett syndrome gene therapy. PLoS One 4: e6810.

38. Barber BA, Liyanage VR, Zachariah RM, Olson CO, Bailey MA, Rastegar M (2013) Dynamic expression of MEIS1 homeoprotein in E14.5 forebrain and differentiated forebrain-derived neural stem cells. Ann Anat 195: 431-440.

39. Kobrossy L, Rastegar M, Featherstone M (2006) Interplay between chromatin and trans-acting factors regulating the Hoxd4 promoter during neural differentiation. J Biol Chem 281: 25926-25939.

40. Rastegar M, Kobrossy L, Kovacs EN, Rambaldi I, Featherstone M (2004) Sequential histone modifications at Hoxd4 regulatory regions distinguish anterior from posterior embryonic compartments. Mol Cell Biol 24: 8090-8103.

41. Nolte C, Rastegar M, Amores A, Bouchard M, Grote D, Maas R, Kovacs EN, Postlethwait J, Rambaldi I, et al. (2006) Stereospecificity and PAX6 function direct Hoxd4 neural enhancer activity along the antero-posterior axis. Dev Biol 299: 582-593.

42. Kriaucionis S, Bird A (2004) The major form of MeCP2 has a novel N-terminus generated by alternative splicing. Nucleic Acids Res 32: 1818-1823.

43. Schneider L, d'Adda di Fagagna F (2012) Neural stem cells exposed to BrdU lose their global DNA methylation and undergo astrocytic differentiation. Nucleic Acids Res 40: 5332-5342.

44. Zachariah RM, Olson CO, Ezeonwuka C, Rastegar M (2012) Novel MeCP2 isoform-specific antibody reveals the endogenous MeCP2E1 expression in murine brain, primary neurons and astrocytes. PLoS One 7: e49763.

45. Schade A, Delyagina E, Scharfenberg D, Skorska A, Lux C, David R, Steinhoff G (2013) Innovative Strategy for MicroRNA Delivery in Human Mesenchymal Stem Cells via Magnetic Nanoparticles. Int J Mol Sci 14: 10710-10726.

46. Rastegar M, Rousseau GG, Lemaigre FP (2000) CCAAT/enhancer-binding protein-alpha is a component of the growth hormone-regulated network of liver transcription factors. Endocrinology 141: 1686-1692.

47. Wu CH, Rastegar M, Gordon J, Safa AR (2001) beta(2)-microglobulin induces apoptosis in HL-60 human leukemia cell line and its multidrug resistant variants overexpressing MRP1 but lacking Bax or overexpressing P-glycoprotein. Oncogene 20: 7006-7020.

48. MacCallum DE, Hall PA (2000) The location of pKi67 in the outer dense fibrillary compartment of the nucleolus points to a role in ribosome biogenesis during the cell division cycle. J Pathol 190: 537-544.

49. Gerdes J, Lemke H, Baisch H, Wacker HH, Schwab U, Stein H (1984) Cell cycle analysis of a cell proliferation-associated human nuclear antigen defined by the monoclonal antibody Ki-67. J Immunol 133: 1710-1715.

50. Cai J, Chen Y, Cai WH, Hurlock EC, Wu H, Kernie SG, Parada LF, Lu QR (2007) A crucial role for Olig2 in white matter astrocyte development. Development 134: 1887-1899.

51. Yokoo H, Nobusawa S, Takebayashi H, Ikenaka K, Isoda K, Kamiya M, Sasaki A, Hirato J, Nakazato Y (2004) Anti-human Olig2 antibody as a useful immunohistochemical marker of normal oligodendrocytes and gliomas. The American journal of pathology 164: 1717-1725.

52. Setoguchi T, Kondo T (2004) Nuclear export of OLIG2 in neural stem cells is essential for ciliary neurotrophic factor-induced astrocyte differentiation. J Cell Biol 166: 963-968.

53. Miyake K, Nagai K (2007) Phosphorylation of methyl-CpG binding protein 2 (MeCP2) regulates the intracellular localization during neuronal cell differentiation. Neurochem Int 50: 264-270.

54. Hayashi S, Mikami T, Murai Y, Takano Y, Imura J (2014) Alpha-tubulin nuclear overexpression is an indicator of poor prognosis in patients with non-Hodgkin's lymphoma. Int J Mol Med 34: 483-490.

55. Goo YH, Sohn YC, Kim DH, Kim SW, Kang MJ, Jung DJ, Kwak E, Barlev NA, Berger SL, et al. (2003) Activating signal cointegrator 2 belongs to a novel steady-state complex that contains a subset of trithorax group proteins. Mol Cell Biol 23: 140-149.

56. Adachi J, Mizoi Y, Fukunaga T, Ogawa Y, Ueno Y, Imamichi H (1991) Degrees of alcohol intoxication in 117 hospitalized cases. J Stud Alcohol 52: 448-453.

57. Vangipuram SD, Lyman WD (2012) Ethanol affects differentiation-related pathways and suppresses Wnt signaling protein expression in human neural stem cells. Alcohol Clin Exp Res 36: 788-797.

58. Hicks SD, Middleton FA, Miller MW (2010) Ethanol-induced methylation of cell cycle genes in neural stem cells. J Neurochem 114: 1767-1780.

59. Zhou FC, Balaraman Y, Teng M, Liu Y, Singh RP, Nephew KP (2011) Alcohol alters DNA methylation patterns and inhibits neural stem cell differentiation. Alcohol Clin Exp Res 35: 735-746.

60. Pappalardo-Carter DL, Balaraman S, Sathyan P, Carter ES, Chen WJ, Miranda RC (2013) Suppression and Epigenetic Regulation of MiR-9 Contributes to Ethanol Teratology: Evidence from Zebrafish and Murine Fetal Neural Stem Cell Models. Alcohol Clin Exp Res 10.1111/acer.12139.

61. Collins AL, Levenson JM, Vilaythong AP, Richman R, Armstrong DL, Noebels JL, David Sweatt J, Zoghbi HY (2004) Mild overexpression of MeCP2 causes a progressive neurological disorder in mice. Hum Mol Genet 13: 2679-2689.

62. Bodda C, Tantra M, Mollajew R, Arunachalam JP, Laccone FA, Can K, Rosenberger A, Mironov SL, Ehrenreich H, et al. (2013) Mild Overexpression of Mecp2 in Mice Causes a Higher Susceptibility toward Seizures. Am J Pathol 183: 195-210.

63. Barker JM, Zhang Y, Wang F, Taylor JR, Zhang H (2013) Ethanol-induced Htr3a promoter methylation changes in mouse blood and brain. Alcohol Clin Exp Res 37 Suppl 1: E101-107.

64. Bleich S, Lenz B, Ziegenbein M, Beutler S, Frieling H, Kornhuber J, Bonsch D (2006) Epigenetic DNA hypermethylation of the HERP gene promoter induces down-regulation of its mRNA expression in patients with alcohol dependence. Alcohol Clin Exp Res 30: 587-591.

65. Huang Y, Pastor WA, Shen Y, Tahiliani M, Liu DR, Rao A (2010) The behaviour of 5-hydroxymethylcytosine in bisulfite sequencing. PLOS ONE 5: e8888.

66. Velez-Bermudez IC, Schmidt W (2014) The conundrum of discordant protein and mRNA expression. Are plants special? Front Plant Sci 5: 619.

67. Riley EP, McGee CL (2005) Fetal alcohol spectrum disorders: an overview with emphasis on changes in brain and behavior. Exp Biol Med (Maywood) 230: 357-365.

68. Samson HH, Grant KA (1984) Ethanol-induced microcephaly in neonatal rats: relation to dose. Alcohol Clin Exp Res 8: 201-203.

69. Rodriguez JJ, Terzieva S, Olabarria M, Lanza RG, Verkhratsky A (2013) Enriched environment and physical activity reverse astrogliodegeneration in the hippocampus of AD transgenic mice. Cell Death Dis 4: e678.

70. Kulijewicz-Nawrot M, Verkhratsky A, Chvatal A, Sykova E, Rodriguez JJ (2012) Astrocytic cytoskeletal atrophy in the medial prefrontal cortex of a triple transgenic mouse model of Alzheimer's disease. J Anat 221: 252-262.

71. Calabrese JM, Sun W, Song L, Mugford JW, Williams L, Yee D, Starmer J, Mieczkowski P, Crawford GE, et al. (2012) Site-specific silencing of regulatory elements as a mechanism of X inactivation. Cell 151: 951-963.

72. Haffner MC, Chaux A, Meeker AK, Esopi DM, Gerber J, Pellakuru LG, Toubaji A, Argani P, Iacobuzio-Donahue C, et al. (2011) Global 5-hydroxymethylcytosine content is significantly reduced in tissue stem/progenitor cell compartments and in human cancers. Oncotarget 2: 627-637.

73. James SJ, Shpyleva S, Melnyk S, Pavliv O, Pogribny IP (2014) Elevated 5-hydroxymethylcytosine in the Engrailed-2 (EN-2) promoter is associated with increased gene expression and decreased MeCP2 binding in autism cerebellum. Transl Psychiatry 4: e460.

74. Zhou FC, Chen Y, Love A (2011) Cellular DNA methylation program during neurulation and its alteration by alcohol exposure. Birth Defects Res A Clin Mol Teratol 91: 703-715.

75. Stevens SA, Nash K, Koren G, Rovet J (2012) Autism characteristics in children with fetal alcohol spectrum disorders. Child Neuropsychol 10.1080/09297049.2012.727791.

76. Bishop S, Gahagan S, Lord C (2007) Re-examining the core features of autism: a comparison of autism spectrum disorder and fetal alcohol spectrum disorder. J Child Psychol Psychiatry 48: 1111-1121.

77. Maliszewska-Cyna E, Bawa D, Eubanks JH (2010) Diminished prevalence but preserved synaptic distribution of N-methyl-D-aspartate receptor subunits in the methyl CpG binding protein 2(MeCP2)-null mouse brain. Neuroscience 168: 624-632.

78. Moykkynen T, Korpi ER (2012) Acute effects of ethanol on glutamate receptors. Basic Clin Pharmacol Toxicol 111: 4-13.

79. Bingham SM, Mudd LM, Lopez TF, Montague JR (2004) Effects of ethanol on cultured embryonic neurons from the cerebral cortex of the rat. Alcohol 32: 129-135.

80. Guerri C, Pascual M, Renau-Piqueras J (2001) Glia and fetal alcohol syndrome. Neurotoxicology 22: 593-599.

81. Valles S, Sancho‐Tello M, Minana R, Climent E, Renau‐Piqueras J, Guerri C (1996) Glial fibrillary acidic protein expression in rat brain and in radial glia culture is delayed by prenatal ethanol exposure. Journal of neurochemistry 67: 2425-2433.

82. Guizzetti M, Costa LG (1996) Inhibition of muscarinic receptor‐stimulated glial cell proliferation by ethanol. Journal of neurochemistry 67: 2236-2245.

83. Guerri C, Pascual Ma, Renau-Piqueras J (2001) Glia and fetal alcohol syndrome. Neurotoxicology 22: 593-599.

84. Miller MW, Potempa G (1990) Numbers of neurons and glia in mature rat somatosensory cortex: effects of prenatal exposure to ethanol. J Comp Neurol 293: 92-102.

85. Zou J, Rabin RA, Pentney RJ (1993) Ethanol enhances neurite outgrowth in primary cultures of rat cerebellar macroneurons. Brain Res Dev Brain Res 72: 75-84.

86. Reiter-Funk CK, Dohrman DP (2005) Chronic ethanol exposure increases microtubule content in PC12 cells. BMC Neurosci 6: 16.

87. Roivainen R, Hundle B, Messing RO (1995) Ethanol enhances growth factor activation of mitogen-activated protein kinases by a protein kinase C-dependent mechanism. Proc Natl Acad Sci U S A 92: 1891-1895.

88. Larimore JL, Chapleau CA, Kudo S, Theibert A, Percy AK, Pozzo-Miller L (2009) Bdnf overexpression in hippocampal neurons prevents dendritic atrophy caused by Rett-associated MECP2 mutations. Neurobiol Dis 34: 199-211.

89. Camarillo C, Miranda RC (2008) Ethanol exposure during neurogenesis induces persistent effects on neural maturation: evidence from an ex vivo model of fetal cerebral cortical neuroepithelial progenitor maturation. Gene Expr 14: 159-171.

90. Wang IT, Reyes AR, Zhou Z (2013) Neuronal morphology in MeCP2 mouse models is intrinsically variable and depends on age, cell type, and Mecp2 mutation. Neurobiol Dis 58: 3-12.

91. Nguyen MV, Du F, Felice CA, Shan X, Nigam A, Mandel G, Robinson JK, Ballas N (2012) MeCP2 is critical for maintaining mature neuronal networks and global brain anatomy during late stages of postnatal brain development and in the mature adult brain. J Neurosci 32: 10021-10034.

92. Maezawa I, Swanberg S, Harvey D, LaSalle JM, Jin LW (2009) Rett syndrome astrocytes are abnormal and spread MeCP2 deficiency through gap junctions. J Neurosci 29: 5051-5061.

93. Ushikoshi H, Takahashi T, Chen X, Khai NC, Esaki M, Goto K, Takemura G, Maruyama R, Minatoguchi S, et al. (2005) Local overexpression of HB-EGF exacerbates remodeling following myocardial infarction by activating noncardiomyocytes. Lab Invest 85: 862-873.

94. Giordano G, Guizzetti M, Dao K, Mattison HA, Costa LG (2011) Ethanol impairs muscarinic receptor-induced neuritogenesis in rat hippocampal slices: Role of astrocytes and extracellular matrix proteins. Biochem Pharmacol 82: 1792-1799.

95. Ballas N, Lioy DT, Grunseich C, Mandel G (2009) Non-cell autonomous influence of MeCP2-deficient glia on neuronal dendritic morphology. Nat Neurosci 12: 311-317.

96. Messing RO, Henteleff M, Park JJ (1991) Ethanol enhances growth factor-induced neurite formation in PC12 cells. Brain Res 565: 301-311.

97. Roivainen R, Hundle B, Messing RO (1995) Ethanol enhances growth factor activation of mitogen-activated protein kinases by a protein kinase C-dependent mechanism. Proceedings of the National Academy of Sciences 92: 1891-1895.

98. Kim JH, Sung DK, Park CW, Park HH, Park C, Jeon SH, Kang PD, Kwon OY, Lee BH (2005) Brain-derived neurotrophic factor promotes neurite growth and survival of antennal lobe neurons in brain from the silk moth, Bombyx mori in vitro. Zoolog Sci 22: 333-342.

4.14 Supplementary information
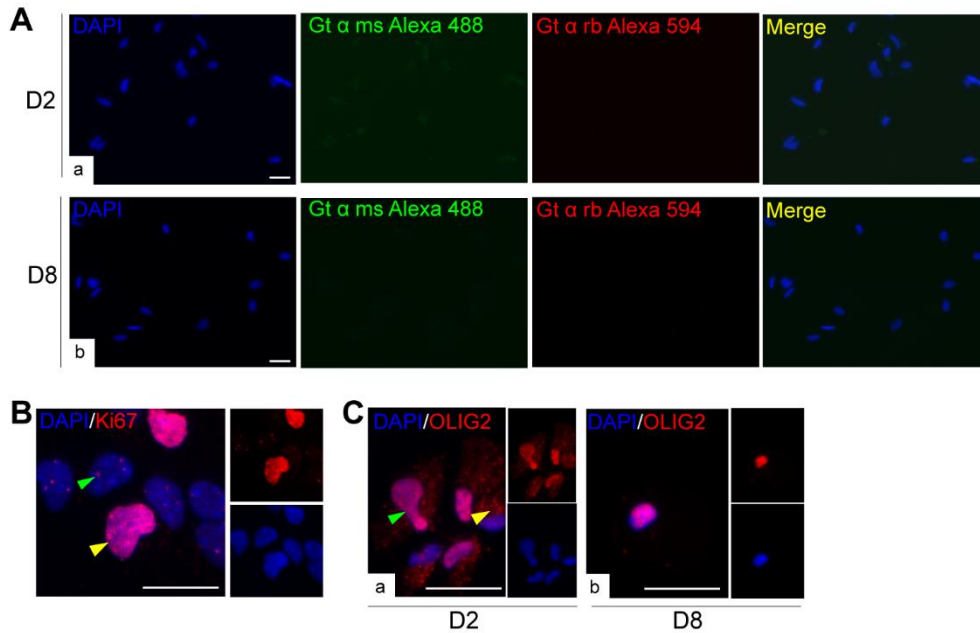
Figure 4.S1 Negative controls for immunocytochemistry and different staining patterns of Ki67 and OLIG2.

A) Primary omission negative controls for the two secondary antibodies used in this study. Secondary antibodies are Goat (Gt) anti (α) mouse (ms) Alexa 488 (green) and Gt α rabbit (Rb) Alexa 594 (red) at (**a**) Day (D) 2 and (**b**) D8. Scale bars represent 20 µm. **B)** Two different localization patterns of Ki67 discussed in the text are shown, green arrow: nucleoli and yellow arrow: diffused. **C)** Two localization patterns of OLIG2, (**a**) nucleo-cytoplasmic (green arrow: nuclear and yellow arrow: cytoplasmic) majorly seen in D2 population; (**b**) nuclear which is mainly seen in D8 cells. Scale bars represent 20 µm.
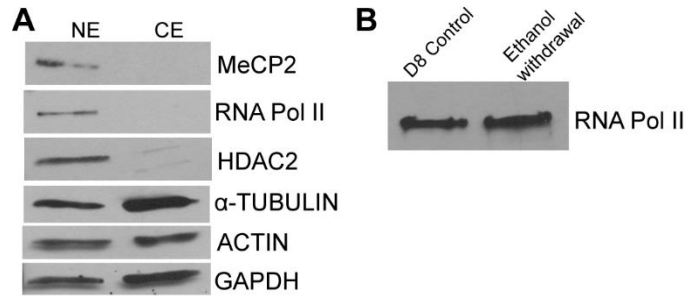
Figure 4.S2 Comparison of MeCP2 detection in the nuclear and cytoplasmic protein extracts to select the best loading controls for the nuclear extracts.

A) Western blot experiments with nuclear extracts (NE) and cytoplasmic extracts (CE) from day (D) 8 control cells. The membrane was re-probed with antibodies specific for MeCP2, nuclear markers RNA Pol II and HDAC2, cytoplasmic marker α-TUBULIN (also known to be present in the nucleus), as well as ACTIN and GAPDH, which are detected in both nucleus and cytoplasm. **B)** Detection of RNA Pol II in D8 control and ethanol-withdrawal samples. The membrane is a re-probe of the same membrane used in Figure 4.2D. Therefore, for the ACTIN loading control refer to Figure 4.2D.
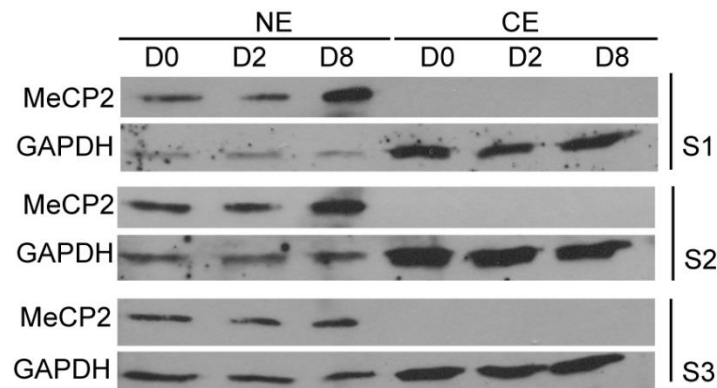
Figure 4.S3 Comparison of MeCP2 detection in the nuclear and cytoplasmic protein extracts during neural stem cell differentiation.

Western blot experiments with nuclear extracts (NE) and cytoplasmic extracts (CE) from day (D) 0 (undifferentiated), D2 (early differentiation stage) and D8 (late differentiation stage) are shown. Membranes were re-probed with antibodies specific for MeCP2, nuclear marker HDAC2 and endogenous loading control GAPDH. S= Set (refers to biological replicates).
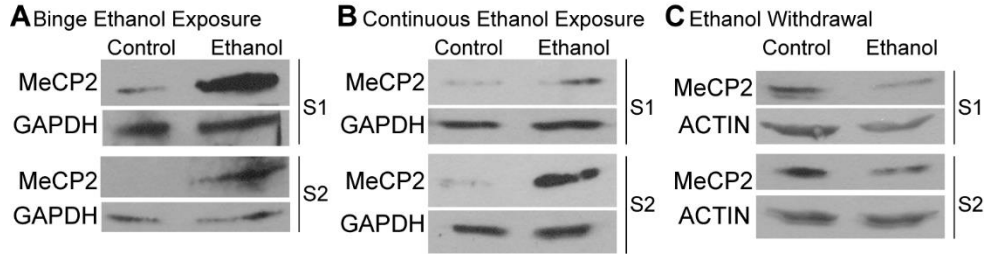
Figure 4.S4 Biological replicates of the Western blot experiments for MeCP2 detection in control and ethanol-treated conditions.

A) Binge ethanol exposure; **B)** Continuous ethanol exposure and **C)** Ethanol withdrawal. S= Set (refers to biological replicates). GAPDH and ACTIN are used as endogenous loading controls. Note that exposure time for each Western blot is different.
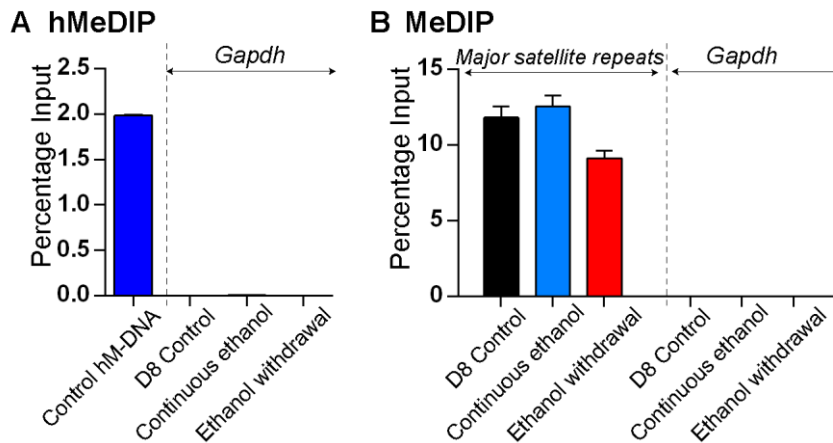
Figure 4.S5 Controls for hMeDIP and MeDIP experiments.

A) Controls for hMeDIP experiments. Enrichment of 5hmC is shown at the positive control DNA (contains 44 5hmC CpGs) and absence of amplification at the *Gapdh* coding region (unmethylated negative control) in day (D) 8 control and ethanol-treated samples. **B)** Controls for MeDIP experiments. Enrichment of 5mC is shown at the *Major Satellite Repeats* as the positive control and absence of amplification at the *Gapdh* coding region (unmethylated negative control) in D8 control and ethanol-treated samples. Data from 2 independent experiments, $N = 2 \pm SEM$.
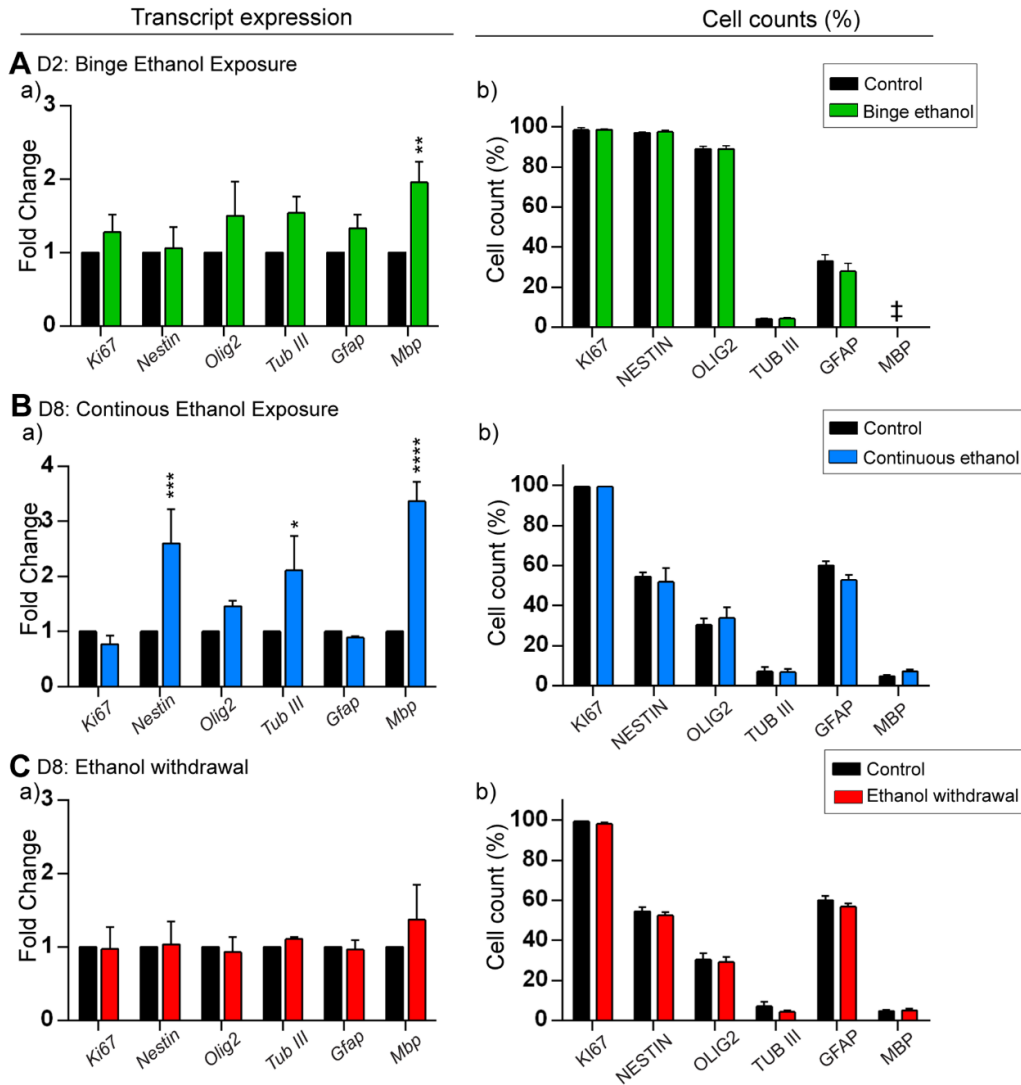
Figure 4.S6 The effect of ethanol on cell populations of differentiating neural stem cells (NSC).

A) Day (D) 2 control and binge ethanol-treated cells, **B)** D8 control and continuous ethanol-treated cells, and **C)** D8 control and ethanol withdrawal cells. Left panel: Transcript detection of cell type-specific markers. Right panel: Cell counts are shown as percentages. The markers are specific for proliferating cells (*Ki67*/Ki67); neural stem/progenitor cells (*Nestin*/NESTIN) and glial/oligodendrocyte progenitors (*Olig2*/OLIG2); neurons (*Tub III*/TUB III); astrocytes (*Gfap*/GFAP) and oligodendrocytes (*Mbp*/MBP) by qRT-PCR (**a**) and immunocytochemistry (**b**). Fold changes are calculated relative to the expression levels in untreated controls. N = 3 ± SEM. ‡ indicates that no positive cells were detected.

Figure 4.S7 Nucleotide and amino acid sequence alignments of Myelin basic protein (MBP). A) (**a**) Nucleotide sequence (mRNA) alignment of the four *Mbp* isoforms (1, 2, 3 and 5) and the forward and reverse primers used in qRT-PCR experiments. The sequence amplified by the primers is shown in red. (**b**) The melt curve generated after qRT-PCR shows a single peak in the reaction indicating that only one single band was amplified with the templates and with no amplification in the negative control sample (no template control). **B)** Amino acid sequence alignment of the four MBP isoforms (1, 2, 3 and 5) is shown. Amino acids corresponding to the mRNA sequence recognized by the RT-PCR primers are shown in red. The C-terminal amino acid sequence used to generate the MBP antibody is underlined. The mRNA and amino acid RefSeq numbers for each *Mbp*/MBP isoform are shown in the table. Multiple sequence alignment was performed using CLUSTAL O (1.2.1).

CHAPTER 5. CELL TYPE-SPECIFIC REGULATION OF MURINE *MECP2E1* AND *MECP2E2*

5.1 Foreword

In Chapters 3 and 4, I presented evidence on the impact of DNA methylation at the *Mecp2* REs and hence its potential role in regulating the expression of *Mecp2e1* and *Mecp2e2* transcripts in differentiating NSC. The data presented in those chapters, as well as other studies (reviewed in [1]), suggest a potential cell type-specific regulation of *Mecp2*/MeCP2 expression and the possibility of the involvement of DNA methylation in this regulation. The third aim of my thesis was to investigate cell type-specific regulation of *Mecp2e1* and *Mecp2e2* transcripts in two major brain cell types; neurons, and astrocytes. The data presented in this chapter addresses aim 3. This chapter is written as a manuscript in progress (work-in-progress) to maintain consistency as a sandwich-type thesis. However, some of the data must be validated by further experiments before publication. This study has been conducted in collaboration with the Rastegar lab members. I have contributed to the majority of the work, which includes performing experiments, data collection, analyses, and interpretation.

Vichithra R. B. Liyanage: Conceived and designed experiments; assistance with cell culture and culture maintenance; sample collection, RNA extraction from female neurons and astrocytes; DNase treatment of trizol-extracted RNA samples collected by Carl Olson; cDNA synthesis and qRT-PCR; molecular identification of male/female cells by PCR, qRT-PCR and agarose gel electrophoresis; data collection, analysis and interpretation including bisulfite pyrosequencing DNA methylation results, correlation analysis between DNA methylation and *Mecp2* expression; preparation of figures and writing.

<u>Robby M. Zachariah:</u> Designed experiments, isolation and culture of primary neurons and astrocytes and sample collections.

<u>Carl Olson:</u> Designed experiments; harvest, sex-separation, and imaging of sex-specific embryos; embryonic forebrain dissections; RNA and DNA extraction from male neurons and astrocytes.

<u>Dr. Mojgan Rastegar:</u> Conceived and designed experiments; isolation and culture of primary male and female neurons and astrocytes, and sample collections; provided research support; contributed reagents/materials/analysis tools; data analyses and interpretation.

Note that the abbreviations used in this chapter have been introduced in previous chapters.

5.2 Abstract

MeCP2 isoforms, MeCP2E1 and MeCP2E2 function as epigenetic regulators in the brain. Expression and functional deficits of MeCP2 are the primary causes of several neurodevelopmental disorders that include RTT, MDS and ASD. Studies have demonstrated the consequences of the loss- and overexpression of *Mecp2/MECP2* in different brain cell types such as neurons and glia. However, the understanding of the mechanisms regulating *Mecp2*/MeCP2 isoform-specific expression in these cell types remains largely elusive. The primary objective of the current study is to characterize sex- and cell type-specific expression of *Mecp2e1* and *Mecp2e2* transcripts in neurons and astrocytes, and investigate the potential role of DNA methylation in *Mecp2* regulation. Previously, we reported six REs in the promoter (R1-R3) and intron 1 silencer element (R4-R6) of *Mecp2*, methylation at these sites affects the expression of *Mecp2* in embryonic NSC and the adult mouse brain. Here, we observed the existence of cell type- and sex-specific expression patterns of *Mecp2e1* and *Mecp2e2* transcripts in neurons and astrocytes. Transcripts of both *Mecp2e1* and *Mecp2e2* were highly expressed in male neurons compared to

male astrocytes. In male neurons, *Mecp2e1* transcript levels were higher than *Mecp2e2*. The higher DNA methylation at three REs (R1, R2, and R6) was associated with lower transcript levels of *Mecp2e1* and *Mecp2e2* in male astrocytes compared to male neurons. Correlation analyses between DNA methylation and transcript levels of *Mecp2e1* and *Mecp2e2* suggested that regulation of *Mecp2* in neurons was complex. Our data fill a significant knowledge gap in the MeCP2 field in terms of sex- and cell type-specific expression of *Mecp2e1* and *Mecp2e2* transcripts and their regulation by DNA methylation.

5.3 Introduction

The X-linked *MECP2/Mecp2* gene encodes for MeCP2 protein which has two isoforms, MeCP2E1 and MeCP2E2. MeCP2 is a major transcriptional regulator in the brain (reviewed in [2]). Altered expression and disrupted functions of *MECP2/Mecp2/*MeCP2 have been linked to RTT [3,4], MDS [5-7], ASD [8,9], and FASD (reviewed in [10]). RTT and MDS are predominantly found in female and male patients, respectively, which is generally referred to as a 'sex-bias' [11]. Such sex bias's may occur because *MECP2* gene is X-linked [12] and the nature of XCI [13]. Despite the extensive research done to identify therapeutic strategies, there is currently no cure for these disorders. Restoring normal levels of MeCP2 could be a potential therapeutic approach. A thorough understanding of the regulation of *Mecp2*/MeCP2 expression is essential to achieve the goal of rescuing deficits in MeCP2 expression. Therefore, investigation of the transcriptional profiles of *Mecp2e1* and *Mecp2e2* transcripts in all neural cell types and the mechanisms by which their expression are regulated in these cell types is important. The current study aims to address this knowledge gap and focuses on *Mecp2* regulation in two major brain cell types; neurons and astrocytes.

Research on MeCP2 expression and functions has been mostly focused in neurons, primarily due to the belief that symptoms associated with the loss-of-*Mecp2* are of neuronal origin [1,2]. However, the discovery of MeCP2 expression in glia, and subsequent studies highlighting the functional consequences of glial *Mecp2*-loss, especially on neuronal phenotypes, caused a paradigm shift in the MeCP2 field [14-16]. Restoration of *Mecp2* expression in neurons, astrocytes, and microglia can rescue the RTT phenotypes in mouse models and *in vitro* cell models [17-20]. While the cell type-specific role of MeCP2 in MDS is unknown, one study showed that elevated *MECP2* levels in neurons might contribute to the neuropsychiatric and cognitive abnormalities seen in MDS patients [21]. For these reasons, the mechanisms by which *MECP2/Mecp2* expression is regulated in different brain cell types should be investigated to ensure accurate modulation of its expression in assisting future therapeutic approaches. We and others have shown that *Mecp2*/MeCP2 and MeCP2E1 expression is higher in neurons as compared to astrocytes [22,23]. This observation led to the hypothesis that *Mecp2e1* and *Mecp2e2* transcripts could be differentially regulated in different brain cell types. Here we studied cell type-specific expression of *Mecp2e1* and *Mecp2e2* transcripts in primary neurons and astrocytes isolated from E18 mouse brain, in a sex-specific manner.

XCI occurs in females to achieve dosage compensation of gene expression between males and females [24]. However, some X-linked genes do escape XCI, and thus expression levels are higher in females compared to males [13,25]. *MECP2/Mecp2* shows bi-allelic expression due to XCI escape in muscle fibroblast cultures [26], suggesting the possibility that *Mecp2* transcript expression may be different based on sex. According to previous studies on other genes that undergo XCI escape [27,28], it is possible that transcriptional, epigenetic and/or post-

transcriptional mechanisms may drive sex-specific expression of *Mecp2e1* and *Mecp2e2* transcripts.

Hyper- and hypomethylation of the *MECP2* promoter has been detected in ASD patients with reduced *MECP2* [8,9], and a rare case of RTT with increased *MECP2* [29], respectively. We have identified six REs in the *Mecp2* promoter (R1-R3) and intron 1 silencer element (R4-R6) that potentially regulate transcription of *Mecp2* by DNA methylation [30] under normal and decitabine- or alcohol-treated conditions in differentiating NSC [30,31]. Our studies also suggested that the methylation at the *Mecp2* intron 1 silencer REs may impact *Mecp2* splicing [30], which is supported by the concept of DNA methylation- and CTCF binding-mediated co-transcriptional splicing [32,33]. DNA methylation at the same REs correlated with the transcript levels of *Mecp2e1* and *Mecp2e2* in different adult mouse brain regions [34]. Correlation analyses of DNA methylation and *Mecp2* expression in our studies suggested that DNA methylation might be important in the regulation of the transcript levels of *Mecp2e1* and *Mecp2e2* in different cell types, implicating the role of DNA methylation in *Mecp2* transcriptional regulation [30,34]. Here we studied the DNA methylation status of the six *Mecp2* REs in male neurons and astrocytes. While understanding of *Mecp2* regulation in brain cell types of both sexes is equally important, this study focused on male neurons and astrocytes.

5.4 Materials and Methods

5.4.1 Ethics

All experiments were performed in agreement with the standards of the Canadian Council on animal care with the approval of the office of research ethics at the University of Manitoba. All

Chapter 5. Aim 3

experimental procedures were reviewed and approved (protocol number 12-031/1/2) by the University of Manitoba Bannatyne Campus protocol management and review committee.

5.4.2 Biological and technical replicates

All experiments were performed in primary cortical neurons or astrocytes isolated from 2-3 separate pregnant mothers, considered as biological replicates [22,30,31,34,35]. The definition of biological and technical replicates was adopted as discussed in Chapter 2 (Section 2.1). For transcript analyses, 3 biological replicates were used for male neurons, female neurons, and female astrocytes. Only 2 biological replicates were available for female neurons.

5.4.3 Primary culture of neurons and astrocytes

Primary neurons and astrocytes from the cortex of E18 CD-1 mice were cultured as previously described [19,22,35]. Embryos were separated based on their sex. Neurons and astrocytes were collected after eight and 15 days in culture, respectively. A detailed protocol is provided in Chapter 2 (sections 2.6, 2.7 and 2.8).

5.4.4 Culture and identification of sex-specific neurons and astrocytes

Genomic DNA was extracted from neurons and astrocytes using the DNeasy blood and tissue kit (Qiagen) as described in Chapter 2 (Section 2.14.2). Semi-quantitative PCR-based amplification of *Sry* was carried out as described previously [36] to identify and confirm that cells were male in origin. *Il3* is detected in both sexes and was used as an internal control for PCR amplification. PCR products were identified based on their size [*Sry:* 402 bp, and *Il3*: 544 bp]. RNA was extracted from male and female cells using the trizol extraction method (Life

Technologies) and the mirVana RNA extraction kit (Thermo Scientific), respectively. Detailed

experimental steps are outlined in Chapter 2 (Section 2.11.1). Quantitative RT-PCR for the *Xist*

gene was done as previously described [30,37] to confirm that cells were indeed of female origin.

Further details can be found in Chapter 2 (Section 2.8.2.2).

5.4.5 Quantitative RT-PCR

RNA that was converted to cDNA and analyzed by qRT-PCR using previously established

protocols [30,34]. Gene expression was calculated relative to that of the housekeeping gene

Gapdh. The extended protocol can be found in Chapter 2 (section 2.11).

5.4.6 DNA *methylation analysis by bisulfite pyrosequencing*

Bisulfite pyrosequencing was performed for the six *Mecp2* REs as reported previously

[30,31,34] by the Hospital for Sick Children, Toronto, Canada as described in Chapter 2 (Section

2.14) and Chapters 3 and 4.

5.4.7 Statistical analyses

All graphs represent the average of 3 independent experiments (N=3) and error bars indicate

SEM unless otherwise specified. For N=3 samples, statistical significance was determined at

****P <0.0001, ***P <0.001, **P <0.01 or *P <0.05. There are no error bars for female neurons

as there were only 2 biological replicates. For graphs representing qRT-PCR data, data points show

all technical replicates as follows; male neurons [Biological replicates (N)=3, technical replicates

(n)=12, male astrocytes (N=3, n=12), female neurons (N=2, n=12) and female astrocytes (N=3,

n=6). Refer to Chapter 2 (section 2.16) for more detail. Pearson's correlation analysis and linear

regression were done between DNA methylation and levels of the *Mecp2e1* and *Mecp2e2* transcripts as previously reported in differentiating NSC and adult mouse brain regions [30,34]. Statistical significance was determined at *P* <0.05. Refer to Chapter 2 (Section 2.14.4) for more detail.

5.5 Results

5.5.1 Culturing sex-specific neurons and astrocytes

As our first aim was to characterize cell type-specific *Mecp2* expression patterns in a sex-specific manner, we isolated and cultured male and female primary embryonic cortical neurons and astrocytes. This was carried out by slightly modifying our previously established protocols for mixed cultures of neurons and astrocytes [19,22,35]. The separation and confirmation of the sex of mice from which the cells were derived were performed based on three techniques. First, we separated the male and female embryos based on the visual observation of testis in male mouse embryos and fallopian tubes and ovaries in female mouse embryos, respectively **(Figure 5.1A)**. The second and third techniques involved molecular identification and confirmation of the sex of the cultured cells as previously reported [30]. Isolated neurons and astrocytes were characterized using qRT-PCR-based detection of *Xist* gene expression; *Xist* transcripts are female-specific [24]. As expected, *Xist* transcripts were exclusively detected in female cells **(Figure 5.1B)**. Multiplex PCR-based detection of *Il3/Sry* genes, with both *Il3-* and *Sry*-specific primers being included in the reaction, was used to distinguish male neurons further. *Sry* detection is male-specific [38] whereas *Il3* is expressed in both sexes. [39]. Male neurons and astrocytes showed both *Sry* and *Il3*, thereby confirming the male origin of these cells **(Figure 5.1C)**.

A Visual examination

B *Xist* gene expression

C *Il3/Sry* detection
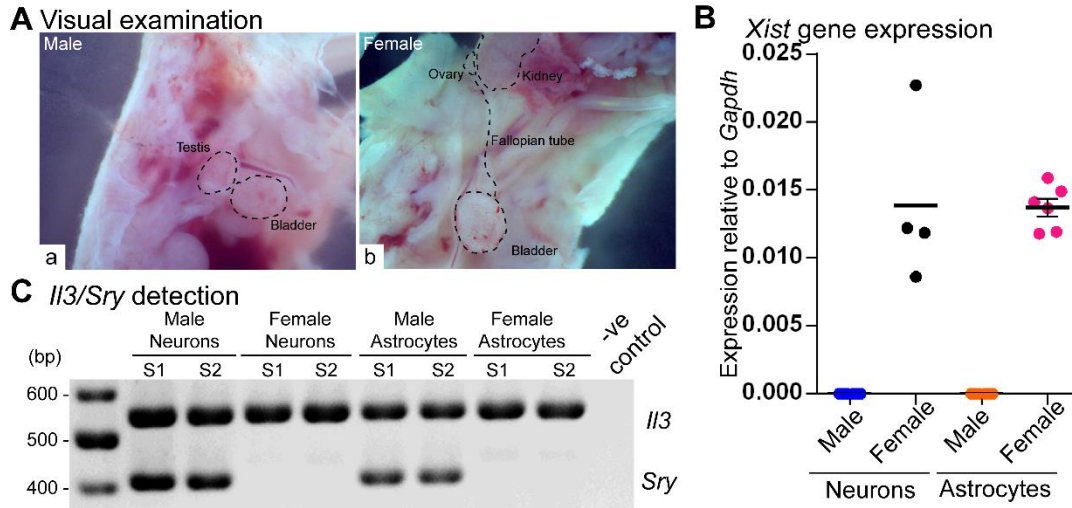
Figure 5.1 Confirmation of sex-specificity of embryos, cultured neurons, and astrocytes.

A) Separation of male (**a**) and female (**b**) embryos based on visual observation of testes and ovaries, respectively. Figure 5.1A is courtesy of Carl Olson from our lab. **B)** Confirmation of sex-specific origin of cultured neurons and astrocytes by detection of female-specific *Xist* gene expression. For male neurons and astrocytes and female astrocytes N=3; female neurons N=2. Error bars represent SEM. Individual data points represent both biological (N) and technical replicates (n) as follows; male neurons [N=3, n=6, male astrocytes (N=3, n=6), female neurons (N=2, n=4) and female astrocytes (N=3, n=6). **C)** *Il3/Sry*-based confirmation of male and female cells. PCR product sizes are 402 bp for *Sry*, and 544 bp for *Il3*.

5.5.2 Mecp2e1 and Mecp2e2 transcripts show cell type- and sex-specific expression in neurons and astrocytes

Mecp2/MeCP2 displays cell type-specific expression patterns in the brain [19,22,23]. *Mecp2* is an X-linked gene that escapes XCI and shows bi-allelic expression as early as the 2-cell stage of mouse embryonic development [40], and consequently, its expression levels are likely to be sex-dependent. Therefore, we first determined *Mecp2e1* and *Mecp2e2* transcript levels in male

neurons and astrocytes and compared them to those determined for female neurons and astrocytes (**Figure 5.2**).
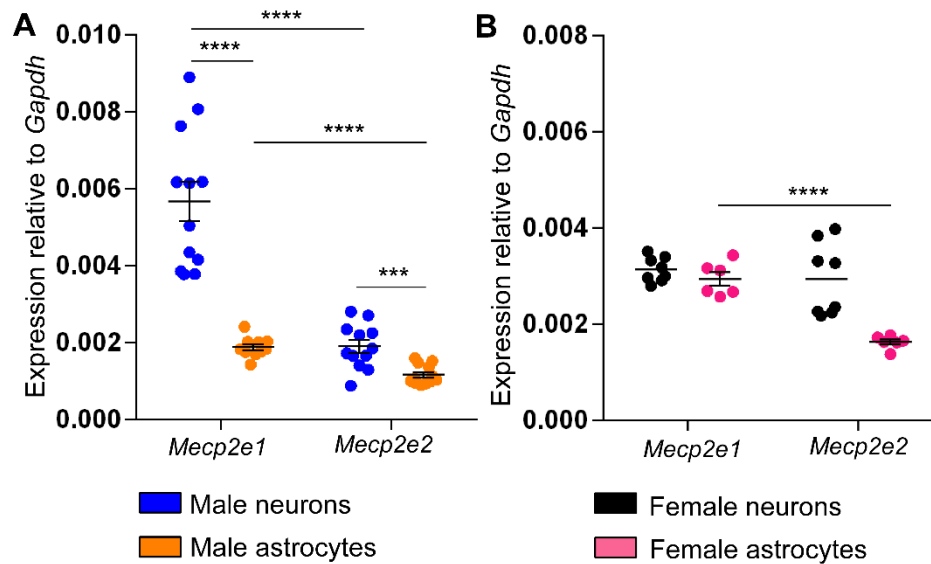
Figure 5.2 Cell type- and sex-specific expression of *Mecp2e1* and *Mecp2e2* transcripts in mouse embryonic neurons and astrocytes.

A) *Mecp2* transcript expression in male neurons and astrocytes. **B)** *Mecp2* transcript expression in female neurons and astrocytes. For male neurons, male astrocytes, and female astrocytes, N=3. Error bars represent SEM. For female neurons N=2. Significant differences are indicated with ****$P <0.0001$, ***$P <0.001$ for samples with N=3. The transcript expression values were normalized to the endogenous control *Gapdh* expression. Individual data points represent both biological and technical replicates as follows; male neurons (N=3, n=12), male astrocytes (N=3, n=12), female neurons (N=2, n=12) and female astrocytes (N=3, n=6).

Expression of *Mecp2e1* was 3.02-fold ($P <0.0001$) higher in male neurons compared to male astrocytes (**Figure 5.2**). Similarly, *Mecp2e2* transcripts were 1.63-fold ($P <0.001$) higher in male neurons compared to male astrocytes. This pattern was not seen in the cells of female origin, however, this observation needs to be verified by additional biological replicates. *Mecp2e1* levels were similar between female neurons and astrocytes (1.06-fold: female neurons *vs.* female

astrocytes). On the other hand, *Mecp2e2* expression was much higher (1.80-fold) in female neurons compared to female astrocytes.

Potential differences in expression of *Mecp2e1* and *Mecp2e2* transcripts in different cell types may also influence their functions, thus warranting an examination of the regulatory mechanisms governing their cell type-specific expression. In male neurons, *Mecp2e1* transcript levels were higher than *Mecp2e2* (2.99-fold, *P <0.0001*) **(Figure 5.2A)**. Similarly, within male astrocytes, *Mecp2e1* levels were higher than *Mecp2e2* levels (1.61-fold, *P <0.0001*). In female neurons, the levels of *Mecp2e1* and *Mecp2e2* were similar (1.07-fold) **(Figure 5.2B)**. Moreover, *Mecp2e1* levels were higher than *Mecp2e2* in female astrocytes (1.80-fold, *P <0.0001*).

Lastly, we studied the sex-specific expression of *Mecp2e1* and *Mecp2e2* transcripts **(Figure 5.2A-B; Table 5.1)**. If XCI occurs, dosage compensation mechanisms in female cell types would lead to comparable expression levels of *Mecp2* between the two sexes. As a previous study in fibroblasts suggested that *Mecp2* escapes XCI, we anticipated XCI-escape in female neurons and astrocytes tested in our study. In agreement with this hypothesis, neither of the *Mecp2e1* and *Mecp2e2* transcripts was equally expressed in male and female cell types **(Figure 5.2)**. However, if XCI-escape occurs in female cell types, the expression of *Mecp2e1* and *Mecp2e2* transcripts in female cells should be higher than in male cells. Consistent with this hypothesis, both *Mecp2e1* and *Mecp2e2* transcript levels were higher in female astrocytes when compared to male astrocytes (*Mecp2e1:* 1.57-fold, *P <0.001; Mecp2e2:* 1.40-fold, *P <0.001*). In neurons, *Mecp2e2* followed an expression pattern that agrees with XCI-escape (M<F: 1.54-fold). As both *Mecp2* transcripts are transcribed from the same locus, if, *Mecp2e2* shows signs of XCI-escape, it is likely that *Mecp2e1* should also escape XCI. However, *Mecp2e1* levels were higher in male neurons in contrast to female neurons (1.81-fold). Therefore, it is possible that mechanisms other than XCI-

escape may be acting in neurons, specifically those involved in regulating *Mecp2e1*-specific

expression and/or *Mecp2* splicing (**Table 5.1**).

Table 5.1 Summary of sex-specific expression of *Mecp2e1* and *Mecp2e2* transcripts in neurons and astrocytes			
Cell type	**Transcript**	**M & F expression**	**Explanation**
Neurons	*Mecp2e1*	M > F	does not agree with XCI-escape
	Mecp2e2	M < F	agrees with XCI-escape
Astrocytes	*Mecp2e1*	M < F	agrees with XCI-escape
	Mecp2e2	M < F	agrees with XCI-escape

M: Male; F: Female

5.5.3 DNA methylation at the Mecp2 REs may contribute to the higher expression of Mecp2 in neurons compared to astrocytes

In order to determine if DNA methylation contributes to the detected differences in transcript

levels of *Mecp2e1* and *Mecp2e2* between male neurons and male astrocytes, we analyzed the DNA

methylation patterns at known *Mecp2* REs [30,31] (**Figure 5.3B**). Previous genome-wide DNA

methylation analyses have indicated differential DNA methylation at CpG island regions, which

are comprised of the CpG island, N shore, N shelf, S shore and S shelf that flank the CpG islands

[41-43] (**Figure 5.3A-B**). The 'shores' are located ~2 kb flanking CpG islands and have been

shown to display dynamic DNA methylation patterns in contrast to the lower DNA methylation

levels seen in CpG islands. The 'shelves' are located ~4 kb away from the CpG islands and, similar

to shores, display differential methylation [43-45]. We analyzed DNA methylation at individual

CpG sites (**Figure 5.3C-D**) as well as the average methylation over the entire RE region (**Figure

5.S1**). Similar to our previous studies, the *Mecp2* promoter regions contained 13, 4 and 2 CpG

sites in R1, R2, and R3, respectively. The intron 1 silencer element has three REs, named R4, R5,

and R6, with 1, 1, and 2 CpG sites, respectively **(Figure 5.3B)**. Based on the general repressive role of DNA methylation we have observed before [30,31,34], we hypothesized that the higher *Mecp2* expression in male neurons is driven by lower DNA methylation at the *Mecp2* REs, and the lower *Mecp2* expression in male astrocytes is associated with higher DNA methylation.
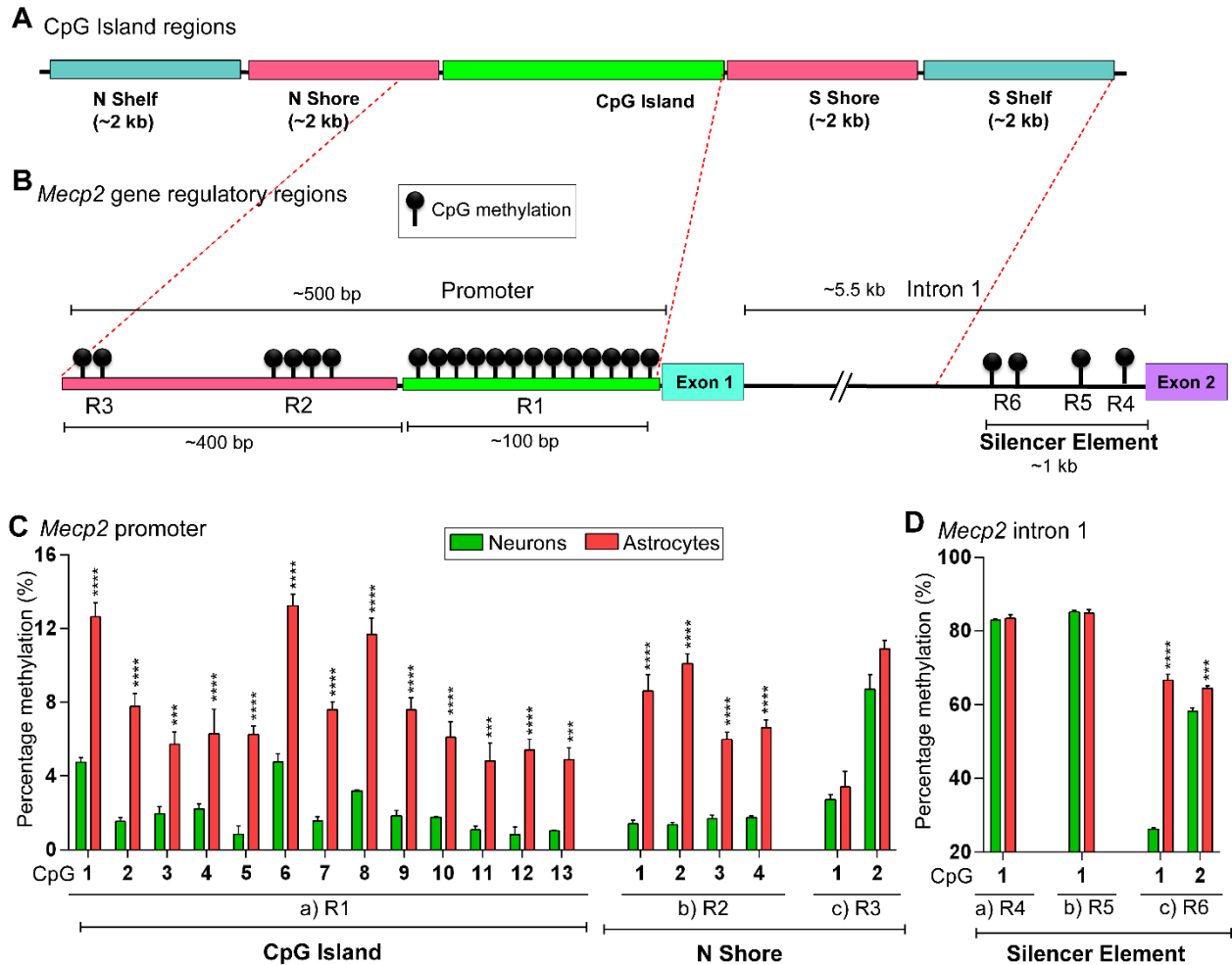
Figure 5.3 Bisulfite pyrosequencing analysis of DNA methylation at the *Mecp2* REs in male neurons and astrocytes.

A) Schematic representation of CpG island regions: CpG island, shelves and shores. Figure modified from [46,47] (not drawn to scale). **B)** Distribution of CpGs and assignment of CpG island regions to the *Mecp2* REs (promoter: R1-R3 REs and intron 1 silencer element: R4-R6). Figure not drawn to scale. Each methylation symbol indicates a single CpG. The number of CpGs within

each RE are: R1: 13 CpGs, R2: 4 CpGs, R3: 3 CpGs, R4: 1 CpG, R5: 1CpG and R6: 2CpGs. **C)** Percentage DNA methylation of CpG sites within the *Mecp2* promoter regions (**a**) R1, (**b**) R2, and (**c**) R3. **D)** Percentage DNA methylation of CpG sites within the *Mecp2* intron 1 silencer element regions (**a**) R4, (**b**) R5, and (**c**) R6. Significant differences between male neurons and astrocytes are indicated with ****P <0.0001, ***P <0.001*. N = 3. Error bars indicate SEM.

First, we assigned the CpG island regions as illustrated in **Figure 5.3A** to *Mecp2* gene REs (**Figure 5.3B**). R1 of the *Mecp2* promoter was assigned to the CpG island, whereas R2 and R3 belong to the N shore (**Figure 5.3B**). As the intron 1 silencer element REs are located more than 4 kb downstream of the CpG island, they do not belong to either the S shelf or S shore. Based on previous studies in autistic patients and a rare RTT patient [8,9,29], we hypothesize that blocks of DNA methylation in the CpG island and/or N-shore may have differentially methylated CpG blocks, which may contribute to the differential *Mecp2* expression in neurons and astrocytes.

Bisulfite pyrosequencing experiments showed that the percentage DNA methylation at all 13 CpGs within the *Mecp2* promoter region R1 was 3.7-8.4% higher in male astrocytes when compared to male neurons (**Figure 5.3C**). Similarly, the percentage DNA methylation at all four CpG sites at the promoter R2 was significantly higher (4.3-8.7%) in male astrocytes compared to neurons. In contrast, DNA methylation at R3 CpG sites, while also low, was not different between astrocytes and neurons in a statistically significant manner. Altogether, the proximal *Mecp2* promoter, showed a higher percentage of DNA methylation in male astrocytes, potentially contributing to the lower *Mecp2e1* and *Mecp2e2* transcript levels in astrocytes as compared to neurons. We then studied the *Mecp2* intron 1 silencer element regions for DNA methylation changes (**Figure 5.3D**). R6 CpGs had a significantly higher percentage DNA methylation (6.3-

40.4%) in male astrocytes compared to male neurons. CpG sites in R4 and R5 were similarly methylated in male astrocytes and neurons.

Another critical observation we had was the percentage methylation levels between the *Mecp2* promoter REs and the intron 1 silencer REs. For instance, in male neurons, the promoter REs showed percentage methylation levels ranging between 1-10% suggesting a lower level of promoter methylation **(Figure 5.3C)**. This is in agreement with published studies that suggested low or no DNA methylation at CpG islands and low methylation levels at its flanking regions [44,48]. In contrast, the intron 1 REs showed percentage methylation levels between ~65-85%, indicating that the intron 1 silencer element is much more highly methylated than the promoter **(Figure 5.3D)**. Similar differential methylation between the promoter and intron 1 silencer element was observed in astrocytes as well **(Figure 5.3C-D)**.

Our previous studies [30,31,34] and a report on autistic patients [8] provided a rationale for investigating the average methylation over blocks of CpGs or REs. Similar to our previous studies, average methylation was calculated for the promoter REs that contain more than one CpG site (R1, R2, and R3) and belonged to CpG island and N-shore of the *Mecp2* core promoter [30,31,34]. Both R1 (+5.59%) and R2 (+6.29%) showed a greater than 5% methylation difference between astrocytes and neurons over the entire region **(Figure 5.S1)**. Although individual CpG sites of R3 were not significantly changed, the average methylation over promoter R3 was slightly higher (+1.44%, *P <0.05*) in male astrocytes. In other words, the difference in average methylation between male neurons and astrocytes was higher in the CpG island (R1) while the difference was reduced further away from the transcription start site (R3).

5.5.4 Mecp2e1 and Mecp2e2 transcript levels show differential correlation with DNA methylation at the Mecp2 REs

Next, we investigated a potential mechanism driving *Mecp2* expression in neurons and astrocytes. As a first step in this objective, we performed a correlational analysis between *Mecp2e1* and *Mecp2e2* transcript levels and DNA methylation at individual CpG sites of the *Mecp2* REs in male neurons **(Figure 5.4A)** and male astrocytes **(Figure 5.4B)**. Based on previous studies [49] and our unpublished data, we assume that *Mecp2e1* and *Mecp2e1* are regulated by a single promoter and the DNA methylation at the intron 1 silencer element may influence *Mecp2* transcription through its silencer activity and/or splicing.
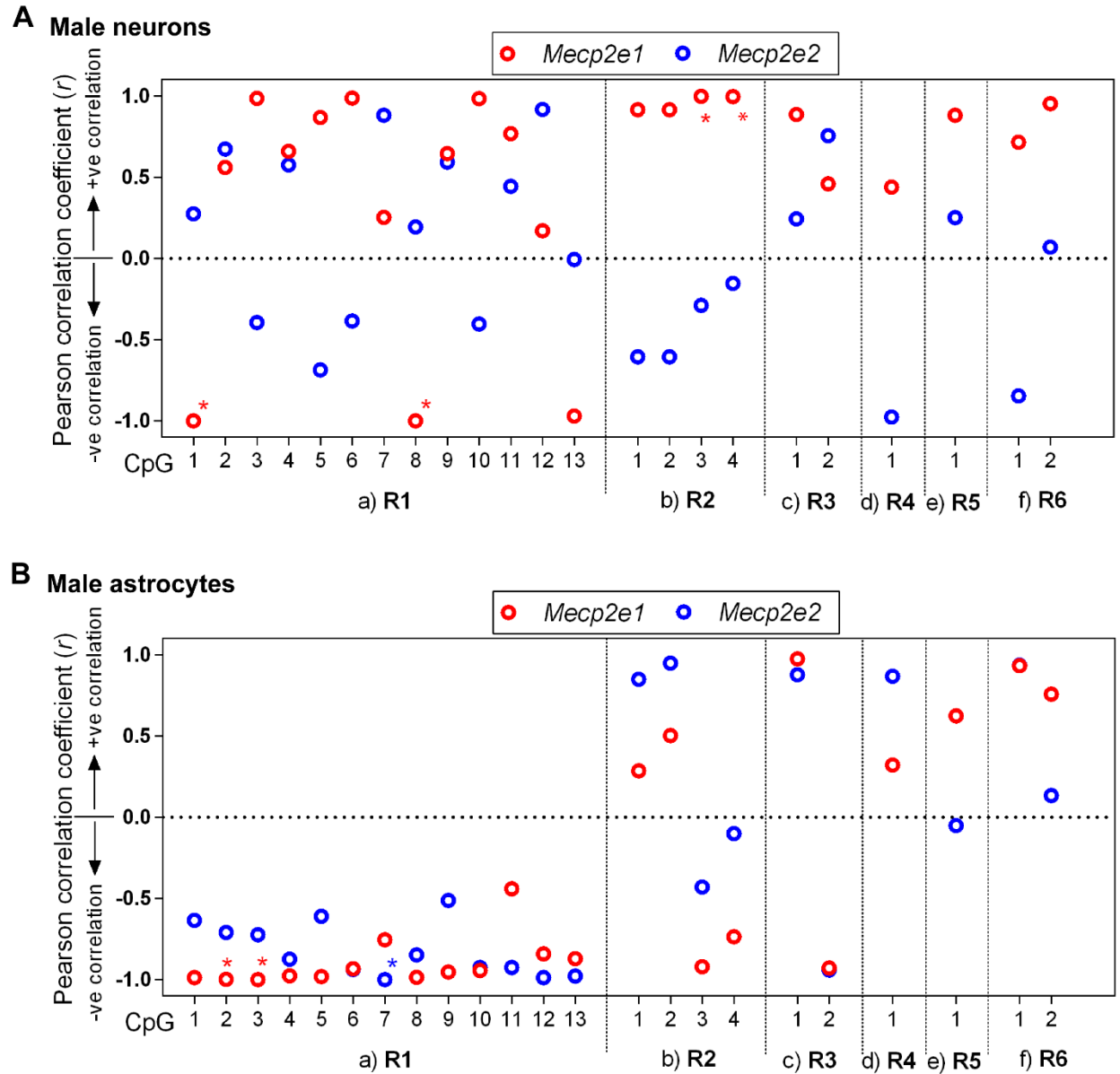
Figure 5.4 Correlation analyses between DNA methylation at the *Mecp2* REs and *Mecp2e1* and *Mecp2e2* transcript levels in male neurons and astrocytes.

A) Male neurons, **B)** male astrocytes. All graphs represent the Pearson correlation coefficient (*r*) for *Mecp2e1* (Red), and *Mecp2e2* (Blue). Statistical significance of the correlation is indicated by *P <0.05*; N = 3. Individual CpG sites at the promoter regions (**a**) R1, (**b**) R2, and (**c**) R3, and intron 1 silencer element regions (**d**) R4, (**e**) R5, and (**f**) R6 are shown on the x-axis.

First, we determined the relationship between *Mecp2e1* transcript levels in male neurons with the methylation levels of individual REs in the *Mecp2* core promoter region. In R1, CpG1 and CpG8 showed a very strong negative correlation with *Mecp2e1* expression (CpG1: $r = -0.99$, $P < 0.05$; CpG8: $r = -0.99$, $P < 0.05$). Although CpG13 also showed a negative correlation with *Mecp2e1*, this relationship was not statistically significant ($r = -0.97$, $P = 0.15$). The other CpG sites (CpG2, 3, 4, 5, 6, 7, 9, 10, 11 and 12) showed varying degrees of positive correlations, which were not statistically significant. DNA methylation at the CpG sites in R2 and *Mecp2e1* expression levels had a very strong positive correlation ($r > -0.9$) and it was statistically significant for CpG3 ($r = +0.99$, $P < 0.05$) and CpG4 ($r = +0.99$, $P = 0.051$). *Mecp2e1* showed a positive but statistically insignificant correlation with DNA methylation at the promoter R3 region, and all the intron 1 silencer element REs (R3, R4, and R6). In contrast, when the correlation between *Mecp2e2* transcript levels and DNA methylation was determined, all *Mecp2* REs showed varying degrees of positive and negative correlations; however, these correlations were statistically insignificant.

Unlike neurons, which showed widely distributed correlational patterns between DNA methylation and transcript levels of *Mecp2e1* and *Mecp2e2,* male astrocytes had a distinct correlational pattern **(Figure 5.4B)**. Both *Mecp2e1* and *Mecp2e2* expression in male astrocytes negatively correlated with DNA methylation of all CpGs in R1, which is in agreement with the repressive role of DNA methylation at R1 previously highlighted [30,31]. Among them, the correlations between *Mecp2e1* and R1:CpG2 ($r=-0.9984$, $P < 0.05$) and CpG3 ($r=-0.9994$, $P < 0.05$) were statistically significant. Similarly, *Mecp2e2* showed a negative and significant correlation with DNA methylation at the R1:CpG7 ($r=-0.9999$, $P < 0.01$). The correlation between DNA methylation at the R2, R3 and intron 1 R4-R6 regions and *Mecp2* transcripts was statistically insignificant. However, R2:CpG1 and R2:CpG2 and R3:CpG1 showed a positive correlation with

both *Mecp2e1* and *Mecp2e2*. In contrast, R2: CpG3 and R2: CpG4 and R3: CpG2 showed a negative correlation with both *Mecp2e1* and *Mecp2e2*. This correlation pattern is opposite to that observed in male neurons. Similar to neurons, DNA methylation at R4-R6 showed a positive, but statistically insignificant correlation with *Mecp2e1*. The correlation between *Mecp2e2* and DNA methylation at R4-R6 in male astrocytes was opposite to that in neurons, even though statistically insignificant.

5.6 Discussion

Understanding how *Mecp2/MECP2*/MeCP2 expression is regulated in major brain cell types is essential for MeCP2-associated health research for the following reasons. First, it aids in understanding how different levels of *Mecp2/MECP2*/MeCP2 and its two transcript isoforms (*Mecp2e1* and *Mecp2e2*) contribute to the maintenance of proper cellular functions and activities in the brain, possibly in a cell type- and sex-specific manner. Second, investigating *Mecp2* cell type-specific expression and regulation provides valuable insights on how regulatory mechanisms can be used to develop therapeutic strategies to recover normal expression levels in MeCP2-associated neurological disorders, possibly in a cell type- and sex-specific manner. Therefore, this study contributes to the field of MeCP2 by establishing the sex- and cell type-specific expression patterns of *Mecp2e1* and *Mecp2e2* and its correlation with DNA methylation status.

Previous studies have indicated that MeCP2E1 levels were higher in neurons than in astrocytes [22,34]. We concluded that both *Mecp2e1* and *Mecp2e2* transcripts show higher expression in male neurons compared to male astrocytes, a pattern not seen in female cells. In both cell types, except for the female neurons, *Mecp2e1* is the major isoform at the transcript level. Therefore, our study suggests that in female neurons and female astrocytes, *Mecp2e1,* at the

transcript level, may not be the major isoform. Whether MeCP2 isoforms at the protein level also follow a similar expression pattern is currently unknown, but needs to be assessed by western blotting.

To my knowledge, this is the first study which explored the expression of *Mecp2e1* and *Mecp2e2* transcripts in a sex-specific manner in neurons and astrocytes. Although numerous studies have reported a loss of *Mecp2* or overexpression of *MECP2* in male and female rodent systems (reviewed in [50]), they have not reported the expression patterns of *Mecp2e1* and *Mecp2e2* in primary male/female neurons and astrocytes. The only exception was a study of *Mecp2*/MeCP2 expression in the rat brain during development [51]. Their findings indicated a higher expression of *Mecp2*/MeCP2 in female amygdala and hypothalamus at postnatal day 1 (P1) compared to male brain regions. In contrast, at P10, males expressed more *Mecp2*/MeCP2 in the preoptic area. The observed higher expression of *Mecp2* in females compared to males observed in the rat brain at P1 is in agreement with XCI-escape and thus further strengthens the theory that *Mecp2* undergoes XCI-escape with some exceptions in specific cell types or brain regions. In agreement with a previous report [51], our study suggests that *Mecp2* expression may change in a sex-dependent, cell type-specific, and *Mecp2* transcript-specific manner. These results may also implicate age/developmental stage-specific regulatory mechanisms.

XCI-escape may explain the higher expression of *Mecp2* in female cells. The male neurons, which showed a deviation from this pattern (*Mecp2e1* M>F; *Mecp2e2* M<F), may be subject to alternative mechanisms such as transcriptional, epigenetic, post-transcriptional or co-transcriptional splicing mechanisms. However, it should be noted that data from female neurons were generated from two biological replicates and thus should be verified by additional experiments. Several other studies have shown that XCI-escape and bi-allelic expression of X-

linked genes such as *Hdac6* and *Kdm6a* were associated with a more accessible chromatin structure at the promoters of these genes as indicated by DNase I hypersensitivity, occupancy of RNA Pol II-S5p, recruitment of CTCF and enrichment of active histone modifications such as H3K4me3 [27,28]. Our data illustrated that neither *Mecp2e1* nor *Mecp2e2* in neurons and astrocytes undergoes dosage compensation by XCI. Based on previous reports on XCI-escape of *Mecp2* gene in fibroblast cells [26], it was speculated that this could partly be due to XCI-escape. In addition to *MECP2*, other X-linked genes such as *GAB3, RPS4X, JARID1C, UBE1, BIRC4* and *SLC16A2* show evidence of XCI-escape in female bovine fetal muscle tissues [26]. Generally, when genes escape XCI, these genes show higher expression in females due to bi-allelic expression when compared to mono-allelic expression in males. Based on our and others' studies, higher expression in cells of female origin was not observed all the time, suggesting that additional regulatory mechanisms might be contributing to sex-specific expression of these genes. Studies on other genes have provided similar evidence [52]. For instance, a microarray-based analysis of cerebellum demonstrated that the *MECP2* unigene cluster (Hs.200716) showed a F/M ratio of 0.8 (M>F), suggesting *MECP2* in the cerebellum may not follow XCI or XCI-escape. On the other hand, 0.8 F/M ratio is ~1 suggesting an agreement with XCI. The cerebellum is a brain region with the highest neuronal density in the brain. Therefore, it is worth questioning whether there are deviating or complex *MECP2/Mecp2* regulatory mechanisms seen in neurons. In our study, *Mecp2e1* and *Mecp2e2* transcripts showed opposing trends in neurons (*Mecp2e1*: M > F; *Mecp2e2*: M < F), which does not fully comply with XCI-escape. However, as *Mecp2e2* shows signs of XCI-escape and both *Mecp2e1/e2* are expressed from the same promoter, it is justifiable to assume that *Mecp2* undergoes XCI escape in female neurons. The discordant observations of *Mecp2e1* and *Mecp2e2* thus could either be due to increased and decreased expression of *Mecp2e1* and *Mecp2e2*

in male neurons and female neurons, respectively, by mechanisms other than XCI-escape. As DNA methylation also regulates co-transcriptional splicing [32], an alternate mechanism would be a shifting in *Mecp2* splicing in male neurons when compared to female neurons. Either way, these observations warrant further investigations in mechanisms that regulate *Mecp2e1* and *Mecp2e2* transcription and splicing, specially in neurons. Studies in human trophoblast stem cells, different strains of mice and human population studies have suggested variable XCI-escape in a tissue-, cell-, developmental stage-, and gene-specific manner [53-57]. These studies also suggest that the variability may arise from epigenetic plasticity of the cell type [55]. Therefore, it is possible that the epigenetic differences between neurons and astrocytes may contribute to the variable XCI-escape of *Mecp2* observed between them in our study.

In accordance with the generally repressive role of DNA methylation (5mC), higher DNA methylation would be expected to reduce gene expression [10]. This is consistent with our conclusion that the higher percentage of DNA methylation at the *Mecp2* promoter (R1-R2) and intron 1 (R6) REs may collectively contribute to the lower *Mecp2* expression in male astrocytes when compared to male neurons. Our data also imply that DNA methylation at R3, R4 and R5 may not play any role in the differential expression of *Mecp2e1* and *Mecp2e2* in male neurons and astrocytes. As this inference was made based on the lack of differential methylation at these REs between male neurons and astrocytes, it should be further validated by analyzing both 5mC and 5hmC levels in these REs. Overall, this analysis showed that male neurons have significantly lower DNA methylation, mainly at the *Mecp2* promoter REs in contrast to astrocytes. suggesting their contribution to the epigenetic regulation of *Mecp2e1* and *Mecp2e2* transcript levels in neurons and astrocytes.

Correlation analyses between *Mecp2* transcript levels and DNA methylation showed both negative (repressive) and positive (active) correlations with specific CpGs. In order to further investigate the nature of these relationships, characterization of 5mC and 5hmC will be necessary. This is because 5mC and 5hmC play different roles in gene expression depending on their genomic context. At promoters 5mC generally plays a transcriptional repressive role while 5hmC may activate transcription [10]. The negative correlations between *Mecp2e1* and specific R1 CpGs in male neurons implicate a repressive role of DNA methylation, similar to our observations in decitabine-treated differentiating NSC [30]. Our data may also suggest that the role of DNA methylation at individual CpG sites of the promoter R1 in male astrocytes could be different from male neurons. For instance, methylation of R1:CpG2 and CpG3 may impact *Mecp2e1* expression while R1:CpG7 may impact *Mecp2e2* expression. A positive correlation between *Mecp2e1* and R2 methylation in male neurons suggested an active role of DNA methylation, which is in agreement with our ethanol studies [31]. In our previous study, we demonstrated that R2 has a relatively higher percentage of 5hmC in contrast to other promoter regions and shows a positive correlation with *Mecp2* transcript expression [31]. Based on this relationship, R2 in male neurons might be enriched with 5hmC. Presence of correlations between DNA methylation and *Mecp2e1* but not with *Mecp2e2* may imply a more prominent role of DNA methylation in regulating *Mecp2e1* in male neurons, even though both transcripts may be transcribed from the same *Mecp2* promoter. The differences in correlation for *Mecp2e1* and *Mecp2e2* with promoter DNA methylation thus may imply the influence of promoter methylation in regulating alternative splicing of *Mecp2*. The lack of statistically significant correlations between DNA methylation and *Mecp2e2* transcript levels may not necessarily indicate the absence of a role for the *Mecp2* promoter DNA methylation in *Mecp2e2* regulation, due to two reasons. First, as both *Mecp2e1*

and *Mecp2e2* transcripts are transcribed from the same promoter, the influence of promoter DNA methylation on both transcripts should theoritically be similar, except if DNA methylation plays a role in splicing or selection of different TSSs for *Mecp2* isoforms. Second, the statistical significance of the correlation analyses depends on the number of biological replicates included (in this case, N=3) and thus the inclusion of more biological replicate may provide further supporting evidence.

Previously, we showed a differential correlation of *Mecp2e1* and *Mecp2e2* transcript levels with DNA methylation at almost all CpG sites when comparing two stages of differentiation [Day (D)2 and D8] of NSC isolated from E14 forebrain [30]. In contrast, when *in vivo* differentiated neurons were isolated from E18 brain, statistically significant correlations were limited to four CpGs in the *Mecp2* promoter and only with *Mecp2e1*. Similarly, the number of statistically significant correlations in male astrocytes isolated from E18 embryos were limited to three CpGs in promoter R1, albeit the correlations were observed for expression levels of both *Mecp2e1* and *Mecp2e2*. This suggests that DNA methylation may play a more critical role in earlier stages of embryonic development and during NSC differentiation, in comparison to differentiated cell types at later embryonic stages.

5.7 Conclusion

In conclusion, studies presented here report cell type-, sex- and transcript-specific expression patterns of *Mecp2e1* and *Mecp2e2* in neurons and astrocytes. As expected, *Mecp2* seems to undergo XCI-escape in female astrocytes. The *Mecp2e1* and *Mecp2e2* transcript expression patterns in neurons may not be fully explained by XCI-escape and may imply potential involvement of alternate mechanisms such as alternative splicing. The higher abundance of

Mecp2e1 and *Mecp2e2* transcripts in male neurons in contrast to male astrocytes could be partially driven by the lower DNA methylation levels at *Mecp2* REs. Within male neurons, *Mecp2e1* was the major transcript isoform with approximately 3-fold higher expression than *Mecp2e2*. Correlation analysis in male neurons suggested that the state DNA methylation at the *Mecp2* promoter may influence *Mecp2e1* transcript levels more than *Mecp2e2* transcript levels, suggesting the involvement of DNA methylation in both transcription and splicing.

The major findings of this study and potential mechanisms driving these results are summarized in **Figure 5.5**. We hypothesize that, the lower DNA methylation at the *Mecp2* promoter in male neurons may induce an 'active chromatin conformation' allowing higher transcription. In contrast, higher DNA methylation at the *Mecp2* promoter in male astrocytes may cause a 'less active and condensed chromatin conformation' leading to lower expression of *Mecp2*. We propose that DNA methylation may act as a switch for fine tuning of *Mecp2* gene expression from 'ON' (active promoter) to 'DIM' (less active promoter) to 'OFF' (repressed promoter).
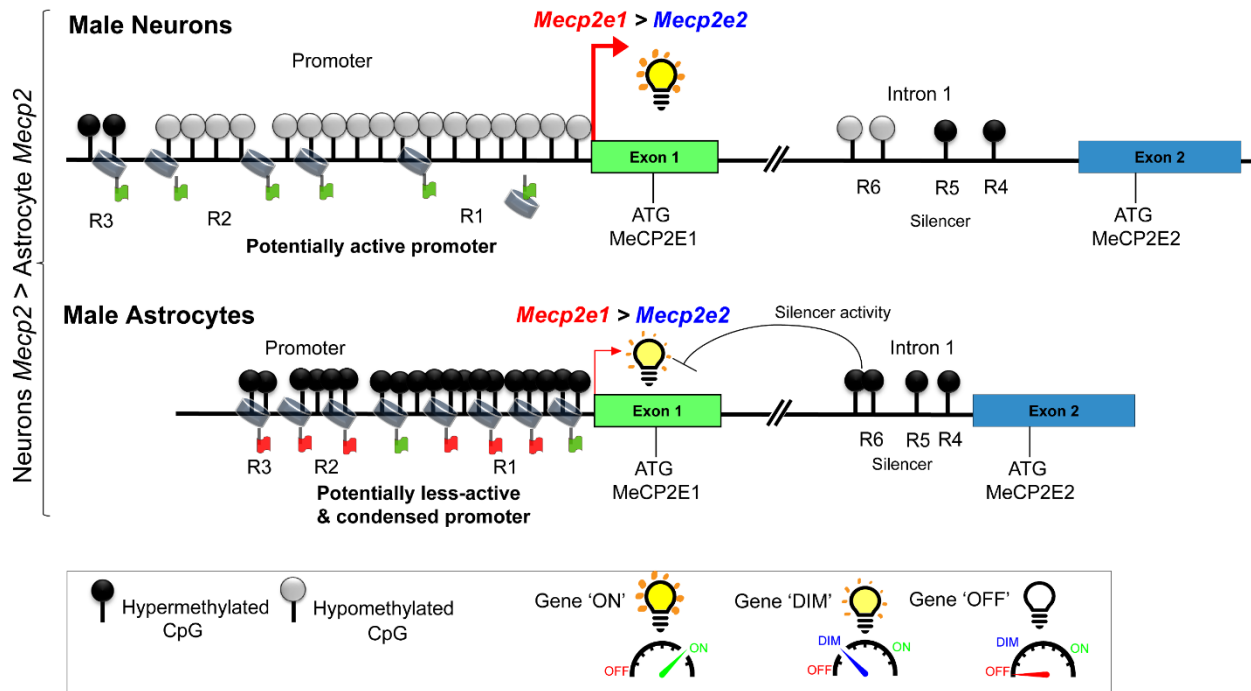
Figure 5.5 Summary and proposed model for the potential regulation of *Mecp2e1* and *Mecp2e2* transcripts by DNA methylation in male neurons and astrocytes.

Based on the findings of this study, this figure illustrates a summary of the proposed mechanism of *Mecp2* regulation by DNA methylation in male neurons and astrocytes. The higher *Mecp2* expression in male neurons compared to male astrocytes could be in part driven by lower DNA methylation. The lower DNA methylation levels in male neurons may be associated with an active or open chromatin conformation while higher DNA methylation in male astrocytes may render a less-active and condensed chromatin conformation.

5.8 References

1. Liyanage VB, Rastegar M (2014) Rett Syndrome and MeCP2. NeuroMolecular Medicine 10.1007/s12017-014-8295-9: 1-34.

2. Zachariah RM, Rastegar M (2012) Linking epigenetics to human disease and Rett syndrome: the emerging novel and challenging concepts in MeCP2 research. Neural Plast 2012: 415825.

3. Wan M, Lee SS, Zhang X, Houwink-Manville I, Song HR, Amir RE, Budden S, Naidu S, Pereira JL, et al. (1999) Rett syndrome and beyond: recurrent spontaneous and familial MECP2 mutations at CpG hotspots. Am J Hum Genet 65: 1520-1529.

4. Amir RE, Van den Veyver IB, Wan M, Tran CQ, Francke U, Zoghbi HY (1999) Rett syndrome is caused by mutations in X-linked MECP2, encoding methyl-CpG-binding protein 2. Nat Genet 23: 185-188.

5. Meins M, Lehmann J, Gerresheim F, Herchenbach J, Hagedorn M, Hameister K, Epplen JT (2005) Submicroscopic duplication in Xq28 causes increased expression of the MECP2 gene in a boy with severe mental retardation and features of Rett syndrome. J Med Genet 42: e12.

6. Ariani F, Mari F, Pescucci C, Longo I, Bruttini M, Meloni I, Hayek G, Rocchi R, Zappella M, et al. (2004) Real-time quantitative PCR as a routine method for screening large rearrangements in Rett syndrome: Report of one case of MECP2 deletion and one case of MECP2 duplication. Hum Mutat 24: 172-177.

7. Van Esch H (1993) MECP2 Duplication Syndrome. In: Pagon RA, Adam MP, Ardinger HH, Wallace SE, Amemiya A et al., editors. GeneReviews(R). Seattle (WA).

8. Nagarajan RP, Hogart AR, Gwye Y, Martin MR, LaSalle JM (2006) Reduced MeCP2 expression is frequent in autism frontal cortex and correlates with aberrant MECP2 promoter methylation. Epigenetics 1: e1-11.

9. Nagarajan RP, Patzel KA, Martin M, Yasui DH, Swanberg SE, Hertz-Picciotto I, Hansen RL, Van de Water J, Pessah IN, et al. (2008) MECP2 promoter methylation and X chromosome inactivation in autism. Autism Res 1: 169-178.

10. Liyanage VR, Jarmasz JS, Murugeshan N, Del Bigio MR, Rastegar M, Davie JR (2014) DNA modifications: function and applications in normal and disease States. Biology (Basel) 3: 670-723.

11. Goh E (2017) Rett syndrome: a sex-biased neurodevelopmental disorder. Gender Medicine: 30-33.

12. Kim KC, Choi CS, Kim JW, Han SH, Cheong JH, Ryu JH, Shin CY (2014) MeCP2 Modulates Sex Differences in the Postsynaptic Development of the Valproate Animal Model of Autism. Mol Neurobiol 10.1007/s12035-014-8987-z.

13. Deng X, Berletch JB, Nguyen DK, Disteche CM (2014) X chromosome regulation: diverse patterns in development, tissues and disease. Nature Reviews Genetics 15: 367-378.

14. Lioy DT, Garg SK, Monaghan CE, Raber J, Foust KD, Kaspar BK, Hirrlinger PG, Kirchhoff F, Bissonnette JM, et al. (2011) A role for glia in the progression of Rett/'s syndrome. Nature 475: 497-500.

15. Maezawa I, Swanberg S, Harvey D, LaSalle JM, Jin LW (2009) Rett syndrome astrocytes are abnormal and spread MeCP2 deficiency through gap junctions. J Neurosci 29: 5051-5061.

16. Okabe Y, Takahashi T, Mitsumasu C, Kosai K, Tanaka E, Matsuishi T (2012) Alterations of gene expression and glutamate clearance in astrocytes derived from an MeCP2-null mouse model of Rett syndrome. PLoS One 7: e35354.

17. Lioy DT, Garg SK, Monaghan CE, Raber J, Foust KD, Kaspar BK, Hirrlinger PG, Kirchhoff F, Bissonnette JM, et al. (2011) A role for glia in the progression of Rett's syndrome. Nature 475: 497-500.

18. Derecki NC, Cronk JC, Lu Z, Xu E, Abbott SB, Guyenet PG, Kipnis J (2012) Wild-type microglia arrest pathology in a mouse model of Rett syndrome. Nature 484: 105-109.

19. Rastegar M, Hotta A, Pasceri P, Makarem M, Cheung AY, Elliott S, Park KJ, Adachi M, Jones FS, et al. (2009) MECP2 isoform-specific vectors with regulated expression for Rett syndrome gene therapy. PLoS One 4: e6810.

20. Luikenhuis S, Giacometti E, Beard CF, Jaenisch R (2004) Expression of MeCP2 in postmitotic neurons rescues Rett syndrome in mice. Proc Natl Acad Sci U S A 101: 6033-6038.

21. Ramocki MB, Peters SU, Tavyev YJ, Zhang F, Carvalho CM, Schaaf CP, Richman R, Fang P, Glaze DG, et al. (2009) Autism and other neuropsychiatric symptoms are prevalent in individuals with MeCP2 duplication syndrome. Ann Neurol 66: 771-782.

22. Zachariah RM, Olson CO, Ezeonwuka C, Rastegar M (2012) Novel MeCP2 isoform-specific antibody reveals the endogenous MeCP2E1 expression in murine brain, primary neurons and astrocytes. PLoS One 7: e49763.

23. Ballas N, Lioy DT, Grunseich C, Mandel G (2009) Non-cell autonomous influence of MeCP2-deficient glia on neuronal dendritic morphology. Nat Neurosci 12: 311-317.

24. Cerase A, Pintacuda G, Tattermusch A, Avner P (2015) Xist localization and function: new insights from multiple levels. Genome biology 16: 166.

25. Prothero KE, Stahl JM, Carrel L (2009) Dosage compensation and gene expression on the mammalian X chromosome: one plus one does not always equal two. Chromosome research 17: 637-648.

26. Nino-Soto M, Nuber UA, Basrur P, Ropers H-H, King W (2005) Differences in the pattern of X-linked gene expression between fetal bovine muscle and fibroblast cultures derived from the same muscle biopsies. Cytogenetic and genome research 111: 57-64.

27. Berletch JB, Ma W, Yang F, Shendure J, Noble WS, Disteche CM, Deng X (2015) Escape from X inactivation varies in mouse tissues. PLoS Genet 11: e1005079.

28. Khalil AM, Driscoll DJ (2007) Trimethylation of histone H3 lysine 4 is an epigenetic mark at regions escaping mammalian X inactivation. Epigenetics 2: 114-118.

29. Vieira JP, Lopes F, Silva-Fernandes A, Sousa MV, Moura S, Sousa S, Costa BM, Barbosa M, Ylstra B, et al. (2015) Variant Rett syndrome in a girl with a pericentric X-chromosome inversion leading to epigenetic changes and overexpression of the MECP2 gene. Int J Dev Neurosci 46: 82-87.

30. Liyanage VR, Zachariah RM, Rastegar M (2013) Decitabine alters the expression of Mecp2 isoforms via dynamic DNA methylation at the Mecp2 regulatory elements in neural stem cells. Mol Autism 4: 46.

31. Liyanage VR, Zachariah RM, Davie JR, Rastegar M (2015) Ethanol deregulates Mecp2/MeCP2 in differentiating neural stem cells via interplay between 5-methylcytosine and 5-hydroxymethylcytosine at the Mecp2 regulatory elements. Exp Neurol 265: 102-117.

32. Shukla S, Kavak E, Gregory M, Imashimizu M, Shutinoski B, Kashlev M, Oberdoerffer P, Sandberg R, Oberdoerffer S (2011) CTCF-promoted RNA polymerase II pausing links DNA methylation to splicing. Nature 479: 74-79.

33. Schor IE, Rascovan N, Pelisch F, Allo M, Kornblihtt AR (2009) Neuronal cell depolarization induces intragenic chromatin modifications affecting NCAM alternative splicing. Proc Natl Acad Sci U S A 106: 4325-4330.

34. Olson CO, Zachariah RM, Ezeonwuka CD, Liyanage VR, Rastegar M (2014) Brain region-specific expression of MeCP2 isoforms correlates with DNA methylation within Mecp2 regulatory elements. PLoS One 9: e90645.

35. Barber BA, Liyanage VR, Zachariah RM, Olson CO, Bailey MA, Rastegar M (2013) Dynamic expression of MEIS1 homeoprotein in E14.5 forebrain and differentiated forebrain-derived neural stem cells. Ann Anat 195: 431-440.

36. Lambert JF, Benoit BO, Colvin GA, Carlson J, Delville Y, Quesenberry PJ (2000) Quick sex determination of mouse fetuses. J Neurosci Methods 95: 127-132.

37. Hartshorn C, Rice JE, Wangh LJ (2002) Developmentally-regulated changes of Xist RNA levels in single preimplantation mouse embryos, as revealed by quantitative real-time PCR. Mol Reprod Dev 61: 425-436.

38. Dewing P, Chiang CWK, Sinchak K, Sim H, Fernagut P-O, Kelly S, Chesselet M-F, Micevych PE, Albrecht KH, et al. Direct Regulation of Adult Brain Function by the Male-Specific Factor SRY. Current Biology 16: 415-420.

39. Lambert J-F, Benoit BO, Colvin GA, Carlson J, Delville Y, Quesenberry PJ (2000) Quick sex determination of mouse fetuses. Journal of neuroscience methods 95: 127-132.

40. Patrat C, Okamoto I, Diabangouaya P, Vialon V, Le Baccon P, Chow J, Heard E (2009) Dynamic changes in paternal X-chromosome activity during imprinted X-chromosome inactivation in mice. Proceedings of the National Academy of Sciences 106: 5198-5203.

41. van Veldhoven K, Polidoro S, Baglietto L, Severi G, Sacerdote C, Panico S, Mattiello A, Palli D, Masala G, et al. (2015) Epigenome-wide association study reveals decreased average methylation levels years before breast cancer diagnosis. Clinical Epigenetics 7: 67.

42. Hansen KD, Timp W, Bravo HC, Sabunciyan S, Langmead B, McDonald OG, Wen B, Wu H, Liu Y, et al. (2011) Increased methylation variation in epigenetic domains across cancer types. Nature genetics 43: 768-775.

43. Irizarry RA, Ladd-Acosta C, Wen B, Wu Z, Montano C, Onyango P, Cui H, Gabo K, Rongione M, et al. (2009) The human colon cancer methylome shows similar hypo-and hypermethylation at conserved tissue-specific CpG island shores. Nature genetics 41: 178-186.

44. Edgar R, Tan PPC, Portales-Casamar E, Pavlidis P (2014) Meta-analysis of human methylomes reveals stably methylated sequences surrounding CpG islands associated with high gene expression. Epigenetics & Chromatin 7: 28.

45. Doi A, Park I-H, Wen B, Murakami P, Aryee MJ, Irizarry R, Herb B, Ladd-Acosta C, Rho J, et al. (2009) Differential methylation of tissue-and cancer-specific CpG island shores distinguishes human induced pluripotent stem cells, embryonic stem cells and fibroblasts. Nature genetics 41: 1350-1353.

46. Huang W-Y, Hsu S-D, Huang H-Y, Sun Y-M, Chou C-H, Weng S-L, Huang H-D (2014) MethHC: a database of DNA methylation and gene expression in human cancer. Nucleic acids research: gku1151.

47. W.Y. Huang SDH, H.Y. Huang, Y.M. Sun, C.H. Chou, S.L. Weng, H.D. Huang (2014) MethHC: A database of DNA Methylation and gene expression in Human Cancer.

48. Deaton AM, Webb S, Kerr ARW, Illingworth RS, Guy J, Andrews R, Bird A (2011) Cell type–specific DNA methylation at intragenic CpG islands in the immune system. Genome Research 21: 1074-1086.

49. Adachi M, Keefer EW, Jones FS (2005) A segment of the Mecp2 promoter is sufficient to drive expression in neurons. Hum Mol Genet 14: 3709-3722.

50. Liyanage VR, Rastegar M (2014) Rett syndrome and MeCP2. Neuromolecular Med 16: 231-264.

51. Kurian JR, Forbes-Lorman RM, Auger AP (2007) Sex Difference in Mecp2 Expression During a Critical Period of Rat Brain Development. Epigenetics 2: 173-178.

52. Talebizadeh Z, Simon SD, Butler MG (2006) X chromosome gene expression in human tissues: Male and female comparisons. Genomics 88: 675-681.

53. Peeters SB, Cotton AM, Brown CJ (2014) Variable escape from X-chromosome inactivation: identifying factors that tip the scales towards expression. Bioessays 36: 746-756.

54. Cotton AM, Ge B, Light N, Adoue V, Pastinen T, Brown CJ (2013) Analysis of expressed SNPs identifies variable extents of expression from the human inactive X chromosome. Genome Biol 14: R122.

55. Dubois A, Deuve JL, Navarro P, Merzouk S, Pichard S, Commere PH, Louise A, Arnaud D, Avner P, et al. (2014) Spontaneous reactivation of clusters of X-linked genes is associated with the plasticity of X-inactivation in mouse trophoblast stem cells. Stem Cells 32: 377-390.

56. Calabrese JM, Sun W, Song L, Mugford JW, Williams L, Yee D, Starmer J, Mieczkowski P, Crawford GE, et al. (2012) Site-specific silencing of regulatory elements as a mechanism of X inactivation. Cell 151: 951-963.

57. Gunter C (2005) Genome biology: she moves in mysterious ways. Nature 434: 279-280.

5.9 Supplementary information
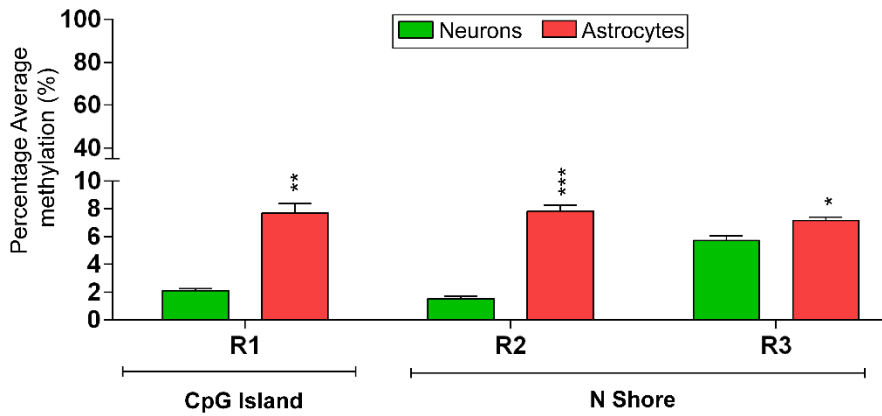
Figure 5.S1 Average DNA methylation patterns over the *Mecp2* promoter REs in male neurons and astrocytes.

Average percentage DNA methylation of all CpG sites in the promoter region R1 (13 CpGs), R2 (4 CpGs) and R3 (2 CpGs), in male neurons and astrocytes. Significant differences between neurons and astrocytes are indicated with *****$P <0.0001$, ****$P <0.001$, ***$P <0.01$ or ***$P <0.05$. N = 3. Error bars indicate SEM.

CHAPTER 6. CONCLUSIONS, DISCUSSION AND FUTURE PERSPECTIVES

6.1 Does DNA methylation indeed '*regulate*' expression of *Mecp2e1* and *Mecp2e2 transcripts*?

One of the major conclusions of my thesis work is that DNA methylation may regulate *Mecp2e1* and *Mecp2e2*. However, the analysis techniques and methodologies such as correlational analyses and treatment with drugs used in this study might not be sufficient to make an irrefutable conclusion. Generally, to prove that an RE regulates a gene's expression, reporter assays should be done proving its active or repressive role. However, the use of reporter assays is insufficient to show the role of DNA methylation at these REs, because recapitulation of DNA methylation patterns observed *in vivo* in an *in vitro* setting is extremely challenging or may be impossible. Based on the studies presented in Chapter 4, each of the *Mecp2* REs showed distinct 5mC and 5hmC patterns. Recapitulation of both 5mC and 5hmC patterns in *in vitro* reporter assays to my knowledge is not feasible. This might be the reason that in almost all cases [except in electrophoretic mobility shift assay (EMSA) experiments [1]] the role of DNA methylation on gene regulation is shown or rather predicted through correlational/association studies [2-4].

The role of these REs in *Mecp2/MECP2* regulation has already been confirmed by previous studies [5,6], which was the basis for the experimental design of REs used in our studies. We show here by drug treatments (decitabine) and ethanol exposure, and correlation analyses between DNA methylation and *Mecp2* transcript levels that DNA methylation at specific REs may play a role in the regulation of *Mecp2* expression in differentiating NSC, neurons and astrocytes and adult mouse brain regions [7-9]. Based on this discussion, I would conclude that the evidence shown in this thesis suggests that DNA methylation regulates *Mecp2* expression in embryonic differentiating NSC, neurons, and astrocytes. A synopsis of all the critical findings of the thesis can be found in **Table A1** in the Appendix.

6.2 Development of 'hypothetical models' of *Mecp2* regulation by DNA methylation: Conceptual basis of epigenetic regulation of gene expression by DNA methylation

In this thesis, the changes in DNA methylation at the *Mecp2* REs and their potential impact on *Mecp2* expression were described. However, DNA methylation changes at the promoter or distant elements, such as the intron 1 silencer element, may trigger other epigenetic and transcriptional changes to either induce or repress the gene expression. Moreover, DNA methylation at the intron 1 silencer element may regulate *Mecp2* splicing. In this section, using known TFs, regulatory complexes and studies on DNA methylation changes, hypothetical models for *Mecp2* expression changes by DNA methylation will be proposed. It should be noted that these are '*hypothetical scenarios*' that need to be empirically validated in the future. As a conceptual basis, I describe below how DNA methylation fine tunes expression to turn the gene 'ON' or 'OFF'.

Chromatin structure is important in the dynamic regulation of transcription. A chromatin conformation that is usually referred to as 'open' drives transcription by providing access to the general transcription machinery, co-activators (E.g., HAT) and chromatin remodelers **(Figure 6.1A)**. This open chromatin conformation is usually defined by dispersed nucleosomes, increased active DNA methylation (i.e. 5hmC) and active hPTMs such as histone acetylation (H3K27ac, H4K20ac) and histone methylation (H3K4me). On the other hand, a 'condensed' chromatin conformation refers to the repressed transcription where a gene is turned 'OFF' by preventing the access to the general transcription machinery **(Figure 6.1A)**. This state is characterized by inactive DNA methylation (5mC), repressive hPTMs (H3K27me3) and recruitment of repressor complexes.
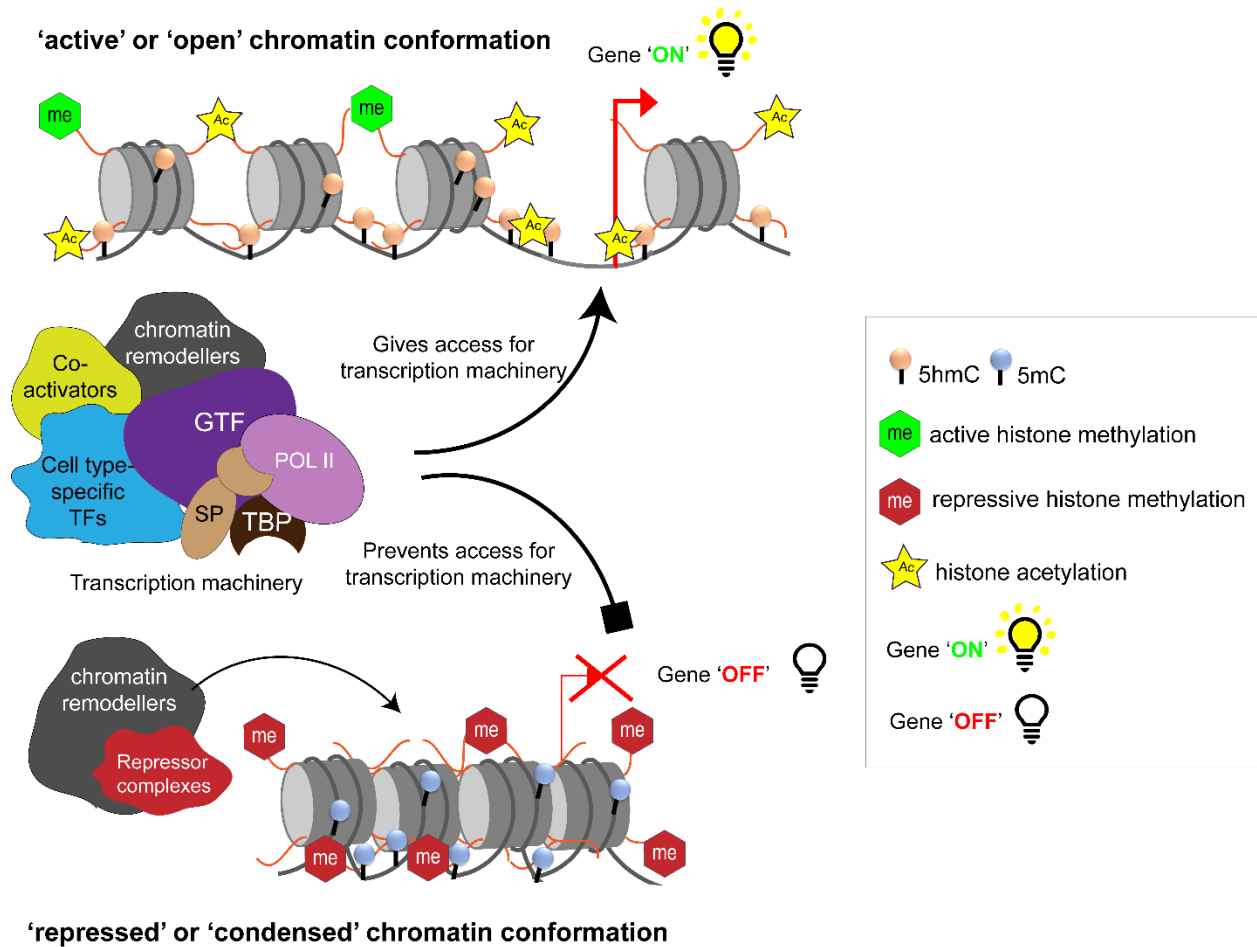
Figure 6.1 Differential states of chromatin mediating gene transcription.
Chromatin conformation states can either be **A)** 'open', or an active conformation allowing gene expression (gene ON), or **B)** 'condensed', which confers an inactive and repressed conformation, thereby turning off gene expression (gene OFF). GTF: General transcription factors, TFs: Transcription factors, TBP: TATA-box binding protein, SP: SP-family TFs, ac: acetylation, me: methylation.

DNA methylation plays diverse roles in transcription depending on their genomic location and recruitment of regulatory proteins. CpG islands, which are short stretches of DNA at proximity to TSS and highly enriched with CpGs, are usually unmethylated or show low methylation levels, mostly 5hmC [10,11]. Differentially methylated regions can be found further away from the core

279

promoter and can contain either 5mC and/or 5hmC [12]. In the case of some genes (E.g., *MECP2*), there are highly 5mC-methylated regions of heterochromatin, insulated by CTCF binding and the loss of CTCF binding leads to the crawling of the heterochromatic state into the promoter region, silencing the gene [13]. Additionally, distant regulatory elements such as silencers and enhancers may also be differentially methylated. For instance, hypermethylation of silencer element that regulates the *H19/Igf2* imprinted locus inactivates silencing activity, while hypermethylation *H19/Igf2* enhancer triggers its activity [14]. Moreover, some silencers are CTCF-dependent and can be differentially methylated depending on the cell or tissue type [15]. Proteins that are recruited to 5mC and 5hmC may also vary. For example, 5mC can bind MeCP2 and MBD1-4 in ESC, mouse brain, and neural precursors, while MeCP2, MBD3 and MBD4 bind to 5hmC in the same cell types [16-18].

Gene expression in neurons and astrocytes is most often regulated by cell type-specific binding of TFs. Neuron-specific TFs (NSTFs) and astrocyte-specific TFs (ASTFs). Examples of NSTFs are NeuroD1, NeuroD6, SP1, SP4, NHLH2, LHX5, DLX1, DLX5, EBF3, TBR1 and BCL11A [19-21]. ASTFs that are highly functional in astrocytes include GLI1, GLI2, GLI3, OTX1, GRHL1, SOX 9, RFX4, PBXIP1, HES5, PAX6, and DBX2 [19-21].

6.3 Proposed 'hypothetical models' of DNA methylation-mediated regulation of *Mecp2*

6.3.1 Basic concept of Mecp2 regulation by DNA methylation

The basic concept used in building these 'hypothetical models' of *Mecp2* regulation relies on the dynamics of chromatin conformation mediated by activating epigenetic modifications, binding of regulatory proteins and cross-talk between them. It was hypothesized that;

i.   Higher levels or induced expression of *Mecp2* in differentiating NSC and neuron/astrocyte cell types is mediated by enrichment of active epigenetic modifications and blocking the potential activity of the intron 1 silencer element. These modifications confer an active and open chromatin conformation of the *Mecp2* promoter regions allowing access to the transcription machinery. These changes ultimately lead to higher or induced *Mecp2* expression.

ii. Lower levels or reduced expression of *Mecp2* in differentiating NSC and neuron/astrocyte cell types is mediated by the enrichment of repressive epigenetic modifications and the potential activity of the intron 1 silencer element. These modifications confer a less-active or repressive chromatin conformation of the *Mecp2* promoter regions by creating a more compact chromatin structure. This prevents or reduces access to the transcription machinery, ultimately leading to lower or reduced *Mecp2* expression.

To build a hypothetical model of *Mecp2* regulation, it was necessary to identify regulatory proteins that have been proven or predicted to bind to *Mecp2* REs. **Table 6.1** summarizes proteins known to bind to the *Mecp2/MECP2* gene REs.

Table 6.1 Proteins known to bind to the *Mecp2/MECP2* promoter and intron 1 REs					
Promoter			Intron 1		
R1	R2	R3	R4	R5	R6
SP1 [5,22]; RNA Pol II [5,22,23]	SP1 [5]; NeuroD1 [24]; MeCP2(*)	CTCF (*)	unknown	unknown	CTCF (*)
TAF1, Nrf1, CTCF, C/EBP, CAP [23]; ngn1/3, STAT, Brn-3, Bcl6 [22]			SRP20/40, hnRNP, YB-1, FOX1, QK1, NOVA1 (§)		

*Preliminary *in silico* analyses by myself using ENCODE and/or CistromeDB

§ Splice factors determined by SF map *in silico* analysis (http://sfmap.technion.ac.il/)

The higher *Mecp2* transcript levels in neurons could possibly be driven by NSTFs (**Table 6.2**) or transcription activators such as MEF2A (**Appendix A3: Figure A1**) [25]. As a TATA-less promoter, *Mecp2* transcription is regulated by the SP-family TFs [5,22,23]. SP family members function in a cell type-specific manner, where SP4 is believed to be highly functional in neurons, and other SP proteins function in many cell types [26]. Therefore, differences in binding of SP-family proteins to the *Mecp2* promoter may contribute to neuron- and astrocyte-specific *Mecp2* transcript expression patterns.

Table 6.2 NSTFs and ASTFs: Potential recruitment to the *Mecp2/MECP2* promoter					
NSTFs			**ASTFs**		
TF	**Function**	**Evidence for binding to *Mecp2/MECP2***	**TF**	**Function**	**Evidence for binding to *Mecp2/MECP2***
NeuroD1	activator	*Mecp2*/ESC to neurons/CistromeDB/[24]	GLI1	activator	*Mecp2*/embryo/ CistromeDB/[27]
NeuroD6	activator	N/A	GLI2	activator/ repressor	*MECP2*/colon cancer/ CistromeDB/[28]
SP1	activator	[22]	GLI3	activator/ repressor	*MECP2*/colon cancer/ CistromeDB/[28]

SP4	activator	*MECP2*/ESC/ CistromeDB/[29]	OTX1	activator	*MECP2*/colon cancer/ CistromeDB/[28]
NHLH2	activator	N/A	GRHL1	activator	*MECP2*/colon cancer/ CistromeDB/[28]

*Evidence was collected from CistromeDB or other publications. N/A: Not available

6.3.2 Mecp2 gene regulation by ethanol exposure and withdrawal
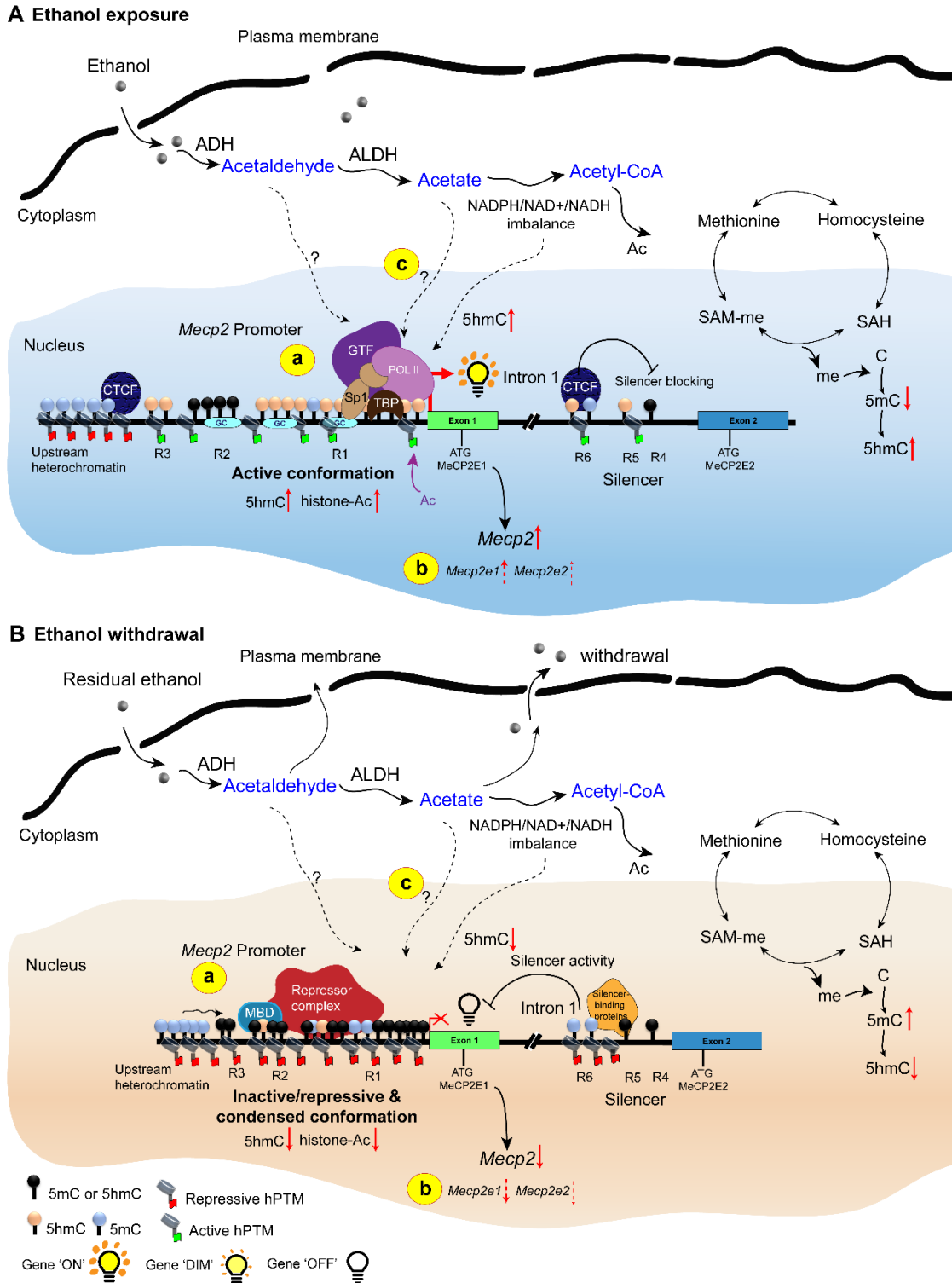
Figure 6.2 'Hypothetical model' of epigenetic and transcriptional regulation of *Mecp2* by ethanol exposure and withdrawal.

The figure illustrates a sequence of chemical reactions and events that occur in NSC after **A)** continuous ethanol exposure and **B)** ethanol withdrawal. **A)** Continuous ethanol exposure: **a**) ethanol enters into the cell results in DNA methylation changes at the *Mecp2* REs located in the *Mecp2* promoter (R1-R3) and intron 1 silencer element (R4-R6). The 5mC and 5hmC levels at specific REs were adapted from Chapter 4 [7]. Note that positioning of 5mC and 5hmC marks on CpGs is only representative. Hypothetically, DNA methylation changes may lead to other changes to the epigenetic signature at the REs mediated by hPTMs and the recruitment of protein complexes. DNA methylation and hPTM changes lead result in an active or more open conformation of the *Mecp2* promoter, resulting in the recruitment of RNA Pol II, and GTFs. CTCF may be protecting the active *Mecp2* promoter from the nearby heterochromatin, while DNA methylation changes and/or CTCF binding to the intron 1 silencer element may block the activity of the silencer. **b**) Ethanol-mediated changes to DNA methylation and other hypothetical changes to the REs have led to increased levels *Mecp2*/MeCP2. It is anticipated *Mecp2e1* and *Mecp2e2* transcripts could be upregulated. **c**) Ethanol is metabolized upon entry to the cell, which may have epigenetic effects such as on the methionine-homocysteine cycle that may change the levels 5mC, 5hmC, histone methylation and histone acetylation. **B)** Ethanol withdrawal: **a**) After ethanol withdrawal DNA methylation at the *Mecp2* REs was changed to a more repressive state and render a repressive *Mecp2* promoter signature. Lack of CTCF binding to the upstream promoter may cause crawling of nearby heterochromatin into the promoter region. The epigenetic signature of the intron 1 silencer element may influence silencer activity. Overall, the repressive signature and compact chromatin status reduce *Mecp2* transcription. **b**) These changes were associated with reduced levels of *Mecp2*/MeCP2 with potential reduction of *Mecp2e1* and *Mecp2e2* transcripts as well. **c**) The adverse effects after ethanol withdrawal may be a result of ethanol metabolites. Information and evidence for the binding of regulatory proteins to *Mecp2* REs are provided in Tables 6.1 and 6.2. *Mecp2* gene-specific and global DNA methylation levels were adapted from Chapter 4 [7].

As continuous ethanol exposure elevated *Mecp2* transcript levels in association with increased 5hmC and decreased 5mC at specific REs, we speculate that the *Mecp2* promoter region may have acquired a 'transcriptionally active' conformation and be less impacted by the intron 1

silencer element **(Figure 6.2A:a)**. Based on previous studies on *MECP2* regulation in human neurons [13], it is possible that CTCF binding to the upstream *Mecp2* promoter region may protect it from nearby heterochromatin regions, thereby maintaining it in an active conformation. We speculate that ethanol induces high 5hmC levels at the R1, likely favoring the recruitment of general transcription machinery and induce *Mecp2* expression. Potential CTCF binding to the intron 1 silencer element may act as a 'silencer blocker', inhibiting the activity of the silencer element. Together, this may contribute to the increased expression of *Mecp2* observed in differentiating NSC exposed to continuous ethanol exposure (Chapter 4) [7].

On the other hand, when ethanol is withdrawn, *Mecp2* expression was downregulated in association with increased 5mC and decreased 5hmC at specific REs. This observation suggests that the *Mecp2* promoter is likely in a repressed or inactive conformation with increased impact from the intron 1 silencer element **(Figure 6.2B:a)**. The reduced 5hmC levels at the promoter R1-R2 may recruit MBDs such as MeCP2, which in turn cross-talks with other repressor protein complexes containing regulatory proteins such as DNMTs, KMT, and HDAC. Together, they may be capable of changing the underlying hPTM signature of the *Mecp2* promoter to a repressive state by increasing histone methylation and decreasing histone acetylation. Formation of these complexes and repressive hPTMs prevent the access of TFs and RNA Pol II to the *Mecp2* promoter. Moreover, the increased 5mC at R6 may exert a silencing effect on the *Mecp2* promoter. Together, these mechanisms may contribute to the decreased expression of *Mecp2* observed in differentiating NSC after ethanol withdrawal (Chapter 4) [7].

Based on our and other studies [9,30], we speculate that the production of *Mecp2e1* transcripts could be more susceptible or sensitive to ethanol exposure than the production of *Mecp2e2* transcripts **(Figure 6.2A-B:b)**. This hypothesis can be evaluated in the future using qRT-

PCR with primers specific for *Mecp2e1* and *Mecp2e2* transcripts. It is likely that *Mecp2* splicing may have also been impacted by changes in DNA methylation (most probably at the intron 1 silencer element) and the associated epigenetic signature. However, we do not currently have sufficient evidence to show any impact of ethanol on *Mecp2* splicing in our system, which could be studied in the future.

In effect, it is the metabolites of ethanol that do the actual damage to cells *via* changing cellular chemical reactions, signaling pathways and gene expression [31]. As described in the introduction, alcohol metabolism produces acetaldehyde, H_2O_2, and acetate, which are among the major teratogens [32]. It is possible that DNA methylation and other associated changes to the epigenetic signature at the *Mecp2* REs may have been caused by metabolites of ethanol (**Figure 6.2A-B:c**). To test this possibility, future experiments could include treatments with acetaldehyde and acetate. Alternatively, ethanol treatment may have changed the levels of SAM, supplementation of which has been shown to attenuate ethanol-induced cellular changes [33]. Treatment with SAM, in the presence and absence of ethanol, may provide further insights into *Mecp2* deregulation by ethanol and its products.

6.3.3 Mecp2 gene regulation in male mouse neurons and astrocytes

We speculate that the chromatin conformation of the *Mecp2* promoter in male neurons that produce high levels of *Mecp2* transcripts may be in an active or open state (**Figure 6.3A; Appendix A3: Figure A1-A2**). While it is natural to believe that the *Mecp2* promoter in male astrocytes, which have lower *Mecp2* transcript levels may have a 'repressive' and condensed promoter conformation, it is possible it may simply have a 'less active' or repressive signature compared to neurons. As astrocytes show some level of transcriptional activity for *Mecp2,* we

speculate that the *Mecp2* promoter in astrocytes is 'less active' than 'repressive' mediated a combination of both active and repressive hPTMs **(Figure 6.3B)**.

I assumed that the CpGs that showed a positive correlation with *Mecp2* might be 5hmC-enriched, while the CpGs that showed a negative correlation with *Mecp2* transcript levels may be 5mC-enriched **(Chapter 5: Figure 5.4)**. In neurons, the *Mecp2* promoter is likely to be more 5hmC-enriched, which may attract active hPTMs and recruitment of the transcription machinery [34]. On the other hand, the *Mecp2* promoter in male astrocytes may have a less-active chromatin conformation. DNA methylation may cause reduced gene expression through the binding of MBD proteins such as MeCP2 which are known to act as epigenetic modulators due to their ability to fine-tune transcription through careful recruitment of protein partners such as DNMTs and HDACs [35]. In neurons, the upstream regions heterochromatin may be insulated by CTCF binding [13], to maintain the *Mecp2* promoter in an active conformation, while the opposite be expected in astrocytes. We also speculate that the activity of the intron 1 silencer element might be minimal in neurons when compared to astrocytes. These influences should be empirically validated in the future by the use of reporter assays. Moreover, the higher *Mecp2* expression in neurons may be driven by NSTFs that may have more potent activity in neurons than the ASTFs that may drive the lower *Mecp2* expression in astrocytes. The binding of the TFs and other regulatory complexes to the *Mecp2* promoter and intron 1 should be evaluated by ChIP using antibodies specific for these proteins, followed by qPCR with *Mecp2* gene-specific primers.
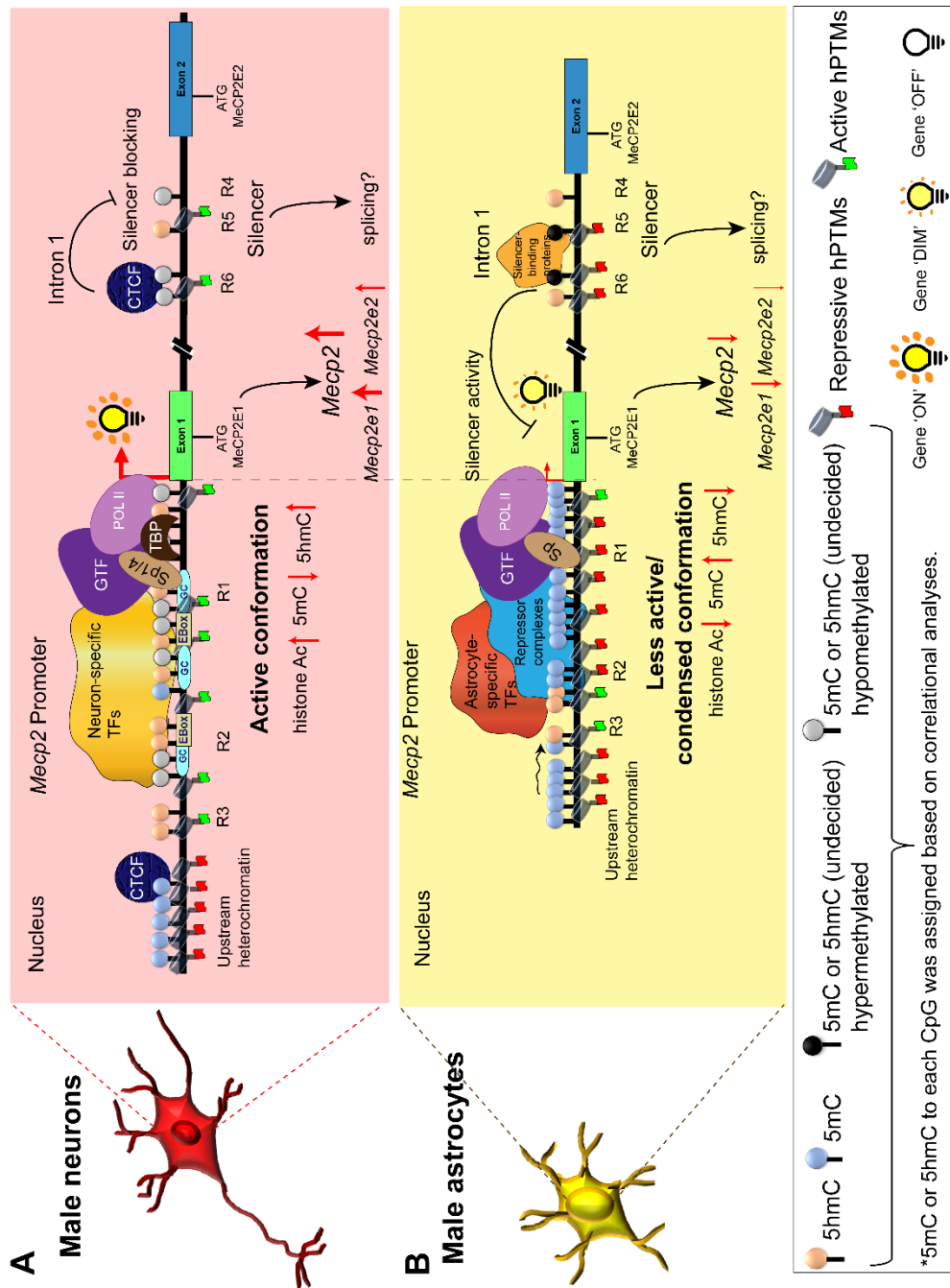
Figure 6.3 'Hypothetical models' of epigenetic and transcriptional regulation of *Mecp2* in male neurons and male astrocytes.

The figure illustrates potential *Mecp2* transcriptional regulation in **A)** male neurons and **B)** male astrocytes. DNA methylation at the *Mecp2* REs located at the promoter (R1-R3) and intron 1 silencer element (R4-R6) are different between them and 5mc/5hmC marks have been assigned

hypothetically based on correlation analyses reported in Chapter 5 (Figure 5.4). The CpGs with unclear methylation status were assigned hypermethylation or hypomethylation based on the Chapter 5 observations (Figure 5.3). Hypothetically, the *Mecp2* promoter in neurons may be in an active conformation mediated by DNA methylation, recruitment of transcription machinery and neuron-specific TFs. Astrocytes may have a less active and condensed promoter with astrocyte-specific TFs, increased 5mC, hypermethylation of CpGs and binding of repressor complexes. Moreover, DNA methylation at the intron 1 silencer element may influence its silencer activity. We speculate that the silencer activity may be blocked in male neurons by CTCF binding. In male astrocytes, silencer activity might further repress the *Mecp2* expression. Additionally, DNA methylation at the intron 1 silencer element may regulate *Mecp2* splicing. Evidence for the binding of regulatory proteins to *Mecp2* REs is provided in Tables 6.1 and 6.2.

In order to prove the role of these regulatory proteins, ChIP experiments should be done in neurons and astrocytes, followed by qPCR with primers-specific for the *Mecp2* promoter. To support the theory of an 'active *Mecp2* promoter in neurons', I did preliminary *in silico* ChIPseq data mining using CistromeDB. This preliminary analysis suggested the enrichment of active promoter markers at the *Mecp2* promoter in neurons **(Appendix A3: Figure A1)**. Therefore, in combination with the hypomethylation of the *Mecp2* promoter, the higher *Mecp2* transcript levels in neurons could be driven by the presence of active hPTMs (e.g., H3K27ac, H4K16ac, H3K4me2 and H3K4me3) [36] and neuronal transcription activators such as MEF2A [25]. The highest enrichment of these factors was observed in the proximity of the TSS found by Adachi *et al.* [5]. This is consistent with the H3K27ac levels (active hPTM) at the *Mecp2* promoter observed in NIH3T3 cells **(Appendix A3: Figure A1)**, which have lower *Mecp2* levels compared neurons and astrocytes (data not shown).

It is important to know whether higher *MECP2* transcript levels are observed in human neurons compared to astrocytes. To my knowledge, there are no studies conducted in human cell

types. As a first step, I used an *in silico* approach to indirectly ask this question. As no microarray or RNAseq data are available in human neurons and astrocytes, I mined ChIPseq data from human Neurons (SK-N-SH_RA: neuroblastoma cell line differentiated with retinoic acid) and human astrocytes (NH-A-Brain) from the ENCODE project. As not all the epigenetic markers were available for both neurons and astrocytes, I carefully incorporated ChIPseq data from relevant epigenetic marks to gain insight on *MECP2* expression **(Appendix A3: Figure A2; Table 2.1)**. The enrichment of hPTMs, EZH2, and POLR2A at the *MECP2* promoter in neurons, in contrast to astrocytes, suggested that *MECP2* expression in neurons. Moreover, the enrichment of H3K27ac and H3K9ac indicated that the expression of *MECP2* in astrocytes is still active, albeit at lower levels. This evidence, at least partly implies that there may be similar *Mecp2/MECP2* transcript expression patterns in neurons and astrocytes in mouse and humans. This suggests that the findings from mouse cells may be valid in human cells as well. In order to empirically test the hypothesis that *MECP2E1* and *MECP2E2* transcript expression is higher in human neurons than human astrocytes, cultured human neurons and astrocytes should be tested for *MECP2* transcript levels (qRT-PCR), DNA methylation at the REs (MeDIP, hMeDIP), and enrichment of hPTMs (ChIP). Another insight gained from this analysis on *MECP2* regulation is the association of CpG island with higher enrichment of H3K4me3 in both neurons and astrocytes. This observation is in agreement with the studies that have shown the role of zinc finger CXXC domain-containing proteins such as CFP1 in inducing H3K4me3 at CpG islands and thereby fine regulating the chromatin structure at the CpG island [37-39]. Therefore, another future experiment would be to study the binding of CFP1 at proximity to CpG island (R1) of *MECP2/Mecp2* promoter and its influence on H3K4me3 enrichment and promoter chromatin conformation.

DNA methylation can also regulate alternative splicing [35]. In our studies in NSC, we speculated that the DNA methylation status at R1 (promoter), R4, and R5 (intron 1 silencer element) might regulate *Mecp2* splicing. The potential of DNA methylation at the *Mecp2* intron 1 silencer element in regulating *Mecp2* splicing in neurons and astrocytes was brought up in Chapter 5 as well. Studying the role of DNA methylation in *Mecp2* splicing was out of the scope of my thesis. However, it is important to investigate the role of DNA methylation in *Mecp2* splicing, as this may modulate the expression of *Mecp2e1* and *Mecp2e2* in neurons and astrocytes. Shukla *et al.* (2011) demonstrated a 'kinetic coupling model' of co-transcriptional splicing *via* a DNA methylation- and CTCF-mediated mechanism [40]. I hypothesize that the loss of CTCF binding to exon 2 may occur in a DNA methylation-dependent manner leading to the generation of *Mecp2e1* transcripts by exon skipping (RNA Pol II skips exon 2) **(Figure 6.4A)**. DNA methylation-dependent binding of CTCF to exon 2 would pause RNA Pol II at exon 2, resulting in the inclusion of exon 2 to generate *Mecp2e2* transcript **(Figure 6.4B)**. A thorough analysis of 5mC and 5hmC distribution in the promoter, exon 1-2, exon-intron boundaries and intron 1 silencer element using oxBS-seq, MeDIP and hMeDIP will provide insights regarding whether DNA methylation can define *Mecp2* exons 1 and 2 as constitutive and alternate exons, respectively. Constitutive exons are enriched with 5hmC compared to alternatively spliced exons [41,42]. Testing this hypothesis would also require confirmation of CTCF binding through ChIP and EMSA studies that would involve the use of 5mC- and 5hmC- methylated probes. CTCF ChIP could be accompanied by testing RNA Pol II recruitment by sequential ChIP with a Ser2-P RNA pol II-specific antibody (elongation). The paused RNA Pol II should be phosphorylated at Ser5-P, which could be assessed using a Ser5-P RNA pol II-specific antibody. Comparison of this mechanism in neurons and

astrocytes may indicate whether DNA methylation and CTCF binding play any role in differential

Mecp2 splicing.
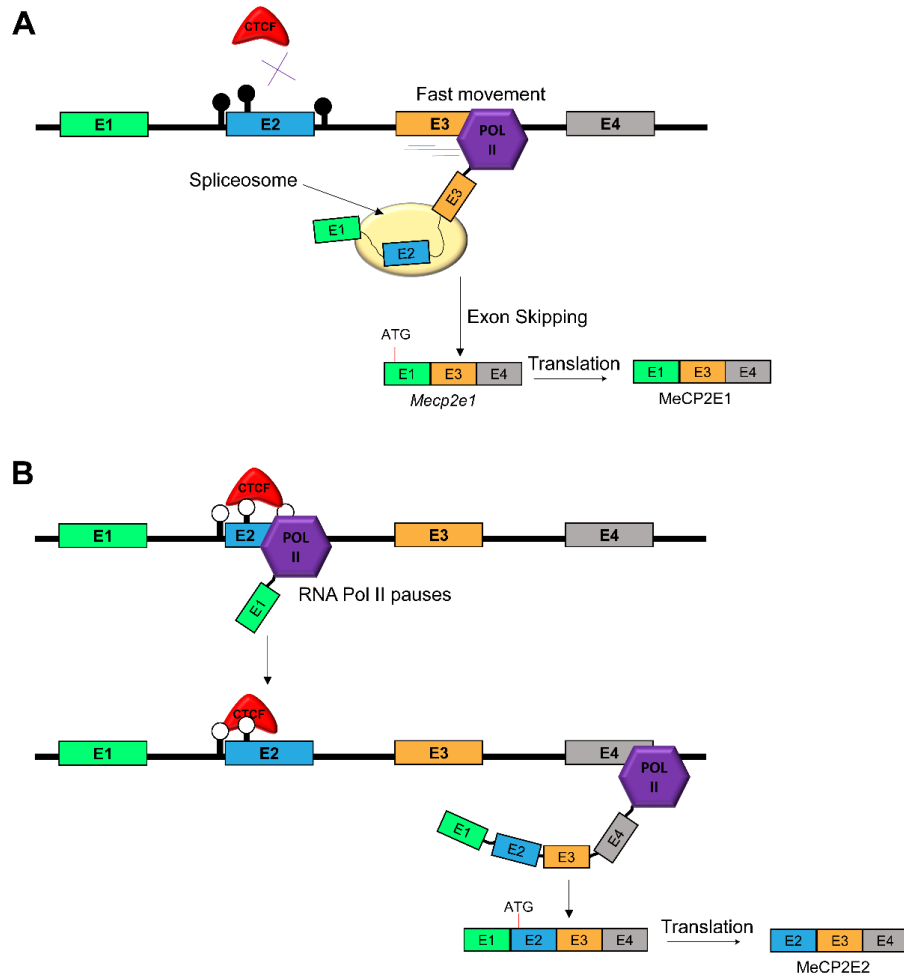
Figure 6.4 Proposed hypothetical mechanism for DNA methylation-dependent and CTCF binding-mediated co-transcriptional *Mecp2* splicing.

The model was developed based on [40,43]. **A)** Generation of the *Mecp2e1*/MeCP2E1 isoform. **B)** Generation of the *Mecp2e2*/MeCP2E2 isoform.

Even though this theory is widely-accepted model of DNA methylation-mediated regulation of alternative splicing, an alternate theory was proposed by Schor et al., 2013 [44]. According to this

theory, RNA Pol II pausing at proximity to an exon results in inclusion of that exon. How DNA methylation contributes to this mechanism is yet to be determined.

6.4 Potential challenges/limitations of the study and possible improvements

6.4.1 Investigation of MeCP2 isoforms at the protein level

In Chapter 3 and 4, we focused on the MeCP2E1 and total MeCP2, without differentiating MeCP2E1 and MeCP2E2 at protein levels. In Chapter 5, only *Mecp2e1* and *Mecp2e2* transcript levels were investigated. As MeCP2E1 and MeCP2E2 protein levels may change depending on how *Mecp2* transcripts are spliced during alternative splicing as well as post-transcriptional and post-translational regulation, future studies should include the analysis of MeCP2 isoform protein levels by western blotting using anti-MeCP2E1 and MeCP2E2 antibodies [8,45].

6.4.2 Investigation of sex-specific Mecp2 expression in NSC system

MeCP2-associated disorders, specifically RTT (females) and MDS (males), show a sex bias while FASD has been detected in both sexes, but with a higher incident in males. Ideally, we would have taken the sex of the embryos used in NSC culture into account in Chapter 3-4 studies. This was at least partly addressed by assessing sex-ratio in the Chapter 3 studies [9]. Future studies should be done in NSC isolated from male and female embryos separately to explore precise mechanisms underlying *Mecp2* extrinsic and intrinsic regulation. Moreover, ideally, we would have sequenced and verified the PCR products of *Sry* and *Il3* during male/female confirmation. The primers were obtained and PCR was carried out as described previously [46], and the expected PCR product sizes were observed ensuring the accuracy of the experiment.

Chapter 6

6.4.3 Cytotoxicity, cell fate, and global gene expression changes

One of the challenges of using decitabine or ethanol during NSC differentiation is their potential adverse effects on cell fate commitment and/or cell death [47-49]. Even though this challenge was partly addressed by quantification of cell type-specific markers of the major cell types (neurons, astrocytes, and oligodendrocytes), it is still possible that decitabine and ethanol may have caused changes to other minor cell types such as microglia. Therefore, a deeper analysis of cell fate commitment using a technique such as RNAseq may provide a detailed view of the cell fate changes as well as cell death through gene expression and cellular signaling pathway analysis. Employment of cell viability assays such as the LDH or MTT cytotoxicity assay may also address this limitation. Additionally, less cytotoxic DNA demethylating agents such as zebularine [50] could be used as an alternate for decitabine. As decitabine may not cause DNA demethylation in non-differentiating cells (Eg. neurons), valproate, a drug that functions independently of DNA replication/cell proliferation, could be used in neurons in the future studies.

The second challenge was the global effects of decitabine and ethanol treatment such as the observed changes in global 5mC and 5hmC levels. Global changes in gene expression and cell signaling, that might have caused by decitabine and ethanol, were out of the scope of the current study, which could be explored by RNAseq analysis followed by cellular pathway analysis in the future. Moreover, our study shows that MeCP2 protein expression was changed by decitabine and ethanol, but the consequences of its change were not analyzed or discussed. Possible consequences include altered MeCP2 binding to its target genes, cellular localization, global gene expression and chromatin architectural changes. Therefore, future studies should include IF and ChIPseq studies of MeCP2 to investigate any localization changes and binding to target genes.

Our study used an NSC differentiation system that is mainly directed towards glial differentiation in a mixed population of neurons, astrocytes, and oligodendrocytes. Even though our NSC differentiation model [7,9,51,52] may closely represent the cell composition in the brain; it would be beneficial to replicate our findings in a system that is directed towards neuronal differentiation. This could be achieved by replacing DMEM with neurobasal media to differentiate NSC towards neurons [53], followed by similar gene expression and DNA methylation analyses.

6.4.4 Advantages and disadvantages of studying DNA methylation in mixed populations of cells

Studying gene regulatory mechanisms in mixed populations of cell cultures or brain regions have certain advantages. The mixed cultures may replicate in part, the conditions, environment and cellular interactions (communications) experienced *in vivo*. Cells do not function in isolation. Particularly in the case of MeCP2-expressing cells, they rely heavily on external cues provided by nearby cells, through non-cell autonomous effects [54,55]. Therefore, investigating epigenetic mechanisms influenced by extrinsic insults such as drugs (decitabine) and alcohol in mixed cell populations can be beneficial. However, results obtained from a mixed population of cultured cells or brain regions may be biased towards a set of cell types or one cell type showing the most distinct changes, depending on the relative abundance of each cell type and the gene expression profiles of each cell type. Therefore, an ideal experimental setup would include parallel experiments being carried out with mixed cultures and homogenous cell populations. Individual homogenous cells can be obtained by cell sorting systems to separate individual cell types from a mixed culture or by isolating of individual cell types from the mouse embryonic forebrain (E14.5 for NSC) for gene expression and DNA methylation analyses. Flow cytometry with cell type-specific markers (TUB III for neurons, GFAP and S100B for astrocytes and OLIG2 and CNPase for oligodendrocytes)

can be used to sort individual cell types. However, one caveat to this approach is the sensitivity of differentiating embryonic cell types to mechanical cues used in cell sorting, and the adverse effects they may have on gene expression and regulation. Additionally, statistical and bioinformatic models can be used to extract cell type-specific transcriptome and epigenome data from heterogeneous populations of cells. This is referred to as deconvolution of cell type-specific epigenetic information from mixed populations of known cell types [56-58]. If such methods were to be applied in our studies of mixed cell cultures, the apriori DNA methylation signatures of neurons, astrocytes, and oligodendrocytes must be known. In the case of studies with drug treatments, it should be determined whether these treatments have changed the cellular composition, as such changes could affect the interpretation of the cell type-specific epigenetic data [59].

6.4.5 Differential 5mC, 5hmC, and CpH methylation analysis

The major DNA methylation analyses in Chapters 3 and 5 were done by bisulfite pyrosequencing, which does not differentiate between 5mC or 5hmC. To differentiate 5mC from 5hmC, methylated MeDIP and hMeDIP should be done in the future as reported in Chapter 4 [7]. In addition, gene expression differences between neurons and astrocytes were previously shown to be partly mediated through CpH methylation, where CpH methylation is relatively higher in neurons compared to glia [60]. Therefore, as a future direction, characterization of CpH methylation patterns could be carried out throughout the *Mecp2* gene in a sex- and cell type-specific manner, as described in other studies [61,62].

Chapter 6

6.4.6 Limitations of the quantification technique used in WB and dot blot

In both Chapters 3 and 4, we used X-ray films to detect WB and dot blot signals; films were then scanned and quantified using Photoshop software as reported previously [8,45,51]. However, X-ray film-based quantification is a semi-quantitative method with a narrow linear range and signals can be easily saturated. A more accurate method would be to use a digital imager (Gel Doc) to develop and detect the WB and dot blot signals, which do not depend on the use of X-ray films. A digital imager is able to capture signals in the linear dynamic range and will also identify the bands that are saturated. Therefore, the generation of a standard curve for protein or DNA quantification would be a more appropriate method.

In dot blot experiments, we have used MB to stain and quantify the total DNA content. I have attempted using a ds-DNA antibody to label total DNA during dot blot experiments. However, this was found to be less-reliable compared to MB labeling, as ds-DNA antibody signals were producing false positive signals in subsequent staining of the same membrane with 5mC or 5hmC antibodies. Even though some of the images of MB staining in Chapter 4 appear to be low in intensity, the quantification of the signal to background noise suggests the presence of DNA. In the future studies, ds-DNA antibody usage could potentially be optimized to reduce cross-reactions with other antibodies or the use of a higher amount of DNA to enhance the detection of total DNA by MB staining more accurately. Perhaps a digital imager system such as the Gel Doc may be used to detect lower intensity signals of MB staining.

6.5 Potential role of *Mecp2* promoter and intron 1 silencer element methylation in regulating expression of *Mecp2e1* and *Mecp2e2* transcripts in the adult mouse brain *in vivo*

In addition to the results outlined in Chapter 3-5, I also analyzed the DNA methylation patterns at the same *Mecp2* REs in adult mouse brain regions. This study aided in strengthening the data obtained from *in vitro* cell models *in vivo*. These data were part of a study published from our lab in 2014, to which I contributed as a co-author [8]. In this analysis, we investigated DNA methylation patterns at the *Mecp2* REs in seven mouse brain regions namely, olfactory bulb, striatum, cortex, hippocampus, thalamus, brain stem and cerebellum (**Figure 6.5; Table A3**). Among the analyzed REs, five CpG sites showed differential DNA methylation in these brain regions. They were R1:CpG5, R3:CpG2, R5:CpG1, R6:CpG1 and R6:CpG2. Therefore, it is possible that the differential *Mecp2* isoform expression observed in this study may be at least partly driven by differential DNA methylation of these CpGs. Additionally, all brain regions showed low promoter methylation (>10%) and high intron 1 silencer element methylation (~20-80%), similar to our studies in differentiating NSC, neurons, and astrocytes [[7,9], Chapter 5].

Similar to the studies presented in the thesis, I performed correlation analyses between *Mecp2e1* and *Mecp2e2* transcripts and average DNA methylation of all brain regions (representative of all brain regions) **(Figure 6.6A)** or individual brain regions **(Figure 6.6B)**. This analysis suggested that when all brain regions are considered collectively, R1:CpG1, R1:CpG10 and R3:CpG1 showed a positive/active correlation, while R1:CpG11 showed a negative/repressive correlation with *Mecp2e1* transcript levels. On the other hand, R1:CpG2, R1:CpG5, R1:CpG10 and R6:CpG2 showed a positive/active correlation with *Mecp2e2* transcript levels, while R3:CpG2 showed a repressive correlation with *Mecp2e2* transcript levels. It was highlighted that R3 CpGs displayed inverse correlations with *Mecp2e1* and *Mecp2e2* transcript levels implicating differential

regulatory mechanisms. This was also observed in studies presented in Chapter 3 in NSC [9]. Moreover, DNA methylation at R6 correlated only with *Mecp2e2* transcript levels raising the possibility that in the brain, R6 could be involved in regulation of the generation of *Mecp2e2* transcripts, which agrees with our initial hypothesis. Differential roles of DNA methylation in regulation of the generation of *Mecp2* transcripts in various cell types that were brought up in Chapters 3-4 and proven in Chapter 5 were further confirmed by the different correlations observed between the levels of *Mecp2e1* and *Mecp2e2* transcripts in various brain regions. Overall, the same *Mecp2* REs that were suggestive of regulating *Mecp2 in vitro* models were proven to be true in the adult brain *in vivo*.
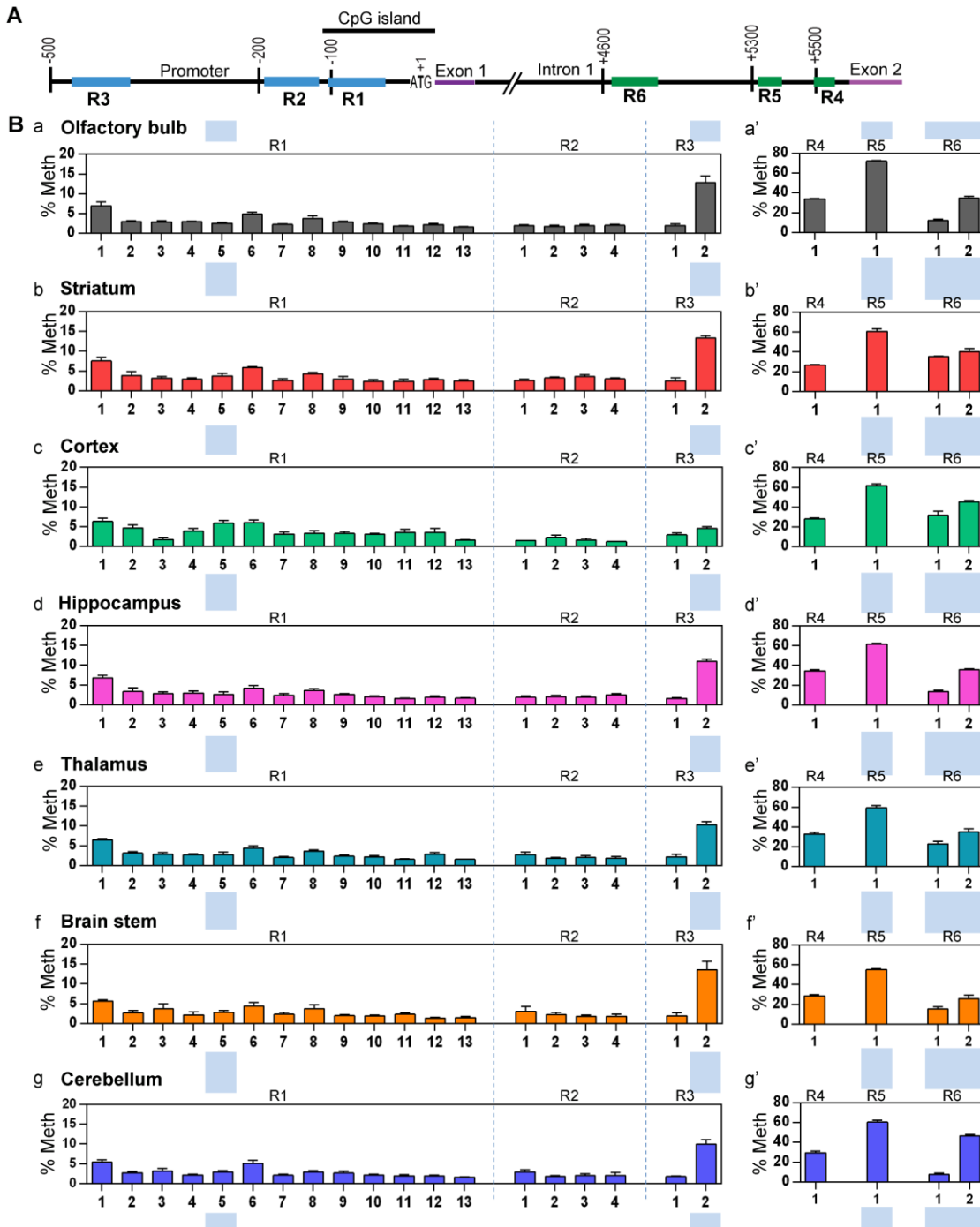
Figure 6.5 Bisulfite pyrosequencing analysis of DNA methylation status at the _Mecp2_ regulatory elements in adult murine brain regions.

A) Schematic representation of regions within the _Mecp2_ promoter (R1-R3) and intron 1 (R4-R6) (not drawn to scale) [9]. The first ATG of exon 1 is marked +1. **B)** The graphs represent the percentage methylation (% Meth) observed at the individual CpG sites within analyzed sequences

in seven indicated brain regions of adult mouse brain. a-a': olfactory bulb, b-b': striatum, c-c': cortex, d-d': hippocampus, e-e': thalamus, f-f': brain stem and g-g': cerebellum. N = 5 ± SEM. Blue shaded regions show statistically significant differences between brain regions. For a detailed comparison of statistical analysis, see Appendix: **Table A3**.

Figure and figure legend reprinted with permission from [8].
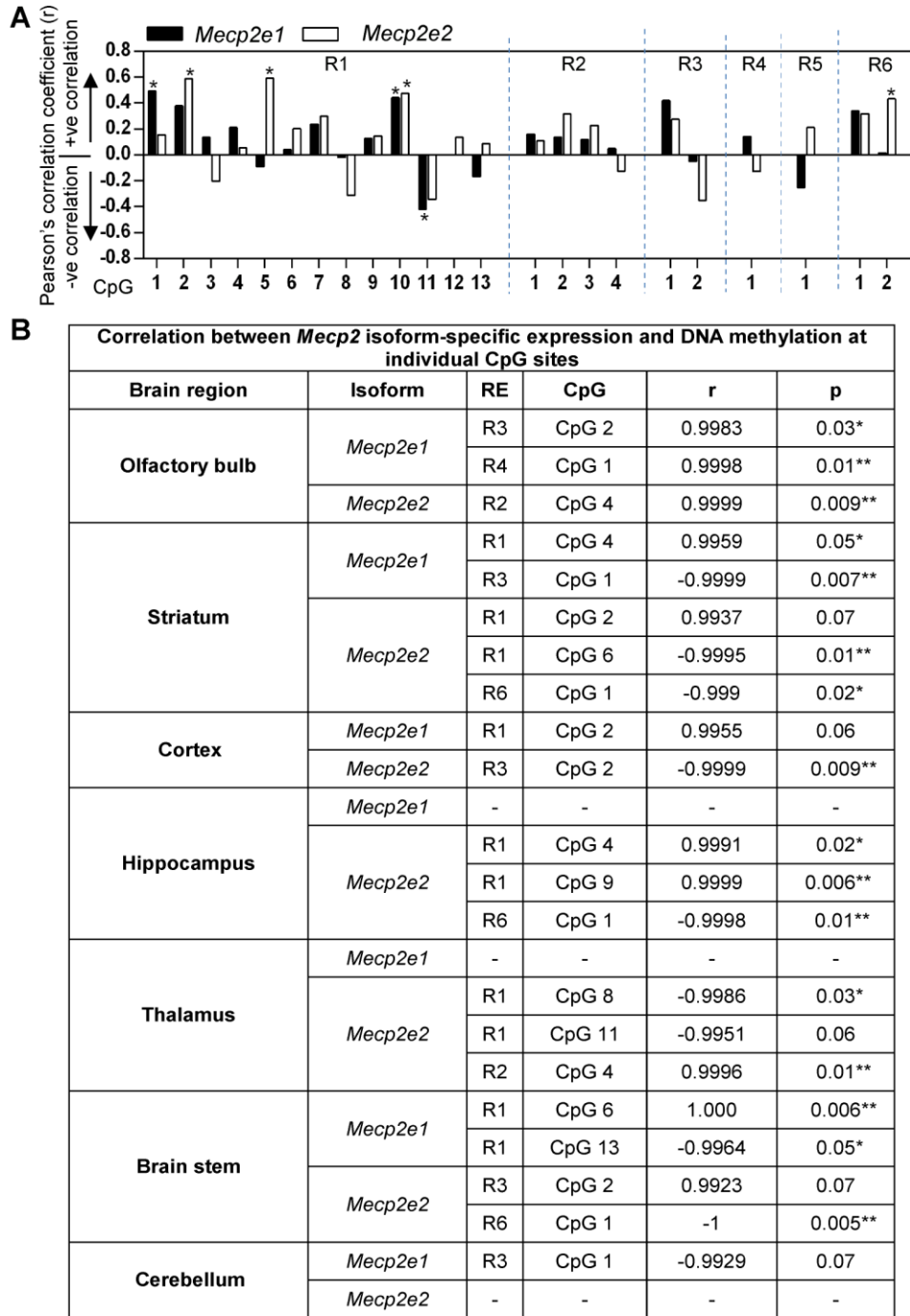
Figure 6.6 Correlation analyses between DNA methylation at the *Mecp2* regulatory elements and the expression of *Mecp2* isoforms in the adult mouse brain regions.

A) Graph represents Pearson's correlation coefficient (*r*) for correlation between DNA methylation at the *Mecp2* regulatory elements and *Mecp2e1* (black), and *Mecp2e2* (white) expression in seven

adult mouse brain regions. Stars (*) indicate statistical significance *P <0.05**. N = 3. **B)** Table representing Pearson's correlation coefficient (*r*) for correlation between DNA methylation at the *Mecp2* regulatory elements and expression of *Mecp2e1* (black), *and Mecp2e2* (white). Stars (*) indicate statistical significance *P <0.05**. N = 3.

Figure and figure legend reprinted with permission from [8].

6.6 Translating DNA methylation patterns at mouse *Mecp2* REs to human *MECP2* and implications of *Mecp2/MECP2* promoter methylation in neurological conditions in mouse models and human patients

6.6.1 Comparison of mouse Mecp2 and human MECP2 promoter CpGs

Conservation of CpGs and/or REs between mouse *Mecp2* and human *MECP2* promoters may determine how the knowledge obtained from mouse can be translated to human. Some of the CpGs found within the mouse *Mecp2* REs are absent in the human *MECP2* promoter and *vice versa* [9]. This comparison is further elaborated in **Figure 6.7A**. For instance, one of the R1 CpGs of the *Mecp2* promoter is missing in the human *MECP2* promoter. There are four extra CpGs in the human *MECP2* promoter between R1 and R2. Due to technical difficulties, seven CpGs between mouse R2 and R3 were not included in our bisulfite pyrosequencing analyses. Within the same regions (between R2 and R3), the human *MECP2* promoter has 22 CpGs, only 5 of which aligned with the mouse CpGs. Finally, among the two CpGs of the *Mecp2* R3, only one CpG has a corresponding CpG in the human *MECP2* promoter. Collectively, while some CpGs can be aligned between mouse and human promoters, there are a few CpGs that cannot be directly linked (**Figure 6.7A**). In addition, it is possible that either corresponding individual CpGs in the human *MECP2* promoter or entire REs (in relation to other epigenetic signatures) may contribute to *MECP2* regulation in human.

As a future direction of this project, I propose that the CpGs between R2 and R3 should be analyzed for DNA methylation. Moreover, to investigate the impact of the upstream promoter heterochromatin regions we discussed in the hypothetical models (section 6.3), more CpGs upstream of R3 should be included in future analyses.
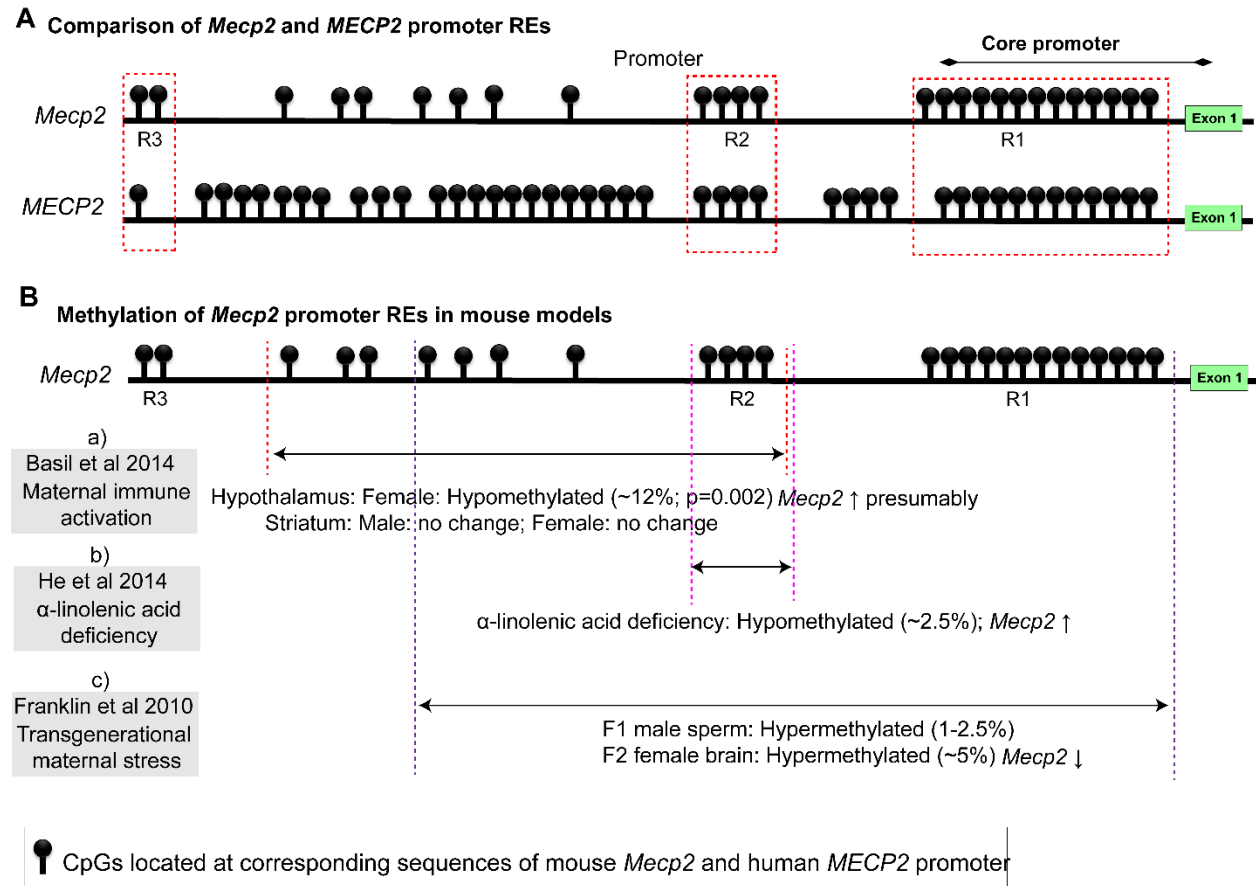
Figure 6.7 Comparison of *Mecp2* and *MECP2* promoter CpGs and their changes in mouse models of neurological conditions.

A) Comparison of CpGs and REs of the mouse *Mecp2* promoter reported in this thesis [7-9] and the human *MECP2* promoter [6,63,64]. The mouse *Mecp2* promoter REs are labeled as R1, R2, and R3 and marked by the red boxes. **B)** These illustrations show changes to the mouse *Mecp2* promoter methylation by three other studies on neurological conditions caused by **a**) maternal immune activation [65], **b**) α-linolenic acid deficiency [66] and **c**) transgenerational maternal stress

[67]. Changes to *Mecp2*/MeCP2 levels are also shown. ↑: upregulation/induction; ↓: downregulation/reduction.

6.6.2 Implications of Mecp2/MECP2 promoter methylation in neurological conditions and similarities/dissimilarities with our studies

My first two studies on *Mecp2* promoter methylation were published in 2013 [9] and 2015 [7], and I also contributed to DNA methylation studies at these REs *in vivo* in the mouse brain (2014) [8]. Since then, there were several studies published implicating *MECP2/Mecp2* promoter methylation in neurological disorders. I emphasize that our studies were the first reports connecting the expression of *Mecp2e1* and *Mecp2e2* transcripts and DNA methylation at the *Mecp2* REs [8,9]. To show the significance and application of our findings in neurological disorders, I have compared DNA methylation at the *Mecp2* promoter reported in other studies in mouse models (**Figure 6.7B**) and human patients with neurodevelopmental disorders (**Figure 6.8**).

6.6.2.1 Methylation of Mecp2 REs in mouse models of neurological disorders

Here, I compared DNA methylation changes at the *Mecp2* promoter REs reported in three mouse models with neurological symptoms caused by a) maternal immune activation (MIA) [65] b) α-linolenic acid-deficiency [66] and c) transgenerational maternal stress [67].

a) MIA model: In this study, MIA was induced by PolyI:C (a viral analog of dsRNA) at E9 [65]. The authors analyzed the average methylation of a *Mecp2* promoter region that overlaps with our R2 (**Figure 6.7B:a**) in hypothalamus and striatum in a sex-specific manner. The percent average DNA methylation at the *Mecp2* promoter in control (saline-treated) hypothalamus and striatum ranged between 25-35% in both male and female mice [65]. In contrast, our study of adult mouse

striatum (mixed sexes) showed less than 5% methylation at R2 **(Figure 6.5B)** [8]. In females, MIA caused *Mecp2* promoter hypomethylation by 12% in the hypothalamus **(Figure 6.7B:a)**. The authors speculated that the role of DNA methylation in *Mecp2* regulation in the MIA model was repressive, thus predicting that *Mecp2* expression may be induced by MIA. They also showed that omega-3 supplementation at E9 was able to reverse the observed *Mecp2* promoter hypomethylation caused by MIA [68]. Therefore, it is hopeful that nutritional supplementation could potentially be used to restore *Mecp2*/*MECP2*/MeCP2 deregulation to some extent. In support of this notion, omega-3 supplementation had been partially successful in reducing the clinical severity of RTT patients [69,70], while it is unknown whether these improvements were caused by direct changes in *MECP2* expression or immunological compensation.

b) α-linolenic acid-deficiency model: This study analyzed *Mecp2* promoter region which overlapped with our R2 and the intron 1 that overlapped with our silencer element [66] **(Figure 6.7B:b)**. Control brain samples analyzed at P19 showed ~5% and ~3% average methylation levels at the *Mecp2* promoter (R2) and intron 1 respectively. While the promoter methylation levels are in accordance with our studies, the lower (3%) intron 1 methylation was a significant deviation from our studies which showed 20-80% average methylation in the adult mouse brain and embryonic cell types [7-9]. α-linolenic acid is a precursor in the omega-3 elongation pathway. In the α-linolenic acid deficient-mouse brain, *Mecp2* expression was reduced in association with reduced *Mecp2* promoter (R2) methylation (~2.5%), but no change in intron 1 methylation **(Figure 6.7B:b)**. This observation suggests a positive correlation (active role) between *Mecp2* promoter methylation and *Mecp2* expression, similar to the observations made in our ethanol studies described in Chapter 4 [7] and thus further strengthens our work. Both *Mecp2* expression and promoter hypomethylation were restored after α-linolenic acid supplementation. They also

provided evidence on the impact of nutrition supplementation on *Mecp2* expression in the mouse brain as the *Mecp2* expression was increased upon α-linolenic acid supplementation.

c) Transgenerational maternal stress model: In our ethanol studies, we suggested that the epigenetic memory of an environmental insult that occurs at the *Mecp2* REs as DNA methylation changes are carried over even after the insult is removed. This transgenerational maternal stress model supports the concepts of epigenetic memory [67]. The *Mecp2* promoter regions analyzed in this study overlapped with R1 and R2 and include additional four CpGs upstream of R2 **(Figure 6.7B:c)**. Prenatal maternal stress caused *Mecp2* promoter (R1-R2) hypermethylation (1-2.5%) in F1-sperm, which was transmitted trans-generationally to the F2-brain of female offspring as *Mecp2* promoter hypermethylation (~5%) and reduced MeCP2 expression **(Figure 6.7B:c)** [67]. Therefore, R1-R2 methylation seems to play a repressive role in the F2 female brain. Moreover, the *Mecp2* promoter methylation levels of control sperm ranged between ~2-8% in agreement with our studies in NSC, neurons, astrocytes and mouse brain. However, control F2 female brain showed ~10-50% promoter methylation which did not agree with our studies, perhaps due to the differences in sex.

Taken together the three studies described here and our studies suggest that depending on the developmental stage, genetic background, treatments, sex and perhaps due to many other environmental factors, the role of the promoter R2 may be either repressive [9,65,67] or active [7,66], and the role of R1 methylation may be repressive [67] or active [7]. Overall, these studies further validate and support the importance of the REs chosen in our studies.

6.6.2.2 Methylation of MECP2 REs in human patients with neurological conditions

Translation of the data obtained in our studies in mouse cells to human patients is the ultimate goal. Therefore, I compared the mouse *Mecp2* REs used in our studies with human *MECP2* promoter methylation changes reported in patients with a) Autism and Down syndrome [6], b) RTT [63], and c) FASD [64].

a) Autism and Down syndrome: This study was pioneering work and showed that *MECP2* promoter methylation is a 'quantitative epigenotype', which set the basis for our studies. The *MECP2* promoter region analyzed contained 15 CpGs that overlapped with our *Mecp2* promoter R3 (**Figure 6.8A**). In control male brain, *MECP2* promoter methylation ranged between 0-5%, in agreement with the lower DNA methylation levels we observed in our studies on mouse NSC, neurons, astrocytes and mouse brain. The human *MECP2* promoter was significantly hypermethylated by ~2.5% in Autism and ~1% Down syndrome patients, when average methylation of 15 CpGs was considered. This observation suggested a repressive role of DNA methylation at the *MECP2* promoter in the human male brain. In a subsequent study, the Nagarajan group extended their analyses to include 200 bp upstream of R3 to interrogate the role of an insulator element regulated by CTCF and DNA methylation in *MECP2* regulation in autism and neurons [13]. I hypothesize that the region upstream of the *Mecp2* promoter R3 could potentially be a region of heterochromatin characterized by high DNA methylation and repressive hPTMs, as shown in our hypothetical models (**Section 6.3**). As these two studies included some CpGs, not investigated in our studies in mouse cells and brain, our future work should extrapolate DNA methylation analysis to this upstream heterochromatin region. Together, this may further establish *Mecp2* promoter methylation as a 'quantitative epigenotype' that determines the transcript levels of *Mecp2e1* and *Mecp2e2* in mouse brain cell types.
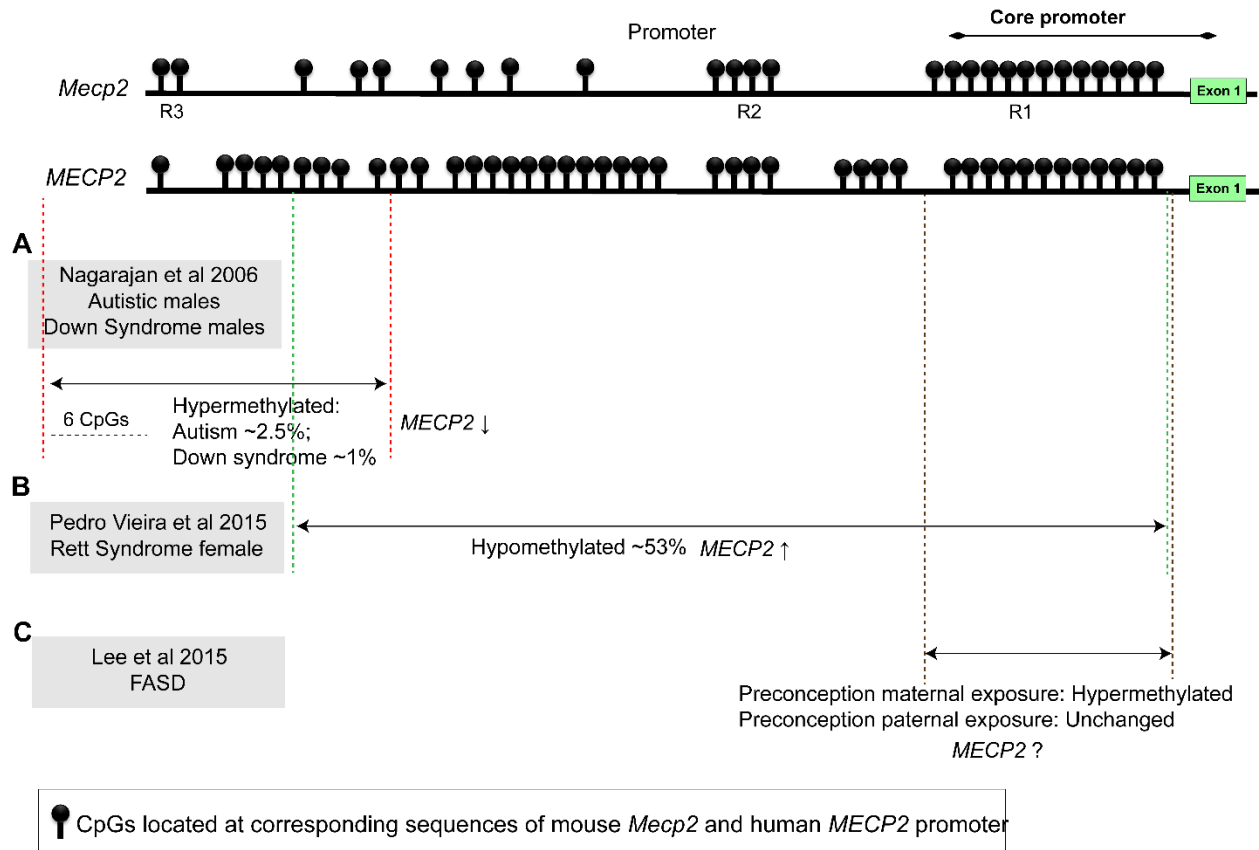
Figure 6.8 Comparison of mouse *Mecp2* REs and human *MECP2* promoter changes reported in patients with neurological disorders.

The schematics show the mouse *Mecp2* promoter REs reported in our studies (Chapters 3-5; [7-9]) and the corresponding *MECP2* promoter. Changes to *MECP2* promoter methylation in three neurological conditions are shown as follows: **A)** Autistic males and Down syndrome males [6], **B)** an RTT female [63], and **C)** FASD patients [64]. The changes to *MECP2* expression depicted as ↑: upregulation/induction; ↓: downregulation/reduction.

b) RTT: The *MECP2* CpG island analyzed in a female RTT patient overlapped with our *Mecp2* R1 and R2 (**Figure 6.8B**). She was a rare RTT patient who showed hypomethylated *MECP2* promoter (~53%) and increased *MECP2* expression in leucocytes [63]. This observation suggested a negative correlation (repressive) between DNA methylation and *MECP2* expression, similar to our observations for *Mecp2* R1 and R2 in male neurons and astrocytes. Based on this repressive

role of R1/R2 DNA methylation observed in human female leucocytes, we hypothesize that DNA methylation at the mouse *Mecp2* R1/R2 may also play a repressive role in female cell types isolated from mouse brain.

c) FASD: This study was highly relevant to our work presented in Chapter 4 as it was related to *MECP2* and FASD [64]. The *MECP2* promoter region they examined overlapped with our R1 (**Figure 6.8C**). Using a method that involves methylation-specific endonuclease digestion followed by qRT-PCR, they analyzed *MECP2* promoter methylation in blood collected from babies whose parents had consumed alcohol preconception. *MECP2* promoter hypermethylation was observed in maternal alcohol exposure but not paternal alcohol exposure. Unfortunately, they did not report the expression levels of *MECP2* in their study nor did their strategy differentiate between 5mC and 5hmC. Based on the general repressive role of DNA methylation, one might postulate that *MECP2* expression was reduced by preconception maternal alcohol exposure. Based on our ethanol studies, it is also possible the hypermethylation may represent an increase in 5hmC levels associated with increased *MECP2*. Therefore, it is of great importance that DNA methylation studies be accompanied with *MECP2* expression analyses to accurately interpret the 'epigenotype.' This study also indicated that the influence of maternal alcohol consumption is more critical than paternal alcohol consumption due to the interactions between the mother and the fetus during the pregnancy [64]. The preconception effects of alcohol on the fetus show transgenerational epigenetic memory. This study provides some hope that the data obtained in mouse NSC could potentially be translated to human studies. While confirmation or further investigation of mechanisms in human FASD patients is the ultimate goal, access to human patient samples (blood or postmortem brain samples) is challenging and will likely require collaborative studies.

Chapter 6

Collectively, these studies show similarities in the *Mecp2*-DNA methylation correlations observed in our studies of mouse brain cells. They also provide valuable insights regarding sex-specific *MECP2* promoter methylation changes that are helpful in extrapolating some of the knowledge gaps we had in the studies presented in my thesis.

6.7 Impact and knowledge translation: Potential of promoter hypomethylation to induce *MECP2* expression

In Chapter 3, I demonstrated that treatment with decitabine upregulates *Mecp2e1*/MeCP2E1, through demethylation of the *Mecp2* REs [9]. DNA demethylating agents that are capable of inducing *Mecp2/MECP2* expression may be helpful in the treatment of RTT, presumably through X-chromosome reactivation (XCR) and/or demethylation of the REs. According to a previous study [71], and our studies presented in Chapter 5, it is possible that *Mecp2/MECP2* may undergo XCI-escape in most of the cell types in the brain. However, it is unknown whether XCI-escape occurs in 100% of the cells, or whether XCI-escape is skewed, similar to XCI skewing observed in MeCP2-associated disorders such as RTT [72-74]. Therefore, there is a possibility that a DNA demethylating agent may be able to cause XCR and induce *MECP2* expression. Fibroblasts isolated from RTT patients did not respond to 5-aza-2′-deoxycytidine at lower concentrations [75], possibly due to its inability to fully reactivate inactive the X chromosome (Xi) [76]. In such cases, hydroxyurea, which is a ribonucleotide reductase (RNR)-inhibitor, can be used simultaneously with 5-aza-2′-deoxycytidine to increase incorporation of 5-aza-2′-deoxycytidine to DNA [76]. Therefore, an extension of the current study would be to treat cells isolated from RTT patients with decitabine and hydroxyurea for different periods of time, followed by an analysis of *MECP2*/MeCP2 expression and DNA methylation at

the REs. RTT patient-derived fibroblasts in Yu *et al.* (2011) [77] were also treated with other DNMT inhibitors zebularine and RG108, as well as HDAC inhibitors TSA and RG108 alone and in combination. None of these treatments were able to re-activate the wild-type *MECP2* from the Xi. The RTT patient contained a truncation mutation (1155del32). As re-activate the Xi might be the most appropriate way to induce *MECP2* expression in such cases (assuming incomplete XCI-escape of *MECP2*), hydroxyurea treatment discussed above [76] could potentially be used in combination with DNA demethylating agents. In contrast, in the cases of RTT-causing *MECP2* non-sense mutations (e.g., R294X, R270X, and R168X), cells can be treated with aminoglycosides such as gentamycin, NB54/NB84 to suppress or read-through the mutant STOP codon [78,79]. In case these treatments do not restore MeCP2 to normal levels, decitabine or other DNA demethylating agents could potentially be used to reactivate the silenced *MECP2*. From a therapeutic point of view, it is questionable whether treatments with decitabine or other DNA demethylating agents would be successful in elevating *Mecp2*/MeCP2 expression in differentiated cell types (E.g., neurons), in later developmental stages, and in adults. Therefore, as a future direction, we suggest treatment of male and female neurons, astrocytes and NSC isolated from different stages of brain development to investigate the ability of decitabine to induce *Mecp2*/MeCP2 expression.

Reduced gene expression by promoter hypermethylation is observed in ASD, and many other studies have used decitabine to induce the expression of genes such as *RORA* (5 µM decitabine for 48 h) [4] and *SHANK3* (1-5 µM decitabine for 14 days [80]. For ASD cases with reduced *MECP2* expression by promoter hypermethylation [81], a similar experimental approach could be used. Lymphocytes from both male and female ASD patients (twins and siblings) can be obtained through the Autism Consortium and the Autism genetic resource exchange (AGRE)

Repository. Cultured ASD and control lymphocytes can be treated with decitabine and hydroxyurea as per previous studies [76]. They can be then tested for expression levels of *MECP2* transcripts, promoter methylation and global DNA methylation and gene expression changes. These studies may provide insights into whether decitabine can be used to re-activate *MECP2 via* promoter demethylation in both male and female patients.

Can this knowledge on the effect of DNA methylation on *Mecp2/MECP2* be used in MDS? In a study conducted in lens epithelial cells, zebularine (a DNMT inhibitor) attenuated MeCP2 expression in a time- and dose-dependent manner [82]. Similarly, in human fetal retinal pigment epithelial cells, 5-aza-2′-deoxycytidine reduced MeCP2 expression in a dose-dependent manner [83]. It is possible that depending on the cell type, the effect of DNA demethylating agents and/or DNMT inhibitors on MeCP2 expression may be different. Therefore, there is some hope that knowledge of DNA methylation may be useful in MDS treatments.

6.8 Concluding remarks

Collectively, for the first time, we provide evidence on potential regulation of *Mecp2e1* and *Mecp2e2* transcript expression by DNA methylation at six REs found within the *Mecp2* promoter and intron 1 silencer element in differentiating NSC, neurons, astrocytes, and adult mouse brain regions. Comparison with studies in mouse models and human patients suggested that DNA methylation changes at the REs are biologically relevant. DNA methylation signatures at these REs may, therefore, be used to establish as a 'quantitative epigenotype' for MeCP2-associated disorders as well as mouse brain cell types. The knowledge gained from this study may also be helpful in the perusal of studies to test the potential of DNA demethylating agents such as decitabine to modulate *MECP2* expression in MeCP2-associated neurological disorders.

Chapter 6

6.9 References

1. Mellen M, Ayata P, Dewell S, Kriaucionis S, Heintz N (2012) MeCP2 binds to 5hmC enriched within active genes and accessible chromatin in the nervous system. Cell 151: 1417-1430.

2. Laird PW (2010) Principles and challenges of genome-wide DNA methylation analysis. Nature Reviews Genetics 11: 191-203.

3. Huang Y-Z, Sun J-J, Zhang L-Z, Li C-J, Womack JE, Li Z-J, Lan X-Y, Lei C-Z, Zhang C-L, et al. (2014) Genome-wide DNA methylation profiles and their relationships with mRNA and the microRNA transcriptome in bovine muscle tissue (Bos taurine). Scientific reports 4: 6546.

4. Nguyen A, Rauch TA, Pfeifer GP, Hu VW (2010) Global methylation profiling of lymphoblastoid cell lines reveals epigenetic contributions to autism spectrum disorders and a novel autism candidate gene, RORA, whose protein product is reduced in autistic brain. The FASEB Journal 24: 3036-3051.

5. Adachi M, Keefer EW, Jones FS (2005) A segment of the Mecp2 promoter is sufficient to drive expression in neurons. Hum Mol Genet 14: 3709-3722.

6. Nagarajan RP, Hogart AR, Gwye Y, Martin MR, LaSalle JM (2006) Reduced MeCP2 expression is frequent in autism frontal cortex and correlates with aberrant MECP2 promoter methylation. Epigenetics : official journal of the DNA Methylation Society 1: e1-11.

7. Liyanage VR, Zachariah RM, Davie JR, Rastegar M (2015) Ethanol deregulates Mecp2/MeCP2 in differentiating neural stem cells via interplay between 5-methylcytosine and 5-hydroxymethylcytosine at the Mecp2 regulatory elements. Exp Neurol 265: 102-117.

8. Olson CO, Zachariah RM, Ezeonwuka CD, Liyanage VR, Rastegar M (2014) Brain region-specific expression of MeCP2 isoforms correlates with DNA methylation within Mecp2 regulatory elements. PLoS One 9: e90645.

9. Liyanage VR, Zachariah RM, Rastegar M (2013) Decitabine alters the expression of Mecp2 isoforms via dynamic DNA methylation at the Mecp2 regulatory elements in neural stem cells. Mol Autism 4: 46.

10. Ndlovu MN, Denis H, Fuks F (2011) Exposing the DNA methylome iceberg. Trends Biochem Sci 36: 381-387.

11. Booth MJ, Branco MR, Ficz G, Oxley D, Krueger F, Reik W, Balasubramanian S (2012) Quantitative sequencing of 5-methylcytosine and 5-hydroxymethylcytosine at single-base resolution. Science 336: 934-937.

12. Kamstra JH, Sales LB, Aleström P, Legler J (2017) Differential DNA methylation at conserved non-genic elements and evidence for transgenerational inheritance following developmental exposure to mono(2-ethylhexyl) phthalate and 5-azacytidine in zebrafish. Epigenetics & Chromatin 10: 20.

13. Nagarajan RP, Patzel KA, Martin M, Yasui DH, Swanberg SE, Hertz-Picciotto I, Hansen RL, Van de Water J, Pessah IN, et al. (2008) MECP2 promoter methylation and X chromosome inactivation in autism. Autism Res 1: 169-178.

14. MacDonald WA (2012) Epigenetic mechanisms of genomic imprinting: common themes in the regulation of imprinted regions in mammals, plants, and insects. Genetics research international 2012.

15. Klochkov D, Rincón-Arano H, Ioudinkova ES, Valadez-Graham V, Gavrilov A, Recillas-Targa F, Razin SV (2006) A CTCF-Dependent Silencer Located in the Differentially Methylated Area May Regulate Expression of a Housekeeping Gene Overlapping a Tissue-Specific Gene Domain. Molecular and Cellular Biology 26: 1589-1597.

16. Spruijt CG, Gnerlich F, Smits AH, Pfaffeneder T, Jansen PW, Bauer C, Munzel M, Wagner M, Muller M, et al. (2013) Dynamic readers for 5-(hydroxy)methylcytosine and its oxidized derivatives. Cell 152: 1146-1159.

17. Iurlaro M, Ficz G, Oxley D, Raiber EA, Bachman M, Booth MJ, Andrews S, Balasubramanian S, Reik W (2013) A screen for hydroxymethylcytosine and formylcytosine binding proteins suggests functions in transcription and chromatin regulation. Genome Biol 14: R119.

18. Yildirim O, Li R, Hung JH, Chen PB, Dong X, Ee LS, Weng Z, Rando OJ, Fazzio TG (2011) Mbd3/NURD complex regulates expression of 5-hydroxymethylcytosine marked genes in embryonic stem cells. Cell 147: 1498-1510.

19. Cahoy JD, Emery B, Kaushal A, Foo LC, Zamanian JL, Christopherson KS, Xing Y, Lubischer JL, Krieg PA, et al. (2008) A transcriptome database for astrocytes, neurons, and oligodendrocytes: a new resource for understanding brain development and function. J Neurosci 28: 264-278.

20. Mao XR, Moerman-Herzog AM, Chen Y, Barger SW (2009) Unique aspects of transcriptional regulation in neurons--nuances in NFkappaB and Sp1-related factors. J Neuroinflammation 6: 16.

21. Zhang Y, Chen K, Sloan SA, Bennett ML, Scholze AR, O'Keeffe S, Phatnani HP, Guarnieri P, Caneda C, et al. (2014) An RNA-sequencing transcriptome and splicing database of glia, neurons, and vascular cells of the cerebral cortex. J Neurosci 34: 11929-11947.

22. Liu J, Francke U (2006) Identification of cis-regulatory elements for MECP2 expression. Hum Mol Genet 15: 1769-1782.

23. Singh J, Saxena A, Christodoulou J, Ravine D (2008) MECP2 genomic structure and function: insights from ENCODE. Nucleic Acids Res 36: 6035-6047.

24. Pataskar A, Jung J, Smialowski P, Noack F, Calegari F, Straub T, Tiwari VK (2016) NeuroD1 reprograms chromatin and transcription factor landscapes to induce the neuronal program. EMBO J 35: 24-45.

25. Akhtar MW, Kim M-S, Adachi M, Morris MJ, Qi X, Richardson JA, Bassel-Duby R, Olson EN, Kavalali ET, et al. (2012) In Vivo Analysis of MEF2 Transcription Factors in Synapse Regulation and Neuronal Survival. PLOS ONE 7: e34863.

26. Johar K, Priya A, Dhar S, Liu Q, Wong-Riley MT (2013) Neuron-specific specificity protein 4 bigenomically regulates the transcription of all mitochondria-and nucleus-encoded cytochrome c oxidase subunit genes in neurons. Journal of neurochemistry 127: 496-508.

27. Peterson KA, Nishi Y, Ma W, Vedenko A, Shokri L, Zhang X, McFarlane M, Baizabal JM, Junker JP, et al. (2012) Neural-specific Sox2 input and differential Gli-binding affinity provide context and positional information in Shh-directed neural patterning. Genes Dev 26: 2802-2816.

28. Yan J, Enge M, Whitington T, Dave K, Liu J, Sur I, Schmierer B, Jolma A, Kivioja T, et al. (2013) Transcription factor binding in human cells occurs in dense clusters formed around cohesin anchor sites. Cell 154: 801-813.

29. Gertz J, Savic D, Varley KE, Partridge EC, Safi A, Jain P, Cooper GM, Reddy TE, Crawford GE, et al. (2013) Distinct properties of cell-type-specific and shared transcription factor binding sites. Mol Cell 52: 25-36.

30. Warita K, Mitsuhashi T, Ohta K, Suzuki S, Hoshi N, Miki T, Takeuchi Y (2013) Gene expression of epigenetic regulatory factors related to primary silencing mechanism is less susceptible to lower doses of bisphenol A in embryonic hypothalamic cells. J Toxicol Sci 38: 285-289.

31. Koop DR (2006) Alcohol metabolism's damaging effects on the cell. Alcohol Res Health 29: 274-280.

32. Liyanage VR, Curtis K, Zachariah RM, Chudley AE, Rastegar M (2017) Overview of the Genetic Basis and Epigenetic Mechanisms that Contribute to FASD Pathobiology. Curr Top Med Chem 17: 808-828.

33. Kharbanda KK, Bardag-Gorce F, Barve S, Molina PE, Osna NA (2013) Impact of Altered Methylation in Cytokine Signaling and Proteasome Function in Alcohol and Viral-Mediated Diseases. Alcoholism: Clinical and Experimental Research 37: 1-7.

34. Liyanage VRB, Zachariah RM, Delcuve GP, Davie JR, Rastegar M (2012) New Developments in Chromatin Research: An Epigenetic Perspective. In: Simpson NM,

Stewart VJ, editors. New Developments in Chromatin Research: Nova Science Publishers pp. 29-58.

35. Liyanage VR, Jarmasz JS, Murugeshan N, Del Bigio MR, Rastegar M, Davie JR (2014) DNA modifications: function and applications in normal and disease States. Biology (Basel) 3: 670-723.

36. Telese F, Ma Q, Perez PM, Notani D, Oh S, Li W, Comoletti D, Ohgi KA, Taylor H, et al. (2015) LRP8-Reelin-Regulated Neuronal Enhancer Signature Underlying Learning and Memory Formation. Neuron 86: 696-710.

37. Blackledge NP, Thomson JP, Skene PJ (2013) CpG island chromatin is shaped by recruitment of ZF-CxxC proteins. Cold Spring Harb Perspect Biol 5: a018648.

38. Clouaire T, Webb S, Skene P, Illingworth R, Kerr A, Andrews R, Lee JH, Skalnik D, Bird A (2012) Cfp1 integrates both CpG content and gene activity for accurate H3K4me3 deposition in embryonic stem cells. Genes Dev 26: 1714-1728.

39. Thomson JP, Skene PJ, Selfridge J, Clouaire T, Guy J, Webb S, Kerr AR, Deaton A, Andrews R, et al. (2010) CpG islands influence chromatin structure via the CpG-binding protein Cfp1. Nature 464: 1082-1086.

40. Shukla S, Kavak E, Gregory M, Imashimizu M, Shutinoski B, Kashlev M, Oberdoerffer P, Sandberg R, Oberdoerffer S (2011) CTCF-promoted RNA polymerase II pausing links DNA methylation to splicing. Nature 479: 74-79.

41. Khare T, Pai S, Koncevicius K, Pal M, Kriukiene E, Liutkeviciute Z, Irimia M, Jia P, Ptak C, et al. (2012) 5-hmC in the brain is abundant in synaptic genes and shows differences at the exon-intron boundary. Nature structural & molecular biology 19: 1037-1043.

42. Maor GL, Yearim A, Ast G (2015) The alternative role of DNA methylation in splicing regulation. Trends in Genetics 31: 274-280.

43. Shukla S, Oberdoerffer S (2012) Co-transcriptional regulation of alternative pre-mRNA splicing. Biochim Biophys Acta 1819: 673-683.

44. Schor IE, Fiszbein A, Petrillo E, Kornblihtt AR (2013) Intragenic epigenetic changes modulate NCAM alternative splicing in neuronal differentiation. The EMBO Journal 32: 2264-2274.

45. Zachariah RM, Olson CO, Ezeonwuka C, Rastegar M (2012) Novel MeCP2 isoform-specific antibody reveals the endogenous MeCP2E1 expression in murine brain, primary neurons and astrocytes. PLoS One 7: e49763.

46. Lambert JF, Benoit BO, Colvin GA, Carlson J, Delville Y, Quesenberry PJ (2000) Quick sex determination of mouse fetuses. J Neurosci Methods 95: 127-132.

47. Kim JJ, Duan L, Tu TG, Elie O, Kim Y, Mathiyakom N, Elashoff D, Kim Y (2014) Molecular effect of ethanol during neural differentiation of human embryonic stem cells in vitro. Genom Data 2: 139-143.

48. Tateno M, Ukai W, Yamamoto M, Hashimoto E, Ikeda H, Saito T (2005) The effect of ethanol on cell fate determination of neural stem cells. Alcohol Clin Exp Res 29: 225S-229S.

49. Tateno M, Ukai W, Ozawa H, Yamamoto M, Toki S, Ikeda H, Saito T (2004) Ethanol inhibition of neural stem cell differentiation is reduced by neurotrophic factors. Alcohol Clin Exp Res 28: 134S-138S.

50. Cheng JC, Matsen CB, Gonzales FA, Ye W, Greer S, Marquez VE, Jones PA, Selker EU (2003) Inhibition of DNA Methylation and Reactivation of Silenced Genes by Zebularine. JNCI: Journal of the National Cancer Institute 95: 399-409.

51. Barber BA, Liyanage VR, Zachariah RM, Olson CO, Bailey MA, Rastegar M (2013) Dynamic expression of MEIS1 homeoprotein in E14.5 forebrain and differentiated forebrain-derived neural stem cells. Ann Anat 195: 431-440.

52. Rastegar M, Hotta A, Pasceri P, Makarem M, Cheung AY, Elliott S, Park KJ, Adachi M, Jones FS, et al. (2009) MECP2 isoform-specific vectors with regulated expression for Rett syndrome gene therapy. PLoS One 4: e6810.

53. Xiong H, Gendelman HE (2014) Current laboratory methods in neuroscience research: Springer.

54. Kishi N, Macklis JD (2010) MeCP2 functions largely cell-autonomously, but also non-cell-autonomously, in neuronal maturation and dendritic arborization of cortical pyramidal neurons. Exp Neurol 222: 51-58.

55. Ballas N, Lioy DT, Grunseich C, Mandel G (2009) Non-cell autonomous influence of MeCP2-deficient glia on neuronal dendritic morphology. Nat Neurosci 12: 311-317.

56. Oldham MC, Konopka G, Iwamoto K, Langfelder P, Kato T, Horvath S, Geschwind DH (2008) Functional organization of the transcriptome in human brain. Nat Neurosci 11: 1271-1282.

57. Montano CM, Irizarry RA, Kaufmann WE, Talbot K, Gur RE, Feinberg AP, Taub MA (2013) Measuring cell-type specific differential methylation in human brain tissue. Genome Biol 14: R94.

58. Guintivano J, Aryee MJ, Kaminsky ZA (2013) A cell epigenotype specific model for the correction of brain cellular heterogeneity bias and its application to age, brain region and major depression. Epigenetics 8: 290-302.

59. Uranova NA, Vostrikov VM, Orlovskaya DD, Rachmanova VI (2004) Oligodendroglial density in the prefrontal cortex in schizophrenia and mood disorders: a study from the Stanley Neuropathology Consortium. Schizophr Res 67: 269-275.

60. Lister R, Mukamel EA, Nery JR, Urich M, Puddifoot CA, Johnson ND, Lucero J, Huang Y, Dwork AJ, et al. (2013) Global epigenomic reconfiguration during mammalian brain development. Science 341: 1237905.

61. Guo JU, Su Y, Shin JH, Shin J, Li H, Xie B, Zhong C, Hu S, Le T, et al. (2014) Distribution, recognition and regulation of non-CpG methylation in the adult mammalian brain. Nature neuroscience 17: 215-222.

62. Kozlenkov A, Wang M, Roussos P, Rudchenko S, Barbu M, Bibikova M, Klotzle B, Dwork AJ, Zhang B, et al. (2016) Substantial DNA methylation differences between two major neuronal subtypes in human brain. Nucleic Acids Research 44: 2593-2612.

63. Vieira JP, Lopes F, Silva-Fernandes A, Sousa MV, Moura S, Sousa S, Costa BM, Barbosa M, Ylstra B, et al. (2015) Variant Rett syndrome in a girl with a pericentric X-chromosome inversion leading to epigenetic changes and overexpression of the MECP2 gene. Int J Dev Neurosci 46: 82-87.

64. Lee BY, Park SY, Ryu HM, Shin CY, Ko KN, Han JY, Koren G, Cho YH (2015) Changes in the methylation status of DAT, SERT, and MeCP2 gene promoters in the blood cell in families exposed to alcohol during the periconceptional period. Alcohol Clin Exp Res 39: 239-250.

65. Basil P, Li Q, Dempster EL, Mill J, Sham PC, Wong CCY, McAlonan GM (2014) Prenatal maternal immune activation causes epigenetic differences in adolescent mouse brain. Translational Psychiatry 4: e434.

66. He F, Lupu DS, Niculescu MD (2014) Perinatal α-linolenic acid availability alters the expression of genes related to memory and to epigenetic machinery, and the Mecp2 DNA methylation in the whole brain of mouse offspring. International journal of developmental neuroscience : the official journal of the International Society for Developmental Neuroscience 36: 38-44.

67. Franklin TB, Russig H, Weiss IC, Gräff J, Linder N, Michalon A, Vizi S, Mansuy IM (2010) Epigenetic Transmission of the Impact of Early Stress Across Generations. Biological Psychiatry 68: 408-415.

68. Basil P, Li Q, Smith R, Wong P, Mill J, Sham P, McAlonan G. Dietary Intervention on the Epigenetic Changes Induced by Environmental Risk Factors in the Adolescent Brain; 2014. Human Genome Organization (HUGO).

69. De Felice C, Signorini C, Durand T, Ciccoli L, Leoncini S, D'Esposito M, Filosa S, Oger C, Guy A, et al. (2012) Partial rescue of Rett syndrome by ω-3 polyunsaturated fatty acids (PUFAs) oil. Genes & Nutrition 7: 447-458.

70. Leoncini S, De Felice C, Signorini C, Zollo G, Cortelazzo A, Durand T, Galano J-M, Guerranti R, Rossi M, et al. (2015) Cytokine dysregulation in MECP2-and CDKL5-related Rett syndrome: relationships with aberrant redox homeostasis, inflammation, and ω-3 PUFAs. Oxidative medicine and cellular longevity 2015.

71. Nino-Soto M, Nuber UA, Basrur P, Ropers H-H, King W (2005) Differences in the pattern of X-linked gene expression between fetal bovine muscle and fibroblast cultures derived from the same muscle biopsies. Cytogenetic and genome research 111: 57-64.

72. Weaving LS, Williamson SL, Bennetts B, Davis M, Ellaway CJ, Leonard H, Thong MK, Delatycki M, Thompson EM, et al. (2003) Effects of MECP2 mutation type, location and X-inactivation in modulating Rett syndrome phenotype. Am J Med Genet A 118A: 103-114.

73. Krepischi AC, Kok F, Otto PG (1998) X chromosome-inactivation patterns in patients with Rett syndrome. Hum Genet 102: 319-321.

74. Camus P, Abbadi N, Perrier MC, Chery M, Gilgenkrantz S (1996) X chromosome inactivation in 30 girls with Rett syndrome: analysis using the probe. Hum Genet 97: 247-250.

75. Yu D, Sakurai F, Corey DR (2011) Clonal Rett Syndrome cell lines to test compounds for activation of wild-type MeCP2 expression. Bioorganic & medicinal chemistry letters 21: 5202-5205.

76. Minkovsky A, Sahakyan A, Bonora G, Damoiseaux R, Dimitrova E, Rubbi L, Pellegrini M, Radu CG, Plath K (2015) A high-throughput screen of inactive X chromosome reactivation identifies the enhancement of DNA demethylation by 5-aza-2′-dC upon inhibition of ribonucleotide reductase. Epigenetics & chromatin 8: 42.

77. Yu D, Sakurai F, Corey DR (2011) Clonal Rett Syndrome cell lines to test compounds for activation of wild-type MeCP2 expression. Bioorg Med Chem Lett 21: 5202-5205.

78. Vecsler M, Ben Zeev B, Nudelman I, Anikster Y, Simon AJ, Amariglio N, Rechavi G, Baasov T, Gak E (2011) Ex vivo treatment with a novel synthetic aminoglycoside NB54 in primary fibroblasts from Rett syndrome patients suppresses MECP2 nonsense mutations. PLoS One 6: e20733.

79. Brendel C, Belakhov V, Werner H, Wegener E, Gartner J, Nudelman I, Baasov T, Huppke P (2011) Readthrough of nonsense mutations in Rett syndrome: evaluation of novel aminoglycosides and generation of a new mouse model. J Mol Med (Berl) 89: 389-398.

80. Zhu L, Wang X, Li XL, Towers A, Cao X, Wang P, Bowman R, Yang H, Goldstein J, et al. (2014) Epigenetic dysregulation of SHANK3 in brain tissues from individuals with autism spectrum disorders. Hum Mol Genet 23: 1563-1578.

81. Nagarajan R, Hogart A, Gwye Y, Martin MR, LaSalle JM (2006) Reduced MeCP2 expression is frequent in autism frontal cortex and correlates with aberrant MECP2 promoter methylation. Epigenetics 1: 172-182.

82. Zhou P, Lu Y, Sun X-H (2011) Zebularine suppresses TGF-beta-induced lens epithelial cell–myofibroblast transdifferentiation by inhibiting MeCP2.

83. He S, Barron E, Ishikawa K, Khanamiri HN, Spee C, Zhou P, Kase S, Wang Z, Dustin LD, et al. (2015) Inhibition of DNA Methylation and Methyl-CpG-Binding Protein 2 Suppresses RPE Transdifferentiation: Relevance to Proliferative VitreoretinopathyDNA Methylation Regulates RPE Transdifferentiation. Investigative ophthalmology & visual science 56: 5579-5589.

APPENDIX

A1. Highlights of the study

Table A1. Highlights of the findings of current thesis		
Aim	**Chapter**	**Highlights**
1	3	• To our knowledge, this is the first report on the regulation of *Mecp2* isoforms by DNA methylation. • We identified six REs in the *Mecp2* promoter and intron 1, DNA methylation at which potentially 'regulate' *Mecp2e1* and *Mecp2e2* transcripts during NSC differentiation. • Treatment with the DNA demethylating agent-decitabine upregulated the expression of *Mecp2e1*/MeCP2E1, suggesting a potential mechanism for inducing *Mecp2*/MeCP2 in *Mecp2*-deficient conditions. • Provides some insights on future therapeutic interventions for neurological conditions caused by deficient of *MECP2*. • This was among the few reports which have shown that a drug that can induce MeCP2 expression and the only report on a drug that can induce the major MeCP2 isoform (MeCP2E1) (reviewed in [1]).
2	4	• First study which reported the effects of binge and chronic ethanol exposure and ethanol withdrawal on *Mecp2*/MeCP2 expression, which filled a significant knowledge gap in the field **(Table 6.2).** • Ethanol exposure and withdrawal during NSC differentiation extrinsically deregulated *Mecp2* expression at least partly *via* intrinsic DNA methylation changes at *Mecp2* REs. • Increased expression of *Mecp2* by ethanol exposure was associated with increased 5hmC and decreased 5mC at specific REs, while the opposite was observed after ethanol withdrawal.

Appendix

		• Reported changes to global 5mC and 5hmC levels and changes in glial size and neuronal morphology as a consequence of ethanol exposure and withdrawal. • Provided supporting evidence for the theory of 'epigenetic memory' in response to environmental insults/stressors through global- and *Mecp2* gene-specific DNA methylation changes. • Provided novel insights into the harmful effects of alcohol on epigenetic programming and epigenetic memory during NSC differentiation, which may help in further explaining the phenotypes observed in FASD patients and individuals with an alcohol addiction.
3	5	• To my knowledge, this is the first study which reported sex- and cell type-specific expression of *Mecp2e1* and *Mecp2e2* transcripts in embryonic neurons and astrocytes. • Our data confirm that *Mecp2* transcript expression in neurons and astrocytes isolated from E18 mouse brain do not follow the rules of XCI and dosage compensation and possibly escapes XCI. • Provided evidence that *Mecp2e1* is not always the major isoform at the transcript level. • Differences in DNA methylation between male neurons and astrocytes may at least partly drive the differential expression levels of *Mecp2e1* and *Mecp2e2* transcripts, presumably in a repressive manner. • Correlation analysis showed a much-conserved relationship between *Mecp2* transcript expression and DNA methylation in male astrocytes in contrast to the rather complex nature observed in male neurons.

There is a significant knowledge gap on the effect of ethanol exposure on *Mecp2/MECP2* expression during brain development. **Table A2** summarizes the studies on *Mecp2*/MeCP2 expression affected by ethanol exposure before conception, during pregnancy and after birth. Addressing a critical aspect of this knowledge gap, our study published in 2015 provided insights

324

Appendix

on not only the expression changes to *Mecp2*/MeCP2 after binge and continuous ethanol exposure

and ethanol withdrawal during NSC differentiation but also a potential epigenetic mechanism [2]

(Table A2).

Table A2. Summary of previous studies on the effects of ethanol on *Mecp2*/MeCP2 expression				
Model animal/system	**Ethanol condition**	**Brain region/cell type**	**Effect on *Mecp2*/MeCP2**	**Ref.**
Preconception paternal ethanol consumption in mice	0.5, 1, 2, and 4 g/kg/day of ethanol for 7 weeks and 1 week of ethanol withdrawal	Cortex and striatum	Decreased MeCP2	[3]
Postnatal day 7 (P7) mature mice	1.0 g/kg of ethanol	Hippocampus and neocortex	Increased MeCP2	[4]
Pregnant rats fed with ethanol during E10-E21 and adult offspring were tested	5% w/v, 35% ethanol	Hippocampus and frontal cortex	Increased MeCP2 in the hippocampus but unchanged MeCP2 in frontal cortex	[5]
Pregnant rats fed with ethanol between E7-E21 and male offspring tested at 60 days after birth	120-150 mg/dl blood alcohol levels	Hypothalamus	Increased *Mecp2*/MeCP2	[6]
Three-trimester model of pregnant rats fed with	4.5 g/kg	Whole brain	Decreased *Mecp2*	[7]

ethanol throughout pregnancy				
Pregnant rats fed with ethanol during E7-E21	1.7-5.0% v/v	Hypothalamus neurons	Increased MeCP2	[8]
Pregnant mice and rats were exposed to ethanol during pregnancy	4 and 6 g/kg/day ethanol	Cerebral cortex and striatum	Decreased MeCP2	[9]
Pregnant mice fed with ethanol during E7-E16.	4% v/v alcohol	Hippocampal neurons	Decreased MeCP2	[10]
E15 embryonic primary cortical neurons: ethanol exposure and withdrawal	75 mM	Primary cortical neurons	Decreased *Mecp2*/MeCP2 by both exposure and withdrawal	[11]

Table reprinted with permission from [12].

Differentiating NSC (isolated from E14.5 mouse embryos) to model binge and continuous ethanol exposure and ethanol withdrawal	70 mM	E14 NSC differentiating to a mixed population of neurons, astrocytes, and oligodendrocytes	Binge ethanol exposure: increased *Mecp2*/MeCP2; Continuous ethanol exposure: increased *Mecp2*/MeCP2; Ethanol withdrawal: decreased *Mecp2*/MeCP2	Current study (Chapter 4) [2]

A2. Validation of the potential role of *Mecp2* promoter and intron 1 methylation in regulating *Mecp2* isoforms in adult mouse brain *in vivo*

	Table A3. Comparison of percentage methylation differences at the individual CpG sites between brain regions													
	R1 CpG 5			R3 CpG 2			R5 CpG 1			R6 CpG 1			R6 CpG 2		
REGION	MD	SIG	P	MD	SIG	P	MD	SIG	P	MD	SIG	P	MD	SIG	P
OB vs. STR	-1.273	ns	>0.9999	0.5617	ns	>0.9999	11.67	***	0.0005	-22.93	***	<0.0001	-5.306	ns	0.3046
OB vs. CTX	-3.336	***	0.0009	8.247	***	<0.0001	10.49	**	0.0024	-19.51	***	<0.0001	-10.55	**	0.0020
OB vs. HIPPO	-0.08033	ns	>0.9999	1.768	ns	0.6119	10.73	**	0.0019	-1.456	ns	0.7941	-0.8000	ns	0.9945
OB vs. THAL	-0.1658	ns	>0.9999	2.523	*	0.0400	12.94	***	<0.0001	-10.59	**	0.0015	0.1360	ns	0.9945
OB vs. BS	-0.3343	ns	>0.9999	-0.7775	ns	>0.9999	17.36	***	<0.0001	-3.076	ns	0.5986	9.134	**	0.0098
OB vs. CERE	-0.4003	ns	>0.9999	2.840	*	0.0101	11.90	***	0.0004	4.424	ns	0.4133	-11.39	***	0.0007
STR vs. CTX	-2.063	ns	0.2311	8.809	***	<0.0001	-1.178	ns	0.9993	3.420	ns	0.5986	-5.245	ns	0.3046
STR vs. HIPPO	1.193	ns	>0.9999	2.330	ns	0.0862	-0.9420	ns	0.9993	21.48	***	<0.0001	4.506	ns	0.3931
STR vs. THAL	1.108	ns	>0.9999	3.084	**	0.0032	1.274	ns	0.9993	12.34	***	0.0001	5.442	ns	0.3046
STR vs. BS	0.9390	ns	>0.9999	-0.2158	ns	>0.9999	5.694	ns	0.3756	19.86	***	<0.0001	14.44	***	<0.0001
STR vs. CERE	0.8730	ns	>0.9999	3.402	***	0.0006	0.2310	ns	0.9993	27.36	***	<0.0001	-6.086	ns	0.2029
CTX vs. HIPPO	3.256	**	0.0014	-6.479	***	<0.0001	0.2360	ns	0.9993	18.06	***	<0.0001	9.751	**	0.0049
CTX vs. THAL	3.170	**	0.0021	-5.725	***	<0.0001	2.452	ns	0.9888	8.921	*	0.0104	10.69	**	0.0019
CTX vs. BS	3.002	**	0.0048	-9.025	***	<0.0001	6.872	ns	0.1601	16.44	***	<0.0001	19.69	***	<0.0001
CTX vs. CERE	2.936	**	0.0065	-5.408	***	<0.0001	1.409	ns	0.9993	23.94	***	<0.0001	-0.8405	ns	0.9945

	MD	SIG	P	MD	SIG	P	MD	SIG	P	MD	SIG	P	MD	SIG	P
HIPPO vs. THAL	-0.0855	ns	>0.9999	0.7542	ns	>0.9999	2.216	ns	0.9913	-9.136	**	0.0089	0.9360	ns	0.9945
HIPPO vs. BS	-0.2540	ns	>0.9999	-2.546	*	0.0363	6.636	ns	0.1867	-1.620	ns	0.7941	9.934	**	0.0042
HIPPO vs. CERE	-0.3200	ns	>0.9999	1.072	ns	>0.9999	1.173	ns	0.9993	5.880	ns	0.1675	-10.59	**	0.0020
THAL vs. BS	-0.1685	ns	>0.9999	-3.300	**	0.0011	4.420	ns	0.6918	7.516	*	0.0461	8.998	*	0.0106
THAL vs. CERE	-0.2345	ns	>0.9999	0.3175	ns	>0.9999	-1.043	ns	0.9993	15.02	***	<0.0001	-11.53	***	0.0006
BS vs. CERE	-0.06600	ns	>0.9999	3.618	***	0.0002	-5.463	ns	0.4143	7.500	*	0.0461	-20.53	***	<0.0001
vs= versus; MD = Mean difference; SIG= Significance; P= P value															
Bonferroni's multiple comparisons test. P≤0.05 was considered statistically significant. N=5															

Reprinted with permission from [13].

Appendix

A3. *In silico* analysis of the enrichment of regulatory proteins and hPTMs at the *Mecp2* promoter in neurons, and *MECP2* promoter in human neurons and astrocytes
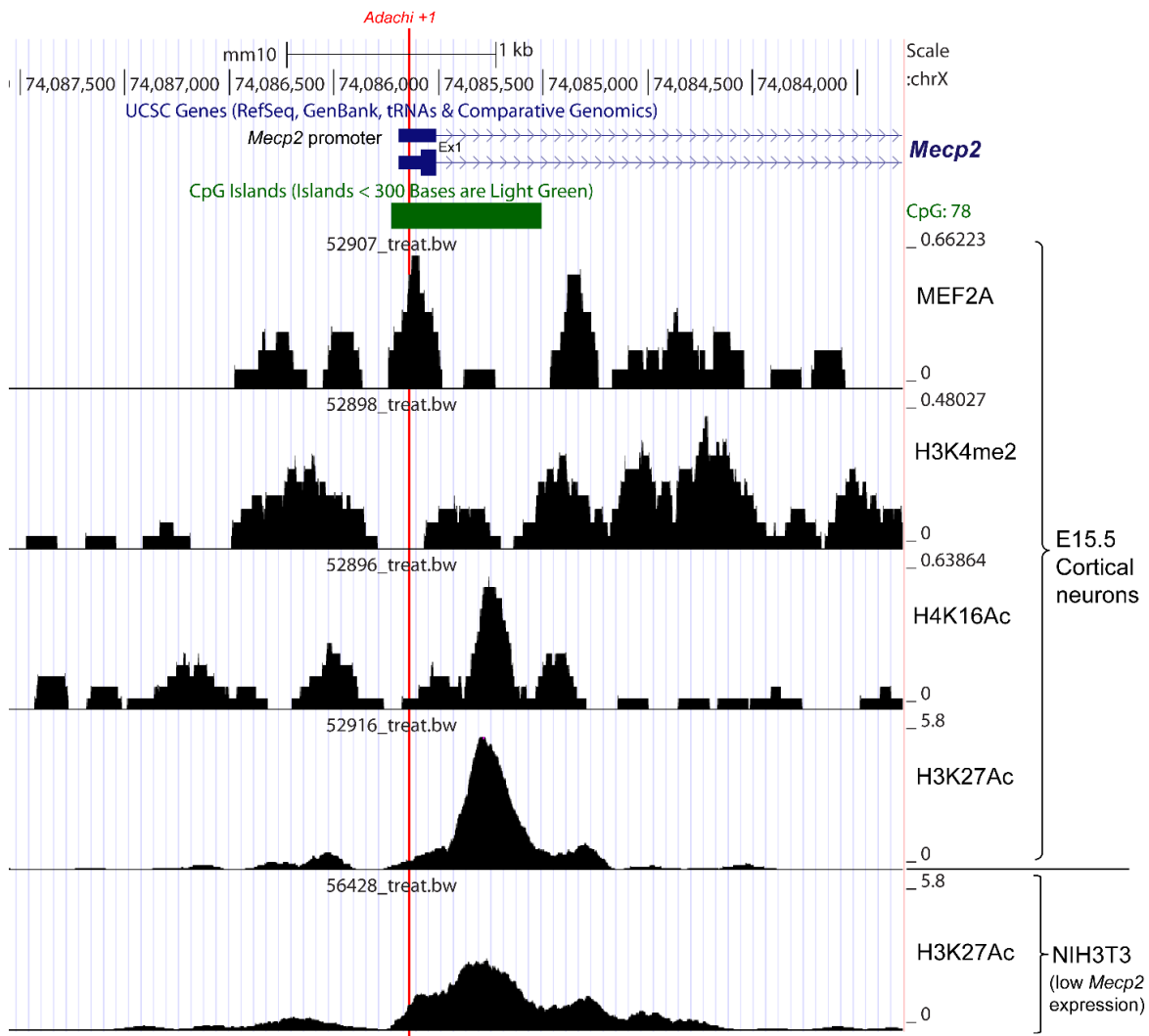

Figure A1 ChIPseq data mining to show active nature of the *Mecp2* promoter in neurons. The active nature of the mouse *Mecp2* promoter in cortical neurons (E15.5) was determined using CistromeDB ChIPseq analysis. ChIPseq data for neurons were extracted from [14] and NIH3T3 from [15]. The TSS reported in Adachi *et al* [16] is also marked. Refer to Chapter 2 (Section 2.15) for methods.
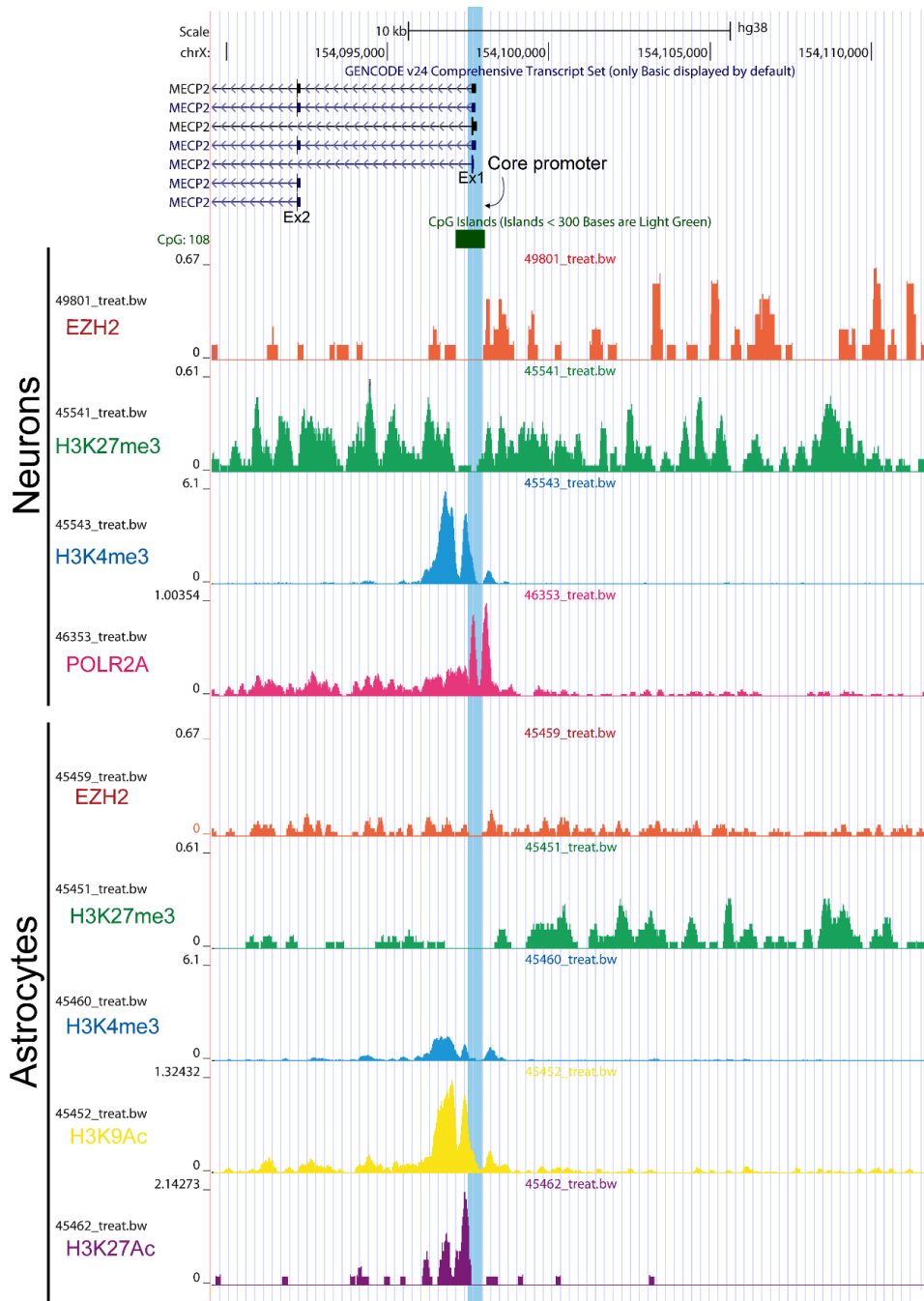
Appendix

Figure A2 Comparison of the distribution of epigenetic and transcriptional signatures at the *MECP2* promoter in human neurons and astrocytes.

ChIPseq data extracted from differentiated SK-N-SH_RA for human neurons and NH-A-Brain for astrocytes from the ENCODE project are represented in the figure. The core human *MECP2* promoter reported by Adachi *et al.* is marked in blue [16]. The epigenetic signatures of the *MECP2*

330

Appendix

promoter in two cell types implies potentially higher *MECP2* expression in neurons than astrocytes. Refer to Chapter 2 (Section 2.15) for methods.

References

1. Liyanage VR, Rastegar M (2014) Rett syndrome and MeCP2. Neuromolecular Med 16: 231-264.

2. Liyanage VR, Zachariah RM, Davie JR, Rastegar M (2015) Ethanol deregulates Mecp2/MeCP2 in differentiating neural stem cells via interplay between 5-methylcytosine and 5-hydroxymethylcytosine at the Mecp2 regulatory elements. Exp Neurol 265: 102-117.

3. Kim P, Choi CS, Park JH, Joo SH, Kim SY, Ko HM, Kim KC, Jeon SJ, Park SH, et al. (2014) Chronic exposure to ethanol of male mice before mating produces attention deficit hyperactivity disorder-like phenotype along with epigenetic dysregulation of dopamine transporter expression in mouse offspring. J Neurosci Res 92: 658-670.

4. Subbanna S, Nagre NN, Shivakumar M, Umapathy NS, Psychoyos D, Basavarajappa BS (2014) Ethanol induced acetylation of histone at G9a exon1 and G9a-mediated histone H3 dimethylation leads to neurodegeneration in neonatal mice. Neuroscience 258: 422-432.

5. Tunc-Ozcan E, Ullmann TM, Shukla PK, Redei EE (2013) Low-dose thyroxine attenuates autism-associated adverse effects of fetal alcohol in male offspring's social behavior and hippocampal gene expression. Alcohol Clin Exp Res 37: 1986-1995.

6. Gangisetty O, Bekdash R, Maglakelidze G, Sarkar DK (2014) Fetal Alcohol Exposure Alters Proopiomelanocortin Gene Expression and Hypothalamic-Pituitary-Adrenal Axis Function via Increasing MeCP2 Expression in the Hypothalamus. PLoS One 9: e113228.

7. Perkins A, Lehmann C, Lawrence RC, Kelly SJ (2013) Alcohol exposure during development: Impact on the epigenome. Int J Dev Neurosci 31: 391-397.

8. Bekdash RA, Zhang C, Sarkar DK (2013) Gestational choline supplementation normalized fetal alcohol-induced alterations in histone modifications, DNA methylation, and proopiomelanocortin (POMC) gene expression in beta-endorphin-producing POMC neurons of the hypothalamus. Alcohol Clin Exp Res 37: 1133-1142.

9. Kim P, Park JH, Choi CS, Choi I, Joo SH, Kim MK, Kim SY, Kim KC, Park SH, et al. (2013) Effects of ethanol exposure during early pregnancy in hyperactive, inattentive and impulsive behaviors and MeCP2 expression in rodent offspring. Neurochem Res 38: 620-631.

10. Chen Y, Ozturk NC, Zhou FC (2013) DNA methylation program in developing hippocampus and its alteration by alcohol. PLoS One 8: e60503.

11. Guo Y, Chen Y, Carreon S, Qiang M (2012) Chronic intermittent ethanol exposure and its removal induce a different miRNA expression pattern in primary cortical neuronal cultures. Alcohol Clin Exp Res 36: 1058-1066.

12. Liyanage VR, Curtis K, Zachariah RM, Chudley AE, Rastegar M (2016) Overview of the Genetic Basis and Epigenetic Mechanisms that Contribute to FASD Pathobiology. Curr Top Med Chem, http://www.ncbi.nlm.nih.gov/pubmed/27086780.

13. Olson CO, Zachariah RM, Ezeonwuka CD, Liyanage VR, Rastegar M (2014) Brain region-specific expression of MeCP2 isoforms correlates with DNA methylation within Mecp2 regulatory elements. PLoS One 9: e90645.

14. Telese F, Ma Q, Perez PM, Notani D, Oh S, Li W, Comoletti D, Ohgi KA, Taylor H, et al. (2015) LRP8-Reelin-Regulated Neuronal Enhancer Signature Underlying Learning and Memory Formation. Neuron 86: 696-710.

15. Schick S, Fournier D, Thakurela S, Sahu SK, Garding A, Tiwari VK (2015) Dynamics of chromatin accessibility and epigenetic state in response to UV damage. J Cell Sci 128: 4380-4394.

16. Adachi M, Keefer EW, Jones FS (2005) A segment of the Mecp2 promoter is sufficient to drive expression in neurons. Hum Mol Genet 14: 3709-3722.